Scaling and singularities in higher-order nonlinear differential equations

Williams, J. F.

Award date:
2003

Awarding institution:
University of Bath

Scaling and singularities in higher-order nonlinear differential equations

Submitted by

J. F. Williams

for the degree of PhD
of the

University of Bath

2003

ProQuest LLC
789 East Eisenhower Parkway
P.O. Box 1346
Ann Arbor, MI 48106-1346

Abstract

Higher-order parabolic equations are ever more important in applications. Despite their simple and familiar structure, few of the rigorous classical tools of analysis can be applied to study them. In this thesis we begin an investigation into the structure of singular solutions to some important canonical higher-order equations. Using a mixture of PDE and ODE methods including similarity transformations, matched asymptotic expansions and bifurcation theory we establish the existence of similarity solutions to problems both with blow-up and decay. Indeed, we show that the classical second-order heat equation with nonlinear reaction is a special case in not having exact similarity solutions. The well known centre-manifold behaviour observed there is a property only of the order of the problem, not of the semilinear structure.

In particular, using a mixture of spectral theory, asymptotics, and numerics we conjecture the existence of at least $2\lfloor m/2 \rfloor$ self-similar solutions to the higher-order semilinear parabolic equation

$$u_t = -(-\Delta)^m u + |u|^{p-1}u, \qquad p > 1, \;\; m > 1.$$

This is in stark contrast to the classical case of $m = 1$ where it is known there are no self-similar solutions. Using a combination of PDE and ODE analysis we prove the existence of a countable spectrum of the so-called very singular solutions to

$$u_t = -(-\Delta)^m u - |u|^{p-1}u, \qquad p > 1, \;\; m > 1,$$

in the sub-critical Fujita range $p < p_0 = 1 + 2m/N$ in space dimension N. Further, we consider the equation

$$u_t = (-\Delta)(\Delta u + |u|^{p-1}u), \qquad p > 1,$$

and prove the existence of a countable spectrum of similarity solutions for the critical exponent $p = 3$ in $N = 1$. This family is then constructed using matched singular asymptotic expansions. Additionally, we prove the existence of a continuous family of global decaying solutions.

All our work is guided by careful numerical investigation and the construction of efficient and robust adaptive numerical schemes for the investigation of singularities in fourth-order nonlinear parabolic problems is a major component of this thesis. To this end we describe the construction and implementation of a conservative moving collocation method for problems of the form

$$\mathbf{f}(x, t, \mathbf{u}, \mathbf{u}_x, \mathbf{u}_{xx}, \mathbf{u}_{xxx}, \mathbf{u}_t) = (\mathbf{g}(x, t, \mathbf{u}, \mathbf{u}_x, \mathbf{u}_{xx}, \mathbf{u}_{xxx}))_x \qquad x \in (x_l(t), x_r(t)) \; t > 0.$$

Acknowledgements

I would like to thank my supervisors Chris Budd and Victor Galaktionov for their endless support, assistance and encouragement. Each of them taught me about what mathematics is, how to do it and many more important things. It will take me years to unravel all the lessons they have impressed upon me.

I am also endebted to Keith Promislov for originally showing me that mathematics is fun, rewarding and a worthwhile endeavour.

I have been very lucky to have been able to discuss my work with many experts. I am grateful to Jan Bouwe van den Berg, Alan Champneys, Jonathan Evans, Joost Hulshof, Ivan Graham, Adrian Hill, John King, Bill Morton, Bob Russell, Bert Peletier, Mark Peletier, Matt Piggott, Alastair Spence and John Toland for kind words and useful insights.

My friends and colleagues, emerging experts themselves, helped immensely by at times distracting me from my own work and always listening and making useful suggestions. My study in Bath has been made immeasurably better by various house- and office-mates: Jörg Berns-Muller, David Cunningham, Ceri Fiddes, Damien Harwin, Andy Holt, Sarah Mitchell, Steven White and Andy Whittle.

My parents have, all through my life, been unreservedly supportive of everything I have done and this has been no exception. Thank you for everything.

Lastly, I could not have done it (why would I even have bothered?) without the love and generosity of Trudy O'Donaghey. Thanks for always being there, even though 'there' was 7567.32 km away.

Statement of results

No work is ever truly done alone and this is certainly the case in this thesis. Five publications have been submitted or are in preparation in connection with this thesis with five co-authors. It is important to be explicit from the beginning what results are contained within and where else they have appeared or have been submitted.

Chapter 1 We motivate many of the more mathematical questions in this thesis with the analysis of blow-up solutions to the Semenov-Rayleigh-Benard problem which models the interaction of convection and reaction in a reacting fluid and which is governed, in the limit of large solutions, by

$$u_t = -u_{xxxx} + \beta[(u_x)^3]_x + e^u.$$

Some of the results in this Chapter appear in 'On a higher-order equation from explosion-convection theory' (Galaktionov and Williams 2002) accepted for publication in the European Journal of Applied Mathematics.

Chapter 2 A general purpose code named MovCol4 has been written to solve systems of fourth-order parabolic equations of the form

$$\mathbf{f}(x, t, \mathbf{u}, \mathbf{u}_x, \mathbf{u}_{xx}, \mathbf{u}_{xxx}, \mathbf{u}_t) = (\mathbf{g}(x, t, \mathbf{u}, \mathbf{u}_x, \mathbf{u}_{xx}, \mathbf{u}_{xxx}))_x.$$

This code is an extension of pre-existing work of R.D. Russell and Wheizhang Whang and some of the results of this Chapter will appear in Williams, Xu and Russell (2003).

Chapter 3 In this Chapter we establish the existence of exact self-similar blow-up solutions to the equation

$$u_t = -(-\Delta)^m u + |u|^{p-1}u, \qquad p > 1, m > 1.$$

A bifurcation analysis suggests the existence of at least $2\lfloor m/2 \rfloor$ solutions, which, by numerical computation is shown to a be lower bound. The results of this Chapter appear in the paper 'Self-similar blow-up in higher-order semilinear parabolic equations.', submitted to the SIAM Journal of Applied Mathematics (Budd, Galaktionov and Williams 2002). We also describe some centre manifold patterns of the SRB problem.

Chapter 4 We describe the so-called Very Singular Solutions (VSS) to the diffusion-absorption equation

$$u_t = -(-\Delta)^m u - |u|^{p-1}u, \qquad p > 1, \;\; m > 1.$$

Using a combination of PDE and ODE analysis the existence of a countable spectrum of solutions for $p < p_0 = 1 + 2m/N$ is established. This work has been submitted to the Journal of Asymptotic Analysis (Galaktionov and Williams 2003b).

Chapter 5 The existence of both blow-up and decaying solutions to

$$u_t = (-\Delta)(\Delta u + |u|^{p-1}u), \qquad p > 1$$

is established. For the critical exponent (in one dimension) $p = 3$, a countable spectrum of blow-up solutions is proven to exist and constructed using matched asymptotic expansions. Whereas for the decay problem a continuous spectrum is proven to exist. This work will appear as 'Blow-up and global asymptotics of the unstable Cahn-Hilliard equation with a homogeneous nonlinearity' (Galaktionov and Williams 2003a). I gratefully acknowledge the assistance of Dr. J.D. Evans in the construction of the multi-scale asymptotic expansions employed in Chapter 5 and particularly in the derivation of formula (5.3.26)

Chapter 6 This Chapter indicates how other current and ongoing work by the author fits into the framework of this thesis and what future work is suggested by the present study.

A human being should be able to change a diaper, plan an invasion, butcher a hog, conn a ship, design a building, write a sonnet, balance accounts, build a wall, set a bone, comfort the dying, take orders, give orders, cooperate, act alone, solve equations, analyze a new problem, pitch manure, program a computer, cook a tasty meal, fight efficiently, die gallantly. *Specialization is for insects!*

- Robert A. Heinlein

Contents

Chapter 1

Introduction: Models and Methodology

In this thesis we shall investigate and exploit the intriguing relationship which exists between scaling, self-similarity, asymptotics and numerical discretizations in studying singularity formation in parabolic partial differential equations. We will treat a number of essentially new models with particular interest in higher-order equations. Many physical processes of great importance are modelled by such equations and we will use the underlying scaling structure for our analysis, be it rigorous, formal or numerical.

Higher-order semilinear parabolic equations arise in many physical applications such as thin film theory, convection-explosion theory, lubrication theory, flame and wave propagation (the Kuramoto-Sivashinskii equation and the extended Fisher-Kolmogorov equation), phase transition at critical Lifschitz points, bi-stable systems and applications from structural mechanics. The effect of fourth-order terms on self-focussing problems in nonlinear optics has also recently been considered by Fibich, Ilan and Papanicolau (2002) and Ben-Artzi, Koch and Saut (2000). Indeed, fourth- (and higher-) order terms are increasingly recognized as being significant in many physical models, and this has lead to the burgeoning literature including the recent book by Peletier and Troy (2001) which lists a number of models and references. Therefore, it is important to know if higher-order semilinear equations exhibit analagous singularity behaviour to their classical second-order counterparts where exact self-similar behaviour is unavailable.

In this thesis we shall concentrate on two fundamental types of behaviour arising from diverse physical applications and as canonical mathemical models. The first is the formation of hot-spots, where, typically the solution u corresponds to a temperature and solutions can become unbounded in finite time. The second is of infinite-time decay wherein the long-time (not rescaled) behaviour is dominated by dissipative rather than reactive effects. In both cases the large time asymptotic behaviour is governed by simple *similarity solutions.*

The fundamental role of similarity solutions in studying partial differential equations (PDEs) stems from the *covariance* principle of physics, see eg. Barenblatt (1996) which states that the fundamental laws of physics are not affected by the co-ordinate system in which they are posed. From this deceptively simple statement follows *dimensional analysis* whereby we may simplify complicated models to their mathematical essence where only terms of the same importance remain. This balancing is a feature of *scaling invariance* wherein solutions are invariant under a group transformation (see Section 1.3). Moreover the scaling structure of a problem often signals the existence of self-similar solutions which, under many circumstances, are attractors for the system under consideration and as such define the intermediate asymptotics, describing the key asymptotic behaviour of the problem at hand. That is, the behaviour of the problem at sufficiently large times that initial data are no longer important but before boundary conditions dominate the solution. Self-similar solutions also reduce the complexity of the problem by transforming partial differential equations into ordinary differential equations (ODEs) or lowering the number of independent variables.

Finite time blow-up is a typical problem in the study of dynamical systems theory, with second-order models having been well studied for the past thirty years. We are interested in new higher-order models for which the standard and well known mathematical techniques do not apply. There is no order-preservation, Maximum Principle or gradient structure for most of these new problems. Consequently, we are interested in a mixture of asymptotic and numerical computation to determine the governing dynamics of these emerging problems. We begin by introducing the key concepts of this thesis in the context of a physical model.

1.1 A typical higher-order model: The Semenov-Rayleigh-Benard problem

As a motivating example for both this introduction and indeed the thesis as a whole we will consider a problem from explosion-convection theory due to Joulin, Mikishev and Sivashinsky (n.d.), the Semenov-Rayleigh-Benard problem, which describes the evolution of temperature in a reacting fluid contained between a heated plate below, and a cooled one above, see Figure 1.1. This is described by the fourth-order PDE

$$u_t = -u_{xxxx} - \left[(2-(u_x)^2)u_x\right]_x - \alpha u + qe^{su}, \tag{1.1.1}$$

where α, q and s are positive constants determined from physical parameters and u defined on $x \in I_0 = (0, 2\pi)$ satisfies periodic boundary conditions.

The above fourth-order one-dimensional semilinear parabolic equation (1.1.1) is derived by studying the interaction between natural convection and the reaction of an

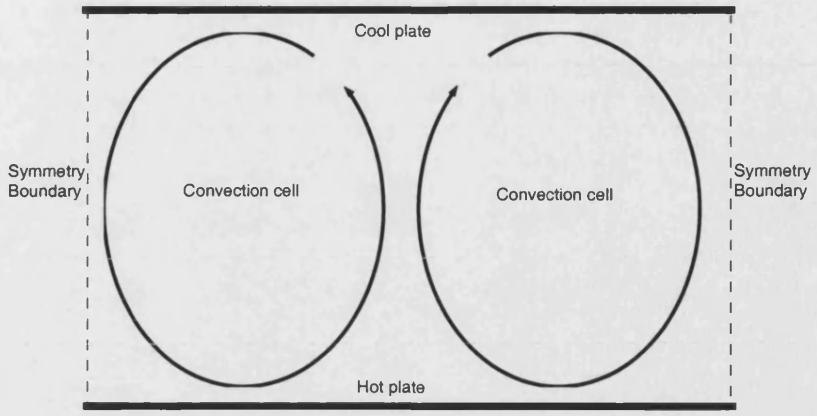

Figure 1.1: Geometry of the Semenov-Ralyleigh-Benard problem

exothermally reactive fluid confined between two isothermal horizontal plates. This is an evolutionary equation for temperature fluctuations in the presence of natural convection (it is assumed that the Rayleigh number is marginally supercritical), small wall losses and chemistry. It can be considered as a formal combination of the equation derived in Gertsberg and Sivashinsky (1981) (see also Chapman and Proctor (1980) wherein the derivation is very similar except for the absence of reactive effects) for the Rayleigh-Benard problem and of the Semenov-like energy balance (Semenov 1935, Frank-Kamenetskii 1969) showing that natural convection and the explosion mechanism may reinforce each other when the convection cells are large enough. In the statement of this problem the solutions $u = u(x,t)$ are 2π-periodic in x with bounded periodic initial data $u(x,0) = u_0(x)$ for $x \in I_0 = [0, 2\pi]$. The previous authors were concerned with the stability of small solutions and the possibility of thermal runaway, they did not consider the spatio-temporal structure of blow-up solutions. Equation (1.1.1) can be considered to be a higher-order generalization of the famous *Frank-Kamenetskii equation* (1938) (the solid fuel model (Zel'dovich, Barenblatt, Librovich and Makhviladze 1985)),

$$u_t = u_{xx} + e^u, \quad x \in \mathbf{R}, \ t > 0. \tag{1.1.2}$$

1.2 Singularity formation phenomena: Finite-time blow-up

While for a great many problems the solution and all its derivatives remain bounded for all time, that is the solution is *globally solvable* in time, it is a wonderful feature of nonlinear problems that this is not always true. One of the central concepts to reaction-diffusion equations is *finite time blow-up* (meaning explosion in Combustion Theory (Zel'dovich et al. 1985)), in the sense that there exists $0 < T < \infty$ such that

$u(x,t)$ exists and is classical on any time-interval $[0,T']$ with $T' \in (0,T)$ and

$$\sup_x |u(x,t)| \to \infty \quad \text{as } t \to T^-. \tag{1.2.1}$$

The fact that solutions of higher-order parabolic equations may blow up is well known, see the surveys by Levine (1990) and Galaktionov and Vazquez (2002) and more recent results in the work of Egorov, Galaktionov, Kondratiev and Pohozaev (2002) and Chaves and Galaktionov (2001) for equations of the form $u_t = -(-\Delta)^m u + f(u)$, where the critical Fujita exponent and estimates on blow-up rates were established for any $m > 1$. The structure of these blow-up solutions is described in detail in Chapter 3.

A general treatment of blow-up processes occurred in the 1930's - 1950's in the context of N.N. Semenov's chain reaction theory, adiabatic explosion and combustion theory (the first blow-up result was by O.M. Todes (1933)), see Gel'fand (1963) and Zel'dovich et al. (1985). On the other hand, in the same period there was a strong influence from the study of blow-up singularities in gas dynamics, in particular, the intense explosion (focusing) problem, admitting similarity solutions of the second kind, was considered by K. Bechert, K.G. Guderley and L.I. Sedov in the 1940's; see Barenblatt (1996, p. 127) and Zel'dovich and Raizer (1966). Another classical area of blow-up processes which developed in the 1960's is nonlinear optics, where the main model is the nonlinear (cubic) Schrödinger equation defined in $\mathbf{R}^2$ or $\mathbf{R}^3$ which is hyperbolic and admits blow-up self-focusing solutions; see references in the book by Sulem and Sulem (1999) and some comments Chapter 6 in this thesis. Finite time blow-up is often seen in the leading order equation of asymptotic expansions where it can represent a breakdown in the model. Therefore it is important to understand the structure of the singularity to determine whether or not small saturating terms ignored at the first level of approximation are truly significant before something physically catastrophic happens in the model.

1.2.1 The SRB-problem

To see that finite-time blow-up is not simply the consequence of pathological models we will first make some comments about the regularity and dynamics of the Semenov-Rayleigh-Benard problem. Equation (1.1.1) is uniformly parabolic with all spatial differential operators appearing in divergence form. For all intitial data in L^∞ it admits a unique classical local in time solution, see the standard parabolic theory in Friedman (1983). The operator on the right-hand side of (1.1.1)

$$\mathbf{N}(u) \equiv -u_{xxxx} - [(2 - (u_x)^2)u_x]_x - \alpha u + qe^{su}$$

is potential in the sense that the equation admits the Lyapunov function

$$L[u](t) = \int_{I_0} \frac{1}{2}(u_{xx})^2 - (u_x)^2 + \frac{1}{4}(u_x)^4 + \frac{\alpha}{2}u^2 - \frac{q}{s}e^{su}\,dx,$$

which is monotone on bounded orbits,

$$\frac{d}{dt}L[u](t) = -\int_{I_0} (u_t)^2 dx \le 0.$$

For such smooth gradient systems, the ω-limit set of any bounded orbit $\{u(\cdot,t),\ t>0\}$,

$$\omega(u_0) = \{f \in C(I_0):\ \exists\ \{t_k\} \to \infty \text{ such that } u(\cdot,t_k) \to f \text{ uniformly}\},$$

is known (Sell and You 2002) to consist of stationary solutions: $\mathbf{N}(f) = 0$ in I_0 for any $f \in \omega(u_0)$. Some results on bifurcation of stationary solutions were obtained in Joulin et al. (n.d.). If the subset of stationary solutions consists of isolated equilibria, the asymptotic behaviour of uniformly bounded orbits does not essentially differ from that for the second-order parabolic equation (1.1.2) where any bounded orbits are known to approach a stationary profile as $t \to \infty$. Despite the gradient structure, the proof of blow-up for the periodic initial value problem for (1.1.1) is straightforward.

Proposition 1.2.1. *Let $u(x,t)$ be a solution of* (1.1.1) *in $I_0 \times \mathbf{R}_+$ with periodic boundary conditions and bounded continuous initial data $u_0(x)$.*
(i) If

$$\alpha < sqe^{1/2\pi}, \tag{1.2.2}$$

then the solution blows up in finite time.
(ii) If (1.2.2) *does not hold, then the solution blows up if the initial data is sufficiently large in the mean sense.*

Proof. Denoting by $\bar{u}(t) = \int u(x,t)dx$ the mean of the solution on I_0 and integrating equation (1.1.1) over I_0, we obtain

$$\bar{u}' = q\int e^{su}dx - \alpha\bar{u}.$$

By Jensen's inequality for convex functions (Hirsch and Lacombe 1999)

$$\int e^{su}dx = 2\pi \int e^{su}\frac{1}{2\pi}dx \ge 2\pi e^{s\bar{u}/2\pi},$$

and we arrive at an *ordinary differential inequality* (ODI)

$$\bar{u}' \ge F(\bar{u}) \equiv 2\pi q e^{s\bar{u}/2\pi} - \alpha\bar{u}. \tag{1.2.3}$$

If (1.2.2) holds, then $F > 0$ in $\mathbf{R}$. Hence, $\bar{u}' > 0$, $\bar{u}(t) > \bar{u}_0$ for $t > 0$ and (1.2.3) implies

that $\bar{u}(t)$ (and $u(x,t)$) blows up at

$$T \leq T_0 = \int_{\bar{u}_0}^{\infty} ds/F(s).$$

(ii) If $\alpha \geq sqe^{1/2\pi}$, then similarly we have that blow-up occurs if $\bar{u}_0 > s_+$, where s_+ is the maximal root of the equation $F(s) = 0$. □

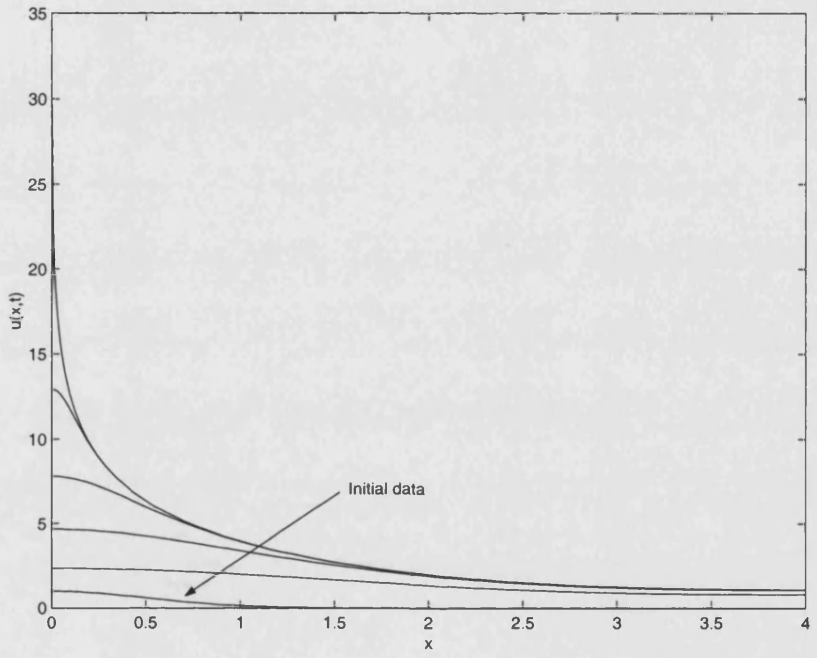

Figure 1.2: Finite time blow-up of (1.1.1) in physical co-ordinates.

The use of ODIs is typical in the construction of blow-up estimates, see for instance Chaves and Galaktionov (2001) or Levine (1990). In Figure 1.2 we show typical profiles of the evolution, showing single-point blow-up at the origin and the formation of the singular final time profile. The numerical methods used for the approximation of this solution will be introduced in Section 1.6 and discussed at length in Chapter 2.

Blow-up is an essential feature of explosion-convection problems and the corresponding parabolic equations under consideration. As for the solid fuel model (1.1.2), the structure of such a blow-up singularity formation is of importance in the present higher-order model. Finite time blow-up involves a delicate balance between the spatial and temporal derivatives and the reaction terms driving the blow-up. This balance is made naturally apparent by considering the scaling invariance of the underlying PDE.

1.3 Scale invariance and similarity variables

Scaling and self-similarity have been known since the 1930's to give fundamental insight into many systems which develop singularities in finite time. For example, consider the simple classical semilinear heat equation with a polynomial reaction term,

$$u_t = u_{xx} + u^p, \quad x \in \mathbf{R}, \ t > 0 \quad \text{with exponent } p > 1 \quad (u(x,t) \geq 0). \tag{1.3.1}$$

We define a group of scaling transformations by

$$t \mapsto \lambda t, \qquad x \mapsto \lambda^{1/2} x, \qquad u \mapsto \lambda^{-1/(p-1)} u, \qquad \lambda > 0. \tag{1.3.2}$$

Then, equation (1.3.1) is *invariant* under (1.3.2) in the sense that solutions are mapped to solutions under this transformation. The existence of such a transformation means that there also exists a family of solutions of (1.3.1) of the form

$$u(x,t) = (T-t)^{-1/(p-1)} f(y), \qquad y = x/(T-t)^{1/2} \tag{1.3.3}$$

with an unknown blow-up time $t = T$ and where $f(y)$ satisfies the ODE,

$$f'' - \frac{1}{2} y f' - \frac{1}{p-1} f + f^p = 0. \tag{1.3.4}$$

The simplicity of the geometric structure of (1.3.1) means that we can reduce the original PDE problem for $u(x,t)$ to an ODE problem for $f(y)$. As we shall see though, the existence of an equation for a similarity profile does not imply the existence of an admissable similarity solution to the full PDE! This can because the ODE has no solution with the appropriate boundary conditions, thus far not discussed, or because of other geometric constraints. However, even in the case that a complete similarity solution does not exist, the leading dynamics of the PDE my well be governed by operators associated with the similarity solutions.

1.3.1 Similarity variables in the SRB-problem

To see the asymptotic similarity structure in (1.1.1) we first rescale

$$su \mapsto u, \quad (qs)^{1/4} x \mapsto x, \quad \text{and} \quad qst \mapsto t$$

in (1.1.1) to obtain the equation

$$u_t = \mathbf{A}(u) - \gamma u_{xx} - \delta u, \quad \gamma = 2/\sqrt{qs}, \ \delta = \alpha/qs, \tag{1.3.5}$$

where $\mathbf{A}$ is the fourth-order operator

$$\mathbf{A}(u) = -u_{xxxx} + \beta[(u_x)^3]_x + e^u, \quad \beta = 1/s^2.$$

Here β is an essential parameter which cannot be removed by scaling. The physically admissible range of the parameter is $\beta \in (0, \infty)$, but we also include the limit case $\beta = 0$ which formally corresponds to $s = \infty$ and leads to the fourth-order *extended Frank-Kamenetskii equation*

$$u_t = -u_{xxxx} + e^u. \tag{1.3.6}$$

We begin our similarity analysis with the unperturbed equation

$$u_t = -u_{xxxx} - \beta[(u_x)^3]_x + e^u \tag{1.3.7}$$

which is a natural simplification of (1.3.5) for large solutions as only the lowest-order (in a sense to be described below) terms have been neglected.

Without loss of generality, we assume that the solution $u(x,t)$ blows up at finite time $t = T$ in the sense of (1.2.1) and that the blow-up set

$$B[u_0] = \{x \in I : \exists \{x_k\} \to x, \ \{t_k\} \to T^- \text{ such that } u(x_k, t_k) \to \infty\} \tag{1.3.8}$$

contains the origin, $0 \in B[u_0]$. We now observe that the reduced equation, (1.3.7), is invariant under the group of transformations

$$t \mapsto \lambda t, \quad x \mapsto \lambda^{1/4} x, \quad u \mapsto u - \ln \lambda, \quad \text{with } \lambda > 0. \tag{1.3.9}$$

Therefore, motivated by the blow-up assumptions, replacing $t \mapsto t - T$ and setting $\lambda = (T-t)^{-1}$ yields the following independent self-similar variables: $y = x/(T-t)^{1/4}$: $I_0 \to \mathbf{R}$ is the new spatial variable, and $\tau = -\ln(T-t)$: $(0,T) \to (\tau_0, \infty)$ with $\tau_0 = -\ln T$ is the new time variable. Then the rescaled solution is given by

$$u(x,t) = -\ln(T-t) + \theta(y,\tau), \tag{1.3.10}$$

and substituting into (1.3.7) gives the rescaled equation

$$\theta_\tau = -\theta_{yyyy} + \beta\left[(\theta_y)^3\right]_y - \frac{1}{4} y\theta_y + e^\theta - 1 \equiv \mathbf{A}_1(\theta). \tag{1.3.11}$$

Using these new variables for the full equation (1.1.1) gives that the rescaled function θ satisfies the following perturbed parabolic equation:

$$\theta_\tau = \mathbf{A}_1(\theta) + \mathbf{C}(\theta, \tau), \tag{1.3.12}$$

where $\mathbf{A}_1$ is the *autonomous* operator in (1.3.11) and $\mathbf{C}$ is a *non-autonomous* pertur-

bation,

$$\mathbf{C}(\theta,\tau) = -\gamma e^{-\tau/2}\theta_{yy} - \delta e^{-\tau}(\tau+\theta),$$

which is *exponentially small* as $\tau \to \infty$ (i.e., as $t \to T^-$) on bounded orbits. From this scaling analysis we see that $\mathbf{C}(\theta,\tau)$ is exponentially small near blow-up and we may ignore it, considering only the reduced model (1.3.7) in which all terms balance. This scaling structure is also important for the numerical methods employed in integrating the full PDE, see Section 2.2.3.

1.4 Model reduction

In many physical problems the derivation will include terms which do not govern the asymptotic dynamics of the problem due to the fact that not all terms will balance over the time period of interest. This is particularly true of models which exhibit finite-time blow-up as we have just seen for the Semenov-Rayleigh-Benard problem and is typical of many problems where the long-time (possibly rescaled) dynamics are governed only by an operator with scaling symmetry. Hence the motivation for studying canonical scaling invariant mathematical models; they capture the essential asymptotic dynamics of many physical problems. However, it is not only the equation which greatly simplifies. Because of the localization phenomena inherent in blow-up, boundary conditions are asymptotically unimportant. Thus, in this thesis we will consider primarily only the Cauchy problem with suitable decay conditions at infinity (numerically we will still need to solve an initial boundary value problem). It is the model reduction property which motivates us, in Chapter 3, to consider the general higher-order parabolic equation with a reaction term of the form $f(u) = e^u, |u|^p$ or $|u|^{p-1}u$,

$$u_t = -(-\Delta)^m u + f(u) \quad (m > 1). \tag{1.4.1}$$

1.4.1 The Cauchy problem for single point blow-up

It follows from the scaling variable y in (1.3.10) that for arbitrarily small fixed $|x| > 0$, the corresponding $|y| \to \infty$ as $\tau \to \infty$ which, in general, corresponds to formation of a *single point singularity.* Therefore, it is natural to consider the *Cauchy problem* for equation (1.3.12) with bounded initial data at $\tau = \tau_0$ given by

$$\theta_0(y) = u_0(T^{1/4}y) - \tau_0 \quad \text{in } \mathbf{R}.$$

The perturbed equation (1.3.12) suggests that we consider first the unperturbed rescaled equation

$$\theta_\tau = \mathbf{A}_1(\theta) \quad \text{in } Q_0 = \mathbf{R}\times(\tau_0,\infty), \quad \theta(y,\tau_0) = \theta_0(y) \quad \text{in } \mathbf{R}. \tag{1.4.2}$$

According to (1.3.10), $\theta(y,\tau)$ is simply the rescaled solution of (1.3.7). However only exactly (rather than asymptotically) self-similar solutions have θ independent of τ. Hence we begin with the construction of blow-up self-similar solutions of (1.3.7) of the form

$$u_*(x,t) = -\ln(T-t) + f(y), \quad y = x/(T-t)^{1/4}, \tag{1.4.3}$$

where f satisfies the following ODE:

$$\mathbf{A}_1(f) = 0 \quad \text{in } \mathbf{R}_+ \tag{1.4.4}$$

supplemented with the symmetry conditions

$$f'(0) = 0, \quad f'''(0) = 0$$

at the origin. The symmetry assumptions are quite natural in blow-up analysis for various second-order parabolic equations. As is typical for blow-up problems, for stable (generic) blow-up profiles are connected with the idea of infinite time symmetrization (as $\tau \to \infty$) in parabolic equations like (1.3.11) and (1.3.12) wherein solutions converge to symmetric profiles. We expect that these should be kept for higher-order equations, but we cannot prove that the ODE (1.4.4) does not admit suitable asymmetric profiles. We note that for the second order equations the proof of eventual symmetrization is usually proved using Alexandrov's Reflection Principle, moving plane techniques and other approaches based on the Maximum Principle, which are not available for any $m > 1$. Due to the exponential nonlinearity purely anti-symmetric solutions are not permitted by the ODE.

The ODE (1.4.4) has a two-parametric bundle of admissible profiles $f(y)$ at infinity,

$$f(y) = (-4\ln|y| + C + o(1)) + C_1\left(e^{-a_0 y^{4/3}} + o(1)\right) \quad \text{as } y \to \infty, \tag{1.4.5}$$

where $a_0 = 3/4^{4/3}$ and $C, C_1 \in \mathbf{R}$ are arbitrary parameters (see the classical asymptotic methods in Coddington and Levinson (1955) and a detailed example in Section 3.2.2). The first coefficient, C, determines the actual far field behaviour of the blow-up solution such that the limit profile $u_*(x,T^-)$ is bounded in a deleted neighbourhood of the origin ($0 \in B[u_0]$). Specifically, we have that for any $x > 0$ and any symmetric profile f, there exists a finite limit (i.e., the final-time profile)

$$\lim_{t\to T} u(x,t) = \lim_{t\to T}\left(-\ln(T-t) + f\left(\frac{x}{(T-t)^{1/4}}\right)\right) = -\ln|x| + C. \tag{1.4.6}$$

The second parameter, C_1 in (1.4.5), has no role in the leading order structure of the solution, but specifies a complicated two-dimensional topology of the ODE solutions.

Numerical approximation of the solution of (1.4.4) subject to symmetry conditions at

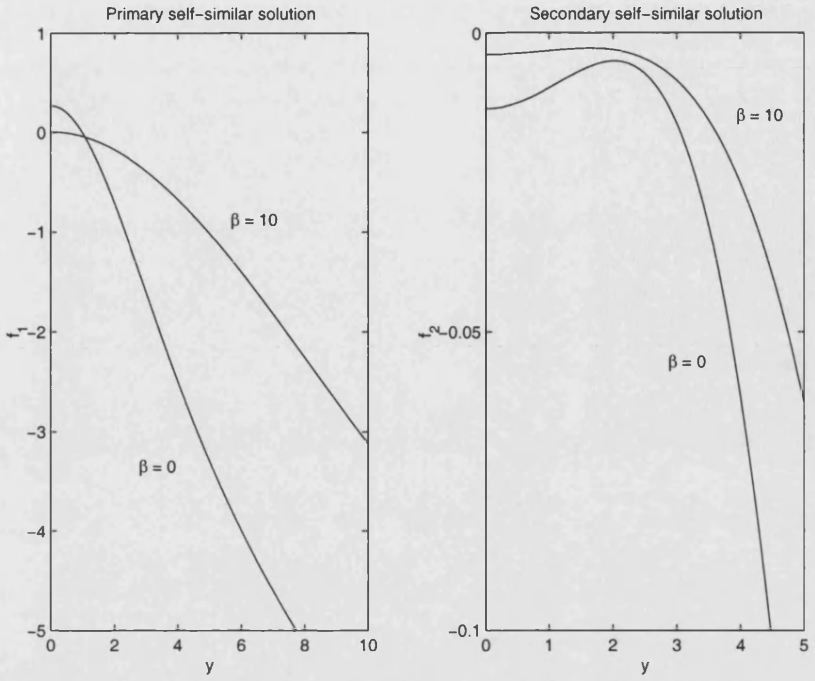

Figure 1.3: Two solutions for equation (1.4.4). The primary solution (found to be stable) has one maximum in $\mathbf{R}$ while the secondary has two.

the origin and slow growth at infinity has uncovered *two* solutions, which are presented in Figure 1.3 and the asymptotic behaviour is shown in detail in Figure 1.4.

1.5 Similarity solutions in classical heat equations with reaction

The results presented in Section 1.4.1 are at odds with what is known for both the Frank-Kamenetskii equation and the heat equation with polynomial reaction, (1.3.1). Because of their importance to many applications, canonical equations from Combustion Theory such as the non-stationary semilinear one-dimensional Frank-Kamenetskii equation, (1.1.2), and its counterpart with power nonlinearity, (1.3.1), have been well studied for the past thirty years and it is known that these both exhibit singularities in finite time. While exact self-similar solutions are known to exist for the related second-order reaction-diffusion *quasilinear* problems (see the references to Chapter 4 in Samarskii, Galaktionov, Kurdyumov and Mikhailov (1995) and Budd and Galaktionov (1998))

$$u_t = (|u_x|^\sigma u_x)_x + e^u \quad \text{or} \quad u_t = (u^\sigma u_x)_x + u^p \quad \text{with} \quad \sigma > 0, \tag{1.5.1}$$

it is somewhat paradoxical that none exist for the above semilinear problems (1.1.2) and (1.3.1). Instead the generic stable asymptotic blow-up behaviour is described by

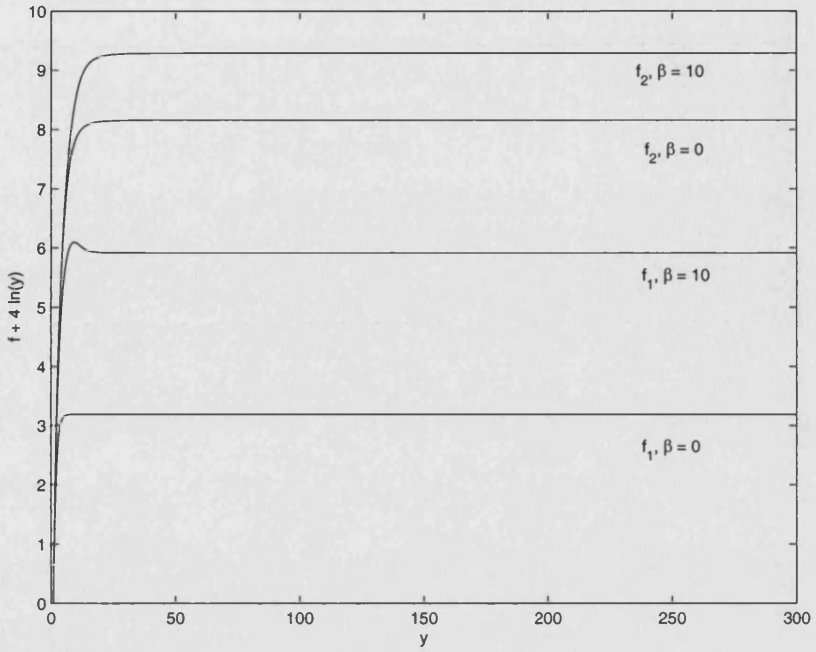

Figure 1.4: Asymptotic behaviour of solutions for equation (1.4.4) showing convergence to the behaviour described in (1.4.5).

approximate similarity solutions satisfying first-order Hamilton-Jacobi equations, see the references in the books by Bebernes and Eberly (1989) and Samarskii et al. (1995) and the surveys by Levine (1990) and Galaktionov and Vazquez (2002). For example in the quasilinear problem (1.5.1) with the power nonlinearity u^p, for any $p > 1$ and $\sigma > 0$ there exists an *exact* non-trivial self-similar solution of the form

$$u_S(x,t) = (T-t)^{-1/(p-1)} f(y), \quad y = x/(T-t)^{(p-1-\sigma)/2(p-1)}, \tag{1.5.2}$$

where T is the finite blow-up time and f is not identically constant and solves a related ODE; see Samarskii et al. (1995, Chap. 4).

In comparison, for the semilinear equation (1.3.1) looking for a similarity solution with the same structure

$$u_S(x,t) = (T-t)^{-1/(p-1)} f(y), \quad y = x/(T-t)^{1/2}$$

yields that for the corresponding ODE the only non-zero similarity profile is the trivial constant one $f \equiv \beta^\beta$, where $\beta = 1/(p-1)$. Such nonexistence results are known from the 1970's, see Hocking, Stewartson and Stuart (1972) for $p = 3$, Ad'jutov and Lepin (1984) for $p > 1$ and Giga and Kohn (1985) for the corresponding equation in $\mathbf{R}^N$ with $1 < p \le p_S = (N+2)/(N-2)_+$. This means that for a wide "dense" subset of general solutions $u(x,t)$ blowing up at $t = T$ at the origin $x = 0$, the similarity

rescaling satisfies (Galaktionov and Poshashkov 1986, Giga and Kohn 1987)

$$\theta(y,t) \equiv (T-t)^{1/(p-1)}u(x,t) \to \beta^{\beta} \quad \text{as } \tau \to T^{-}$$

uniformly on compact subsets in y. The spatial variation of the blow-up solutions can be observed on larger subsets, and the generic asymptotic behaviour is as follows:

$$u(x,t) = \left[(p-1)(T-t)(1+C_*\eta^2)\right]^{1/(p-1)}(1+o(1)) \tag{1.5.3}$$

uniformly on compact subsets in $\eta = x/[(T-t)|\ln(T-t)|]^{1/2}$, where the constant $C_* = (p-1)/4p$ does not depend on initial data (nor, in fact, on the space dimension). The non scaling-invariant "hot-spot variable" η with an extra logarithmic factor was first formally derived by Hocking et al. (1972) and was rigorously established twenty years later, see the references in the survey by Galaktionov and Vazquez (2002). The stable behaviour (1.5.3) is essentially equivalent to the fact that the ODE for the self-similar solutions, which is obtained by a symmetry reduction of the original PDE, has no solution (other than the constant one) with an appropriate decay rate at infinity. Comparing (1.5.2) and (1.5.3) shows that nonexistence of non-trivial ODE similarity profiles implies a fundamental change of the basic spatial scale of singularity formation phenomena. The observation that the blow-up behaviour of these second order problems is only approximately self-similar (in dimensions $N = 1$ and 2) with a new logarithmically perturbed backward heat kernel variable is an essential feature of many related reaction diffusion problems and the corresponding parabolic equations under consideration. Similar results are known for (1.1.2), see Bebernes and Troy (1987), Eberly (1988) and references in the book by Bebernes and Eberly (1989).

The analysis of both these problems is analagous and begins with a centre manifold expansion about a constant solution to the ODE for the similarity profile. Rigorous proof of this behaviour relies on the Maximum Principle and self-adjointness of the associated linear operators, (Giga and Kohn 1987, Filippas and Kohn 1992). Neither of these properties is available here hence the requirement for robust and reliable numerical computations and asymptotic methods. Of course, while proof of non-existence of stationary similarity profiles implies the non-existence of full similarity solutions to the PDE, existence of stationary similarity profiles does not guarantee the existence of stable, attractive similarity solutions to the full PDE. To understand the dynamics of the full PDE problem we first need very careful numerical compuations. It should be mentioned that the history of the numerical investigation of blow-up is riddled with false starts. The first numerical study of the similarity solution to (1.1.2) suggested the existence of a similarity profile while the first computations of (1.3.1) and the nonlinear Schrödinger equation in the critical dimension both suggested the wrong blow-up rates.

1.6 Geometric integration

All of the problems under consideration have a natural scaling structure and many models exhibit finite time blow-up. As a singularity forms, there is convergence to a similarity profile in rescaled co-ordinates, however, in the natural co-ordinates, changes occur on increasingly small length scales and as the time T is approached, on increasingly small timescales. Because for many of the problems we examine, the long time behaviour was not known before this work, reliable and efficient numerical methods are essential. In order to preserve and utilize the underlying scaling structure and capture any emergent scalings we have chosen to use adaptive methods from the newly developing field of geometric integration.

Classical adaptive numerical methods are designed to make decisions based on estimates of local truncation errors with no regard to global qualitative features of the system under examination. The basic philosophy of geometric integration is that the global properties of the solution such as conservation of mass or energy, or positivity of solutions are more important to the underlying problem than the local information given by the problem in terms of differentials. This philosophy, where applicable, can often generate algorithms which are more computationally efficient and robust than standard approches in that they guarantee the preservation of the key qualitative geometric features, (Hairer, Lubich and Wanner 2002).

Given that we expect scale-invariant solutions to be attractors of most initial data it is natural to consider methods which are also scale-invariant under the same transformations. Note that we are not enforcing similarity or a particular solution structure. Also for one of the problems we will need to ensure conservation of mass.

The key to the methods we use is to introduce a co-ordinate transformation from a computational variable ξ to the physical variable x, governed by a monitor function $M(x) > 0$ such that the *moving* grid, $x(\xi, t)$, affords the same scaling transformation as the full PDE being solved on that grid. This means that in the presence of (asymptotically) self-similar behaviour computational nodes can move on the level sets of the (emerging) similarity variable. We now give an example of this in practice but delay a detailed discussion until Section 2.2.

1.6.1 Numerical solution to the SRB-problem

Knowing that solutions to (1.1.1) with suitable initial data will exhibit finite time blow-up, we need a numerical method which is adaptive in both space and time. We will also use a method which inherits any emergent scalings in the PDE but does not assume or enforce any particular solution structure. In Figure 1.5 we see the rescaled solutions converging as the blow-up time is approached. Recall from the rescaling (1.3.9) that this corresponds to localization at the origin. We are able to approximate

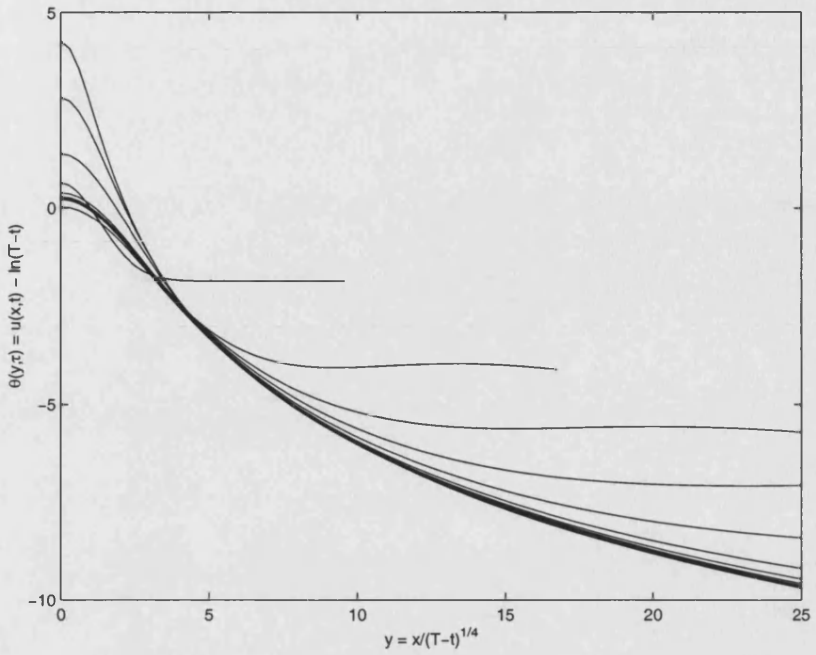

Figure 1.5: Convergence of rescaled solutions to (1.1.1) to the similarity profile (1.4.4). These are the rescaled profiles seen in Figure 1.2 .

this solution very well because the mesh points are also converging to the origin at the appropriate rate, as is seen in Figure 1.6. Notice in this Figure that, close to the origin (the blow-up point), the mesh trajectories lie essentially on level sets of the similarity variable. Because we have a fixed number of points there is some drift due to boundary effects. The PDE profiles in Figure 1.5 are converging to the solution of (1.4.4) displayed in Figure 1.3. Because the blow-up time T is not known a-priori we cannot immediately compare the solutions to the expected asymptotic profiles. To reconstruct the convergence onto the self-similar solution from time integrations of the PDE (1.1.1) we rescale under (1.3.10) in the following way. At each time t we define $\lambda = \exp(u(0,t))$ and set

$$\theta(y,\tau) = -\ln\lambda + u(x\lambda^{1/4}, t), \quad \text{where } \tau = 1/\lambda.$$

Figure 1.5 presents a typical example of convergence of the rescaled solution $\theta(y,\tau)$ (shown with solid lines) to the first similarity profile $f_1(y)$ (shown with a dashed line [hidden below the rescaled PDE solutions]). Under this rescaling the profiles are defined on ever larger ranges of $y = x/(T-t)^{1/4}$ as is seen in Figure 1.6. In this figure, we see constant motion of some mesh lines in y which corresponds to clustering in the physical variable x.

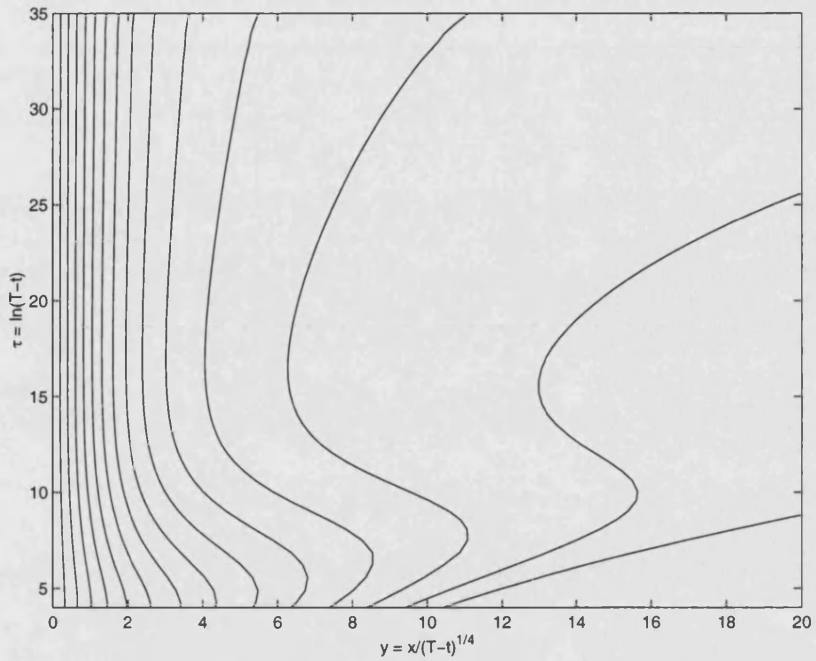

Figure 1.6: Scale-invariant mesh trajectories. This is the mesh for the solution to (1.1.1) as seen in Figures 1.2 and 1.5.

1.7 Organization of the thesis

Numerical solutions complement all the analysis in this thesis and in some cases have even directed it. As such we first describe the numerical methods used, both the general philosophy of scale-invariant adaptivity and the practical implementation of the moving collocation method used for most of the computations discussed herein are described in Chapter 2.

In Chapter 3 we present one of the most significant contributions of this thesis by describing the existence of self-similar solutions for two canonical semilinear equations of arbitrary order. By careful examination of an associated linear operator we establish that there exist at least $2\lfloor m/2 \rfloor$ ($\lfloor x \rfloor$ is the integer part of x) non-trivial self-similar solutions to semilinear equations of the form

$$u_t = -(-\Delta)^m u + f(u) \qquad \text{where } f(u) = e^u \text{ or } |u|^{p-1}u \ (p > 1). \tag{1.7.1}$$

This is in stark contrast to the second-order equivalent of this problem. The asymptotic calculations are supported with numerical evidence. We also make detailed calculations regarding the spectrum of solutions to the Semenov-Rayleigh-Benard problem (1.1.1) constructing both nonlinear and linear patterns.

In Chapter 4 we continue the study of semilinear equations by analyzing the higher

order *absorption* problem

$$u_t = -(-\Delta)^m u - |u|^{p-1}u \qquad (m > 1, p > 1) \tag{1.7.2}$$

wherein the dynamics are governed by, should they exist, the so-called *very singular solutions* (VSS) of the form

$$u(x,t) = t^{-1/p-1}V(y), \quad y = x/t^{1/4}, \quad V(y) \to 0 \text{ exponentially fast as } y \to \infty.$$

As opposed to solutions to (1.7.1) which can blow-up in finite-time, solutions to (1.7.2) decay in infinite time. While the theory for the heat equation with absorption

$$u_t = \Delta u - u^p \qquad (u \geq 0)$$

is essentially complete from the 1980's, the lack of the Maximum Principle or a gradient structure for the corresponding rescaled equation to (1.7.2) means that the theory of asymptotic solutions to such higher-order problems is open. In Chapter 4 we use a combination of asymptotics and analysis to construct a countable spectrum of radially symmetric VSSs for general order of the derivative $2m$ and spatial dimension N. Because of the more mathematically tractable nature of the absorption problem in this Chapter we are able to rigorously prove the existence of solutions (in a particular limit), rather than simply construct them asymptotically.

In Chapter 5 we consider the conservative divergent fourth-order equation

$$u_t = -\Delta(\Delta u + |u|^{p-1}u) \qquad (p > 1) \tag{1.7.3}$$

paying particular attention to the *critical* exponent $p = 3$ (for $N = 1$) for which the similarity solutions are conservative. This is the limit case of the 'unstable' Cahn-Hilliard equation from phase transitions, which belongs to a class of pseudo-parabolic equations with well-known local properties. In Novick-Cohen (1992) and Bernoff and Bertozzi (1995) the authors analyzed a particular case, a model from solidification theory,

$$u_t = -\Delta(\Delta u + u^2) \qquad x \in \mathbf{R} \text{ or } \mathbf{R}^2.$$

In Chapter 5 we show that in general, for all $p > 1$, solutions may either blow-up in finite time or decay in infinite time (essentially, there is no critical Fujita exponent) and that in all cases, regardless of conservation, the dynamics are governed by similarity solutions. The general equation (1.7.3) is of interest not only because of physical applications but because it represents an 'intermediate' equation with connections to both the second-order problem (1.3.1) and the higher-order model (1.7.1).

1.7.1 Underlying themes

The key structural features linking all of these PDEs are the same, as are the mathematical tools for understanding them and the numerical methods for approximating them. We use a dynamical framework wherein the asymptotic behaviour (as $t \to T^-$ or $t \to \infty$) of all these problems approaches similarity solutions of rescaled problems. The solutions of these rescaled PDE problems are first understood by examining the associated ODE problems describing the profiles of exact similarity solutions. We construct spectra of both nonlinear and linear patterns through a combination of bifurcation and branching theory and parameter continuation in the underlying linear equations. From this recurring base we then analyze each problem as appropriate. Similarity solutions to equations of the from (1.7.1) are constructed using matched asymptotic expansions. Rigorous results from bifurcation theory are used to prove existence of VSSs to (1.7.2). Existence of solutions to (1.7.3) is proven via a shooting argument and blow-up profiles are constructed with a singular perturbation expansion. In all cases numerical experiments are key and so we begin by describing the numerical methods developed to study all the PDE problems mentioned thus far.

Chapter 2

MovCol4: A high resolution moving collocation scheme for evolutionary partial differential equations

2.1 Introduction

In each of the problems examined in this thesis, important structures occur at scales which change over the duration of the time-period of interest, and could even move. That is, no one computational grid will be appropriate at all times of interest. Many approaches have been brought to bear on the approximation of such problems numerically. For instance, Berger and Kohn (1988), Bernoff and Bertozzi (1995), Budd, Huang and Russell (1996), Sulem and Sulem (1999), Stockie, MacKenzie and Russell (2000) and Beckett, Mackenzie, Ramage and Sloan (2001) all have features in common with the one-dimensional approach implemented here. Our approach is based primarily on the work of Huang, Ren and Russell (1994a) and (1994b) and Huang and Russell (1996) and (1997). In the context of finite elements or finite differences, the most common approaches are static regridding (h-refinement) or moving meshes (r-refinement). The method of h-refinement is most commonly associated with a-posteriori error methods. These methods are applicable to a wide class of problems, but we do not believe them to be appropriate here because of the nature of blow-up problems. All a-posteriori methods will be plagued by the fact that any arbitrarily small error in time at any stage in the calculation will lead to an arbitrarily large error near the blow-up time. A proper a-posteriori method will recognize this error and try to correct for it by reducing the stepsize and refining the grid. The main problem is that a-posteriori methods will try and find a solution with precisely the same blow-up time as the exact solution

without recognizing that such errors are not important. Instead we consider moving mesh methods and in particular we consider an approach from the emerging field of geometric integration: scale-invariant moving mesh methods. In this approach no extraordinary effort to control the temporal error is made and thus there may be large errors in time compared to the exact solution. However, what really matters is the solution in the rescaled co-ordinates (displaying the key geometric features) and this should be excellent. This may at first seem odd, but shift errors in the prediction of the blow-up time are scaled out when solutions are examined in the similarity variables.

In this Chapter we describe the construction and implementation of the extension of a known method to fourth-order evolutionary PDEs. We also extend the error analysis in Huang and Russell (1996) from the discrete collocation points to all points in the interval of approximation. Lastly, we further the understanding of the advantages of the *conservative* collocation scheme introduced by Huang and Russell (1996) for problems on moving grids which may not have any inherent conservation structure.

Some of the contents of this chapter will appear in the paper 'MovCol4: A high resolution moving collocation scheme for evolutionary partial differential equations', (2003) in collaboration with X. Xu and R. Russell. Three codes which implement the method described in this Chapter have been written. The first two, of which I am the sole author, are based in Matlab; one uses DDASSL, (Brenan, Campbell and Petzold 1996), for the time integration via a MEX interface, the other uses the Matlab routine `ode15i.m`. The final implementation is a port of the Matlab code to Fortran77 merged with an existing code by Huang and Russell (1996) performed in collaboration with X. Xu and R. D. Russell.

2.2 Scale invariant adaptivity for partial differential equations in one space dimension

In order to utilize the scaling structure of the PDEs under consideration we are interested in numerical methods which adapt to qualitative changes of the solution determined by the symmetry properties of that solution.

2.2.1 Equidistribution and optimal meshes

Associated with the approximation of any infinite dimensional problem by a finite dimensional one is the notion of discretization error. When constructing error estimates based on finite difference or finite element methods, one often produces bounds based on a high derivative of the exact solution. It seems perfectly natural that the way to minimize the total error would be to commit the same error in each computational cell, or *equidistribute*, (de Boor 1973), the error and, in fact, it is optimal, as we show

below. If we define a *computational* variable ξ and a monitor function $M(x) > 0$, then, by definition, the equidistributed mapping satisifies

$$\int_0^{x(\xi)} M(s)ds = \xi \int_0^1 M(s)ds. \tag{2.2.1}$$

Differentiating with respect to ξ gives the differential form of the equidistribution principle

$$Mx_\xi = 1 \tag{2.2.2}$$

for a suitably normailized monitor function M ($\int M = 1$). Note that this is a mapping with a specified Jacobian.

As a motivation for the use of a general equidistribution principle, we will now show that equidistributed grids are optimal (with regard to errors) if the monitor function is suitably chosen.

For an arbitrary indicator function $Q(x)$ and a positive scalar α suppose that we define

$$L = x_\xi^\alpha Q(x). \tag{2.2.3}$$

For instance, the L^2 and H^1 errors of a second-order approximation to $u(x)$ on a uniform grid in ξ are both given by

$$E = (\Delta\xi)^{\alpha-1} \int_0^1 L dx$$

with $\alpha = 5$ and 3 respectively and $Q(x) = |u''(x)|^2$.

Lemma 2.2.1. *Equidistribution of errors produces optimal meshes.*

Proof. To find the optimal mesh we use the calculus of variations. The Euler-Lagrange equation associated to (2.2.3) satisfies

$$\frac{d}{d\xi}\left(\frac{\partial L}{\partial x_\xi}\right) - \frac{\partial L}{\partial x} = 0.$$

Expanding directly, we have

$$\alpha x_\xi^{\alpha-1} Q_\xi + \alpha(\alpha-1)x_\xi^{\alpha-2} x_{\xi\xi} Q - Q_\xi \xi_x x_\xi^\alpha = 0,$$

or $\alpha x_\xi^{\alpha-2} x_{\xi\xi} Q + x_\xi^{\alpha-1} Q_\xi = 0$. Multiplying by x_ξ and integrating yields $x_\xi^\alpha Q =$ constant, hence , $Mx_\xi = 1$ for appropriate M. □

This result recovers the optimal mesh results of Carey and Dinh (1985) for finite difference methods applied to second-order boundary value problems but in this form is

originally due to deBoor [1].

Solving (2.2.2) directly in concert with a PDE leads to a highly coupled nonlinear Differential Algebraic Equation with fully half of the variables being algebraic. To avoid this very difficult numerical problem various regularizations have been proposed. These are the so-called Moving Mesh PDEs (MMPDEs). Most importantly, the MMPDEs offer *stabilization*, (Huang, Ren and Russell 1994b), as (2.2.2) is only neutrally stable in time meaning that small errors can accumulate in time.

2.2.2 Moving mesh PDEs

If we begin with the equidistribution principle in integral form, (2.2.1), and consider a mapping in both time and computational space, $x(\xi, t)$, we can write down an evolutionary equation for the mesh:

$$\tau x_t = -\left(\int_0^{x(\xi,t)} M(s)ds - \xi \int_0^1 M(s)ds \right).$$

(The sign indicates that the node concentration will increase in under-equidistributed regions.) Differentiating twice with respect to ξ recovers MMPDE6 (Huang et al. 1994b)

$$x_{t\xi\xi} = -\frac{1}{\tau}(Mx_\xi)_\xi. \tag{2.2.4}$$

The positive parameter $\tau \ll 1$ is the relaxation time and defines the time-scale over which a mesh converges to steady-state (2.2.2). Another common MMPDE is MMPDE4

$$(Mx_{t\xi})_\xi = -\frac{1}{\tau}(Mx_\xi)_\xi \tag{2.2.5}$$

which, for reasons of scaling, we will not use. From Huang et al. (1994b) we also have that, when solved exactly, neither MMPDE6 nor MMPDE4 produce mesh crossings. That is, the mapping is well defined for all time.

The key to a succesful MMPDE method is the proper choice of the monitor function. Methods based on error control have been used by Beckett et al. (2001), while monitor functions to cluster nodes based on qualitative solution properties have been used by Budd et al. (1996), Stockie et al. (2000) and Mackenzie and Robertson (2002) amongst others while Guerra, Peletier and Williams (2003) use both. Because we are interested in the scaling properties of our PDEs, we will concentrate on monitor functions which also make (2.2.4) invariant under the same scale transformation as the physical PDE.

[1] R.D. Russell, private communication 2003

2.2.3 Scale-invariant monitor functions

Because our PDEs are governed (at least asymptotically) by scale-invariant operators we will use methods which preserve the geometric structure of the dynamics. To do this we use not the error as the monitor function but rather a function of the solution chosen so as to preserve the scaling of the underlying system and cluster mesh points in the regions they will be required as the solution evolves in a possibly unknown manner. It is for this reason that we have chosen to use MMPDE6 rather than MMPDE4. For example, consider a general PDE invariant under the scaling

$$t \mapsto \lambda t, \qquad x \mapsto \lambda^{\alpha} x, \qquad u \mapsto \lambda^{\beta} u, \qquad \lambda > 0, \tag{2.2.6}$$

and a monitor function of the general form

$$M = M(x, u, u_x, u_{xx}).$$

Then, for MMPDE6 to also be invariant under (2.2.6), we require

$$M(\lambda^{\alpha} x, \lambda^{\beta} u, \lambda^{\beta-\alpha} u_x, \lambda^{\beta-2\alpha} u_{xx}) = \lambda^{-1} M(x, u, u_x, u_{xx}). \tag{2.2.7}$$

Given this, the complete system of the physical PDE and the moving mesh PDE are invariant under the same transformation, the transformation which governs the key underlying dynamics of the PDE. For blow-up problems, this also suggests a uniform relative error estimate. Defining the relative local truncation error estimate as

$$R = \frac{\text{LTE}}{|u|}, \tag{2.2.8}$$

we have the following observation for blow-up problems understood in a natural sense.

Proposition 2.2.2. *Given a scale-invariant monitor function M, and a discretization whose local truncation error is of the form*

$$LTE = Ch^p |u^p|,$$

the relative local truncation error is asymptotically uniform in the blow-up region.

Proof. Given that $h \simeq x_\xi$ scales as x, $x_\xi \mapsto \lambda^{\alpha} x_\xi$ and that near blow-up solutions are asymptotically rescaled stationary profiles with $\lambda = \lambda(t)$, we have

$$\text{RLTE} = \frac{h^p |u^p|}{|u|} \simeq \frac{\lambda^{p\alpha} (x_\xi)^p \lambda^{\beta - p\alpha} |f_s^{(p)}|}{\lambda^{\beta} |f_s|} = (x_\xi)^p \frac{|f_s^{(p)}|}{|f_s|} \tag{2.2.9}$$

for some reference similarity profile f_s. □

This property was seen in Figure 1.6 where the inner portion of the blow-up solution is resolved on a mesh which follows the level sets of the similarity variable y.

2.2.4 Scale-invariant semi-discretizations

The strategy described in this Chapter uses the semi-discretization based *method of lines* wherein a spatial discretization is introduced and then the coefficients defining this discretization are integrated forward in time. This approach has the advantage that existing robust adaptive ODE codes, eg DDASSL, (Brenan et al. 1996) can be used for this aspect of the problem. We denote $U_i(t)$ as the approximation to $u(x,t)$ at the mesh point $X_i(t),t)$, hence $U_i(t) \simeq u(X_i(t),t)$.

Given that the approximation $(U_i(t), X_i(t), t)$ is the solution of our semi-discrete ODE system, we have that the semi-discretization is scale-invariant if (in the absence of boundary conditions) the set of points

$$(\lambda^a U_i(t), \lambda^\beta X_i(t), \lambda t)$$

is also a solution of the semi-discrete system.

Our approach is scale-invariant *in space* because we are using scale-invariant monitor functions and from the fact that scaling and discretization commute. This means that our method *admits* scale-invariant similarity solutions should they emerge. However, this approach is not scale-invariant in time. To make it so we would need to introduce a transformation in time that would depend on the solution in such a way that the present algorithm would be insufficient. As a trade-off between complete scale-invariance and a simple and flexible code we have chosen to use a standard time-discretization of a spatially scale-invariant method.

In Budd and Piggott (2001) it is shown that scale-invariant methods for ODEs can generate uniform errror estimates, even in the case of singularities. Unfortunately this is not the the case for PDEs. The above estimate (2.2.9) holds only for $h \ll 1$. Clearly as mesh points concentrate in one region the remainder of the interval loses points. There are two possible remedies for this, one to compute on an ever shrinking domain as in the dynamic resaling method for the nonlinear Schrödinger equation, (Sulem and Sulem 1999). The other to construct an (hr)-method and add nodes as required. Both these approaches require an adhoc extension to the general method presented here which would vary from problem to problem. Due to the large number of problems considered in this thesis we have chosen to construct only one algorithm which is as flexible as possible.

Our approach differs from one of the earliest adaptive numerical methods for blow-up problems due to Berger and Kohn (1988) in that they required knowledge of the structure of the particular solution being approximated. Bernoff and Bertozzi (1995)

performed adaptivity based on scaling, but used a static approach. We will discuss a static regridding routine based, like theirs, on scale-invariance in Section 2.7.1. While our method makes no direct effort to predict the blow-up time exactly (as an a-posteriori method would), the solution in the rescaled co-ordinates should be very good, as demonstrated in Chapter 1.

2.3 Adaptive methods for higher-order problems

Once decided on the continuous form our method will take we need next to choose upon a discretization. Because we are solving high-order problems on a non-uniform grid, a compact scheme is preferable to a wide finite-difference scheme. A scheme with a wide stencil will have errors which are dependent on the local mesh regularity over the width of the stencil. This can lead to the difficulties described in Saucez, Wouwer, Schiesser and Zegeling (2001), where large numbers of nodes (as many as 1000) were required to solve the problems

$$u_t + (u^m)_{xx} + (u^n)_{xxx} = 0,$$
$$u_{tt} - u_{xx} + u_{xxxx} + (u^2)_{xx} = 0,$$
$$u_t + 10uu_{xxx} + 25u_xu_{xx} + 20u^2u_x + u_{xxxxx} = 0.$$

They used finite differences and the same adaptive strategy we do and found that great care needed to be taken to reliably approximate the high-derivatives on a non-uniform grid. In this thesis we are also interested in solving a broad class of problems and thus would like a method which can easily be modified with the least possible effort to solve many different problems.

A natural choice satisfying these requirements is collocation. This discretization, combined with the MMPDE (as described in Section 2.2.2) approach to adaptivity, has already been demonstrated to work for second-order problems by Huang and Russell (1996). Our objective in this Chapter is to develop a method which is an extension of their approach to fourth-order problems. Their original motivation was to create a scheme which was flexible and robust for a variety of parabolic problems on both static and moving grids, hence a collocation scheme and the moving mesh adaptive procedure (Huang et al. 1994b, Huang et al. 1994a, Huang and Russell 1997). This method has been used succesfully to compute solutions to second-order problems with finite time blow-up by Budd, Chen and Russell (1999), Budd, Rottschäffer and Williams (2003) and Guerra et al. (2003) amongst others. We now show how this method extends to higher-order problems in the most efficient way. In fact many of the strengths of the coupling of these two ideas, collocation and MMPDEs, are greatly enhanced for higher-order problems as we shall describe below. An additional reason to use collocation is that our problems may have boundary conditions depending (possibly nonlinearly)

on as high as the third derivative. Such conditions are easily and reliably met with collocation but this is generally not true for a finite difference scheme.

Although at present we are only interested in problems of the form

$$\begin{aligned} &u_t = f(t, x, u.u_x, u_{xxx}, u_{xxxx}) \quad \text{for } t > 0, x \in I \equiv (a, b), \\ &u(x, 0) = u_0(x), \\ &0 = g_{a1}(a, t, u(a), ..., u_{xxx}(a)),\ 0 = g_{a2}(a, t, u(a), ..., u_{xxx}(a)), \\ &0 = g_{b1}(b, t, u(b), ..., u_{xxx}(b)),\ 0 = g_{b2}(b, t, u(b), ..., u_{xxx}(b)), \end{aligned} \tag{2.3.1}$$

the scheme described in this chapter is valid for systems of such equations which also depend nonlinearly on $\boldsymbol{u_t}$ and its first three spatial derivatives.

We begin by collecting the required background material to describe the collocation scheme and to be able to establish error estimates for the non-standard *conservative* discretization used for the physical PDEs. This material all relates to ODEs because we are using the method of lines. Although we are primarily interested in fourth-order (in space) problems, we consider the general case of m-th-order problems first. With a basic understanding of the coupling between the non-uniform grid and the collocation scheme the advantages of this approach over finite differences is made apparent. We conclude by discussing a sequence of test problems to highlight the features and advantages of our approach.

In the remainder of this Chapter the capital letters U and X will be used to refer to the numerical approximations to the dependent continuous variables u and x respectively. The independent variables are the time t and the computational spatial variable ξ.

2.4 Mathematical background

A collocation method is a Petrov-Galerkin discretization where the test functions are Dirac-δ functions, (Bulirsch and Stoer 1980). One can also consider it as an implicit Runge-Kutta finite difference formulation (Ascher, Mattheij and Russell 1988). Consider first a nonlinear ordinary differential equation of the form

$$N(u(x), x) \equiv u^{(m)} + f(x, u, u', ..., u^{(m-1)}) = 0 \qquad \forall x \in I = (a, b), \tag{2.4.1}$$

and boundary conditions

$$\boldsymbol{g}_a(a, u(a), u'(a), ..., u^{(m-1)}(a)) = \mathbf{0}, \quad \boldsymbol{g}_b(b, u(b), u'(b), ..., u^{(m-1)}(b)) = \mathbf{0},$$

where $g_a : R^{m+1} \to R^{n_a}$, $g_b : R^{m+1} \to R^{n_b}$ and $n_a + n_b = m$. We represent the approximation $U(x)$ to the function $u(x)$ as a linear combination of basis functions

$$U(x) = \sum_j \phi_j(x)$$

and determine the parameters specifying the basis functions by enforcing

$$N(U(x_i)) = 0 \tag{2.4.2}$$

at each collocation node x_i. In the particular case of a piecewise polynomial representation we have that

$$U(x) = \sum_{i=1}^{n-1} \phi_i(x)\chi_{I_i},$$

where χ_{I_i} is the indicator function on the interval $I_i = [x_i, x_{i+1}]$ and $\phi_i(x)$ is an interpolating polynomial over that interval. First, we describe classical interpolation which is at the heart of our basis functions. The choice of collocation nodes is related to optimal quadrature. Although standard, we now collect all the required details to construct and analyze our method, see also Ascher et al. (1988, Sections 2.6, 5.4 and 5.6) or Bulirsch and Stoer (1980).

2.4.1 Interpolation

Given $n + 1$ distinct data points $\{x_i\}$, Lagrange interpolation, (Ascher et al. 1988), defines the unique polynomial $L_n(x)$ of a function $y = f(x)$ based on pairs (x_i, y_i) such that for all $i = 0, ..., n$, $L(x_i) = f(x_i)$, whence,

$$L_n(x) = \sum_{i=0}^{n} y_i \tilde{L}_i(x), \quad \text{where } \tilde{L}_i(x) = \prod_{\substack{j=0 \\ j \neq i}}^{n} \frac{x - x_j}{x_i - x_j} \quad i = 0, ..., n\,. \tag{2.4.3}$$

The error associated with (2.4.3) is

$$E(x) \equiv f(x) - L_n(x) = \frac{f^{(n+1)}(\zeta)}{(n+1)!} \prod_{i=0}^{n} (x - x_i), \tag{2.4.4}$$

with $\zeta = \zeta(x) \in I$.

With uniform subdivision this problem quickly becomes ill-conditioned as n becomes large. Also, for many of the problems under consideration, the exact (possibly weak) solutions have derivatives which become successively larger as n increases and hence this error estimate could become increasingly worse. To avoid the ill-conditioning of approximation with high-order polynomials, one typically uses *piece-wise* polynomials, see Figure 2.1, in which the interval I is partitioned $I = \sum I_i$ with $I_i = (x_i, x_{i+1})$

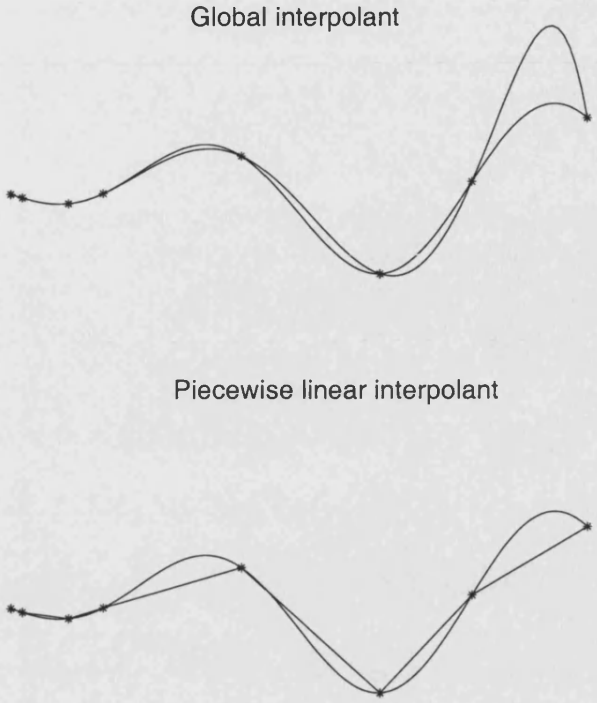

Figure 2.1: Lagrangian interpolation

and a polynomial interpolant is fit on each sub-interval with some matching conditions across the interval endpoints $\{x_i\}$. For the case of Lagrange interpolation with the subintervals defined by the nodes $\{x_i\}$ this defines a piece-wise linear interpolant,

$$L_i(x) = \frac{(x_{i+1} - x)}{(x_{i+1} - x_i)} y_i + \frac{(x - x_i)}{(x_{i+1} - x_i)} y_{i+1}, \quad x_i \leq x \leq x_{i+1}\,.$$

Because we are interested in fourth-order problems a piece-wise linear representation is insufficient. Instead we will use Hermite interpolation which is a generalization of Lagrange interpolation to the case where the derivatives of f are also known at the nodes $\{x_i\}$. Let us suppose then that the given data are

$$\{x_i, f^{(k)}(x_i)\} \quad \text{with } i = 0, ..., n \text{ and } k = 0, ..., m_i,$$

at distinct nodes. Defining $N = \sum_{i=0}^{n}(m_i + 1)$ it can be shown, (Ascher et al. 1988), that there exists a unique polynomial H_{N-1} satisfying

$$H_{N-1}^{(k)}(x_i) = y_i^{(k)}, \quad \text{for } i = 0, ..., n \text{ and } k = 0, ..., m_i.$$

H_{N-1} is called the Hermite interpolation polynomial and takes the form

$$H_{N-1}(x) = \sum_{i=0}^{n} \sum_{k=0}^{m_i} y_i^{(k)} L_{ik}(x), \tag{2.4.5}$$

where $y_i^{(k)} = f^{(k)}(x_i)$ for $i = 0, ..., n$, $k = 0, ..., m_i$.

The functions L_{ik} satisfy the relations

$$\frac{d^p}{dx^p} L_{ik}(x_j) = \begin{cases} 1 & \text{if } i = j \text{ and } k = p, \\ 0 & \text{otherwise,} \end{cases} \tag{2.4.6}$$

and are constructed recursively

$$L_{ij}(x) = l_{ij}(x) - \sum_{k=j+1}^{m_i} l_{ij}^{(k)}(x_i) L_{ik}(x), \qquad j = m_i - 1, m_i - 2, ..., 0, \tag{2.4.7}$$

where the polynomials l_{ij} are defined as

$$l_{ij}(x) = \frac{(x - x_i)^j}{j!} \prod_{\substack{k=0 \\ k \neq i}}^{n} \left(\frac{x - x_k}{x_i - x_k} \right)^{m_k + 1}, \quad i = 0, ..., n, j = 0, ..., m_i,$$

and $L_{im_i}(x) = l_{im_i}(x)$ for $i = 0, ..., n$. In each sub-interval I_i, H_{N-1} satisfies the following error estimate:

$$f(x) - H_{N-1}(x) = \frac{f^{(N)}(\zeta)}{N!} \prod_{i=0}^{n} \prod_{k=0}^{m_i} (x - x_i) \quad \forall x \in I_i, \text{ for some } \zeta(x) \in I_i.$$

To combine the ideas of collocation with Hermite (and Lagrange, see Section 2.7) interpolation we divide our interval I into cells defined by the nodes $\{x_i\}$ and construct an interpolating polynomial over each cell corresponding to the function value and its three derivatives at each node. In each cell, I_i, we pose a solution representation of the form

$$U_i(x) = \sum_{j=0}^{1} \sum_{k=0}^{3} y_j^k L_{jk} \; x \in I_i.$$

This gives us a function which is $C^\infty(I_i)$ and $C^3(I)$, and the error estimate for this representation takes the form

$$f(x) - U_i(x) = \frac{f^{(8)}(\zeta)}{8!} (x - x_i)^4 (x - x_{i+1})^4, \quad x, \zeta(x) \in I_i. \tag{2.4.8}$$

Note that this defines the lowest order polynomial which has a continuous third derivative on all I. One might expect that the high-derivative in the error term would suggest

we use a lower order method for problems such as ours which exhibit finite-time singularities, and hence increasingly large derivatives. However, because of the adaptive method we are using the solutions are relatively smooth in the computational variable and this is not the dominant issue when the mesh is suitably chosen. In fact, as seen in Section 2.2.2 the relative error is essentially constant near a singularity throughout the time-interval of integration.

2.4.2 Collocation, implicit Runge-Kutta methods and optimal quadrature

Collocation can be thought of as a Petrov-Galerkin method, (Bulirsch and Stoer 1980), in the sense that the basis functions are determined by setting

$$\langle N(U(x)), \delta_{x_i} \rangle = 0 \text{ for all } i.$$

However, this does not give any insight into an appropriate choice of the collocation nodes, $\{x_i\}$. For the special case of first-order problems, the connection between collocation and implicit Runge-Kutta methods makes the choice evident.

Consider the first-order problem, $y' = f(x, y)$. A $k-$stage Runge-Kutta method is defined by

$$y_{i+1} = y_i + h_i \sum_{j=1}^{k} \beta_j f_{ij}, \qquad 1 \leq i \leq N, \tag{2.4.9}$$

where

$$f_{ij} = f\left(x_{ij}, y_i + \sum_{l=1}^{k} \alpha_{jl} f_{jl} \right) .$$

The points $x_{ij} = x_i + h_i \rho_j$ are scaled translations of the canonical points $\{\rho_j\}$ which satisfy

$$0 \leq \rho_1 < \rho_2 < \ldots < \rho_k \leq 1 .$$

From (2.4.3) the Lagrange interpolant to $f(x, y)$ satisfies

$$y'(x) = \sum_i \sum_{l=1}^{k} y'(x_{il}) \tilde{L}_l \left(\frac{x - x_i}{h_i} \right) + E(x). \tag{2.4.10}$$

To see that this defines a Runge-Kutta method, observe that integrating (2.4.10) recovers (2.4.9) with the coefficients defined as

$$\beta_j = \int_0^1 \tilde{L}_j(t) dt, \quad \alpha_{jl} = \int_0^{\rho_j} \tilde{L}_l(t) dt .$$

The choice for the canonical points $\{\rho_j\}$ is now clear from the theory of optimal quadra-

ture, (Ascher et al. 1988). For the case

$$0 < \rho_1 < \rho_2 < \ldots < \rho_k < 1,$$

the error $E(x)$ is minimized, in the sense of being of highest order in the interval length, by taking the Gauss points, whereas

$$0 = \rho_1 < \rho_2 < \ldots < \rho_k = 1,$$

specifies the Lobatto points. Both of these sets of points are determined by the zeros of certain orthogonal polynomials. For the Gauss points the j-th (of k) canonical point is the j-th zero of the Legendre polynomial

$$P_k = \frac{1}{k!}\frac{d^k}{ds^k}\left(s(s-1)\right)^k. \tag{2.4.11}$$

In the case of the Lobatto points, ρ_j is the $(j-1)$st zero of $P'_{k-1}(s), 2 \leq j \leq k-1$ with P_{k-1} again defined by (2.4.11). The first Gauss method is the mid-point rule with $\rho_1 = 1/2$ whereas the first Lobatto method is the trapezoidal method, $\rho_1 = 0, \rho_2 = 1$. A sketch of the Hermite interpolant to a given function and the interior collocation nodes is given in Figure 2.2.

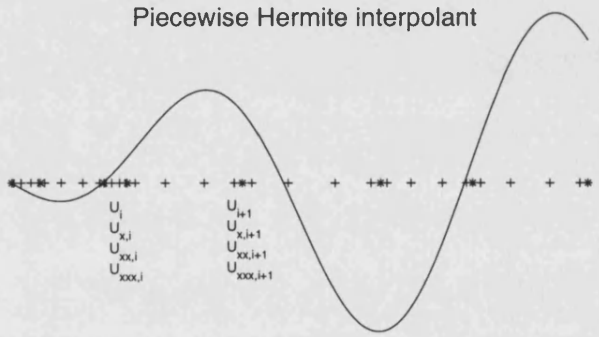

Figure 2.2: Hermite interpolation. The interval endpoints are indicated by $'*'$ while the collocation points (see (2.7.4) are marked by $'+'$.

To see that this formulation also defines a collocation method in the sense of (2.4.2), we observe that by construction (2.4.10) is exact at the points $\{x_{ij}\}$, thus satisfying (2.4.2). Clearly this is an implicit method as the function $f(x, y)$ depends on y at each collocation point in the interval. Normally when solving initial value problems one attempts to avoid implicit methods because they are much more difficult to solve. We are solving nonlinear boundary value problems thus explicit methods are unavailable and symmetric methods which have no preferred direction are more suitable.

For the more general case of higher-order problems, such as those that we are interested in, one can prove similar results, again using properties of orthogonal polynomials, see

for instance, Ascher et al. (1988, Theorems 5.142 and 5.147), from which we have paraphrased the following theorem.

Theorem 2.4.1. *Let $u(x)$ be an isolated solution to (2.4.1) where f, g_a and g_b have continuous second partial derivatives and that the k canonical points, $\{\rho_l\}$, satisfy the orthogonality conditions*

$$\int_0^1 \phi(t) \prod_{l=1}^{k} (t - \rho_l) dt = 0 \tag{2.4.12}$$

for all polynomials $\phi(s)$ of order $p-k$, $\phi = \sum_{j=0}^{p-k-1} c_j s^j$. Then, the collocation approximation $U(x)$ satisfies

$$|u^{(j)}(x) - U^{(j)}(x)| = \mathcal{O}(h_i^{k+m-j}) + \mathcal{O}(h^p), \quad 0 \le j \le m-1,\ 1 \le i \le N, \tag{2.4.13}$$

being superconvergent at the mesh points,

$$|u^{(j)}(x_i) - U^{(j)}(x_i)| = \mathcal{O}(h^p), \quad 0 \le j \le m-1,\ 1 \le i \le N, \tag{2.4.14}$$

with $h = \max_i h_i$, and, given that $p > k + m$,

$$\begin{aligned} u^{(j)}(x) - U^{(j)}(x) = {} & h_i^{k+m-j} u^{(k+m)}(x_i) P^{(j)}\left(\frac{x - x_i}{h_i}\right) \\ & + \mathcal{O}(h_i^{k+m-j+1}) + \mathcal{O}(h^p), \qquad x_i \le x \le x_{i+1}, \end{aligned} \tag{2.4.15}$$

where

$$P(t) = \frac{1}{k!(m-1)!} \int_0^t (t-s)^{m-1} \prod_{l=1}^{k} (s - \rho_l) ds\ .$$

The importance of the Gauss and Lobatto points is clear also as, by construction, the Gauss points give the optimal value of $p = 2k$ in (2.4.12) whereas the Lobatto points maximize $p = 2k - 2$ in the case $\rho_1 = 0, \rho_k = 1$. These estimates, particularly (2.4.15), motivate what follows. The superconvergence property, (2.4.14), is one of the most important aspects of any collocation method but one which we are not taking advantage of here. Typically superconvergence can be used to control mesh adaptation in the solution of boundary value problems (Ascher et al. 1988).

2.5 A moving collocation method

The preceding discussion deals exclusively with stationary in time boundary value problems and is the approach taken in the BVP solvers used for the construction of all the bifurcation diagrams presented in Chapters 3-5 (Doedel, Champneys, Fairgrieve, Kuznetsov, Sandstede and Wang 1997, Shampine and Kierzenka 2001). To solve time-dependent problems, we will use a method of lines approach, discretizing first in space

using Hermite collocation and then passing the resulting system of ODEs in time to an ODE solver. At each stage in time we have a problem of the form as described thus far where now a difference approximation to the time derivative contributes a spatially dependent forcing term to the problem.

Our method is made more complicated because of the singular nature of many of the problems under consideration. In order to be able to resolve finite-time singularities we couple the physical PDE of interest to the MMPDE as described in Section 2.2.2. Because we are currently considering problems in only one space dimension, solving the MMPDE and the physical PDE simultaneously for both the transformation $x(\xi, t)$ and the physical solution $u(x(\xi, t), t)$ is reasonable computationally. This avoids the need to interpolate the solution between different grids and that a method of lines discretization for the entire system may be integrated with existing efficient codes. An alternate strategy is mesh decoupling in which the physical and mesh PDEs are solved in turn, see for instance Beckett et al. (2001). There is no technical requirement for the mesh and physical PDEs to be discretized in the same way. Following Huang and Russell (1996) we use Hermite collocation for the physical PDE but only central differences for the mesh. The mesh need not be solved as accurately as the physical PDE as errors here do not affect the order of convergence of the solution on a given mesh. Also, we do not want to introduce any additional stiffness to the full system of ODEs.

Collocation has many advantages over a standard finite difference approximation: it affords a continuous representation of the solution and its first $(m-1)$ spatial derivatives, it provides a higher order of convergence, is simple and flexible to program, easily handles arbitrary boundary conditions and provides error estimates independent of mesh grading. This last point is perhaps the most important for a moving mesh method, particularly for higher-order problems. By using collocation, we are able to avoid problems of approximating high-order derivatives via differences over a wide non-uniform stencil, see Saucez et al. (2001).

It should be noted that the existing code of Huang and Russell (1996) can, in theory, solve the problems as discussed in this thesis. It is a general purpose code to solve systems of the form

$$\boldsymbol{f}(t, x, \boldsymbol{u}_t, \boldsymbol{u}_x, \boldsymbol{u}_{xx}, \boldsymbol{u}_{xt}) = (\boldsymbol{g}(t, x, \boldsymbol{u}_t, \boldsymbol{u}_x, \boldsymbol{u}_{xt}))_x$$

using the same strategies as described in this Chapter. Clearly, a system of the form

$$\boldsymbol{u} = (v, v_{xx})^T$$

could be used to solve higher-order problems. However, this definition sets $\boldsymbol{u}_2 = v_{xx}$

and hence means solving

$$(u_1)_{xx} = u_2$$

for which u_2 is an algebraic, rather than a differential variable making the system much more difficult to both start and integrate, this is especially true on a moving grid. The alternate relationship

$$(u_1)_{txx} = (u_2)_t$$

recovers a completely differential system but is, in the general case, at best neutrally stable in time. Also, in the conservative case described below, any such system approach is less efficient in that it requires solving for extraneous unknowns. This method also means that our approximation has a continuous third derivative in all I whereas a system approach would not. Additionally, because of the stability proeprties of the DAE computations of the Cahn-Hilliard equation on a moving grid using the system approach have been shown to fail (Williams et al. 2003).

2.5.1 Collocation discretization of the physical PDE

When considering a discretization with a coordinate transformation one can either write the PDE in terms of the physical variable x and discretize on a non-uniform mesh, or solve a transformed PDE in terms of the computational variable ξ on a uniform mesh. The latter approach is typical of moving finite difference approximations. However with the flexibility of the collocation method it is simpler to discretize the PDE with respect to the physical variable x (this approach is only valid in one dimension).

Suppose at a time $t \in [0, t_f]$ the mesh

$$x_L(t) = X_1(t) < X_2(t) < ... < X_{N+1}(t) = x_R(t)$$

solves the MMPDE. The physical solution $u(x,t)$ is approximated by the piecewise septic Hermite polynomial

$$\begin{aligned} U(x,t) = {} & U_i(t)L_{0,0}(s) + U_{x,i}(t)H_i(t)L_{0,1}(s) + U_{xx,i}(t)H_i^2(t)L_{0,2}(s) \\ & + U_{xxx,i}(t)H_i^3L_{0,3}(s) + U_{i+1}(t)L_{1,0}(s) + U_{x,i+1}(t)H_i(t)L_{1,1}(s) \\ & + U_{xx,i+1}(t)H_i^2(t)L_{1,2}(s) + U_{xxx,i+1}(t)H_i^3L_{1,3}(s), \end{aligned} \tag{2.5.1}$$

for $x \in [X_i(t), X_{i+1}(t)]$, $i = 1, ..., N$, where $U_i(t), U_{x,i}(t), U_{xx,i}(t)$ and $U_{xxx,i}(t)$ denote $U(X_i(t),t), U_x(X_i(t),t), U_{xx}(X_i(t),t)$ and $U_{xxx}(X_i(t),t)$ respectively. The local coordinate s is defined by

$$s = \frac{x - X_i(t)}{H_i(t)} \in [0,1], \qquad H_i(t) = X_{i+1}(t) - X_i(t).$$

The Hermite interpolating polynomials are given explicity in a form analogous to the

interpolating formula of Lagrange. Recall that the shape functions are determined recursively by the formula (2.4.7) which for $n = 1$ and $m_0 = m_1 = 3$ works out to

$$\begin{aligned}
L_{0,0}(s) &= \left(20s^3 + 10s^2 + 4s + 1\right)(s-1)^4, \\
L_{0,1}(s) &= s\left(10s^2 + 4s + 1\right)(s-1)^4, \\
L_{0,2}(s) &= \frac{s^2}{2}(4s+1)(s-1)^4, \\
L_{0,3}(s) &= \frac{s^3}{6}(s-1)^4, \\
L_{1,0}(s) &= -\left(20s^3 - 70s^2 + 84s - 35\right)s^4, \\
L_{1,1}(s) &= s^4(s-1)\left(10s^2 - 24s + 15\right), \\
L_{1,2}(s) &= -\frac{s^4}{2}(s-1)^2(4s-5), \\
L_{1,3}(s) &= \frac{s^4}{6}(s-1)^3.
\end{aligned}$$

The derivatives of the solution for $x \in [X_i(t), X_{i+1}]$ are determined by direct differentiation of (2.5.1), for instance,

$$\begin{aligned}
U_x(x,t) = \frac{1}{H_i}\Bigg(&U_i(t)\frac{dL_{0,0}}{ds} + U_{x,i}(t)H_i(t)\frac{dL_{0,1}}{ds} + U_{xx,i}(t)H_i^2(t)\frac{dL_{0,2}}{ds} \\
&+ U_{xxx,i}(t)H_i^3\frac{dL_{0,3}}{ds} + U_{i+1}(t)\frac{dL_{1,0}}{ds} + U_{x,i+1}(t)H_i(t)\frac{dL_{1,1}}{ds} \\
&+ U_{xx,i+1}(t)H_i^2(t)\frac{dL_{1,2}}{ds} + U_{xxx,i+1}(t)H_i^3\frac{dL_{1,3}}{ds}\Bigg),
\end{aligned} \tag{2.5.2}$$

and

$$\begin{aligned}
U_t(x,t) = &\frac{dU_i}{dt}L_{0,0} + \left(\frac{dU_{x,i}}{dt}H_i + U_{x,i}\frac{dH_i}{dt}\right)L_{0,1} + \left(\frac{dU_{xx,i}}{dt}H_i^2 + 2U_{xx,i}H_i\frac{dH_i}{dt}\right)L_{0,2} \\
&+ \left(\frac{dU_{xxx,i}}{dt}H_i^3 + 3U_{xxx,i}H_i^2\frac{dH_i}{dt}\right)L_{0,3} + \frac{dU_{i+1}}{dt}L_{1,0} \\
&+ \left(\frac{dU_{x,i+1}}{dt}H_i + U_{x,i+1}\frac{dH_i}{dt}\right)L_{1,1} + \left(\frac{dU_{xx,i+1}}{dt}H_i^2 + 2U_{xx,i+1}H_i\frac{dH_i}{dt}\right)L_{1,2} \\
&+ \left(\frac{dU_{xxx,i+1}}{dt}H_i^3 + 3U_{xxx,i+1}H_i^2\frac{dH_i}{dt}\right)L_{1,3} - U_x(x,t)\left(\frac{dX_i}{dt} + s^{(i)}\frac{dH_i}{dt}\right).
\end{aligned} \tag{2.5.3}$$

Additional mixed derivatives are computed analagously but have been neglected for brevity. The goal now is to write down an system of ODEs for the unknowns $U_i(t)$, $U_{x,i}(t)$, $U_{xx,i}(t)$ and $U_{xxx,i}(t)$. There are several ways to do this. The standard approach would be to minimize the local truncation error (by maximizing the order); this means collocation at the Gauss points and we describe this method first. However, we are also interested in methods which may be less stiff in time or provide some additional geometric property of the problem. In addition, we also describe a second scheme,

conservative collocation, which does both of these, though at the expense of losing detailed information about the error of the approximate solution and with twice the number of function evaluations.

2.6 Gaussian collocation

Given a problem of the form

$$u_t = \mathcal{N}(t, x, u, u_x, u_{xx}, u_{xxx}, u_{xxxx}), \quad t > 0,\ x \in I = (a, b), \tag{2.6.1}$$

supplemented with the initial condition

$$u(x, 0) = u_0(x), \quad x \in (a, b),$$

and separated boundary conditions

$$g_{a,1} = 0,\ g_{a,2} = 0,\ g_{b,1} = 0,\ g_{b,2} = 0, \tag{2.6.2}$$

where $g_{y,i} = g_{y,i}(t, y, U_t(y), U(y), U_x(y), U_{xx}(y), U_{xxx}(y))$, the standard approach would be to solve for the $(4+1)(N+1)$ unknowns of the solution, U and its first three spatial derivatives as well as the $(N+1)$ mesh points $X_i(t)$ by enforcing the residual

$$U_t - \mathcal{N}(t, x, U, U_x, U_{xx}, U_{xxx}, U_{xxxx}) = 0 \tag{2.6.3}$$

at the 4 Gauss points in each interval. The MMPDE, $X_{t,\xi\xi} = -\frac{1}{\tau}(MX_\xi)_\xi$ is approximated with central differences at the $(N-1)$ interior points,

$$X_{t,i-1} - 2X_{t,i} + X_{t,i+1} = -\frac{1}{\tau}\left(M_{i+1/2}(X_{i+1} - X_i) - M_{i-1/2}(X_i - X_{i-1})\right),$$

where $M_{i+1/2}$ and $M_{i-1/2}$ are approximations to the average of the monitor function over cells I_i and I_{i-1} respectively. The system is closed by satisfying the boundary conditions (2.6.2) and $X_1 = a, X_{N+1} = b$. This gives a system of $5(N+1)$ equations in $5(N+1)$ unknowns. The spatial local truncation error of such a method can then be estimated from (2.4.15). Using $m = 4$, $k = 4$ and $p = 2k = k + m$, we have

$$|u(x) - U(x)| = \mathcal{O}(h^8) \quad \text{for all } x \in I, \quad \text{where } h = \max_i h_i.$$

Problems of the form

$$u_t = (g(t, x, u, u_x, u_{xx}, u_{xxx}))_x$$

occur regularly in applications and satisfy the obvious property that

$$\frac{d}{dt}\int_I u = g(b) - g(a).$$

On a fixed grid, the method as described satisifies this conservation law only for *linear* functions

$$g(u, u_x, u_{xx}, u_{xxx}) = \alpha_1 u + \alpha_2 u_x + \alpha_3 u_{xx} + \alpha_4 u_{xxx}. \tag{2.6.4}$$

Lemma 2.6.1. *Gaussian collocation conserves discrete linear integrals.*

Proof. Denoting $U_i^{(k-1)} = U_i, U_{x,i}, U_{xx,i}, U_{xxx,i}$ for $k = 1, 2, 3, 4$, we have that

$$\begin{aligned}
\frac{d}{dt}\int_I U dx &= \int_I \alpha_1 U_x + \alpha_2 U_{xx} + \alpha_3 U_{xxx} + \alpha_4 U_{xxxx} dx \\
&= \sum_i \sum_j \alpha_j \left(\sum_{k=0}^{3} (H_i)^{k-j+1} \left(U_i^{(k)} \int_0^1 \frac{d^j}{ds^j} L_{0,k}(s) ds + U_{i+1}^{(k)} \int_0^1 \frac{d^j}{ds^j} L_{1,k}(s) ds \right) \right) \\
&= \sum_i \sum_j \alpha_j (U_{i+1}^{(j-1)} - U_i^{(j-1)}) \text{ (by definition of the basis functions, (2.4.6))} \\
&= \sum_j \alpha_j (U_{N+1}^{(j-1)} - U_1^{(j-1)}) \\
&= G(X_{N+1}) - G(X_1).
\end{aligned}$$

□

This is quite a reasonable approach for many problems and we present examples of it in practice in Section 2.8. Clearly we would like a method which is conservative for a class of general equations rather than just the class (2.6.4). Also, for problems with singularity formation, each successive spatial derivative is considerably larger than the previous and the fourth derivative is represented the least well, both with the worst error and being only piece-wise continuous. Because we are solving evolutionary problems on a moving grid both of these issues add to the stiffness of the ODE system. To avoid computing with the fourth derivative directly, we now discuss an integrated form of our problem.

2.7 Conservative collocation

Consider the equation

$$f(t, x, u_t, u, u_x, u_{xx}, u_{xxx}) = (g(t, x, u_t, u, u_x, u_{xx}, u_{xxx}))_x. \tag{2.7.1}$$

This satisfies the generalized conservation property

$$\int_I f dx = g|_{x=b} - g|_{x=a}. \tag{2.7.2}$$

Any problem of the form

$$u_t = \mathcal{N}(t, x, u_t, u, u_x, u_{xx}, u_{xxx}, u_{xxxx})$$

may be written (perhaps awkwardly) in the form (2.7.1). To enforce property (2.7.2) and to eliminate any dependence on U_{xxxx} in our system or ODEs we now construct a cell-averaged approach to (2.7.1).

We begin by approximating f by its Lagrange interpolant as defined in (2.4.3),

$$F_i = \sum_{j=0}^{3} f_{ij} \tilde{L}_j, \tag{2.7.3}$$

where the canonical points are the four Gauss points on the unit interval

$$\rho_1 = \frac{1}{2} - \frac{\sqrt{525 + 70\sqrt{30}}}{70}, \ \rho_2 = \frac{1}{2} - \frac{\sqrt{525 - 70\sqrt{30}}}{70}, \ \rho_3 = 1 - \rho_1, \ \rho_4 = 1 - \rho_2 \tag{2.7.4}$$

and $f_{ij} = f(x_i + H_i \rho_j)$. Integrating equation (2.7.1) between the five Lobatto points on the unit interval,

$$\tilde{\rho}_1 = 0, \ \tilde{\rho}_2 = \frac{1}{2} - \frac{\sqrt{21}}{14}, \ \tilde{\rho}_3 = \frac{1}{2}, \ \tilde{\rho}_4 = \frac{1}{2} + \frac{\sqrt{21}}{14}, \ \tilde{\rho}_5 = 1, \tag{2.7.5}$$

using the approximation to f given by (2.7.3) gives a system in each interval I_i,

$$A\boldsymbol{F}_i = B\boldsymbol{G}_i / H_i. \tag{2.7.6}$$

The matrix A is defined by

$$A_{jk} = \int_{\tilde{\rho}_j}^{\tilde{\rho}_j + 1} \tilde{L}_k dt \quad j, k = 1, 2, 3, 4$$

and the matrix B has the form

$$B_{jk} = \begin{cases} 1 \text{ if } j = k, \\ -1 \text{ if } k = j + 1, \\ 0 \text{ else.} \end{cases} \quad \text{for } j = 1, ..., 4 \text{ and } k = 1, ..., 5,$$

Finally, the vectors $\boldsymbol{F}_i$, $\boldsymbol{G}_i$ satisfy

$$(\boldsymbol{F}_i)_j = F_i(x_i + H_i \rho_j), \quad j = 1, 2, 3, 4,$$

$$(\boldsymbol{G}_i)_j = G_i(x_i + H_i\tilde{\rho}_j), \quad j = 1,2,3,4,5\ .$$

Note that by direct construction (enforcement of cell-averaging), we have that

$$\int_{I_i} F_i = G(X_{i+1}) - G(X_i)$$

and hence the following lemma.

Lemma 2.7.1. *The collocation scheme* (2.7.6) *enforces discrete conservation.*

Proof.

$$\int_I F dx = \sum_i \int_{I_i} F_i dx = \sum_i G(X_{i+1}) - G(X_i) = G(X_{N+1}) - G(X_1).$$

□

To generate an approximation to u, we again approximate u by its Hermite interpolant U as defined in (2.5.1) and choose the coefficients $U_i(t), U_{x,i}(t), U_{xx,i}(t), U_{xxx,i}(t)$ such that in each interval

$$H_i\boldsymbol{F}_i = W\boldsymbol{G}_i,$$

where the differentiation matrix $W = A^{-1}B$. This again gives four equations in each cell, the same as the Gaussian method previously described. We now have a formulation which does not rely on U_{xxxx}, however, if naively coded, it requires 9 function evaluations per interval, f is evaluated at the 4 Gauss points and g at the 5 Lobatto points as opposed to 4 for the Gaussian case. Because the two extreme Lobatto points, $\tilde{\rho}_1 = 0$ and $\tilde{\rho}_5 = 1$ coincide at successive intervals an efficient implementation can be reduced to $8N + 1$ function evaluations, but this is still twice that of the Gaussian formulation.

2.7.1 Conservation on adaptive grids

Unfortunately, on a moving grid conservation is not ideal. To see this, consider the conservation of an arbitrary discrete quantity M on a moving grid. Denoting H_iM_i as the representation of integral of M over I_i then

$$\frac{d}{dt}\int_I M dx = \frac{d}{dt}\sum_i H_iM_i.$$

However if M is *equidistributed* in the sense of (2.2.1) then

$$H_iM_i = \frac{\int_I M dx}{N} \qquad \forall i, \forall t$$

and thus we have discrete conservation if M is the conserved quanitity g. However, if M is not exactly equidistributed, or the monitor function M is not conserved, then

$$\frac{d}{dt}\sum_i H_i M_i = \sum_i M_{t,i} H_i + H_{t,i} M_i$$

and due to the magnitude of $H_{t,i}$ (true for blow-up, but not always the case) small relative errors can lead to significant pollution of the conserved quantity due to numerical error. To overcome this when the conserved quantity is not a suitable monitor function we shall now consider a *static regridding* algorithm which is loosely based on preserving the scale-invariance (2.2.6). This algorithm is described pictorially in Figure 2.3.

Algorithm: Scale-invariant static regridding

1) Define the parameters
   $M(U)$ - the monitor for regridding, eg. $M = \|U\|_\infty$
   λ_0 - the initial regridding parameter, eg. $M(u_0)$
   λ_1 - the regridding factor, eg. 2
   I_s - the initial interval of support, eg I
2) Integrate the PDE on the fixed grid
3) If $M(U) > \lambda_1 \lambda_0$ then
   a) $\lambda_0 = M$
   b) $I_s = M^{\beta/\alpha} I_s$
   c) Subdivide I_s such that are at least N nodes in the new interval of support I_s.
   d) Evaluate the solution on the new grid.
   e) Goto 2.

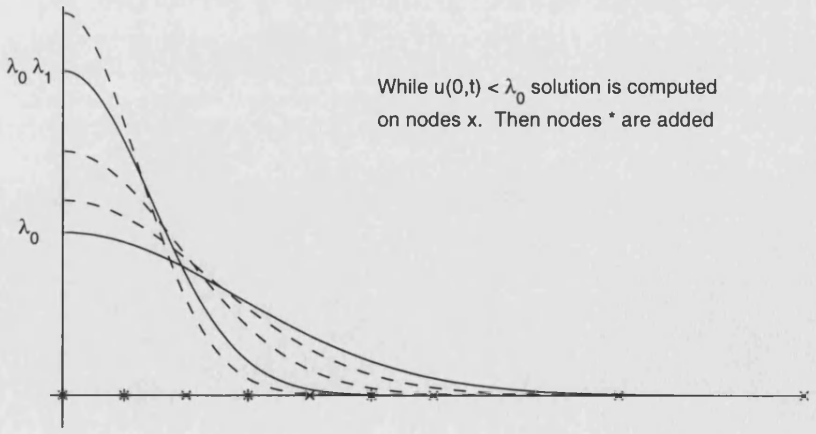

Figure 2.3: Sketch of the static regridding procedure

This algorithm is only useful for the case of localization at a known point. As a singularity develops more nodes are added according to the natural scaling of the problem (as α and β are taken from (2.2.6)), so that the solution is resolved at all times.

Because of the need to restart the ODE solver this algorithm is considerably less efficient than the MMPDE approach, however it has better conservation properties. Note that conservation is exact under this algorithm only provided that we never remove nodes. This is due to the fact that when we add nodes we never interpolate but rather simply evaluate the continuous collocation polynomial at additional points. But, should we remove nodes there is no guarantee that the conserved quantity will remain unchanged.

2.7.2 Error estimates

Despite the non-standard fomulation, the classical theory presented in Theorem 2.4.1 can still be used for error bounds for the conservative collocation scheme when examined in the proper way. We can find the local truncation error for our equations by considering the problem

$$g_x = f$$

as an equation for g. This approach extends the error estimate derived in Huang and Russell (1996) which is valid only at the Gauss points to a spatially global one.

Theorem 2.7.2. *The conservative collocation scheme* (2.7.6) *is globally fourth-order accurate with superconvergence of order five at the Gauss points.*

Proof. We can use the results of Theorem 2.4.1 to estimate $G_x - g$ where there are $k = 5$ Lobatto points, with precision $p = 2k - 2 = 8$ to solve this first-order problem ($m = 1$). The error in the Lagrange approximation to f is given by equation (2.4.4) and thus

$$\begin{aligned}(G_x - F) &= (G_x - g_x) - (F - f) \\ &= H_i^5 \frac{g^{(6)}}{6!} \prod_{j=1}^{5} (s - \tilde{\rho}_j) - H_i^4 \frac{g^{(5)}}{5!} \prod_{j=1}^{4} (s - \rho_j) \end{aligned} \tag{2.7.7}$$

for all points $x_i \leq x \leq x_i$, and $s = (x - x_i)/H_i$. □

Here we have used the fact that the exact solution satisfies $g_x = f$. For this method there is superconvergence at the Gauss points $\{\rho_i\}$ at which this equation is enforced. For the standard Gaussian form we have error estimates for $u - U$ specifically whereas for the conservative case we only have estimates for $g - G$ which, in the general case, may not easily give information about $u - U$. Instead, however we have eliminated all dependence on U_{xxxx} in the ODEs and that we have enforced discrete conservation.

In addition to the standard local error estimates we have also satisfied the global geometric features of scale-invariance and conservation. We have chosen to enforce these additional conditions on the mesh and the discretization because they accurately describe the essential governing geometry of the problem.

2.8 Examples

In this section we display the efficiency, accuracy and robustness of the moving collocation method by testing it on a variety of examples. These examples are mostly singular parabolic problems in keeping with those studied in the remainder of this thesis. However, the code is much more generally applicable and additional examples of different types of problems may be found in Williams et al. (2003). Unless otherwise indicated the following parameters have been used throughout this section

$$N = 25, \quad \text{atol} = .01, \quad \text{rtol} = .0001, \quad \tau = .001.$$

2.8.1 Finite time blow-up

In Chapter 3 we will analyze the following equation; introduced in Chapter 1 and given by

$$u_t = -u_{xxxx} + |u|u, \tag{2.8.1}$$

$$u(x,0) = u_0(x) \in C(\mathbf{R}) \quad \text{such that} \lim_{|x|\to\infty} u_0(x) = 0, \tag{2.8.2}$$

and show that it possesses a blow-up self-similar solution of the form

$$u(x,t) = (T-t)^{-1} f(y), \quad y = x/(T-t)^{1/4},$$

where T is the finite blow-up time. In this section we are interested in studying how the use of conservative discretization affects the integration of this equation. Note that there is no natural quantity which is inherently conserved in this problem. However, the ODE problem is less stiff due to the lack of dependence on u_{xxxx}. Equation (2.8.1) is invariant under the scaling

$$t \mapsto \lambda t, \quad x \mapsto \lambda^{1/4} x \quad \text{and} \quad u \mapsto \lambda^{-1} u, \quad \lambda > 0,$$

hence from (2.2.7) we use the asymptotically scale-invariant monitor function

$$M = 1 + |u|.$$

The floor factor 1 makes the method easier to start as when the solution is small the grid is almost uniform but, as blow-up approaches it is incidental to the self-similar structure as it is vanishingly small in the rescaled variables. The initial data is given by

$$u_0(x) = e^{-x^2}.$$

Symmetry at the origin is enforced by requiring

$$u_x(0,t) = 0 \quad \text{and} \quad u_{xxx}(0,t) = 0.$$

Because of the single-point blow-up the far field boundary conditions are unimportant. We truncate the semi-infinite interval at $L = 8$ and impose

$$u(L,t) = 0 \quad \text{and} \quad u_x(L,t) = 0.$$

In Figure 2.4 we present a typical set of solution profiles and the associated mesh

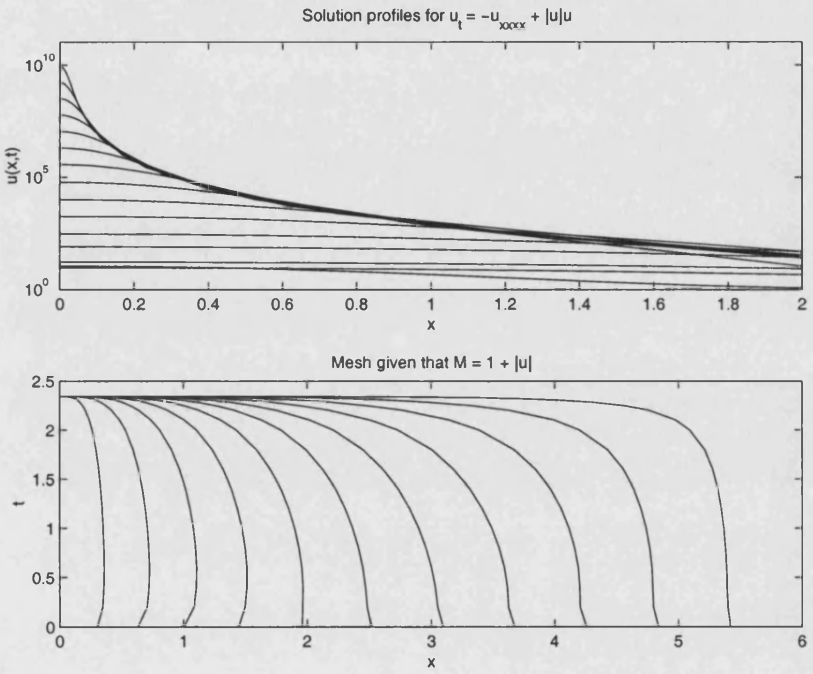

Figure 2.4: Solution and mesh for equation (2.8.1)

while in Table 2.1 we compare the properties of the standard Gaussian and conservative discretizations. These results clearly show that the conservation structure is advantageous for the integration of this problem. As the singularity is approached the non-conservative equations become considerably more stiff with the ODE solver failing when the L^∞-norm is two orders of magnitude less than for the conservative discretization.

2.8.2 Finite time blow-up with conservation

To test the role of the conservative discretization, we now consider an equation related to a simplified model for the evolution of fronts in solidification theory, (Novick-Cohen

	$u(0,t)$	Steps	Fcn.	Jac.
Conservative Discretization	$3.1\,10^{13}$	2505	7527	2922
	10^{12}	2311	6752	2535
	10^{10}	1412	3244	811
	10^{8}	1175	2798	772
	10^{6}	927	2367	724
Gaussian Discretization	3.710^{11}	8737	33162	16026
	10^{10}	3265	11272	1508
	10^{8}	1730	1265	711
	10^{6}	534	946	299

Table 2.1: Comparison of the computational complexity for (2.8.1).

1992)

$$u_t = -(u_{xx} + u^3)_{xx}. \tag{2.8.3}$$

Notice that for this equation

$$\frac{d}{dt}\int u(x,t)dx = -\int (u_{xx} + u^3)_{xx}dx = 0$$

for solutions with sufficient decay as $|x| \to \infty$. We again take intitial data

$$u_0(x) = e^{-x^2},$$

but now the monitor function takes the form

$$M = 1 + |u|^3$$

to preserve the scaling invariance of the combined system. However, to compare the conservation properties of the method we will also test

$$M = 10^{-4} + |u|$$

which, for $u > 0$ and M equidistributed should preserve u very well, because we are using MMPDE6 we expect at worst an $\mathcal{O}(\tau)$ error in the equidistribution of M. Lastly, we will also test the static regridding algorithm. Because for this problem the scaling invariance is

$$t \mapsto \lambda t, \quad x \mapsto \lambda^{1/4}x, \quad u \mapsto \lambda^{-1/4}u, \quad \lambda > 0,$$

whenever the $u(0,t)$ doubles in magnitude we will halve a proportion of the cells closest to the origin.

Again we see from Table 2.2 that the conservative discretization is more efficient and can integrate (marginally) further into the blow-up regime. While in the L^∞ sense it

	$u(0,t)$	Steps	Fcn.	Jac.
Conservative Discretization	2517	1248	2234	184
	1000	1116	1998	167
	500	1008	1817	156
	100	811	1470	137
	50	681	1229	119
Gaussian Discretization	2438	1731	3393	571
	1000	1503	3171	496
	500	1393	2967	487
	100	1159	2555	455
	50	711	1312	130

Table 2.2: Comparison of the computational complexity for (2.8.3).

may appear that we have not been able to compute solutions to this equation nearly as well as for (2.8.1), it should be noted that for (2.8.3) the self-similar profiles are of the form

$$u(x,t) = (T-t)^{-1/4} f(y), \qquad \text{where } y = x/(T-t)^{1/4},$$

and thus we are able to integrate until $(T-t) \simeq 10^{-12}$ in both cases. In Figure 2.5

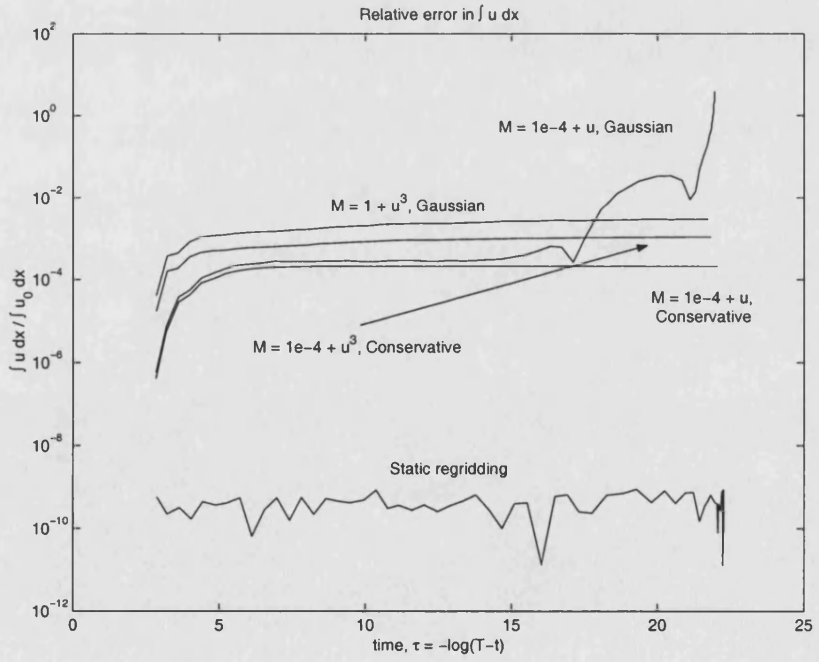

Figure 2.5: Relative variation of $\int u$ over time for (2.8.3)

we show the conservation of $\int u\,dx$ over time. Clearly, the static regridding algorithm does the best and as expected using the conserved quantity as the monitor function

does better than the scale-invariant monitor function. Also, we see that the conservative discretization does a better job than the generic Gaussian case. In the case of $M = |u| + 10^{-4}$, the final grids are completely insufficient to resolve the solution localized near the origin, hence the eventual order one error in the mass. Qualitatively, the conservative solution is no better–it has simply managed to preserve the mass properly despite not representing the solution properly as can be seen in Figure 2.6. The continuous polynomial representation afforded by our method means that the solution is much smoother than those with $M = |u| + 10^{-4}$ seen in Figure 2.6, the piece-wise linear representation has been displayed to show more easily the lack of nodes in the blow-up region with this sub-optimal monitor function. Lastly we consider the time

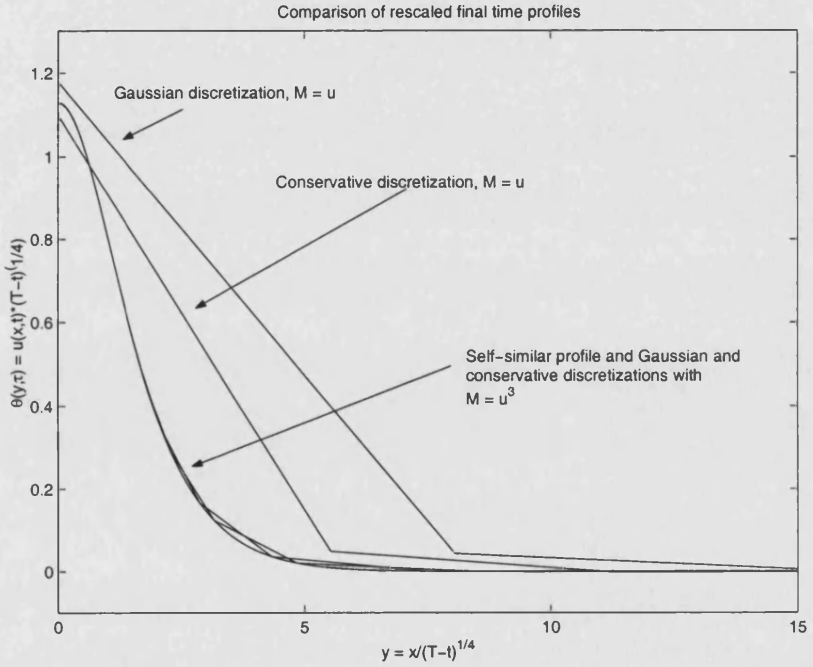

Figure 2.6: Comparison of final profiles for (2.8.3)

required to perform the calculations discussed in this subsection. In Figure 2.7 we present the timing for the four different moving mesh approximations to (2.8.3). In this figure we see that it takes the simpler monitor function, $|u|$, less time to generate an equidistributed mesh and that initially the Gaussian method requires less time. But, as the solution becomes more difficult to compute, despite the fact that each function evaluation requires twice as much work, the conservative discretization soon becomes quicker. Because of multiple restarts, the static re-gridding computation took *hours* rather than seconds.

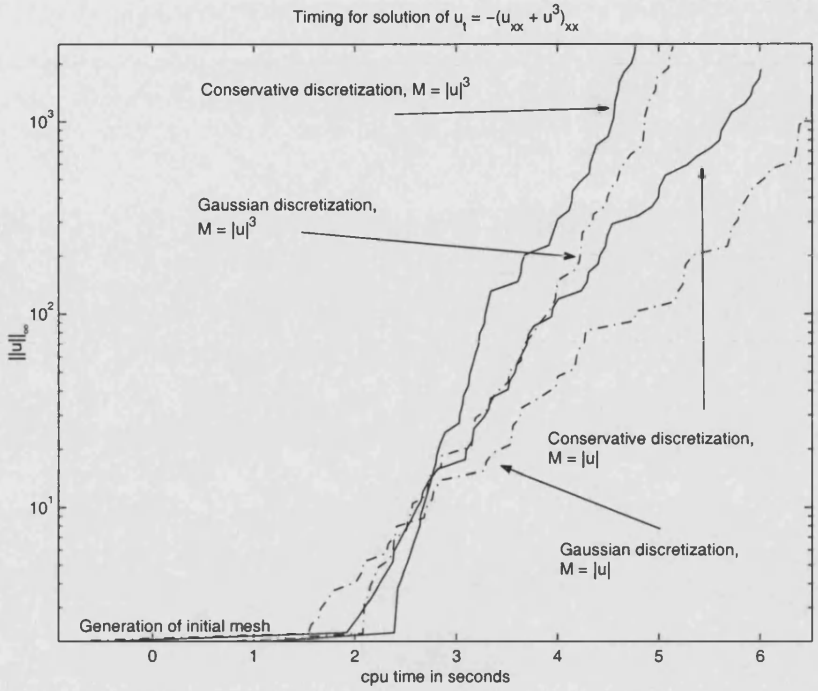

Figure 2.7: Computational time.

2.8.3 Quasilinear finite-time blow-up

A simple quasilinear extension of the semilinear equations considered in Chapter 3 is the PDE,

$$u_t = u(-u_{xxxx} + u^2), \tag{2.8.4}$$

which is only parabolic for $u > 0$. We are interested in the numerical investigation of this equation to test whether or not our method will preserve positivity and whether or not the conservative discretization is at all helpful in this case when there is clearly no inherent conservation property. We will test two possible conservative representations for this equation

$$u_t - u^3 - u_x u_{xxx} = -(u u_{xxx})_x \tag{2.8.5}$$

and

$$\frac{u_t}{u} - u^2 = -(u_{xxx})_x \,. \tag{2.8.6}$$

To ensure parabolicity in the face of numerical error, i.e. preserve $u > 0$, there are two possible regularizations, first we could consider initial data of the form

$$u_0(x) = e^{-x^2} + \alpha^2$$

or replace the quasilinear term u by $|u| + \varepsilon$, where $\varepsilon > 0$ (this approach is effective for the nonlinear diffusion equation (Budd, Piggott and Williams 2003)). We have tested

both approaches and found that the performance of our algorithm depends highly on the value of α and less so on ε. In Table 2.3 we compare the results of the three discretizations taking $\alpha = 10^{-3}$ and $\varepsilon = 10^{-6}$. Here we see that the conservative discretizations can integrate further into the singularity but require more steps, moreover equation (2.8.5) performs better than (2.8.6). This is not surprising due to the term u_t/u. For $\alpha = 1$ the results in Table (2.4) tell a different story. Now both the

	$u(0,t)$	Steps	Fcn.	Jac.
Conservative	$3.9\,10^6$	1852	3536	415
Discretization	10^6	1788	3394	402
$(uu_{xxx})_x$	10^4	1699	3156	385
	10^2	1406	2443	250
Conservative	$2.7\,10^6$	1891	3959	581
Discretization	10^6	1856	3883	575
$(u_{xxx})_x$	10^4	1771	3654	558
	10^2	1525	3378	536
Gaussian	$9.6\,10^5$	1622	3017	307
Discretization	10^4	1489	2732	286
	10^2	1014	1915	143

Table 2.3: Comparison of the computational complexity for (2.8.4) with $u_0(x) = 2e^{-x^2} + 10^{-4}$.

conservative discretizations beat the standard Gaussian one and now the rather unnatural looking formulation (2.8.6) is the best, both in how far the numerical method can integrate and in the required number of steps taken by the ODE solver.

	$u(0,t)$	Steps	Fcn.	Jac.
Conservative	$2.59\,10^6$	875	1859	293
Discretization	10^6	832	1766	285
$(uu_{xxx})_x$	10^4	667	1455	264
	10^2	336	626	55
Conservative	$1.3\,10^7$	744	1548	156
Discretization	10^6	687	1357	141
$(u_{xxx})_x$	10^4	554	1081	118
	10^2	310	550	37
Gaussian	$2.4\,10^6$	951	1985	309
Discretization	10^6	888	1871	301
	10^4	729	1543	282
	10^2	359	668	58

Table 2.4: Comparison of the computational complexity for (2.8.4) with $u_0(x) = 2e^{-x^2} + 1$.

In all cases $-(\min u)/(\max u) \gg \epsilon$.

2.9 Conclusions

In this Chapter we have discussed the implementation of a high-resolution collocation method to integrate fourth-order evolutionary equations on adaptive grids. By carefully choosing the monitor functions we have been able to admit scale-invariant solutions such as are often seen as attractors in the long-time behaviour of our model problems. Also, by using a cell-averaged discretization we have been able to satisfy a general discrete conservation property and also reduce stiffness in the associated ODE problem. However, it is clear that each problem must be considered carefully to determine the appropriate adaptive strategy, monitor function and discretization.

Appendix: Implementation

To solve the problems under consideration in this thesis an implementation of the strategy described above has been made in MatLab. The time integration arising from the method of lines semi-discretization is done using DDASSL (Brenan et al. 1996) called through a MEX interface. DDASSL is a well known code for solving stiff differential algebraic equations of the form

$$F(t, y, y') = 0$$

using backward differentiation formulae to approximate the first derivative term. The resulting method is efficient from both user- and run-time standpoints. There are three user editable routines, two of which we include here to highlight the advantages of this method when solving numerous problems.

File `params.m`

```
N = 20;            % number of nodes
Tau = 1e-4;        % relaxation time
rtol = 1e-5;       % Relative tolerance for DDASSL
atol = 1e-5;       % Absolute tolerance for DDASSL
m = 3;             % Number of neighbouring nodes to smooth the monitor over
```

File `driver.m`

```
function sol = driver(x,xt,u,ux,uxx,uxxx,uxxxx ut,t, FUNC);
% The pde is of the form f = g_x.
p = 1;
switch FUNC
   case 1
% The RHS of the pde, f
      sol = ut - u.*abs(u).^p;
   case 2
% The LHS of the pde, g
      sol = -uxxx;
   case 3
% The initial data
      v = 5*(.2+exp(-.5*x.^2));
      ders = ndiff(x,v,3);
      sol = [v ders(:,1) ders(:,2) ders(:,3)];
```

```
    case 4
% The initial data for the time derivs.
       v = 5*(.2+exp(-.5*x.^2));
       ders = ndiff(x,v,4);
       v4 = ders(:,4);
       vt = -(v4-abs(v).^(p+1));
       ders = ndiff(x,vt,4);
       sol = [vt ders(:,1) ders(:,2) ders(:,3)];
    case 5
% The physical left BCs.  Please use local conditions as a banded
% Jacobian has been assumed!
       sol = [ux(1); uxxx(1)];
    case 6
% The physical right BCs
       sol = [ux(end); uxx(end)];
    case 7
% The monitor function at t = 0.
       sol = 1e-4+abs(u).^(p);
    case 8
% The monitor function for t > 0.
       sol = 1e-4+abs(u).^(p);
    case 9
% The mesh BCs.
       sol = [x(1); x(end) - 8];
end;
```

The third user-editable file `defout.m` defines the output and stopping criterion and is not crucial to using the code. For more details or to download the code see `http://www.bath.ac.uk/~mapjfw/work/MC4`.

With this interface two completely different PDEs with different initial and boundary data can be integrated using different monitor functions with having to modify at most 17 short lines of MatLab code.

Chapter 3

Blow-up in higher-order semilinear parabolic equations

3.1 Introduction

In this Chapter we show that the higher-order generalizations of the second-order model (1.1.2), the extended Frank-Kamenetskii equation,

$$u_t = (-1)^{m+1} D_x^{2m} u + e^u, \quad x \in \mathbf{R},\ t > 0 \quad (D_x = \partial/\partial x), \tag{3.1.1}$$

and (1.3.1)

$$u_t = (-1)^{m+1} D_x^{2m} u + |u|^{p-1} u, \quad x \in \mathbf{R},\ t > 0, \tag{3.1.2}$$

have exact, self-similar blow-up solutions and hence their evolution is somewhat simpler than in the case $m = 1$, though, of course, for $m > 1$ the problem of rigorous justification of the results becomes much more delicate. Fundamentally, we would like to understand the importance of the semilinear structure in these equations, (3.1.1) and (3.1.2), and its role in self-similarity. Additionally, we consider (1.1.1) in greater detail, constructing a countable spectrum of non-similarity blow-up profiles.

In Section 3.2 we introduce the relevant mathematical definitions, formulation of similarity variables and rescaled equations. In Section 3.3 we present the properties of the underlying linearized operator which governs the "dynamics" of both equations (3.1.1) and (3.1.2) near certain blow-up solutions.

In Section 3.4 we consider an extension of the linearized problem which makes clear the structure of the nonlinear spectrum. In particular, we analyze bifurcation points associated with a linearized operator and present an argument for the existence of self-similar solutions. This local argument is strengthened with numerical and asymptotic evidence. Section 3.5 is devoted to the asymptotic behaviour of solutions close to bifurcation points.

Lastly, in Sections 3.6 and 3.7 we construct the blow-up profiles asymptotically and compare them with numerical solutions of both the ODE for the self-similar profile and rescaled profiles from simulations of the full PDEs. Here we use the methods constructed in Chapter 2 to give numerical approximations to the solutions.

This Chapter is mainly devoted to the study of self-similar blow-up for higher-order semilinear parabolic equations, though we discuss some related centre manifold structures. Countable spectra of other blow-up patterns which are approximately self-similar and are constructed by matching of different asymptotic regions are studied in Section 3.8.3, see also Galaktionov (2001).

3.2 Finite time blow-up solutions and similarity variables

3.2.1 Similarity variables and rescaled PDEs

Because of their semilinear structure, the PDEs (3.1.1) and (3.1.2) have similar scaling symmetries, so that (3.1.2) is invariant with respect to the scaling transformation

$$t \mapsto \lambda t, \quad x \mapsto \lambda^{1/2m} x, \quad u \mapsto \lambda^{-1/(p-1)} u \quad \text{for all } \lambda > 0,$$

while (3.1.1) is invariant under the group of transformations

$$t \mapsto \lambda t, \quad x \mapsto \lambda^{1/2m} x, \quad u \mapsto u - \ln \lambda.$$

As usual, we assume that the solution $u(x,t)$ blows up at finite time $t = T$ in the sense of (1.2.1) and the blow-up set $B[u_0]$, defined by (1.3.8), contains the origin. Motivated by this assumption and looking for invariants of the above groups of transformations, we introduce the following self-similar spatial variable:

$$y = x/(T-t)^{1/2m} : \mathbf{R} \to \mathbf{R}, \quad t \in [0,T),$$

and the new time variable

$$\tau = -\ln(T-t) : (0,T) \to (\tau_0, \infty) \quad \text{with } \tau_0 = -\ln T.$$

Then for the polynomial nonlinearity we define a new dependent variable (the rescaled solution) $\theta(y,\tau)$ by

$$u(x,t) = (T-t)^{-1/(p-1)} \theta(y,\tau), \tag{3.2.1}$$

and for the exponential nonlinearity by

$$u(x,t) = -\ln(T-t) + \theta(y,\tau). \tag{3.2.2}$$

Rescaling (3.1.2) in terms of the new variables by substituting (3.2.1), we obtain the following PDE for the rescaled solution θ:

$$\theta_\tau = \mathcal{L}\theta + G_p(\theta), \quad y \in \mathbf{R},\ \tau > \tau_0, \quad \text{where } G_p(\theta) = |\theta|^{p-1}\theta - \theta/(p-1), \tag{3.2.3}$$

and the linear differential operator $\mathcal{L}$ is given by

$$\mathcal{L} \equiv (-1)^{m+1} D_y^{2m} - \frac{y}{2m} D_y. \tag{3.2.4}$$

Similarly, rescaling (3.1.1) leads to the PDE

$$\theta_\tau = \mathcal{L}\theta + G_e(\theta), \quad y \in \mathbf{R},\ \tau > \tau_0, \quad \text{where } G_e(\theta) = e^\theta - 1. \tag{3.2.5}$$

It is important that unlike the well understood case $m = 1$, for any $m > 1$ the operators on the right-hand sides *are not potential* and equations (3.2.3) and (3.2.5) do not possess Lyapunov functions and hence the classical gradient dynamical systems stability theory is not applicable.

3.2.2 Preliminaries: local and asymptotic properties of self-similar solutions

Exactly (not just asymptotically) self-similar solutions are those which are invariant under the group of transformations, i.e., correspond to suitable stationary solutions $\theta(y)$ of which are independent of the rescaled time τ. Any exact self-similar solution to (3.1.2) takes the form

$$u_S(x,t) = (T-t)^{-1/(p-1)} f(y), \tag{3.2.6}$$

where $f(y)$ satisfies the ODE

$$\mathcal{L}f + G_p(f) = 0 \quad \text{in } \mathbf{R}. \tag{3.2.7}$$

It is natural to impose the symmetry conditions at the origin

$$f'(0) = f'''(0) = ... = f^{(2m-1)}(0) = 0. \tag{3.2.8}$$

Then the existence of a stable (generic) self-similar solution with a suitable similarity profile f in (3.2.6) means that for a sufficiently wide subset of global symmetric non-stationary solutions to (3.2.3) there holds

$$\theta(y,\tau) \to f(y) \quad \text{as} \quad \tau \to \infty$$

in a suitable metric (or even pointwise). For such a stable similarity solution (3.2.6) to have non-vanishing trace in the limit $t \to T^-$ and to rule out constant solutions, we need to impose a special decay condition on $f(y)$ as $y \to \infty$. In particular, we will demand that there exists a finite limit $u(x,t) \to u(x,T^-)$ as $t \to T^-$ for arbitrarily small fixed $|x| > 0$. This corresponds to looking for similarity solutions which are compatible with the Cauchy problem on $\mathbf{R}^N$ for (3.1.1) or (3.1.2).

Asymptotic behaviour at infinity

Because we are interested in the Cauchy problem for u with suitable decay at infinity, we need to understand the possible asymptotics of small solutions to (3.2.7) satisfying $f(y) \to 0$ as $y \to +\infty$. We will define as admissible similarity profiles those which tend to zero as $y \to \infty$. The topology of such profiles is charaterized by the number of decaying solutions to the linearization of (3.2.7) about $f = 0$,

$$\mathcal{L}f - f/(p-1) = 0, \quad y > 0. \tag{3.2.9}$$

In order to determine the balance between the autonomous $2m-$th order term and the non-autonomous *growing* coefficient of f', $y/2m$, we set $z = y^\nu$ with $\nu = 2m/(2m-1)$ to reduce (3.2.9) to

$$f^{(2m)} - a_1 f' - a_2 z^{-1} f + \mathbf{B}(z)f = 0, \tag{3.2.10}$$

where $a_1 = (-1)^{m+1}\nu^{1-2m}/2m$, $a_2 = (-1)^{m+1}\nu^{-2m}/(p-1)$. Here

$$\mathbf{B}(z)f = \sum_{j=1}^{2m-1} \gamma_j z^{j-2m} f^{(j)}$$

is a linear operator with bounded and decaying coefficients as $z \to \infty$, where the first coefficient of the derivative f' is of order $O(z^{1-2m})$. By the perturbation theory of higher-order linear ODEs (see Chapters 3-5 in Coddington and Levinson (1955)), we have that the leading terms of exponentially decaying solutions are described by the operator in (3.2.10) with constant coefficients,

$$f^{(2m)} - a_1 f' = 0. \tag{3.2.11}$$

Setting $f = e^{pz}$, $p \neq 0$, gives the characteristic equation $p^{2m} - a_1 p = 0$, whence

$$p^{2m-1} = a_1 = (-1)^{m+1}/2m\nu^{2m-1} \equiv \rho_0^{2m-1}(-1)^{m+1}, \quad \text{where } \rho_0 > 0. \tag{3.2.12}$$

For any $m \geq 1$, there exist $2m-1$ roots $\{p_0, p_1, ..., p_{2m-2}\}$ given by

$$p_k = \rho_0 e^{i(2k+1)\pi/(2m-1)}, \ m = 2l; \quad p_k = \rho_0 e^{i2\pi k/(2m-1)}, \ m = 2l+1, \tag{3.2.13}$$

where $m-1$ roots have negative real parts ($\mathrm{Re}\, p_k < 0$). These correspond to $l \le k \le 3l-2$ for even $m = 2l$ and $l+1 \le k \le 3l$ for odd $m = 2l+1$. The linearized equation (3.2.9) has an $(m-1)$-dimensional subspace of exponentially decaying solutions as $y \to \infty$. For the second-order case $m = 1$, it is empty.

On the other hand, equation (3.2.10) admits a solution with algebraic decay (rather than exponential) as $z \to \infty$ described by the first-order operator

$$-a_1 f' - a_2 z^{-1} f = 0 \quad \Longrightarrow \quad f(z) = c\, z^{-(2m-1)/(p-1)}.$$

The existence of solutions with such a decay for the perturbed equation (3.2.10) is established by a standard expansion analysis by calculating solutions via a Kummer-type series (generalized confluent hypergeometric equations) converging uniformly for $z \gg 1$. For the linearized equation (3.2.9) the leading order behaviour is thus algebraic,

$$f(y) = C|y|^{2m/(p-1)}(1 + o(1)) \quad \text{as } y \to \infty, \text{ with } C \neq 0. \tag{3.2.14}$$

In summary, these results yield that equation (3.2.9) admits an

$$m\text{-dimensional subset of admissible solutions as } y \to \infty. \tag{3.2.15}$$

Subsequently, for the nonlinear equation (3.2.7) we are going to look for profiles $f(y)$ having the algebraic decay given by (3.2.14). Then for such similarity solutions (3.2.6) the limit-time profile is bounded for any $x \neq 0$ and is given by

$$u_S(x, T^-) = C|x|^{-2m/(p-1)}. \tag{3.2.16}$$

Asympotic and numerical computations suggest that the solutions of (3.2.7) which satisfy (3.2.14) are *isolated* and that the constant C plays a role of a *nonlinear* eigenvalue. That is we expect there to be only a discrete set of possible solutions, which will be seen to be a feature of the blow-up problems in this thesis, but not of the decay problems.

Likewise for (3.1.1), the self-similar solution is given by

$$u_S(x,t) = -\ln(T-t) + f(y), \tag{3.2.17}$$

where the function $f(y)$ satisfies the ODE

$$\mathcal{L}f + G_e(f) = 0 \tag{3.2.18}$$

with the symmetry conditions (3.2.8). We look for similarity profiles $f(y) \to -\infty$ "slowly" as $y \to \infty$. The limit as $f \to -\infty$ in $G_e(f) = -1$ so we first consider the "linearized" equation

$$\mathcal{L}f = 1. \tag{3.2.19}$$

Setting $f(y) = -2m \ln y + g(y)$ for $y > 0$, we obtain

$$\mathcal{L}g = 1 + 2m\,\mathcal{L} \ln y \;=\; 2m(-1)^{m+1} D_y^{2m} \ln y = O(y^{-2m}) \quad \text{as } y \to +\infty. \tag{3.2.20}$$

As above, the homogeneous equation $\mathcal{L}g = 0$ has an $(m-1)$-dimensional subspace of exponentially decaying solutions. The inhomogeneous equation (3.2.20) has solutions $g(y) = C + o(1)$ as $y \to +\infty$, so that (3.2.15) holds for equation (3.2.19) admitting an m-dimensional subset of solutions satisfying

$$f(y) = -2m \ln |y| + C + o(1) \quad \text{as} \quad y \to \infty. \tag{3.2.21}$$

In this case the limit-time profile is given by

$$u_S(x, T^-) = -2m \ln |x| + C,$$

where again the constant $C \in \mathbf{R}$ is a certain isolated nonlinear eigenvalue which can be approximated asymptotically, see Section 3.5.

Obviously, the ODEs (3.2.7) and (3.2.18) admit constant solutions $f_{p,e}^*$ satisfying

$$G_p(f_p^*) = 0, \; f_p^* = \beta^\beta \quad \text{and} \quad G_e(0) = 0, \; f_e^* = 0,$$

respectively (the trivial solution $f = 0$ also solves (3.2.7) but plays no part in blow-up). The linearization of the operator $\mathcal{L} + G_p$ about $\beta^\beta = 1/(p-1)^{(}1/(p-1))$ and $\mathcal{L} + G_e$ about 0 coincide and are equal to $\mathcal{L} + I$, where I is the identity operator. The spectral properties of this asymmetric operator in a weighted L^2-space play an important part in our analysis and are necessary to describe the perturbation of the solutions from the constant state. They are essential to describe the long time dynamics of both of the PDEs (3.2.3) and (3.2.5) and so we briefly review them before moving on to the asymptotic analysis.

3.3 The spectral properties of $\mathcal{L}$ and its adjoint

In this Section we study the spectral properties of the linear differential operator $\mathcal{L}$ and its adjoint $\mathcal{L}^*$ given by

$$\mathcal{L}^* = (-1)^{m+1} D_y^{2m} + \frac{1}{2m} y \frac{d}{dy} + \frac{1}{2m} I. \tag{3.3.1}$$

Both operators are not symmetric and do not admit a self-adjoint extension. To determine the nature of the stability of the constant solution and also to apply the Fredholm alternative to compute asymptotic solutions of the ODEs, it is necessary to determine the spectrum and corresponding eigenfunctions of both $\mathcal{L}$ and $\mathcal{L}^*$. We present some

results from Egorov et al. (2002) and Galaktionov (2001) which describe these.

3.3.1 The fundamental solution

We start by determining the spectrum and the eigenfunctions of the adjoint operator $\mathcal{L}^*$. To first find the null eigenfunction, we begin with the fundamental solution of the corresponding linear $2m$th-order parabolic operator. Consider the linear equation

$$u_t = (-1)^{m+1} D_x^{2m} u \quad \text{in } \mathbf{R} \times \mathbf{R}_+. \tag{3.3.2}$$

The fundamental solution of (3.3.2) has the standard self-similar form

$$b(x,t) = t^{-1/2m} F(y), \quad y = x/t^{1/2m}. \tag{3.3.3}$$

Substituting $b(x,t)$ into (3.3.2) yields that the radially symmetric profile $F(y)$ is the unique even square integrable solution of the linear ODE

$$\mathcal{L}^* F = 0 \quad \text{in } \mathbf{R}, \tag{3.3.4}$$

and is the null eigenfunction of $\mathcal{L}^*$. Taking a Fourier transform leads to

$$F(y) = \alpha \int_0^\infty e^{-s^{2m}} \cos(sy) ds. \tag{3.3.5}$$

The coefficient α is chosen to normalize $\int F = 1$, so that

$$\alpha = \left(\int_0^\infty \int_0^\infty e^{-s^{2m}} \cos(sy)\, ds\, dy \right)^{-1}.$$

The rescaled kernel $F(y)$ then satisfies a standard pointwise estimate (Eidelman 1969)

$$|F(y)| \le d_1 e^{-d_2 |y|^\nu} \quad \text{in } \mathbf{R}, \qquad \text{where } \nu = \frac{2m}{2m-1}, \tag{3.3.6}$$

where d_1 and d_2 are positive constants. Applying the Fourier transform to equation (3.3.2) and performing the rescaling, we have

$$\mathcal{F}(b(\cdot,t))(\xi) = e^{-\xi^{2m} t} \quad \text{and} \quad \hat{F}(\omega) = \mathcal{F}(F(\cdot))(\omega) = e^{-\omega^{2m}}. \tag{3.3.7}$$

3.3.2 The discrete real spectrum and eigenfunctions of the adjoint operator $\mathcal{L}^*$

We describe the spectrum $\sigma(\mathcal{L}^*)$ of the adjoint operator in the weighted space $L^2_{\rho^*}(\mathbf{R})$ with the exponential weight

$$\rho^*(y) = e^{a|y|^\nu} > 0 \quad \text{in } \mathbf{R} \tag{3.3.8}$$

where $a \leq 2d_2$ is a sufficiently small positive constant. Denoting by $\langle \cdot, \cdot \rangle_*$ and $\| \cdot \|_*$ the corresponding inner product and the induced norm respectively we introduce a weighted Hilbert space of functions $H^{2m}_{\rho^*}(\mathbf{R})$ with the inner product and the norm

$$\langle v, w \rangle_* = \int_{\mathbf{R}} \rho^*(y) \sum_{k=0}^{2m} D^k v(y)\, \overline{D^k w(y)}\, dy, \quad \|v\|_*^2 = \int_{\mathbf{R}} \rho^*(y) \sum_{k=0}^{2m} |D^k v(y)|^2\, dy.$$

Then $H^{2m}_{\rho^*}(\mathbf{R}) \subset L^2_{\rho^*}(\mathbf{R}) \subset L^2(\mathbf{R})$, and $\mathcal{L}^*$ is a bounded linear operator from $H^{2m}_{\rho^*}(\mathbf{R})$ to $L^2_{\rho^*}(\mathbf{R})$. With these definitions, the spectral properties of the operator $\mathcal{L}$ are given by the following Lemma (Egorov et al. 2002, Galaktionov 2001).

Lemma 3.3.1. *(i) The spectrum of $\mathcal{L}^*$ (and hence of $\mathcal{L}$) comprises real simple eigenvalues only,*

$$\sigma(\mathcal{L}^*) = \{\lambda_k = -k/2m,\ k = 0, 1, 2, ...\}. \tag{3.3.9}$$

(ii) The eigenfunctions of $\mathcal{L}^*$, $\psi^*_k(y)$ are given by

$$\psi^*_k(y) = \frac{(-1)^k}{\sqrt{k!}} D^k F(y), \quad k = 0, 1, 2, ..., \tag{3.3.10}$$

and form a complete subset in $L^2(\mathbf{R})$ and in $L^2_{\rho^*}(\mathbf{R})$. (Here F is as defined in (3.3.5).) *(iii) The resolvent $(\mathcal{L}^* - \lambda I)^{-1} : L^2_{\rho^*}(\mathbf{R}) \to L^2_{\rho^*}(\mathbf{R})$ for $\lambda \notin \sigma(\mathcal{L}^*)$ is a compact integral operator.*

Most importantly, the operators $\mathcal{L}^*$ and $\mathcal{L}$ have zero Morse index (no eigenvalues have positive real part).

3.3.3 The polynomial eigenfunctions of the operator $\mathcal{L}$

We now consider the operator $\mathcal{L}$ (3.2.4) in the weighted space $L^2_\rho(\mathbf{R})$ ($\langle \cdot, \cdot \rangle$ and $\| \cdot \|$ are the inner product and the norm) with the exponentially decaying weight function

$$\rho(y) \equiv 1/\rho^*(y) = e^{-a|y|^\nu} > 0, \tag{3.3.11}$$

and ascribe to $\mathcal{L}$ the domain $H^{2m}_\rho(\mathbf{R})$, which is dense in $L^2_\rho(\mathbf{R})$. Then $\mathcal{L}:\ H^{2m}_\rho(\mathbf{R}) \to L^2_\rho(\mathbf{R})$ is a bounded linear operator, $\mathcal{L}^*$ is adjoint to $\mathcal{L}$ and denoting by $\langle \cdot, \cdot \rangle$ the inner

product on $L^2(\mathbf{R})$, we have

$$\langle \mathcal{L}v, w\rangle = \langle v, \mathcal{L}^* w\rangle \quad \text{for any } v \in H^{2m}_{\rho}(\mathbf{R}),\ w \in H^{2m}_{\rho^*}(\mathbf{R}). \tag{3.3.12}$$

The eigenfunctions of $\mathcal{L}$ take a particularly simple polynomial form and are as follows.

Lemma 3.3.2. *(i) The eigenfunctions $\psi_k(y)$ of $\mathcal{L}$ are polynomials in y of order k given by*

$$\psi_k(y) = \frac{1}{\sqrt{k!}} \sum_{j=0}^{\lfloor -\lambda_k \rfloor} \frac{(-1)^{mj}}{j!} D^{2mj} y^k, \quad k = 0, 1, 2, ..., \tag{3.3.13}$$

and form a complete subset in $L^2_{\rho}(\mathbf{R})$. (Here $\lfloor \cdot \rfloor$ denotes the integer part.)
(ii) $\mathcal{L}$ has compact resolvent $(\mathcal{L} - \lambda I)^{-1}$ in $L^2_{\rho}(\mathbf{R})$ for $\lambda \notin \sigma(\mathcal{L})$.

Corollary 3.3.3. *With the definition* (3.3.10) *of the adjoint basis, integrating by parts, we have that the orthonormality condition*

$$\langle \psi_k, \psi_l^* \rangle = \delta_{k,l} \quad \text{for any } k, l \geq 0, \tag{3.3.14}$$

holds where $\delta_{k,l}$ is the Kronecker delta.

Corollary 3.3.4. *If $m = 2$, then there are coefficients α_j (depending on k) such that for $k = 4r + 2$ and $k = 4r$*

$$\psi_{4r+2} = y^2 \sum_{j=0}^{r} \alpha_j y^{4j} \quad \text{and} \quad \psi_{4r} = \sum_{j=0}^{r} \alpha_j y^{4j},\ \alpha_0 \neq 0.$$

For example, if $m = 2$ (a case we consider in detail first), then the first four even eigenfunctions are

$$\psi_0(y) = 1, \quad \psi_2(y) = y^2/\sqrt{2}, \quad \psi_4(y) = (y^4 + 24)/\sqrt{24}, \quad \psi_6(y) = y^2(720 + y^4)/\sqrt{6!}, \tag{3.3.15}$$

with corresponding eigenvalues $0, -1/2, -1, -3/2$.

3.4 Local asymptotic analysis: invariant subspaces and bifurcation points

In this section we use the spectral properties of the linearized operators to determine the local stability of the constant solutions of the rescaled PDEs (3.2.3) and (3.2.5). We begin with the linearized stability analysis and describe the invariant subspaces.

3.4.1 Invariant eigenspaces

Since the nonlinearities under consideration satisfy $G_p'(\beta^\beta) = G_e'(0) = 1$, let us consider solutions of (3.2.3) and (3.2.5) as perturbations of the constant solution of the form

$$\theta(y,\tau) = f^* + g(y,\tau) \quad \text{with } \|g\|_\rho \ll 1.$$

In both cases g satisfies a perturbed PDE

$$g_\tau = (\mathcal{L} + I)g + \bar{G}(g), \quad \text{where } \bar{G}(g) = G(f^* + g) - g, \tag{3.4.1}$$

with a quadratic nonlinear perturbation $\bar{G}$

$$\bar{G}(g) = c_2 g^2 + c_3 g^3 + ... \quad \text{as} \quad g \to 0, \tag{3.4.2}$$

with the coefficients depending on the nonlinearity, $c_2 = 1/2$, $c_3 = 1/6$,... for G_e and $c_2 = p(p-1)^{1/(p-1)}/2$, $c_3 = p(p-1)^{2/(p-1)}(p-2)/6$,... for G_p.

In what follows we restrict our attention to symmetric in x solutions $u = u(|x|,t)$ and hence to symmetric in y rescaled solutions $\theta = \theta(|y|,\tau)$ and $g = g(|y|,\tau)$. In the space $L^2_{0,\rho}(\mathbf{R})$ of symmetric functions, it follows from (3.3.9), that $\mathcal{L} + I$ has the spectrum

$$\sigma(\mathcal{L} + I) = \{\tilde{\lambda}_k = 1 - k/2m, \ k = 0, 2, 4, ...\}. \tag{3.4.3}$$

By the completeness of the eigenfunctions (Lemma 3.3.2) we have that

$$L^2_{0,\rho}(\mathbf{R}) = E^u(0) \oplus E^c(0) \oplus E^s(0),$$

where $E^u(0)$, $E^c(0)$ and $E^s(0)$ are the unstable, centre and stable subspaces of $\mathcal{L} + I$, and for $m > 1$ are given by

$$\begin{aligned} E^u(0) &= \text{Span}\{\psi_0, \psi_2, ..., \psi_{2m-2}\}, \\ E^c(0) &= \text{Span}\{\psi_{2m}\}, \\ E^s(0) &= \text{Span}\{\psi_{2m+2}, \psi_{2m+4}, ...\}. \end{aligned}$$

In particular the dimension of the unstable subspace is precisely m.

Consider the two one-dimensional unstable subspaces corresponding to the first two positive eigenvalues of the operator $\mathcal{L} + I$ namely

$$\tilde{\lambda}_0 = 1, \ \psi_0(y) = 1 \quad \text{and} \quad \tilde{\lambda}_2 = 1 - 1/m, \ \psi_2(y) = y^2/\sqrt{2}. \tag{3.4.4}$$

As is usual in blow-up problems, the first unstable mode with $k = 0$ corresponds to the instability of blow-up behaviour with respect to perturbations of the blow-up time T.

In contrast, the second mode with $k = 2$ describes an actual instability of the constant solution which is in the direction of $\psi_2(y)$ and is in the space of rescaled solutions having the same fixed blow-up time T. (The first odd mode with eigenvalue $\tilde{\lambda}_1 = 1 - 1/2m$ corresponds to shifts of the blow-up point $x = 0$.) From our asymptotic calculations and numerical experiments we expect that the orbits which arise from the instability of the constant solution in the PDEs (3.2.5) and (3.2.3) when $m > 1$ are uniformly bounded, and stabilize to one of the self-similar solutions. Namely, the first such unstable mode with $\tilde{\lambda}_2 = 1 - 1/m > 0$ gives a heteroclinic connection of f^* with a non-constant stable (generic) similarity profile $f_1(y)$.

It is significant that when $m = 1$ there is no such unstable mode. In contrast the dimension of the unstable subspace is one, corresponding only to the change in the blow-up time. The eigenfunction ψ_2 then has eigenvalue zero and the behaviour of the perturbations of the constant solution must be studied on the centre manifold. It is this which leads to the approximately self-similar behaviour (1.5.3) mentioned in the Introduction.

Before performing some formal invariant manifold analysis for higher-order PDEs, note that the basic properties of connecting equilibria and transversality of intersections of the corresponding stable and unstable manifolds are known for the one-dimensional second-order parabolic equations

$$u_t = u_{xx} + f(x,u) \quad \text{in } (0,1) \times \mathbf{R}_+, \quad u = 0 \text{ at } x = 0,1 \text{ for } t > 0,$$

and were obtained in Henry (1985) and Angenent (1986) using Sturm's Theorem on the non-increase of the number of zeros (intersections) of solutions to linear second-order parabolic equations. The general the structure of connecting orbits remains an important open problem as the Sturmian property is not true for the fourth and higher-order parabolic equations (owing to the lack of a maximum principle in these cases).

3.4.2 The centre subspace

Consider the centre subspace $E^c(0)$ in the case of general m. From Lemma 3.2, it follows that the null eigenfunction of the operator $\mathcal{L}$ is given by ψ_{2m} so that

$$\tilde{\lambda}_{2m} = 0 \quad \text{and} \quad \psi_{2m}(y) = \left(y^{2m} + (-1)^m (2m)!\right) / \sqrt{(2m)!}\,. \tag{3.4.5}$$

We now present a simple calculation showing that the behaviour on the centre manifold is semi-stable.

Proposition 3.4.1. *Let $g(\cdot,\tau) \in H^{2m}_{0,\rho}(\mathbf{R})$ exhibit the centre subspace dominance, so*

that

$$g(\cdot,\tau) = a_{2m}(\tau)\psi_{2m}(\cdot) + w(\cdot,\tau) \quad \textit{for } \tau \gg 1, \tag{3.4.6}$$

where $w \in \mathcal{L}^{\perp}$ *and* $w(\cdot,\tau) = o(\|g(\cdot,\tau)\|_{\rho}) = o(|a_{2m}(\tau)|)$ *as* $\tau \to \infty$. *Then*

$$a_{2m}(\tau) = -\frac{1}{\gamma_0 \tau}(1 + o(1)) \quad \textit{as } \tau \to \infty, \textit{ where } \gamma_0 = c_2\langle(\psi_{2m})^2, \psi^*_{2m}\rangle \neq 0. \tag{3.4.7}$$

It follows from (3.4.7) that $a_{2m}(\tau)$ cannot change sign in any neighbourhood of $\tau = \infty$ meaning a one-sided instability of the centre manifold behaviour.

Proof. We look for a solution of (3.4.1) via a uniformly convergent eigenfunction expansion

$$g(\cdot,\tau) = \sum a_k(\tau)\psi_k(\cdot). \tag{3.4.8}$$

Substituting this expression into (3.4.1) and taking the inner product with ψ^*_k in $L^2(\mathbf{R})$, we arrive at a dynamical system for the expansion coefficients

$$\dot{a}_k = \tilde{\lambda}_k a_k + \langle \bar{G}(g), \psi^*_k\rangle, \quad k = 0, 2, \ldots. \tag{3.4.9}$$

Consider equation for the coefficient a_{2m} with $\tilde{\lambda}_{2m} = 0$. In view of assumption (3.4.6) and (3.4.2), assuming that $|a_{2m}(\tau)| \ll 1$, it follows that

$$\dot{a}_{2m} = (\gamma_0 + o(1))a^2_{2m} \quad \text{for } \tau \gg 1. \tag{3.4.10}$$

Calculating γ_0 by using the adjoint eigenfunction $\psi^*_{2m} = D^{2m}_y F/\sqrt{2m!}$ and (3.4.5), we obtain that

$$\gamma_0 = c_2(-1)^{m+1}\sqrt{(2m!)}\left(\frac{(4m)!}{[(2m)!]^2} - 2\right). \tag{3.4.11}$$

Integrating (3.4.10) as a standard ODE, we deduce that any small solution for $\tau \gg 1$ has the asymptotic behaviour (3.4.7). □

It follows from the quadratic "ODE" (3.4.10) that the centre manifold behaviour exhibits a typical semi-stable ("saddle-node") structure. Because the constant profile β^{β} is only semi-stable small perturbations in the unstable direction may evolve to self-similar solutions. Asymptotic support for this conjecture is presented in Section 3.5 and numerical evidence in 3.6. An evolutionary argument may be found in Budd et al. (2002).

In view of the known spectral and sectorial properties of the operators $\mathcal{L}$ and $\mathcal{L}^*$ (Egorov et al. 2002), (Galaktionov 2001), we expect that the centre (and stable, see Section 3.7) manifold behaviour can be justified by the invariant manifold theory posed in interpolation spaces, see Lunardi (1995, Chap. 9).

3.4.3 Bifurcation points

In this subsection we extend the ODEs (3.2.7) and (3.2.18) for similarity profiles and consider the family of ODEs with a parameter $\mu \geq 0$

$$(-1)^{m+1} D_y^{2m} f - \mu f' y + G(f) = 0 \quad \text{for } y > 0 \text{ with conditions (3.2.8).} \tag{3.4.12}$$

Recall that for single-point blow-up we need to impose an extra condition (of the type (3.2.14) or (3.2.21) with $1/2m \mapsto \mu$) on the decay of $f(y)$ at infinity.

If we take $\mu = 1/2m$ and the appropriate nonlinearity, $G = G_p$ or G_e, then we obtain the ODEs (3.2.7) and (3.2.18) for the rescaled self-similar profiles. More generally, suitable solutions of (3.4.12) are expected to depend smoothly upon $\mu \approx 1/2m$ and coincide with the self-similar solutions when $\mu = 1/2m$. In either case we define a corresponding linearized operator $\mathcal{L}_\mu$ by

$$\mathcal{L}_\mu = (-1)^{m+1} D_y^{2m} - \mu y D_y + I \equiv \mathcal{L} + (1 - \mu + 1/2m) I. \tag{3.4.13}$$

Changing the independent variable to

$$y = z/(2m\mu)^{1/2m}, \tag{3.4.14}$$

we have

$$\frac{1}{2m\mu} \mathcal{L}_\mu = (-1)^{m+1} D_z^{2m} - \frac{1}{2m} z \frac{d}{dz} + \frac{1}{2m\mu} I \equiv \mathcal{L} + \frac{1}{2m\mu} I. \tag{3.4.15}$$

Hence $\mathcal{L}_\mu : H^{2m}_{0,\rho}(\mathbf{R}) \to L^2_{0,\rho}(\mathbf{R})$ is a bounded linear operator (with a change in the coefficient a in the weight function (3.3.11) if necessary). By Lemma 3.3.1 the spectrum $\mathcal{L}_\mu$ in the space $L^2_{0,\rho}(\mathbf{R})$ of radial functions is given by

$$\sigma(\mathcal{L}_\mu) \equiv 2m\mu\sigma\left(\mathcal{L} + \frac{1}{2m\mu} I\right) = \{1 - 2\mu l,\ l = 0, 1, 2, ...\}, \tag{3.4.16}$$

with eigenfunctions ψ_{2l} as before, rescaled according to the transformation (3.4.14).

We next compute bifurcation points from the constant solution f^*. Since the weight function (3.3.11) is exponentially decaying as $y \to \infty$, in general, the inclusion $f \in H^{2m}_\rho$ does not imply the boundedness of f unlike the adjoint case with the increasing weight (3.3.8) where $H^{2m}_{\rho^*} \subset C$. The nonlinearity $G(f)$ is not uniformly Lipschitz continuous on bounded subsets from H^{2m}_ρ. To overcome this we truncate the nonlinearity in (3.4.12) by replacing G by G_n satisfying

$$G_n(f) \equiv G(f) \text{ for } |f| \leq n, \ \ n = 1, 2, \ ...$$

and $G_n(f)$ is sufficiently smooth and uniformly Lipschitz continuous in $\mathbf{R}$. For $G = G_e$

we need only perform the truncation for $f > n$. We have

$$G_n(f) \to G(f) \quad \text{as } n \to \infty \text{ uniformly on compact subsets.}$$

Replacing the full problem by the truncated one,

$$(-1)^{m+1} D_y^{2m} f - \mu y f' + G_n(f) = 0. \tag{3.4.17}$$

is permissible because we are interested in bounded solutions f for which the nonlinearities $G_p(f)$ and $G_e(f)$ have finite range.

Proposition 3.4.2. *For any $m \geq 1$, the values of μ for which the spectrum of $\mathcal{L}_\mu$ contains zero,*

$$1 - 2\mu l = 0 \implies \mu_l = 1/2l, \; l = 1, 2, \ldots, \tag{3.4.18}$$

are bifurcation points for problem (3.4.17).

Proof. Using rescaling (3.4.14) and setting $f = f^* + g$, equation (3.4.17) takes the form

$$(\mathcal{L} - I)g = \tilde{\mu} g + (1 + \tilde{\mu}) G_n(g), \quad \text{where } \tilde{\mu} = -1 - 1/2m\mu. \tag{3.4.19}$$

Consider the Hammerstein operator $(\mathcal{L} - I)^{-1} G_n$. By Lemma 3.3.2, $(\mathcal{L} - I)^{-1}$ is a compact operator in $L^2_{0,\rho}$ with simple eigenvalues $\{-1/(1 + l/m) \leq -1, \, l = 0, 1, 2, \ldots\}$. By construction, G_n is uniformly Lipschitz continuous, $|G_n(g)| \leq C_1 + C_2|g|$ in $\mathbf{R}$, and hence $G_n : L^2_{0,\rho} \to L^2_{0,\rho}$. Therefore, the product $(\mathcal{L} - I)^{-1} G_n$ is a compact operator in $L^2_{0,\rho}$, see e.g. Krasnosel'skii (1964, Chap. 5). Hence, in the nonlinear integral equation written as a fixed point problem

$$g = \mathbf{A}(g, \tilde{\mu}) \equiv \tilde{\mu} (\mathcal{L} - I)^{-1} g + (1 + \tilde{\mu})(\mathcal{L} - I)^{-1} G_n(g), \tag{3.4.20}$$

bifurcation from the origin occurs if and only if $\tilde{\mu}$ coincides with the characteristic values of $(\mathcal{L} - I)^{-1}$ (simple eigenvalues of $\mathcal{L} - I$), i.e., at $\tilde{\mu}_l = -1 - l/m$ (Krasnosel'skii 1964). This yields (3.4.18). □

It is worth mentioning that in passing to the limit $n \to \infty$, some of the bifurcation sub-branches (which are not of physical interest) may disappear, so that we always need to check which sub-branches are available for $n = \infty$. On the other hand, it is interesting to know for which values of μ, lesser or greater than μ_l, there exist non-constant solutions and how many. Since the spectrum of the Frechet derivative $\mathbf{A}'(0, \tilde{\mu}_l)$

$$\sigma(\mathbf{A}'(0, \tilde{\mu}_l)) = \{(1 + l/m)/(1 + k/m), \; k = 0, 1, 2, \ldots\} \tag{3.4.21}$$

always contains 1 (for $k = l$), the local asymptotic behaviour of bifurcation branches for $\mu \approx \mu_l$ is a delicate problem, and often there exist at least two solutions even in the

cases of analytic nonlinearities, see a general theory in Vainberg and Trenogin (1974). Therefore we will need an extra matching analysis to specify the "correct" branches which have the required behaviour at infinity and hence correspond to single-point blow-up similarity profiles.

It is important to mention another reason for extending the operator (3.2.4) in (3.2.7) and (3.2.18) to the operator in (3.4.12) parameterized by μ. Setting $\mu = 0$, in the case of the polynomial nonlinearity with $G = G_p$, we recover a well-studied Hamiltonian system, see Amick and Toland (1992) and the book by Peletier and Troy (2001), and the solutions considered in this case can, in principle, be followed as μ increases to the physically important value of $1/2m$. Alternatively, by setting μ close to the bifurcation points (3.4.18) we can construct asymptotic descriptions of solutions which are local perturbations of the constant solution. This calculation is presented in the next section. Once we have constructed such solutions we may extend again varying μ to determine branches of solutions that extend to the value $\mu_m = 1/2m$.

In other words, problem (3.4.12) for $\mu \in [0, 1/2m]$ describes the *transition* phenomenon between Hamiltonian systems for $\mu = 0$ with a potential and leading self-adjoint differential operators and the singularity formation problem for $\mu = 1/2m$ with no potential structure or symmetry properties of the operators involved.

3.4.4 A conjecture on the existence of a set of self-similar solutions

For any $m > 1$, the questions of the solvability of problem (3.4.12) with $\mu = 1/2m$ (with the appropriate decay of $f(y)$ at infinity) and of the number of solutions seem to be very hard. It is a multi-dimensional problem of matching of the m-dimensional bundle of orbits as $y \to \infty$ (see (3.2.15)) with the m-dimensional bundle at $y \approx 0$ depending on the parameters $\{f(0), f''(0), ..., f^{(2m-2)}(0)\}$ (a multi-dimensional shooting problem whose complexity increases dramatically as m increases). For $m = 1$, such problems for quasilinear equations (1.5.1) are well understood in one dimension (see Samarskii et al. (1995) and Budd and Galaktionov (1998)), though a complete proof of the number, finite or infinite, of solutions for equations in $\mathbf{R}$ and in $\mathbf{R}^N$ is still missing.

We now use the above local bifurcation analysis to estimate the number of solutions from below. In view of Proposition 3.4.2 there exist branches of solutions $f(y;\mu)$ emanating at $\mu = 1/2l$ from constant solutions $f = f^*$ for each value of $l = 1, ..., m-1$ (though we still do not know which bifurcation branches correspond to single point blow-up profiles with the required decay at infinity). In particular, if we fix m, then a self-similar solution occurs at $\mu_m = 1/2m$. However, there are $m-1$ bifurcation points at $\mu_l = 1/2l > \mu_m = 1/2m$ for $l = 1, ..., m-1$. The numerical calculations of Section 3.6 strongly imply that each such bifurcation leads to a branch of solutions $f(y)$ with far-field behaviour of the type (3.2.14) or (3.2.21), which persists until μ_m giving rise to a self-similar solution. Furthermore, due to the semi-stability properties of the

centre manifold patterns and the positivity properties of the associated eigenfunctions (see further comments in Section 3.5) we expect from the observations of the previous section, that there is an additional solution of the ODE when m is even. This detail is also supported by both the asymptotic calculations presented in Section 3.5 and the numerical calculations of Section 3.6. Combining these observations, let us state the following conjecture suggested by our understanding of the dynamics of the linearized operator, asymptotic constructions and a number of numerical experiments.

Conjecture 3.4.3. *For all $m > 1$, the problems (3.2.18), and (3.2.7) have at least $2\lfloor m/2 \rfloor$ solutions.*

Hence we conjecture that the non-existence of exact self-similar blow-up solutions is a feature only of the second-order semilinear equations, not of all the semilinear equations of the forms (3.1.1) and (3.1.2). This conjecture is indeed a lower bound and is based only on the properties of the linear operator presented in this Chapter. Numerical calculations imply the existence of more solutions not connected to the bifurcation problem (3.4.20), in fact, we expect that there may be up to $m(m-1)$ solutions.

Further, we note that bifurcations in the limit problem (3.4.12) hold for arbitrary $L^2_{0,\rho}$-solutions of (3.4.19), not necessarily satisfying the appropriate decay conditions at infinity. There may also exist non-constant solutions which correspond to stabilization as $y \to \infty$ to another equilibrium,

$$f(y) \to \beta^\beta \text{ for } G = G_p \quad \text{and} \quad f(y) \to 0 \text{ for } G = G_e\,. \tag{3.4.22}$$

One can see from (3.2.6) and (3.2.17) that these self-similar solutions create *global blow-up*, where

$$u(x,t) \to \infty \quad \text{as } t \to T^- \text{ uniformly in } \mathbf{R}. \tag{3.4.23}$$

Such behaviour is unavailable for $m = 1$ as the dimension of the stable manifold about f^* is $(m-1)$ as there is no algebraically decaying mode . For $m > 1$, no such solutions have yet been detected, numerically or otherwise.

3.5 The asymptotic behaviour of the solutions close to the bifurcation points

In this Section we again consider μ to be a continuous parameter in (3.4.12) and construct an asymptotic description of solutions $f(y;\mu)$ (with the appropriate decay at infinity, see a precise statement below) for μ close to the bifurcation points at $\mu_l = 1/2l$. We set

$$\mu = \mu_l + \sigma_l \varepsilon \quad \text{with } 0 < \varepsilon \ll 1 \text{ and } \sigma_l^2 = 1, \tag{3.5.1}$$

and look for solutions to the ODEs in $\mathbf{R}_+$ for $l = 1, 2, ...$

$$(-1)^{m+1} f^{(2m)} - (\mu_l + \sigma_l \varepsilon)\, y f' + G_p(f) = 0, \tag{3.5.2}$$

$$(-1)^{m+1} f^{(2m)} - (\mu_l + \sigma_l \varepsilon)\, y f' + G_e(f) = 0. \tag{3.5.3}$$

We seek solutions with symmetry conditions (3.2.8) satisfying the decay condition

$$f(y) = C y^{-1/(p-1)\mu}(1+o(1)) \quad \text{or} \quad f(y) = -\mu^{-1} \ln y + C + o(1) \quad \text{as } y \to +\infty. \tag{3.5.4}$$

Here $\sigma_l = \pm 1$ indicates the direction that the branch departs from the constant solution, which we shall show depends upon l and m. Because of the polynomial structure of the eigenfunctions of the linear operator $\mathcal{L}$ (and hence of $\mathcal{L}_\mu$) the asymptotic calculations are similar in spirit for each bifurcation point, $\mu = 1/2l$, although for each order $2m$ of the differential operator there are m slightly different types of expansion. As such we will illustrate the calculations by first considering the case $m = 2$ close to arbitrary bifurcation points, then close to the particular bifurcation points of interest to fourth order PDEs, namely $\mu_1 = 1/2$ and $\mu_2 = 1/4$. Lastly, we construct solutions close to the specific bifurcation points $\mu_m = 1/2m$ for the case of general m to complement the calculations of the centre manifold behaviour described in the previous section and our conjecture regarding the existence of self-similar solutions of the ODE when $\mu = 1/2m$.

3.5.1 The case of fourth-order ODEs: $m = 2$

We shall first consider the two ordinary differential problems, namely finding the slowly growing/bounded solutions of the fourth order equations with $l = 1, 2, ...$

$$-f'''' - (\mu_l + \sigma_l \varepsilon)\, y f' + |f|^{p-1} f - f/(p-1) = 0, \tag{3.5.5}$$

$$-f'''' - (\mu_l + \sigma_l \varepsilon)\, y f' + e^f - 1 = 0. \tag{3.5.6}$$

The calculation proceeds by identifying three key regions (see Figure 3.1) in which asymptotic solutions of three different scalings of the above equations are derived. The three different asymptotic descriptions of the solutions are then matched together. The first region is given by considering solutions for which $\varepsilon^\gamma y$ is small and where

$$\gamma = \begin{cases} \frac{1}{4l} \text{ for } l \text{ odd}, \\ \frac{1}{2l} \text{ for } l \text{ even}. \end{cases} \tag{3.5.7}$$

Here the solution is near constant and we can express the solution in terms of the eigenfunctions of the linear operator $\mathcal{L}_\mu$ in (3.4.13). Next is a mid-range region for which $\varepsilon^{-\gamma} < y < e^{1/\varepsilon}$ where the appropriately rescaled differential equations reduce to an integrable first order equation. Lastly, there is the region $y > e^{1/\varepsilon}$ where the

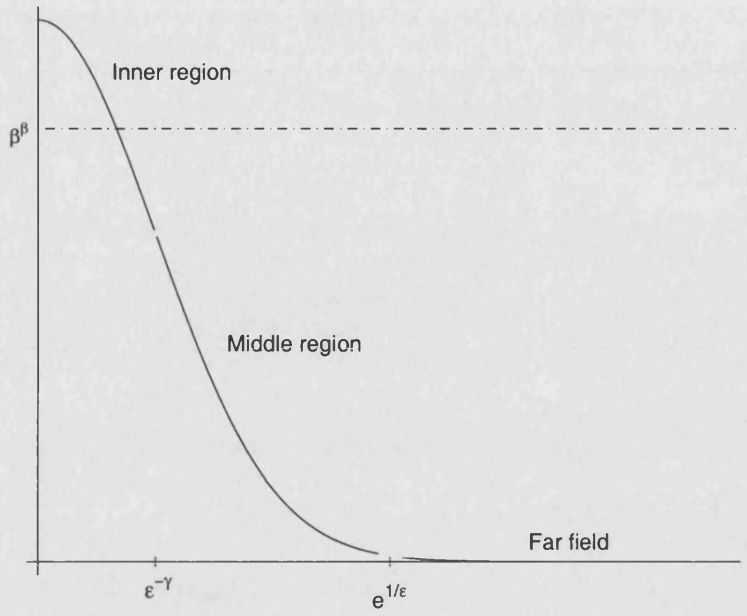

Figure 3.1: Sketch of the asymptotic regions.

solution coverges to the far-field behaviour (3.5.4).

The behaviour of $f(y)$ for $\varepsilon^\gamma y \ll 1$

We begin by seeking solutions to (3.5.5) and (3.5.6) which are valid for small $\varepsilon^\gamma|y|$ and which are close to the constant solutions of the respective nonlinearities. Consider the corresponding equation (3.4.20) for fixed points. Since by (3.4.21), 1 is an eigenvalue of $\mathbf{A}'(0,\tilde{\mu}_l)$ with the one-dimensional eigenspace E_l, according to the general branching theory in (Vainberg and Trenogin 1974, Chap. 5) in this special case we seek solutions in the form of the rational series

$$f(y) = f_0 + \varepsilon^q f_1(y) + \varepsilon^{2q} f_2(y) + \dots , \tag{3.5.8}$$

where we denote $f_0 = f^*$. The exponent $q = 1/n$, with an unknown integer $n \geq 1$, is to be determined from the solvability of the corresponding nonlinear systems on the expansion coefficients (the branching equation). Since dim $E_l = 1$, the branching equation is always one-dimensional. The rational power q of the order parameter depends on the coefficients of the asymptotic expansion which are different depending on whether l is even or odd. Substituting the expansion (3.5.8) into the ODEs, (3.5.2) or (3.5.3), leads, at lowest order, to an ODE for $f_1(y)$ of the form

$$\mathcal{L}_{1/2l} f_1 \equiv -f_1'''' - \frac{1}{2l} y f_1' + f_1 = 0.$$

Accordingly, the leading order approximation to $f - f_0$ is given by a linear multiple of the eigenfunction $\psi_{2l}((2/l)^{1/4}y)$, see (3.4.14). From the description of the spectrum of the operator $\mathcal{L}$ given in Lemma 3.1, using Corollary 3.2, we know that (as $m = 2$) the transformed operator $\mathcal{L}_{1/2l}$ has null eigenfunctions ψ_{2l} which are polynomials and take the form

$$\psi_{2l}(y) = y^2 \sum_{j=0}^{(l-1)/2} \alpha_j y^{4j} \text{ for } l \text{ odd} \quad \text{and} \quad \psi_{2l}(y) = \sum_{j=0}^{l/2} \alpha_j y^{4j} \text{ for } l \text{ even},$$

as defined by (3.3.13) after the change of variable $y \mapsto (2/l)^{1/4}y$.

The difference between the cases of l even and l odd is important and arises as follows. In the asymptotic expansion, the higher powers of $f_1(y)$ become forcing terms to equations involving the operator $\mathcal{L}_{1/2l}f_j$. In the case of odd l these terms will always be polynomials in y^4. Because of the separation of terms in the eigenfunctions these have no contribution which resonates with the null eigenfunction ψ_{2l} of $\mathcal{L}$. In contrast, the powers of $f_1(y)$ for even l will always have contributions which resonate with $\psi_{2l}(y)$. As a consequence, the cases l even and l odd lead to distinctly different forms of asymptotic expansion, in particular, $q = 1/2$ for odd l and $q = 1$ for even l. In other words, for l even and odd the expansion changes its type. Generically, there will be m distinct expansions in powers of $\varepsilon^{i/m}$, $i = 1, 2, ..., m$, see a general classification in Vainberg and Trenogin (1974, Section 12).

A THE CASE OF $m = 2$ AND l ODD. We take $l = 2r+1$ so that the bifurcation point is at $\mu = 1/(4r+2)$, $r = 0, 1, \ldots$. We express $f(y)$ as an asymptotic expansion ($q = 1/2$)

$$f = f_0 + \varepsilon^{1/2}f_1 + \varepsilon f_2 + \varepsilon^{3/2}f_3 + \ldots \ . \tag{3.5.9}$$

This expansion corresponds to the case of the branching equation as described in Theorem 12.2 in Vainberg and Trenogin (1974) where there exist two solutions either for $\mu < \mu_l$ or for $\mu > \mu_l$. Substituting the expansion (3.5.9) into either equation (3.5.5) or (3.5.6), gives a sequence of ODE problems of the form

$$O(\varepsilon^{1/2}): \quad \mathcal{L}_{1/2l}f_1 \equiv -f_1'''' - \frac{1}{4r+2}yf_1' + f_1 = 0, \tag{3.5.10}$$

$$O(\varepsilon): \quad \mathcal{L}_{1/2l}f_2 = -c_2f_1^2, \tag{3.5.11}$$

$$O(\varepsilon^{3/2}): \quad \mathcal{L}_{1/2l}f_3 = \sigma_l yf_1' - 2c_2f_1f_2 - c_3f_1^3, \ \ldots, \tag{3.5.12}$$

where $c_2, c_3, \ldots$ are as given in (3.4.2). In each case we seek solutions from $H_\rho^{2m}(\mathbf{R})$. In view of the asymptotic properties of the linearized operators in Section 3.2, the solutions are assumed to grow slowly (at worst polynomially) as y increases and which will ultimately be matched to solutions of the ODEs (3.5.2) and (3.5.3) which have the

correct behaviour at infinity, (3.5.4).

As observed above, it follows from (3.4.16) that the lowest order equation (3.5.10) can be solved in terms of a rescaling of the null eigenfunction ψ_{2l} of $\mathcal{L}_{2l}$. Applying in (3.3.13) the scaling $y \mapsto (2/(2r+1))^{1/4}y$, it follows that there is a constant α such that

$$f_1(y) = \alpha \tilde{f}_1(y), \quad \text{where } \tilde{f}_1(y) = \sum_{j=0}^{r} \left(\frac{(2r+1)}{2}\right)^{j-r-1/2} \frac{1}{j!} D^{4j} y^{4r+2}. \tag{3.5.13}$$

For example $f_1(y) = \alpha y^2$ when $r = 0$ and $\mu = 1/2$. Here the constant α is unspecified at this level of expansion and will be determined by a solvability condition for the higher order terms.

Applying the Fredholm alternative to the second equation (3.5.11) has a solution in $H^{2m}_{\rho}(\mathbf{R})$ at order ε only if the orthogonality condition.

$$\langle f_1^2, \psi_{2l}^* \rangle = 0, \tag{3.5.14}$$

holds, where $\psi_{2l}^*(y)$ defined in (3.3.10) is the eigenfunction of the adjoint operator $\mathcal{L}_{1/2l}^*$ and $y \mapsto (2/l)^{1/4}y$. If $r = 0$ and $l = 1$ then the first three even eigenfunctions of $\mathcal{L}_{1/2}$ are given in (3.3.15). Since ψ_2^* is the null eigenfunction of $\mathcal{L}_{1/2l}^*$, it follows that $\langle \psi_2^*, \psi_0 \rangle = 0$ and $\langle \psi_2^*, \psi_4 \rangle = 0$. Hence $\langle \psi_2^*, y^4 \rangle = \langle \psi_1, f_1^2 \rangle = 0$ so that the orthogonality (3.5.14) holds and there exists solutions of equation (3.5.11) at this order. This is the lack of resonance condition that we described earlier.

For arbitrary r, by (3.5.13),

$$f_1^2(y) = \alpha^2 \sum_{j=0}^{2r} a_j y^{4j+4}.$$

We can construct an exact solution of (3.5.11) in the form of a particular polynomial

$$\alpha^2 \tilde{f}_2(y) = -c_2 \alpha^2 \sum_{j=-1}^{2r} b_j y^{4j+4}. \tag{3.5.15}$$

Substituting it into the equation and equating the coefficients gives

$$b_{2r} = -a_{2r}, \qquad b_{-1} = 4!\, b_0 \qquad \text{and} \tag{3.5.16}$$

$$b_j = \frac{2r+1}{2(r-j)-1} \left(a_j + b_{j+1} \frac{(8+4j)!}{(4+4j)!} \right) \quad \text{for } j = 2r-1, \ldots, 0. \tag{3.5.17}$$

Hence, the orthogonality condition (3.5.14) holds. The general solution of (3.5.11) is then given by

$$f_2(y) = \alpha^2 \tilde{f}_2(y) + \alpha_1 \tilde{f}_1(y), \tag{3.5.18}$$

where α_1 is an extra real unknown.

The unknowns α and α_1 are determined by applying the Fredholm alternative at the next orders of expansion. In equation (3.5.12), similar to (3.5.14), the solvability condition is given by

$$\langle \sigma_l y f_1' - 2c_2 f_1 f_2 - c_3 f_1^3, \psi_{2l}^* \rangle = 0. \tag{3.5.19}$$

Substituting (3.5.13) and (3.5.18) yields the algebraic equation

$$\alpha A - \alpha^3 B + \alpha\alpha_1 C = 0, \tag{3.5.20}$$

where $A = \langle \sigma_l y f_1', \psi_{2l}^* \rangle$, $B = \langle c_3 \tilde{f}_1^3 + 2c_2 \tilde{f}_1 \tilde{f}_2, \psi_{2l}^* \rangle$ and the third coefficient C vanishes by the first solvability criterion (3.5.14),

$$C = -2C_2 \langle \tilde{f}_1^2, \psi_{2l}^* \rangle = 0. \tag{3.5.21}$$

Equation (3.5.20) is a cubic equation for the first unknown α only, $\alpha(\alpha^2 - \sigma_l \gamma) = 0$, where γ can be computed explicitly. The $\alpha = 0$ case simply corresponds to the constant solution (the trivial expansion (3.5.9)) and can be discarded. Hence, we have two solutions

$$\alpha = \pm\sqrt{\sigma_l \gamma}\,. \tag{3.5.22}$$

The sign of σ_l is thus the same as that of γ while the sign of α follows from matching to the far field solution (see Section 3.5.2). In general, the second unknown α_1 (together with an extra one α_3 obtained from the homogeneous equation (3.5.12), etc.) is to be determined from the solvability conditions of equations for the coefficients f_4, f_5,... of higher-order perturbations. Although not presented, higher approximations follow in a similar manner.

Example. To illustrate this calculation, we now look at the two cases of $l = 1$ and $l = 3$ for the quadratic nonlinearity with $p = 2$, where $G_p(f) = |f|f - f$. These are chosen so that the corresponding bifurcation points at $\mu = 1/2$ and $\mu = 1/6$ are on either side of the "self-similar" value of $\mu_2 = 1/4 = 1/2m$.

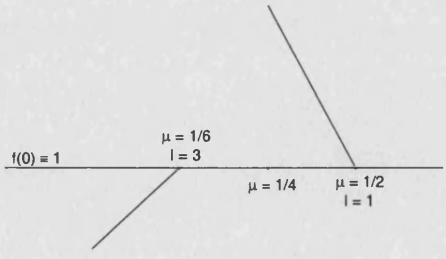

Figure 3.2: Sketch of the bifurcation points under consideration.

The first bifurcation point: $\mu_1 = 1/2$ ($l = 1$, $r = 0$). As observed above, when $l = 1$ we have $f_0 = 1$ and $f_1 = \alpha y^2$. A simple calculation then gives $\tilde{f}_2 = \alpha^2(y^4 + 24)$

and expansion (3.5.9) takes the form

$$f(y) = 1 + \alpha\varepsilon^{1/2}y^2 + \varepsilon\left(\alpha^2(y^4+24) + \alpha_1 y^2\right) + \varepsilon^{3/2}f_3(y) + \dots . \tag{3.5.23}$$

Observe that since $c_3 = 0$, the solvability condition (3.5.19) for f_3 is then given by

$$\langle 2\sigma_1\alpha y^2 - 2\alpha^3 y^2(y^4+24), \psi_2^*\rangle = 0, \quad \psi_2^* = \psi_2^*(2^{1/4}y). \tag{3.5.24}$$

To calculate α we exploit the fact that by (3.3.7) and (3.3.10) $\hat{\psi}_2^*(\omega) = -\omega^2 e^{-\omega^4}/\sqrt{2}$. Recall also that if a function $f(y)$ has Fourier transform $\hat{f}(\omega)$, then

$$\langle f, y^{2n}\rangle = (-1)^n \hat{f}^{(2n)}(0). \tag{3.5.25}$$

Taking $\psi_2^* = \psi_2^*(2^{1/4}y)$ yields $\langle\psi_2^*(2^{1/4}y), y^2\rangle = 1/2^{1/4}$, $\langle\psi_2^*(2^{1/4}y), y^6\rangle = -180/2^{1/4}$, the solvability condition (3.5.24) reduces to the cubic equation $\sigma_1\alpha + 156\alpha^3 = 0$ and hence

$$\sigma_1 = -1 \quad \text{and} \quad \alpha = \pm\frac{1}{\sqrt{156}} = \pm\frac{\sqrt{39}}{78}, \tag{3.5.26}$$

so that (3.5.23) yields

$$f(y) = 1 \pm \varepsilon^{1/2}\frac{y^2}{\sqrt{156}} + \varepsilon\left(\frac{1}{156}(y^4+24) + \alpha_1 y^2\right) + \dots . \tag{3.5.27}$$

The sign of α will be determined by matching to the solution in the mid-range. We show presently that $\alpha < 0$ so that

$$f(y) = 1 - \varepsilon^{1/2}\frac{y^2}{\sqrt{156}} + \varepsilon\left(\frac{1}{156}(y^4+24) + \alpha_1 y^2\right) + \dots$$

and, in particular, since $\varepsilon > 0$

$$f(0) = 1 + 2\varepsilon/13 + \dots > 1. \tag{3.5.28}$$

The resulting branch thus bifurcates to the left, and exists locally only for $\mu < 1/2$, there is no possible matching to a decaying solution for $\mu > 1/2$. The numerical calculations reported in the next section indicate that the branch persists globally, so that a solution exists at the self-similar value $\mu_2 = 1/4$.

THE THIRD BIFURCATION POINT: $\mu_l = 1/6$ $(l = 3,\ r = 1)$. We again have $f_0 = 1$ and now $f_1(y) = \alpha(y^6 + 540y^2)$ and $f_2 = \alpha^2(y^{12} - 32400y^8 - 164170800y^4 - 3940099200)$, so that the expansion is

$$\begin{aligned} f = {} & 1 + \varepsilon^{1/2}\alpha\left(y^6 + 540y^2\right) \\ & + \varepsilon\left(\alpha^2\left(y^{12} - 32400y^8 - 164170800y^4 - 3940099200\right) + \alpha_1\tilde{f}_1\right) + \dots . \end{aligned}$$

A similar (but much longer) analysis of the orthogonality condition (3.5.19) with eigenfunction $\psi_6((2/3)^{1/4}y) = (y^6 + 540y^2)/12\sqrt{5}$ then indicates that the branch again bifurcates to the left and exists locally for $\mu < 1/6$.

B THE CASE OF $m = 2$ AND l EVEN. In the case $l = 2r$ the bifurcation occurs at the point $\mu_{2r} = 1/4r$. Because of the presence of a constant term in the eigenfunction ψ_{2l}, the effect of the "forcing terms" yf' comes in at lower order than in the previous case. This leads to a standard asymptotic expansion for $f(y)$ of the form (cf. Theorem 12.1 in (Vainberg and Trenogin 1974))

$$f = f_0 + \varepsilon f_1 + \varepsilon^2 f_2 + \dots . \tag{3.5.29}$$

Substituting this expression for f into (3.5.5) or (3.5.6) gives

$$O(\varepsilon): \quad \mathcal{L}_{1/2l} f_1 \equiv -f_1'''' - \frac{1}{4r} y f_1' + f_1 = 0, \tag{3.5.30}$$

$$O(\varepsilon^2): \quad \mathcal{L}_{1/2l} f_2 = \sigma_l y f_1' - c_2 f_1^2. \tag{3.5.31}$$

As before, we express f_1 as a multiple of the (scaled) eigenfunction $\psi_{2l}(r^{-1/4}y)$,

$$f_1(y) = \alpha \tilde{f}_1(y) \equiv \alpha \sum_{j=0}^{r} \frac{r^{j-r}}{j!} D^{4j} y^{4r}. \tag{3.5.32}$$

The value of α is determined by considering the solvability condition for equation (3.5.31) at $O(\varepsilon^2)$. From the analysis above, it follows that for f_2 to exist we must have

$$\langle \sigma_l y f_1' - c_2 f_1^2, \psi_{2l}^* \rangle = 0 \quad \text{with } \psi_{2l}^* = \psi_{2l}^*((2/l)^{1/4} y). \tag{3.5.33}$$

This leads to a quadratic equation in α of the form $\alpha(\alpha - \gamma) = 0$, where γ may again be determined explicitly. This is the case of a unique nontrivial solution existing for both $\mu > \mu_l$ and $\mu < \mu_l$, and again we will need an extra matching argument to determine the correct sub-branch.

To illustrate this calculation we again take $p = 2$, $G_p(f) = |f|f - f$ and now consider the case of $l = 2$. This is an especially important value as it corresponds to $\mu_2 = 1/4$, at which the ODE is satisfied by the self-similar solution, if it exists. In this case we have $f_0 = 1$ and $f_1 = \alpha(y^4 + 24)$. The solvability condition for α is now

$$\langle \sigma_2 y f_1' - f_1^2, \psi_4^*(y) \rangle = \langle 4\sigma_2 \alpha y^4 - \alpha^2 (y^4 + 24)^2, \psi_4^*(y) \rangle = 0.$$

We have that $\hat{\psi}_4^*(\omega) = \omega^4 e^{-\omega^4}/2\sqrt{6}$ and it follows that the quadratic equation satisfied by α is given by

$$96\sigma_2 \alpha + 39168\alpha^2 = 0 \quad \Longrightarrow \quad \alpha = -\sigma_2/408. \tag{3.5.34}$$

We show presently that to match with the mid-range, $\alpha < 0$ so that $\sigma_2 = 1$. Hence

$$f(y) = 1 - \frac{\varepsilon}{408}\left(y^4 + 24\right) + \varepsilon^2\left(\tilde{f}_2(y) + \alpha_1 \tilde{f}_1(y)\right) \ldots, \tag{3.5.35}$$

where the third term (actually we do not need to compute it) explains the spatial non-monotonicity of such a solution. If $\varepsilon > 0$, then

$$f(0) = 1 - \varepsilon/17 + O(\varepsilon^2) < 1. \tag{3.5.36}$$

The mid-range $\varepsilon^\gamma < y < e^{1/\varepsilon}$

The mid-range behaviour is governed by the solutions of a first-order equation, which is different for each nonlinearity. However, the calculation now takes the same form for both l even and odd and uses a regular asymptotic expansion. To study the mid-range in all cases we rescale the underlying ODEs in space according to the transformation

$$s = \varepsilon^\gamma y \geq 0 \qquad (\gamma \text{ as in (3.5.7)}). \tag{3.5.37}$$

The outer limit of the inner region can be matched to the mid-range region by taking s to be small and y to be large.

A THE CASE $G_p(f) = |f|^{p-1}f - f/(p-1)$. Under the spatial rescaling (3.5.37), the equation (3.5.5) becomes

$$-\varepsilon^{4\gamma} f'''' - (\mu_l + \sigma_l \varepsilon)\, s f' + |f|^{p-1}f - f/(p-1) = 0, \quad l = 1, 2, \ldots, \tag{3.5.38}$$

where $' = d/ds$. To solve this we pose an asymptotic expansion of the form

$$f = f_0 + \varepsilon^{4\gamma} f_1 + \varepsilon^{8\gamma} f_2 + \ldots. \tag{3.5.39}$$

To leading order we have simply the first-order ODE $-y f_0'/2l + |f_0|^{p-1} f_0 - f_0/(p-1) = 0$, which has a family of bounded positive exact solutions

$$f_0(s) = \left((p-1) + \kappa s^{2l}\right)^{-1/(p-1)}, \tag{3.5.40}$$

where $\kappa > 0$ is a positive constant.

Note that for *small* s we have

$$f_0(s) = \beta^\beta \left(1 - \frac{\kappa}{(p-1)^2} s^{2l} + \frac{p\kappa^2}{2(p-1)^4} s^{4l} + O(s^{8l})\right), \tag{3.5.41}$$

while for *large* s

$$f_0(s) = \kappa^{-1/(p-1)} s^{-2l/(p-1)} + \ldots. \tag{3.5.42}$$

We now consider the next term in the asymptotic expansion, looking at the two cases of small s and large s separately. The function f_1 satisfies the equation

$$-\frac{1}{2l}sf_1' + \left(\frac{p}{(p-1)+\kappa s^{2l}} - \frac{1}{(p-1)}\right) f_1 = \sigma_l s f_0' + f_0''''.$$

We consider for simplicity the case of $p = 2$, and look at the three cases of $l = 1, 2$ and 3.

If $l = 1$, $4\gamma = 1$ and then for small s we have $f_0(s) = 1 - \kappa s^2 + \frac{1}{2}\kappa^2 s^4 + \ldots$, thus the leading order contribution to $\sigma_l s f_0' + f_0''''$ is simply $12\kappa^2$ and hence we have, to leading order as $s \to 0$

$$f_1(s) = 12\kappa^2 + \ldots.$$

If $l = 2$, $4\gamma = 1$ and then for small s, $f_0(s) = 1 - \kappa s^4 + \frac{1}{2}\kappa^2 s^8 + \ldots$ so that, to leading order

$$f_1(s) = -24\kappa + \ldots.$$

If $l = 3$, $4\gamma = 1/3$ and then for small s, $f_0(s) = 1 - \kappa s^6 + \frac{1}{2}\kappa^2 s^{12} + \ldots$ so that, to leading order $f_0'''' = -360\kappa s^2$ and

$$f_1(s) = -540\kappa s^2 + \ldots.$$

We conclude that the small s limit of the mid-range solution is

$$f = 1 - \kappa s^2 + \kappa^2 s^4/2 + \ldots + \varepsilon(12\kappa^2 + \ldots), \quad \text{if} \quad l = 1, \tag{3.5.43}$$

$$f = 1 - \kappa s^4 + \kappa^2 s^8/2 + \ldots - \varepsilon(24\kappa + \ldots), \quad \text{if} \quad l = 2, \tag{3.5.44}$$

$$f = 1 - \kappa s^6 + \kappa^2 s^{12}/2 + \ldots - \varepsilon(540\kappa^2 s^2 + \ldots), \quad \text{if} \quad l = 3. \tag{3.5.45}$$

In terms of the original variable y we have

$$f = 1 - \varepsilon^{1/2}\kappa y^2 + \varepsilon\kappa^2(y^4/2 + 12) + \ldots, \quad \text{if} \quad l = 1, \tag{3.5.46}$$

$$f = 1 - \varepsilon\kappa(y^4 + 24) + \varepsilon^2\kappa^2 y^8/2 + \ldots, \quad \text{if} \quad l = 2, \tag{3.5.47}$$

$$f = 1 - \varepsilon^{1/2}\kappa(y^6 + 540y^2) + \varepsilon\kappa^2 y^{12}/2 + \ldots, \quad \text{if} \quad l = 3. \tag{3.5.48}$$

We can now consider matching the above expressions to the expressions given in the last sections for the overlap region of large y but small s.

If $l = 1$, then comparing with (3.5.27) we have a perfect match provided that $\kappa = -\alpha$. As $\kappa > 0$ it follows that $\alpha = -1/\sqrt{156}$. Thus in the mid-range when $l = 1$ we have

$$f_0(y) = (1 + \varepsilon^{1/2} y^2/\sqrt{156})^{-1}.$$

As remarked earlier, this bifurcation branch exists only if $\mu < 1/2$.

If $l = 2$, then comparing with (3.5.35) we again have a perfect match if $\kappa = -\alpha > 0$. Thus in the mid-range when $l = 2$ we have

$$f_0(y) = (1 + \varepsilon^{1/2} y^4/408)^{-1}.$$

Note, that this expression is only meaningful if $\varepsilon > 0$. As in this case $\sigma_2 = 1$ it follows that locally the branch of solutions which bifurcates from $\mu = 1/4$ exists only if $\mu > 1/4$. Numerically we observe that this curve continues globally for values of $\mu < 1/4$ and hence we conjecture the existence of a fold bifurcation at some point $\mu = \mu_* > 1/4$, with a *non-zero* solution on the branch existing at $\mu = 1/4$. This corresponds to a self-similar solution distinct from that lying on the branch bifurcating from the point $\mu = 1/2$. The existence of such a solution is consistent with the semi-stability of the centre manifold determined in the last section. We generalize this result presently.

If $l = 3$ then comparing with the inner expansion, we again have a match if $\kappa = -\alpha > 0$. Thus in the mid-range we have

$$f_0(y) = (1 - \alpha \varepsilon^{1/2} y^6)^{-1} \quad (\alpha < 0).$$

Now consider the behaviour for $s \gg 1$ when $p = 2$. For these values of s, to leading order, the function f_1 satisfies the ODE $-\mu_l s f_1' - f_1 = -2l\sigma_l/\kappa s^{2l} + \ldots$, hence,

$$f_1(s) = 4l^2 \sigma_l \ln s/\kappa s^{2l} + \ldots \quad \text{as } s \to \infty.$$

Or, returning to the original variable y,

$$f(y) = \frac{1}{\kappa \varepsilon^{l/2} y^{2l}} \left(1 + 4l^2 \sigma_l \ln y + \ldots\right) \quad \text{as } y \to \infty. \tag{3.5.49}$$

B *The case of* $G = e^f - 1$. Under the same spatial rescaling as before, the equation (3.5.6) becomes

$$-\varepsilon f'''' - (\mu_l + \sigma_l \varepsilon) s f' + e^f - 1 = 0, \quad l = 1, 2, \ldots.$$

Posing expansion (3.5.39), substituting into the ODE and solving the leading order equation gives

$$f_0(s) = -\ln(1 + \kappa s^{2l}). \tag{3.5.50}$$

The analysis now proceeds as above, and again matching in the limit $s \to 0$ fixes $\kappa > 0$, see similar calculations in Section 3.8.3.

Far field behaviour

The correct far field behaviour is determined by assuming slow growth in both (3.5.2) and (3.5.3), $f''''(y) \to 0$ as $y \to \infty$ and hence $|f|f \ll f$ for small $f > 0$ in (3.5.5) while $e^f \ll 1$ for $f \ll -1$ in (3.5.6). In the case of (3.5.5) this gives

$$f = Cy^{-1/\mu}(1 + o(1)) \equiv Cy^{-2l/(1+2l\sigma_l\varepsilon)}(1 + o(1)) \quad \text{as } y \to \infty.$$

Expanding this for $\varepsilon \ll 1$, we have

$$f = Cy^{-2l}\left(1 + 4l^2\sigma_l\varepsilon \ln y\right) + \ldots \quad (\varepsilon|\ln y| \ll 1).$$

This matches with (3.5.49) if $C = 1/\kappa\varepsilon^\gamma$.

3.5.2 Bifurcations from $\mu_m = 1/2m$ for general m

As remarked, for $m = 2$ we can also postulate existence of the new profile f_2 from the shape of the branch associated with $\mu_2 = 1/4$ as the branch leaves the bifurcation point to the right and then is expected to fold back. In fact this behaviour can be understood for general m.

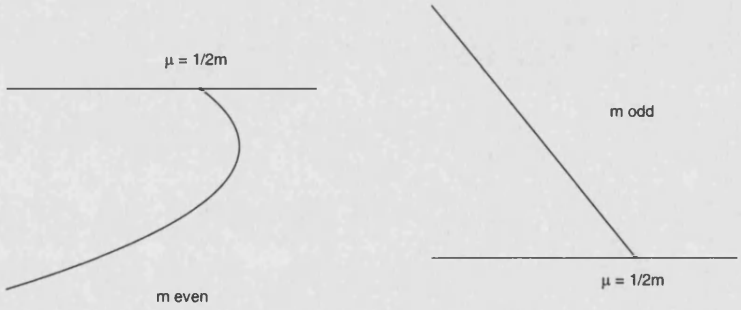

Figure 3.3: Schematic of the distinction between even and odd m.

For all m, the bifurcation point $\mu_m = 1/2m$ is associated with a zero eigenvalue of the linearized operator $\mathcal{L} + I$ in the PDE (3.4.1). Further evidence for the existence of a nonlinear pattern associated with this point comes from the local structure of the bifurcation diagram. Looking for small solutions near this point, we solve

$$(-1)^{m+1}D_y^{2m}f - \mu_m y D_y f + f + \sigma_{2m}\varepsilon y D_y f + \bar{G}(f - f_0) = 0,$$

where $\bar{G}$ is the quadratic perturbation (3.4.2). At $\mu_m = 1/2m$ we have the regular expansion (3.5.39) and expanding as before gives

$$\mathcal{L}_{1/2m}f_1 = 0 \quad \Longrightarrow \quad f_1 = \alpha\left(y^{2m} + (-1)^m(2m)!\right) \quad \text{with unknown } \alpha \in \mathbf{R}.$$

At the next order we have

$$\mathcal{L}_{1/2m} f_2 = \sigma_{2m} y f_1' - c_2 f_1^2 = -2m\sigma_{2m}\alpha y^{2m} - c_2\alpha^2 \left([(2m)!]^2 + 2(2m)! y^{2m} + y^{4m}\right). \tag{3.5.51}$$

By the Fredholm alternative this can be solved only if

$$\left\langle \sigma_{2m}\alpha 2m y^{2m} - c_2\alpha^2 \left(((2m)!)^2 + (-1)^m 2(2m)! y^{2m} + y^{4m}\right), \psi_{2m}^*(y)\right\rangle = 0.$$

By (3.3.10) $\hat{\psi}_{2m}^*(\omega) = \omega^{2m} e^{-2m}/\sqrt{(2m)!}$ so that, after a little manipulation, the solvability condition becomes

$$\sigma_{2m}\alpha 2m(2m)! + c_2\alpha^2(-1)^{m+1}\left((4m)! - 2[(2m)!]^2\right) = 0.$$

Thus the solvability condition implies that

$$\alpha = (-1)^m \sigma_{2m} c_2 \frac{2m\,(2m)!}{(4m)! - 2\left((2m)!\right)^2}$$

and hence

$$f(y) = f_0 - (-1)^m \varepsilon \sigma_{2m} c_2 \frac{2m(2m)!}{(4m)! - 2\left((2m)!\right)^2}\left(y^{2m} + (-1)^m (2m)!\right) + \ldots.$$

But, to match with the mid-range, with $\alpha < 0$ we require that $f_1 \to -\infty$ as $y \to \infty$ which sets

$$\sigma_{2m} = (-1)^m \quad \text{for} \quad \varepsilon > 0.$$

Hence, for even m the branches initially increase in μ and thus, if they have folded back, contribute an extra similarity profile $f_m(y)$ at $\mu = 1/2m$ whereas there need be no such contribution for odd m. This agrees with the centre manifold calculation of Section 3.4.2.

3.6 Numerical calculations of the self-similar profiles

We next present a numerical calculation of the solutions of the problem (3.4.12) parameterized by μ and taking $G_p(f) = |f|f - f$. (As indicated from the analysis of the previous sections, the case $G_e(f) = e^f - 1$ is fundamentally the same and has already been presented in the Introduction.) This calculation allows us to extend the asymptotic analysis of the last section, and in particular to study the global behaviour of the branches which bifurcate from the first two bifurcation points at $\mu_1 = 1/2$ and $\mu_2 = 1/4$. The solutions were obtained using a collocation code which guarantees a small residual tolerance (Shampine and Kierzenka 2001). The initial points on each curve were obtained by setting $\mu = 0$. The continuation of each solution was then done by using the pseudo arc-length routine in AUTO (Doedel et al. 1997). Symmetry con-

ditions were imposed at the origin and minimal growth was enforced at the far field by solving the problem on the finite interval $(0, 1000)$ and setting the highest derivatives to zero at the right hand boundary.

3.6.1 The fourth-order case $m = 2$

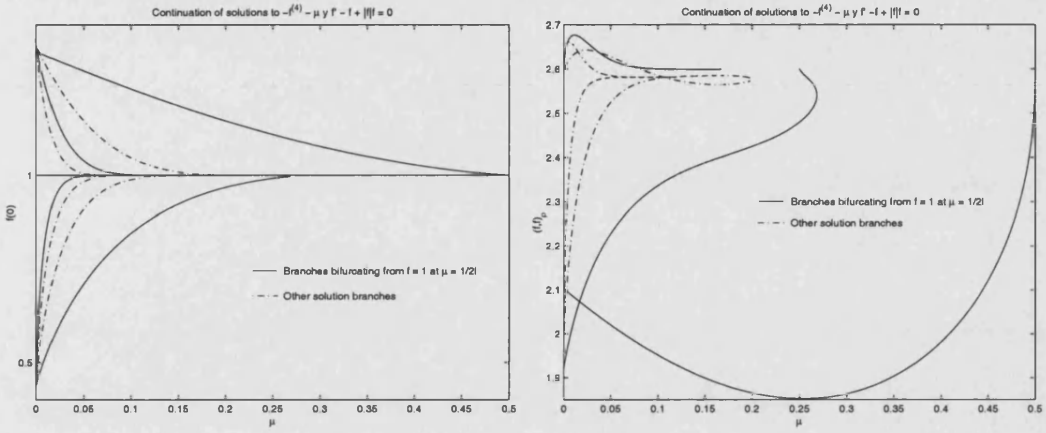

Figure 3.4: Continuation of solutions to $-f'''' - \mu y f' - f + |f|f = 0$ in μ. On the left (a) the measure is $f(0)$ while on the right (b) the measure is the L^2_ρ-norm.

In Figure 3.4a we present the results of the numerical calculations for different values of the parameter μ looking at the fourth-order ordinary differential equations given by taking $m = 2$. In this figure we use $f(0)$ as a measure of the size of the solution as it is easiest to compare this measure with the asymptotic calculations of the previous Section. The existence of branches bifurcating from each of the points $\mu_l = 1/2l$ (displayed as solid lines) is clear. Also plotted in dashed lines are other solutions obtained from continuing solutions from $\mu = 0$ which do not bifurcate from the constant solution $f \equiv 1$. In this format it is difficult to distinguish the solutions which bifurcate from the linear spectrum from the additional "nonlinear" solutions. To make this distinction clear we plot the same solutions in Figure 3.4b using the L^2_ρ-norm as the solution measure.

We observe firstly that the curve bifurcating from $\mu_1 = 1/2$ appears to exist for all values of $\mu \in [0, 1/2]$ and in particular there is a non-constant solution $f_s(y)$ (the subscript s denotes stable, see Section 3.7) for a numerical example of PDE evolution with the value of $\mu_2 = 1/4$. This solution gives a self-similar solution of the underlying PDE (3.1.2). In Figure 3.5 we compare the numerical solution to the boundary-value problem (3.2.7), (3.2.8) with the asymptotic construction (3.5.27). In Figure 3.6 we present an enlargement of Figure 3.4 close to the point $\mu = 1/2$ allowing a direct comparison with the asymptotic calculation of $f(0)$ given by (3.5.28).

In contrast, the curve bifurcating from $\mu = 1/4$ appears to exist for all $\mu \in [0, 1/4 + \delta]$,

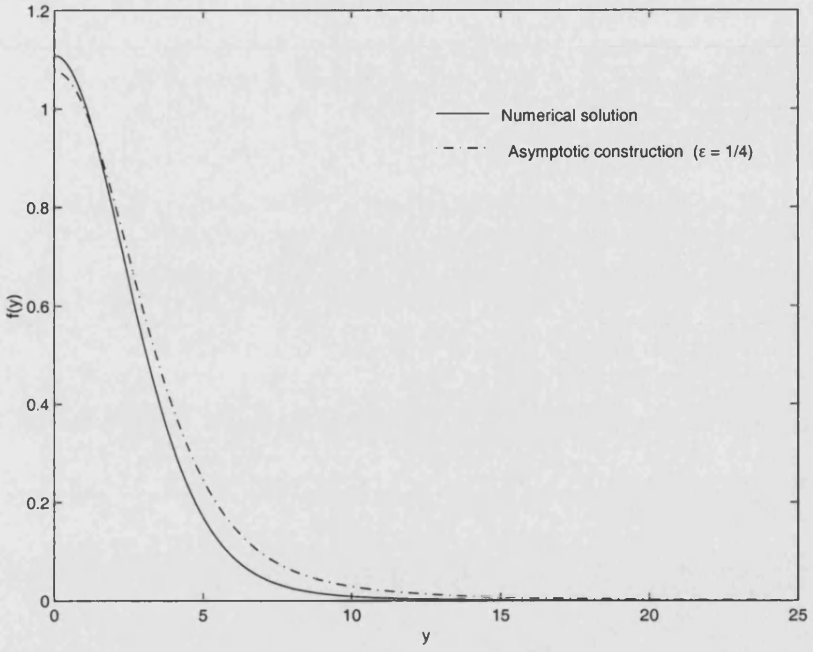

Figure 3.5: Comparison of asymptotic and numeric solutions.

where δ is a small positive constant. This behaviour can be seen more clearly in the enlargement of Figure 3.4 close to $\mu = 1/4$ which is presented in Figure 3.6. Again, we can compare this figure to the asymptotic calculation of $f(0)$ given by (3.5.36), and the associated discussion on the unstable centre manifold behaviour in Section 3.5, which predicts the existence of the bifurcating curve for a range of values of $\varepsilon > 1/4$. This asymptotic calculation is clearly only valid for a small range of values of $\mu > 1/4$, and the curve of solutions folds back at $\mu \simeq 0.26841...$.

In particular, we observe a second non-zero solution $f_u(y)$ (the subscript u denotes unstable, see Section 3.7) of (3.4.12) at $\mu = 1/4$. The existence of this solution implies the existence of a further non-zero self-similar solution of the PDE. As remarked earlier, this result is consistent with the semi-stability of the centre manifold when $m = 2$. The profiles of the two distinct self-similar solutions $f_s(y)$ and $f_u(y)$ are given in Figure 3.7.

Observe that the form of $f_s(y)$ is qualitatively similar to the profile of the solution computed close to $\mu = 1/2$ and described asymptotically in the last section. In particular, it appears to be a monotone decreasing function of y. In contrast the self-similar solution $f_u(y)$ is *increasing* for small values of y and decreasing for larger values. This possible small non-monotonicity is the expansion (3.5.35) is described by the terms at $O(\varepsilon^2)$.

We also present in Figure 3.6 a detail of the neighbourhood of $\mu = 1/6$. Although this branch does not lead to a self-similar solution, its local form is interesting. As predicted by the asymptotic analysis, it bifurcates to the left, but then folds back twice locally

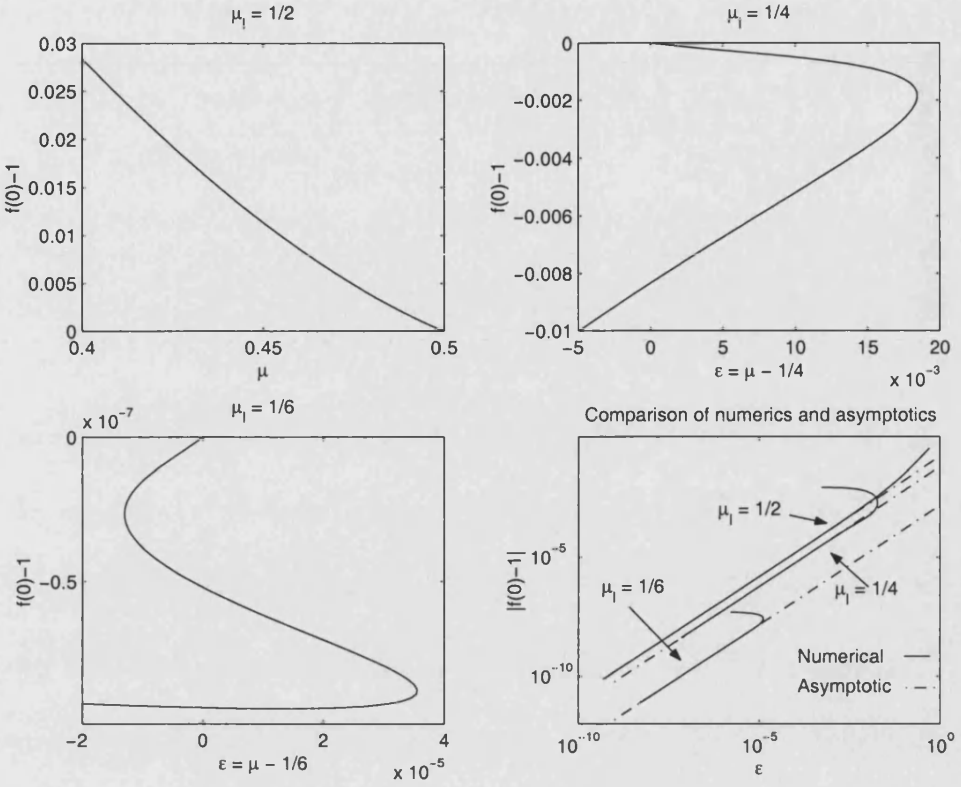

Figure 3.6: Detail of branches at $\mu = 1/2, 1/4, 1/6$. for $m = 2$ and $p = 2$.

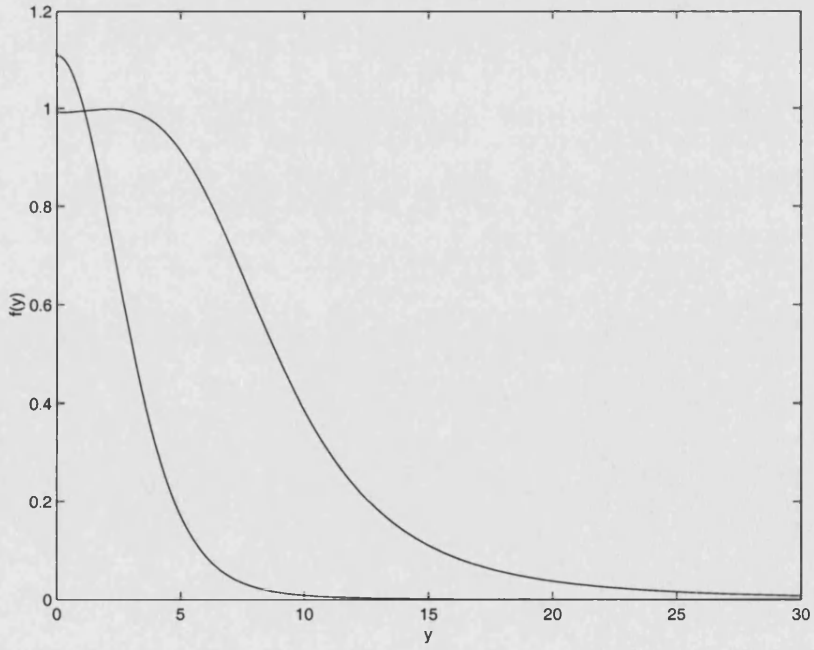

Figure 3.7: The two self-similar profiles f_s, f_u for $m = 2$.

before continuing backwards to $\mu = 0$. From these calculations we make the following conjecture.

Conjecture 3.6.1. *If $m = 2$, then each of the curves bifurcating from the point $\mu_l = 1/2l$ continues globally to include the point $\mu = 0$, and has $l - 1$ fold bifurcations in the vicinity of $\mu = 1/2l$.*

Such fold bifurcations may occur, (Krasnosel'skii 1964), if

$$0 \in \sigma(\mathcal{L}_\mu + G'(f)I). \tag{3.6.1}$$

This equation determines a difficult eigenvalue problem for higher-order operators with non-constant coefficients. The zero eigenvalues of this problem correspond to the turning points of the solution branches indicated in Figure 3.6.

Lastly in Figure 3.6 we compare our asymptotic construction of the bifurcation diagram with the numerical computations. Away from all folds the agreement is excellent even with only a linear approximation.

3.6.2 The sixth-order case $m = 3$

A bifurcation diagram to similar Figure 3.4 but now for the case of the sixth order differential equations when $m = 3$ is presented in Figure 3.8. In this case the far field boundary condition is (3.5.4).

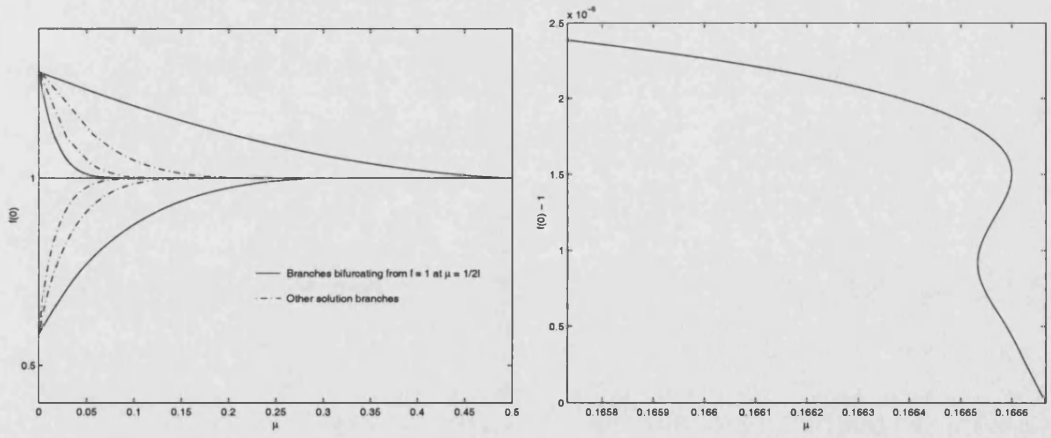

Figure 3.8: Continuation of solutions to $f^{(6)} - \mu y f' - f + |f|f = 0$. (a) Bifurcation diagram for $m = 3$. (b) Detail near $\mu = 1/6$.

This picture is qualitatively similar to Figure 3.4, with the solutions at $\mu_3 = 1/6$ of interest. As before, the monotone decreasing (in a neighbourhood of the origin) solution bifurcating from $\mu = 1/2$ extends backwards to $\mu_3 = 1/6$ as does the solution bifurcating from $\mu = 1/4$. This leads to two self-similar solutions f_s and f_u. A detail

of Figure 3.8a in the neighbourhood of $\mu = 1/6$ is given in Figure 3.8b. As predicted by the asymptotic analysis of Section 3.5, this curve bifurcates *to the left* and there are no non-zero (and hence no self-similar) solutions on this branch when $\mu = 1/6$. Consistent with the previous analysis we observe two self-similar solutions associated with the unstable sub-space and none associated with the centre subspace.

A plot of f_s and f_u is given in Figure 3.9. It is of special interest that for this value of m we see *four* other self-similar solutions that arise from paths which start at $\mu = 0$. These are also plotted in Figure 3.9. Observe that $2 + 4 = 6 = m(m-1)$ for $m = 3$, cf. the second last comment in Section 3.4.

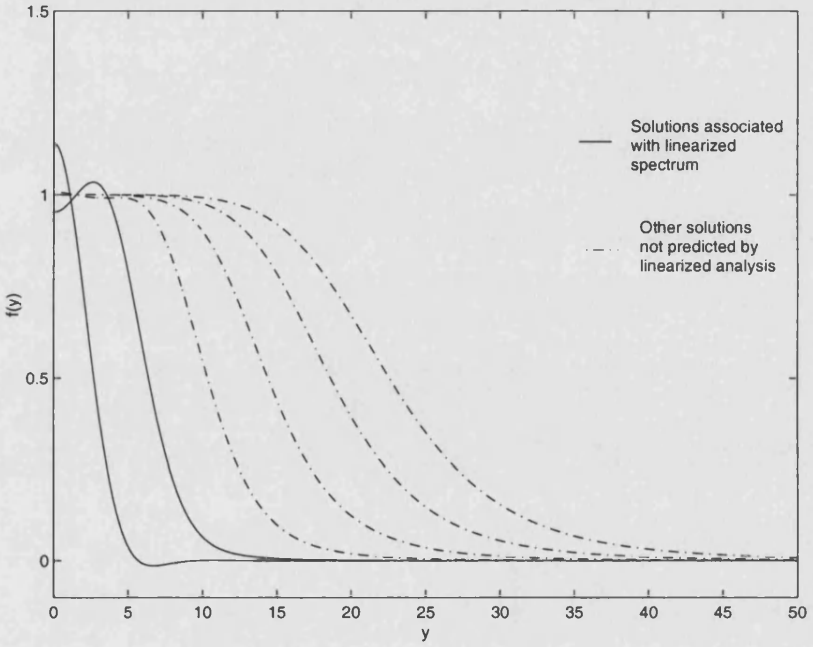

Figure 3.9: Six self-similar profiles for $m = 3$, of which two arise from the weakly nonlinear analysis and four do not.

3.7 Numerical simulations of the solutions of the PDE

While the self-similar solutions of (3.1.2) and (3.1.1) are important, they only give a partial picture of the overall dynamical behaviour of the solutions of these systems. For example, we have not even established whether the self-similar solutions are stable in the rescaled sense (strictly speaking, existence is not even fully established). As we have mentioned, for $m > 1$, the operators in (3.2.3) and (3.2.5) are not potentials and do not generate gradient flows as in the second-order case. For $m = 1$ a Lyapunov function exists and this essentially simplifies the asymptotic analysis, see the first results in Galaktionov and Poshashkov (1986) for $N = 1$ and Giga and Kohn (1985) and Giga and

Kohn (1987) for $N \geq 1$. Moreover, compactness of the rescaled orbits $\{\theta(\tau), \tau > \tau_0\}$ remains an open problem (the only known L^∞-estimate for the blow-up rate is a lower one, (Chaves and Galaktionov 2001), (Galaktionov and Pohozaev 2003)). This makes the asymptotic stability for higher-order equations extremely difficult.

In this section we investigate the dynamics of (3.1.2) in the case of $m = 2$ by using the scale-invariant adaptive numerical method described in Chapter 2. The spatial grid is chosen to equidistribute the monitor function $M(u) = |u|^{p-1}$. By doing this mesh points are clustered where $M(u)$ and hence u is large. This choice of $M(u)$ also preserves the scale invariance of the underlying system.

Example 1. For the first calculation we consider the polynomial nonlinearity (3.1.2) with as initial data the function

$$u_0(x) = 2e^{-x^2}.$$

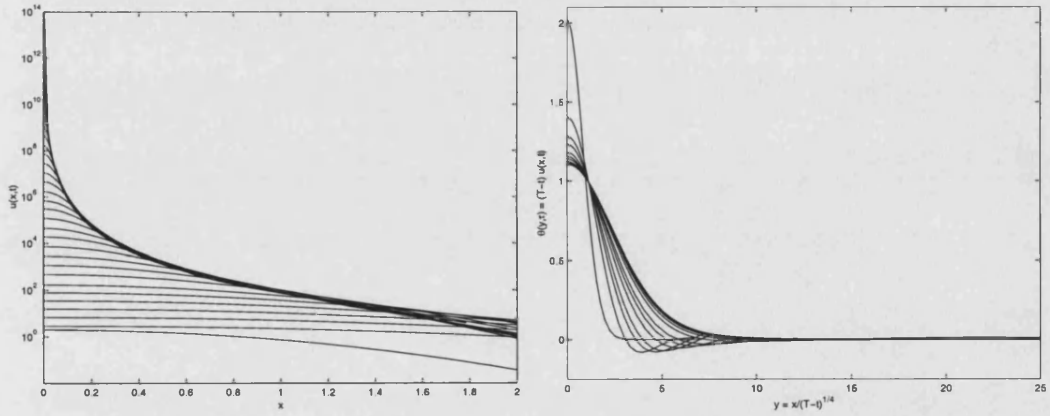

Figure 3.10: The solution of (3.1.2) in the physical variables (a) and the rescaled variables (b).

Firstly, we present the evolution from this data in the original variables in Figure 3.10a, here the formation of the singularity can be seen clearly. In Figure 3.10b we present *the same* data this time in the scaled variables θ and y. Here, the blow-up time T is estimated by a least squares fit of $u(0,t) = f_0/(T-t)^{1/(p-1)}$ with both f_0 and T unknown. The most significant aspect of this figure is that the solutions rapidly converge (exponentially in τ) to the first monotone function $f_s(y)$. The solution of the ODE (3.2.7) is plotted on Figure 3.10 for comparison and is indistinguishable from the large τ solutions to the full PDE and we deduce that the self-similar solution is a stable atractor in this case.

Example 2. For our final calculation we take as initial data the second solution to

(3.2.7), the solution which extends from the bifurcation point $\mu_l = 1/4$.

$$u(x,0) = f_u(x).$$

This is seen to be unstable. While remaining close to the initial data as the magnitude increases several orders eventually the rescaled solution converges to the primary profile as in Example 1, see Figure 3.11.

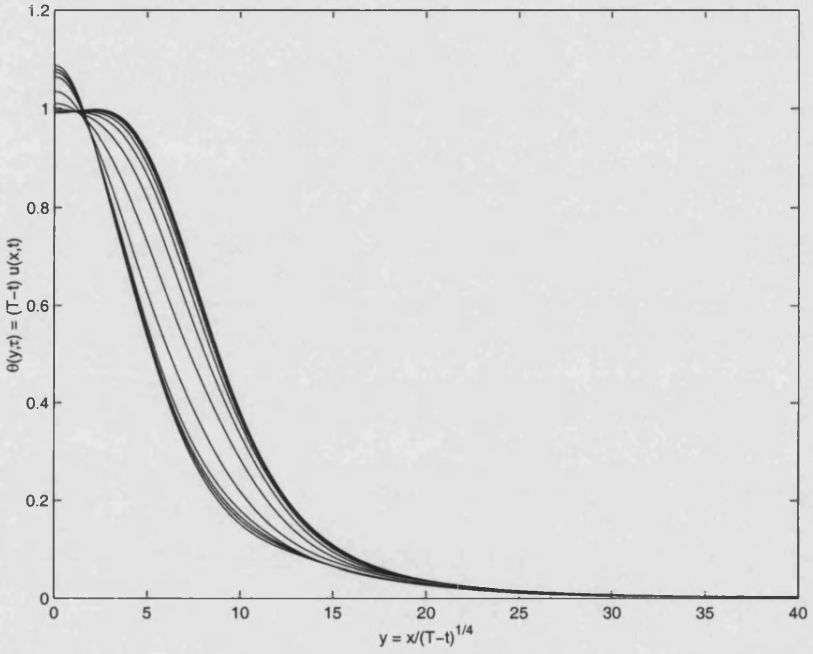

Figure 3.11: The solution of (3.1.2) in the rescaled variables.

3.8 Self-similar profiles and generic blow-up in the SRB-problem

We now return to the Semenov-Rayleigh-Benard problem as first described in the Introduction. We use the general results of the previous Sections for the case $m = 2$ to understand this physical problem in greater detail. Let us write down equation (1.3.11) in terms of the linearized operator (3.2.4),

$$g_\tau = (\mathcal{L} + I)g + \mathbf{D}(g) \tag{3.8.1}$$

with the nonlinear operator

$$\mathbf{D}(g) = \mathbf{A}_1(g) - (\mathcal{L} + I)g \equiv \beta[(g_y)^3]_y + e^g - (1 + g).$$

On solutions $g(\cdot,\tau) \in H^4_\rho(\mathbf{R}^N)$ the perturbation is quadratic,

$$\mathbf{D}(g) = \frac{1}{2}g^2 + \frac{1}{6}g^3 + \beta(g_y^3)_y + ... = \frac{1}{2}g^2 + O(\|g\|^3_{\rho^*}) \quad \text{as } \|g\|_{\rho^*} \to 0. \tag{3.8.2}$$

Hence, all the analysis of Section 3.5 holds and we have two self-similar profiles. These were first seen in the Introduction in Figure 1.3.

3.8.1 Countable family of other blow-up patterns

We now identify other types of blow-up patterns, which are not stable but can occur in the present explosion-convection problem creating special singularity formation phenomena and a discrete "spectrum" of final-time profiles. For equations (1.3.7) and (1.3.5) we construct such blow-up patterns generated by the invariant manifold analysis associated with the centre and stable subspaces of the linearized operator $\mathcal{L}^* + I$ in (3.8.1). It turns out that such an analysis can be done similarly to that for the semilinear equation with the power nonlinearity, (3.1.2), for arbitrary order $2m \geq 4$, see Galaktionov (2001).

3.8.2 Centre manifold pattern: solutions taking infinite values on moving boundaries

By virtue of Proposition 3.4.1 and assuming the asymptotic behaviour (3.4.7), on any compact subset $\{|y| \leq c\}$, $c > 0$, the rescaled solution has the form

$$g(y,\tau) = \frac{1}{\gamma_0 \tau}\frac{1}{\sqrt{24}}\left(y^4 + 24\right) + o(\frac{1}{\tau}) > 0 \quad \text{as } \tau \to \infty. \tag{3.8.3}$$

We now introduce the new rescaled variable

$$\zeta = y/\tau^{1/4} \equiv x/[(T-t)|\ln(T-t)|]^{1/4}, \tag{3.8.4}$$

so that (3.8.3) implies that as $\tau \to \infty$,

$$g = \gamma_1 \zeta^{2m}(1 + o(1)) > 0 \quad \text{for small } \zeta > 0, \quad \gamma_1 = 1/\sqrt{24}\gamma_0 = 1/816. \tag{3.8.5}$$

This extra rescaling forms a remarkable spatial variable (3.8.4) with an additional logarithmic factor. For the second-order heat equations like (1.1.2) a similar variable occurs with the exponent $1/2$ instead of $1/4$. The idea of such non scaling invariant hot-spot variable goes back to the beginning of the 1970's in Hocking et al. (1972), where the equation $u_t = u_{xx} + u^3$ was studied.

Applying the scaling (3.8.4) in equation (1.4.2), we deduce that $g = g(\zeta,\tau)$ satisfies the

following perturbed equation:

$$g_\tau = \mathbf{H}_4(g) + \frac{1}{\tau}\mathbf{F}(g) \quad \text{for } \tau > \tau_0, \tag{3.8.6}$$

with the first-order operator

$$\mathbf{H}_4(g) = -\frac{1}{4}\zeta g_\zeta + e^g - 1, \quad \text{and} \quad \mathbf{F}(g) = -g_{\zeta\zeta\zeta\zeta} + \beta\left((g_\zeta)^3\right)_\zeta - \frac{1}{4}\zeta g_\zeta.$$

As $\tau \to \infty$, (3.8.6) is an asymptotically small singular perturbation of order $O(1/\tau)$ (it is of crucial importance that the perturbation is not integrable, $1/\tau \notin L^1((1,\infty))$) of the first-order Hamilton-Jacobi equation

$$h_\tau = \mathbf{H}_4(h). \tag{3.8.7}$$

Such singularly perturbed dynamical systems occur in several reaction-diffusion equations, see Galaktionov and Vazquez (1991), where a general stability theorem is available. The main hypothesis of this stability approach is the uniform Lyapunov stability of the ω-limit set of the unperturbed equation (3.8.7) established in Galaktionov and Vazquez (1994, Sect. 3), for general equations such as (3.8.7) in a Banach space $C_\rho(\mathbf{R}_+)$ with a singular weight. For such higher-order parabolic problems compactness of rescaled orbits is a difficult open problem and the analysis below is formal.

Assuming that we can pass to the limit in the singularly perturbed equation (3.8.6), we have that the orbit approaches the stationary profiles satisfying

$$\mathbf{H}_4(f) = 0 \quad \text{for } \zeta > 0, \quad f(0) = 0.$$

Integrating this ODE in the class of nonnegative functions $f \geq 0$, which is one of the matching conditions due to the positivity of expansions (3.8.3) and (3.8.5), we obtain a one-parameter family of the limit profiles,

$$f(\zeta) = -\ln(1 - A\zeta^4) \quad \text{with a parameter } A \geq 0. \tag{3.8.8}$$

Since $f(\zeta) = A\zeta^4 + O(\zeta^8)$ as $\zeta \to 0$, comparing with (3.8.5) for the intermediate values of ζ yields the unique stable profile (3.8.8), $f_*(\zeta)$, with the constant $A = \gamma_1$.

Thus, in terms of the new rescaled variable (3.8.4) with the extra logarithmic factor, the centre manifold behaviour is governed by a unique stationary solution of the Hamilton-Jacobi equation (3.8.7):

$$f_*(\zeta) = -\ln(1 - \gamma_1\zeta^4).$$

This means that in the original variables (x,t), the corresponding blow-up pattern takes

the asymptotic form

$$u_4(x,t) = -\ln(T-t) - \ln(1-\zeta^4/816) + ..., \quad \zeta = x/[(T-t)|\ln(T-t)|]^{1/4},$$

i.e., it blows up as $t \to T$ in a shrinking domain $\{|x| \le 4\sqrt{3}[(T-t)|\ln(T-t)|]^{1/4}\}$ and $u_* = +\infty$ on its lateral boundary. Such an infinite Dirichlet condition on moving boundaries is a typical feature for fourth-order PDEs like (1.1.1), (1.3.5) or (1.3.6) (unlike the second-order heat equation (1.1.2) where such initial-boundary value problems are not locally solvable in general in natural functional classes). Note that the ODE (1.4.4) admits solutions $f(y)$ blowing up as $y \to y_0 \pm 0$ for any finite y_0 with the singularity given in the first approximation by the equation $f'''' = e^f$.

3.8.3 Stable manifold patterns

We now describe the rest of the blow-up patterns associated with the stable subspaces of the linearized operator. The patterns on the stable manifold tangent to $E^s(0)$ are generated by the corresponding eigenfunctions with the following asymptotic behaviour of solutions of (3.8.1) for $\tau \gg 1$. On compact subsets

$$g(y,\tau) = Ce^{(1-k/4)\tau}\psi_k(y) + ..., \quad k = 6,8,... \quad \text{(hence } \tilde{\lambda}_k = 1 - k/4 < 0), \qquad (3.8.9)$$

where $C \neq 0$ depends on the initial data. The eigenfunctions ψ_k given by (3.3.13), do not change sign. Therefore, as we will show, positive C in (3.8.9) correspond to blow-up patterns in shrinking domains as $t \to T$, while negative values of C generate blow-up patterns which are well-defined in $\mathbf{R} \times (0,T)$.

We concentrate on negative C and set $C \mapsto -C$. Then (3.8.9) yields for large y as $\tau \to \infty$,

$$g(y,\tau) = -Be^{(1-k/4)\tau}y^k(1+o(1)) + ... \equiv -B\zeta^k + ..., \ |\zeta| \ll 1, \qquad (3.8.10)$$

and $B = C/\sqrt{k!} > 0$,where ζ is the new spatial variable

$$\zeta = ye^{-\tau(k-4)/4k} \equiv |x|/(T-t)^{1/k}, \quad k = 6,8,....$$

Then $g = g(\zeta,\tau)$ satisfies the exponentially perturbed equation

$$g_\tau = \mathbf{H}_k(g) - e^{-(1-4/k)\tau}\left(-g_{\zeta\zeta\zeta\zeta} + \beta\left((g_\zeta)^3\right)_\zeta\right), \qquad (3.8.11)$$

with the Hamilton-Jacobi operator

$$\mathbf{H}_k(g) = -\frac{1}{k}\zeta g_\zeta + e^g - 1.$$

Using the same stability arguments, similar to the above centre case $k = 4$, we conclude that, under necessary compactness hypotheses, the orbit $\{g(\cdot, \tau)\}$ approaches the stationary subset of the unperturbed equation (3.8.11) corresponding to $\tau = \infty$. Solving the ODE $\mathbf{H}_k(f) = 0$ in the class of nonpositive solutions, we obtain the family

$$f(\zeta) = -\ln(1 + A\zeta^k) \quad \text{with a parameter} \quad A \geq 0.$$

Matching the expansion $f(\zeta) = -A\zeta^k + O(\zeta^{2k})$ as $\zeta \to 0$ with (3.8.10), we obtain

$$A = B = C/\sqrt{k!}\,.$$

We thus obtain the following approximate representation of the stable manifold pattern on compact subsets in ζ:

$$u_k(x,t) = -\ln\Big((T-t)(1 + A\zeta^k)\Big) + ..., \quad \zeta = |x|/(T-t)^{1/k}.$$

Passing to the limit $t \to T$, we derive a countable subset of final-time profiles created at $t = T$ via such a blow-up evolution

$$u_k(x, T^-) = -k \ln|x| - \ln A + ... \quad \text{as } x \to 0, \quad k = 6, 8, ... \tag{3.8.12}$$

Thus, the final-time profiles *are not* arbitrary and there exists only a countable family (3.8.12) of those which can occur in the fourth-order PDE (1.3.7).

3.9 Conclusions

It is clear from this study that the (self-similar) behaviour of the blow-up solutions of a relatively straightforward higher-order partial differential equation is quite different, and in a sense simpler, than that of related second order equations. It is very likely that similar behaviour will be observed in a much wider class of higher-order equations. The numerical and asymptotic calculations presented in this Chapter have suggested a number of open questions in analysis which deserve further investigation, in particular, a fully rigorous proof of the existence of the self-similar solutions and the uniqueness of the "most" monotone stable profiles. We leave this as a subject for future study.

Chapter 4

Very singular similarity solutions

Given the detailed understanding of the operators $\mathcal{L}$ and $\mathcal{L}^*$ and their role in describing the blow-up problem for higher-order parabolic equations, we now consider the absorption problem which admits global solutions decaying as time tends to infinity. In the classical second-order case study of these solutions led to the development of a significant amount of new mathematics. While we establish asymptotically that the behaviour of solutions for $m > 1$ is, unlike in the blow-up problem, not significantly different from $m = 1$, we show that fundamentally new mathematics will be required to prove this rigorously.

4.1 Introduction: very singular similarity solution

In this Chapter we consider the Cauchy problem for the $2m$-th order semilinear parabolic equation

$$u_t = -(-\Delta)^m u - u^p \quad \text{in } \mathbf{R}^N \times \mathbf{R}_+, \quad u(x,0) = u_0(x) \in L^\infty(\mathbf{R}^N) \cap L^1(\mathbf{R}^N), \quad (4.1.1)$$

where, in most cases the initial data $u_0(x)$ are assumed to decay exponentially fast as $x \to \infty$ (see (4.1.12)). For convenience, we use the notation

$$u^p := |u|^{p-1}u, \quad p > 1.$$

The operator on the right-hand side of (4.1.1) is monotone, coercive, and affords a unique global weak solution (see the book by Lions (1969)), which is a bounded classical solution for a wide parameter range. We shall study the behaviour of such global solutions as $t \to \infty$.

From the beginning of the 1980's the problem of asymptotics for the semilinear heat equation (4.1.1) with $m = 1$, which became a canonical diffusion-absorption equation, led to the study of a new class of similarity solutions called *Very Singular Solutions*

(VSS). Various asymptotic techniques were developed to prove existence, uniqueness and global stability of the VSS in the *subcritical* parameter range $1 < p < p_0 = 1 + 2/N$ (for nonnegative solutions). Interesting new asymptotic phenomena were also discovered in the supercritical range $p > p_0$, and in the critical case $p = p_0$. We refer to the papers (Brezis and Friedman 1983, Kamin and Peletier 1985, Kamin and Peletier 1986, Brezis, Peletier and Terman 1986, Galaktionov, Kurdyumov and Samarskii 1986, Escobedo and Kavian 1987, Kamin and Véron 1988, Bricmont, Kupiainen and Lin 1994, Bricmont and Kupiainen 1996) (this list of references is not complete and includes only the papers to be used herein); see also a survey in Samarskii et al. (1995, Chap. 2). Historically, the term VSS arose because the first solutions to be discovered for the second-order equation

$$u_t = \Delta u - u^p \tag{4.1.2}$$

with a Dirac measure as initial data were termed 'singular solutions' but are not as singular as the VSS (for which $u(x,0)$ is not a measure) as they did not arise from *very* singular initial data (Kamin and Peletier 1985).

The study of VSS-like asymptotics generated numerous barrier, comparison, reflection, Lyapunov and variational techniques based on the Maximum Principle and later applied to a wide class of semilinear and quasilinear second-order parabolic equations describing various reaction, diffusion, absorption and convection processes. The VSS asymptotics of nonlinear parabolic equations discovered in studying the model equation (4.1.1) with $m = 1$ represented an important new class of stable generic asymptotics of evolutionary PDEs.

The structure of equation (4.1.1) dictates that the critical absorption exponent p_0 establishes a certain balance between the elliptic "diffusivity" operator and the algebraic absorption operator, and this phenomenon is expected to exist for any order $2m \geq 2$. It is of principal importance to reveal properties of higher-order equations similar to those which are well understood for their second-order counterparts. We present the results of asymptotic analysis for the $2m$-th order semilinear equations where the semigroups are not order-preserving and the positivity of solutions is not an invariant property. We consider general initial data with exponential decay at infinity and classify the asymptotic behaviour of solutions by describing various countable and continuous subsets of special patterns. Our main goal is to show that the general portrait of asymptotic patterns remains the same for any $m \geq 1$ including the classical case $m = 1$ for solutions which change sign, where some of our results are new. Indeed, the mathematics of higher-order equations becomes essentially more delicate (any self-adjoint, potential and order-preserving properties of the operators and semigroups involved are lost) and the rigorous justification of some of our conclusions remains an important open problem. Consequently, while our results extend the known behaviour for $m = 1$ to $m > 1$, fundamentally new methods will be required to fully justify our conclusions as we show

that the classical methods no longer apply.

The organization of this Chapter is as follows. In the remainder of this section we introduce self-similar solutions and briefly describe our main results. The next three Sections contain some preliminary and auxiliary results. Section 4.2 is devoted to the asymptotic analysis of the ODE for similarity profiles and Sections 4.3-4.6 present a PDE analysis of (4.1.1). In Section 4.3 we describe three different types of asymptotic patterns formed, loosely speaking, by the unstable, stable and centre manifold behaviour of the rescaled PDE. In Section 4.4 we consider a related bifurcation problem for the ODE which motivates our estimate on the number of possible solutions. We also prove existence of a stable VSS profile for $p \approx p_0^-$ and present supporting numerical evidence. In Section 4.5 we show that the rescaled equation is not a gradient system, and hence general stability results, such as those of Lyapunov and La Salle, do not apply, unlike the case $m = 1$. In Section 4.6, for completeness, we briefly discuss a continuous spectrum of similarity solutions corresponding to data with algebraic (non-exponential) decay at infinity.

4.1.1 The first critical absorption exponent

We begin by reviewing existing results concerning the asymptotic behaviour of global solutions with initial data decaying exponentially at infinity (see (4.1.12) with the precise functional setting in a weighted L^2 space detailed in Section 3.3). It is known that in equation (4.1.1)

$$p_0 = 1 + 2m/N \tag{4.1.3}$$

is a *critical* exponent in the following sense:

(i) In the supercritical range $p > p_0$, for a class of sufficiently small initial data, the solutions behave, as $t \to \infty$, as the fundamental solution (up to a constant multiplier $C \neq 0$ which is specified by the initial data),

$$b(x,t) = t^{-N/2m} F(y), \quad y = x/t^{1/2m}, \tag{4.1.4}$$

of the linear parabolic equation (3.3.2) The rescaled kernel F is the unique radial solution of the elliptic equation (3.3.4). We refer to (Egorov et al. 2002) in which perturbation techniques are applied to any equation like (4.1.1) with the lower-order term replaced by $\pm|u|^p$ or $\pm|u|^{p-1}u$. For the reaction-diffusion equations $u_t = -(-\Delta)^m u + |u|^p$, (4.1.3) becomes the critical Fujita exponent, (Egorov et al. 2002), (Galaktionov 2001).

(ii) The critical case $p = p_0$ is studied in Galaktionov (2002) where it is established that for some initial data, global solutions have the following logarithmically perturbed fundamental asymptotic behaviour as $t \to \infty$:

$$u(x,t) = \pm C_0 (t \ln t)^{-N/2m} \left(F\left(x/t^{1/2m}\right) + o(1) \right). \tag{4.1.5}$$

The constant $C_0 \neq 0$ depends on m and N but is independent of initial data.

For the *semilinear heat equation* with $m = 1$, (4.1.2), posed for solutions $u \geq 0$, these results were established in the 1980's. In this case $p_0 = 1 + 2/N$ coincides with the critical Fujita exponent for the reaction-diffusion equation $u_t = \Delta u + u^p$; see Samarskii et al. (1995, Chap. 2) and an extended list of references therein. Moreover, a complete classification for this semilinear equation is available and in addition to (i) and (ii) above we have the following asymptotic property.

(iii) $(m = 1)$ In the subcritical range $p \in (1, p_0)$, the asymptotic behaviour of *positive* solutions is described by the *unique* VSS

$$u_*(x,t) = t^{-1/(p-1)} V(y), \quad y = x/t^{1/2}, \tag{4.1.6}$$

where $V > 0$ solves a nonlinear ODE (see below, (4.1.8)). We refer to Brezis et al. (1986) (an ODE proof of existence of the VSS), Galaktionov et al. (1986) (a PDE proof of existence and stability), Kamin and Véron (1988) (uniqueness of the VSS) and Kamin and Peletier (1985) (construction of the VSS by monotone approximation of "very" singular initial data).

4.1.2 The main result: VSSs in the subcritical range

For the higher-order equation (4.1.1) with $m \geq 2$, we study the existence and multiplicity of similarity solutions and show that in the subcritical range $p \in (1, p_0)$ there exist VSSs of the form (cf. (4.1.6))

$$u_*(x,t) = t^{-1/(p-1)} V(y), \quad y = x/t^{1/2m}, \tag{4.1.7}$$

where V is a non-trivial radial solution of the elliptic equation

$$\mathcal{L}_1^* V - V^p \equiv -(-\Delta)^m V + \frac{1}{2m} \nabla V \cdot y + \frac{1}{p-1} V - V^p = 0 \quad \text{in} \quad \mathbf{R}^N, \tag{4.1.8}$$

$$V(y) \text{ decays exponentially fast as } |y| \to \infty. \tag{4.1.9}$$

The condition on exponential decay at infinity, (4.1.9), is most naturally enforced by introducing weighted L^2 and Sobolev spaces, as described Section 3.3. The linear part of the operator $\mathcal{L}_1^*$ in equation (4.1.8) is connected with the operator (3.3.1) for the rescaled kernel F in (4.1.4)

$$\mathcal{L}_1^* = \mathcal{L}^* + c_1 I, \quad \text{where } c_1 = N(p_0 - p)/2m(p-1). \tag{4.1.10}$$

One of the main goals of this Chapter is to show by analytical and numerical methods that in the *radial setting*, the ODE problem (4.1.8), (4.1.9) admits at least

$$M(m,p,N) = \sharp_{\rm even}\,(N(p_0-p)/(p-1)) \tag{4.1.11}$$

different non-trivial radial solutions $f = f(|y|)$, where $\sharp_{\rm even}(z)$ for $z \geq 0$ denotes the number of non-negative even numbers $0, 2, 4, ...$ not exceeding the integer part $\lfloor z \rfloor$.

We also study the asymptotic stability of the VSS and describe a countable subset of other self-similar or approximately self-similar patterns in the Cauchy problem (4.1.1). We show that in the supercritical range $p > p_0$, no *generically* stable (see Section 4.3 for a precise definition) non-trivial VSSs exist. On the other hand, there does exist an uncountable family of different similarity solutions which are not in L^1 and have special stability properties.

Results on the global existence of solutions in the subcritical Sobolev range (Hirsch and Lacombe 1999), $p < p_S = (N+2m)/(N-2m)_+$, and satisfying a restriction on the initial data,

$$u_0(x) = o(e^{-k|x|^\nu}) \quad \text{as } x \to \infty \quad (\nu = 2m/(2m-1)), \tag{4.1.12}$$

may be found in Galaktionov and Williams (2003b).

4.2 Preliminaries: the exponential bundle in the ODE as $y \to \infty$

In this section we describe the asymptotics of radial solutions of the ODE (4.1.8) such that $V(y) \to 0$ as $y \to +\infty$, where y now denotes the radial variable, $|y| \geq 0$. The linearization of (4.1.8) about $V = 0$ gives

$$\mathcal{L}_1^* V = 0 \quad \text{for } y > 0. \tag{4.2.1}$$

On such decaying solutions, (4.1.8) is an asymptotically small perturbation of the linear equation (4.2.1). Proceeding as in Section 3.2.2, we begin with the ODE (4.2.1),

$$(-1)^{m+1}\left(V^{(2m)} + \frac{m(N-1)}{y}\,V^{(2m-1)} + ...\right) + \frac{1}{2m}V'y + \frac{1}{p-1}V = 0, \tag{4.2.2}$$

and set $z = y^\nu$, giving the following equation:

$$V^{(2m)} - \tilde{a}_1 V' - z^{-1}\tilde{a}_2 V + z^{-1}\mathbf{C}(z)V = 0. \tag{4.2.3}$$

Here $\tilde{a}_1 = (-1)^m \nu^{1-2m}/2m = -a_1$, $\tilde{a}_2 = (-1)^m \nu^{-2m}/(p-1) = -a_1$ (cf (3.2.10)) and $\mathbf{C}(z)V = \sum_{j=1}^{2m-1} \gamma_j z^{j+1-2m} V^{(j)}$. Recalling the analysis of Section 3.2.2 with

$$a_1 \mapsto -a_1, \quad \text{and} \quad a_2 \mapsto -a_2$$

we conclude that as $y \to \infty$, there exists an m-dimensional bundle of exponentially decaying solutions. For the second-order case $m = 1$, the bundle is only one-dimensional, making it possible to use a phase-plane analysis to prove existence of the VSS (Brezis et al. 1986), or apply a monotone parabolic method via simple super and sub-solutions of the PDE (Galaktionov et al. 1986).

In addition, (4.2.3) admits a solution corresponding to the characteristic root $\mu = 0$ with algebraic decay as $z \to \infty$ described by the first-order operator

$$-\tilde{a}_1 V' - z^{-1} \tilde{a}_2 V = 0 \quad \Longrightarrow \quad V(z) = C z^{-(2m-1)/(p-1)}.$$

For the linearized equation (4.2.1) we obtain the algebraic asymptotic behaviour,

$$V(y) = C|y|^{-2m/(p-1)}(1 + o(1)) \quad \text{as } y \to \infty, \text{ with any } C \neq 0. \tag{4.2.4}$$

Such solutions do not satisfy condition (4.1.9) and represent another family of asymptotic similarity patterns for the PDE (4.1.1) to be discussed in Section 4.6.

Comparing these results with those from Chapter 3, we see the essential difference between the similarity ODEs for blow-up and decay problems: the size of the decaying and growing exponential bundles is reversed. For the blow-up problems we have a larger *unstable* exponential bundle than *stable*, whereas it is the opposite for the decay problems. This increase in the number of free parameters at infinity leads to an uncountable spectrum of solutions to the absorption problem. However, for VSSs we also require exponential decay and will again recover a countable spectrum of admissible solutions.

Summarizing this asymptotic ODE analysis, we have that if V is a VSS profile satisfying problem (4.1.8), (4.1.9) with far field behaviour from the exponentially decaying bundle, then the following global estimate holds:

$$|V(y)| \le D_1 e^{-d_1 |y|^\nu} \quad \text{in } \mathbf{R}^N, \quad D_1, d_1 > 0. \tag{4.2.5}$$

Passing to the limit $t \to 0^+$ in (4.1.7), it follows that such VSSs satisfy

$$u_*(x,t) \to 0 \quad \text{for } x \neq 0, \quad \text{and} \quad |u_*(x,t)|^\beta \to \text{const}\, \delta(x), \quad \beta = (p-1)N/2m \tag{4.2.6}$$

in the sense of bounded measures in $\mathbf{R}^N$. Solutions with algebraic decay (4.2.4) form

the following initial data with uniform convergence only on $[\varepsilon, \infty)$, $\varepsilon > 0$:

$$u_*(x, 0^+) = C|x|^{-2m/(p-1)}. \tag{4.2.7}$$

Formally, this coincides with the limit time profile of blow-up solutions as $t \to T$, (3.2.16) described in the previous Chapter.

4.3 Stability analysis and two types of asymptotic patterns

As (4.1.10) suggests, in order to study the VSS, we need to consider the spectral properties of $\mathcal{L}^*$ and the corresponding adjoint operator $\mathcal{L}$ which will play a role in the further asymptotic analysis of the nonlinear PDE. These operators are posed in weighted L^2-spaces with the weight functions induced by the exponential estimate of the rescaled kernel (3.3.6) and are detailed in Section 3.3.

4.3.1 The stability of the zero solution

Following (4.1.7), we use the similarity scaling

$$u = (1+t)^{-1/(p-1)}v, \quad y = x/(1+t)^{1/2m}, \quad \tau = \ln(1+t) : \mathbf{R}_+ \to \mathbf{R}_+ . \tag{4.3.1}$$

The rescaled solution $v = v(y, \tau)$ then solves the autonomous equation

$$v_\tau = \mathcal{L}_1^* v - v^p \quad \text{for } \tau > 0, \quad v(y, 0) = v_0(y) \equiv u_0(y). \tag{4.3.2}$$

The VSS profiles satisfying (4.1.8), (4.1.9) are the stationary solutions of (4.3.2). We show that at $p = p_0$ the trivial stationary solution $v \equiv 0$ changes its stability, which is a crucial characterization of the critical exponent. As is well known in the general stability and bifurcation theory (Krasnosel'skii and Zabreiko 1984), often this means that $p = p_0$ is a bifurcation point of equilibria (a result to be proved in Section 4.4).

Proposition 4.3.1. *The trivial solution $v \equiv 0$ of equation (4.3.2) is unstable for $p \in (1, p_0)$, and is stable for $p > p_0$.*

Proof. It follows from (4.1.10), (3.3.9) that operator $\mathcal{L}_1^*$ in (4.3.2) (derived by linearizing about $v \equiv 0$) has the discrete spectrum

$$\sigma(\mathcal{L}_1^*) = \{\nu_l = c_1 - l/2m, \, l = 0, 1, 2, ...\}, \tag{4.3.3}$$

so that $\nu_0 > 0$ for $p \in (1, p_0)$ (for which $c_1 > 0$) and $\nu_0 < 0$ for $p > p_0$ (when $c_1 < 0$). In view of the known spectral properties of $\mathcal{L}^*$ (see Lemma 3.3.1 and (Egorov et al. 2002)),

this stability/instability result in $X = H^{2m}_{\rho} \cap L^{\infty}$ follows from the principle of linearized stability, see e.g. Lunardi (1995, Chap. 9). □

4.3.2 Nonexistence of a generically stable VSS for $p > p_0$

In the next sections we will show that the stationary problem (4.1.8), (4.1.9) can admit an arbitrarily large number of different non-trivial solutions $\{V_k,\ k = 0, 1, 2, ...M\}$ (an estimate of M is given below) together with the zero solution denoted by $V^0 \equiv 0$. In order to choose the "most" stable one, we use the following definition under natural assumptions that each profile V_k has a stable manifold $W^s(V_k)$ (of finite co-dimension) and a finite-dimensional unstable one $W^u(V_k)$ associated with the stable, centre and unstable subspaces of the linearized operator

$$\mathbf{D}_k = \mathcal{L}_1^* - p|V_k|^{p-1}I \tag{4.3.4}$$

having discrete spectrum, see Section 4.4.

Definition 4.3.1. *We say that V_0 is* generically stable *in X if:*

(i) $W^u(V_0) = \emptyset$,
(ii) $W^u(V_k) \neq \emptyset$ for all $k = 1, 2, ..., M$, and
(iii) for any $v_0 \notin (\cup_{k=1}^{M} W^s(V_k)) \cup W^s(0)$, $v(\tau) \to V_0$ as $\tau \to \infty$.

Note that (iii) includes the global property of stabilization to a stationary solution in the dynamical system (4.3.2) on X, which is not known for general orbits since (4.3.2) is not a gradient system, see Section 4.5. Therefore, we mainly study the usual (local) stability properties of the VSS for $p < p_0$ (Section 4.4). The above definition is currently used to establish a "weak" nonexistence result for $p > p_0$.

Corollary 4.3.2. *For $p > p_0$, a non-trivial generically stable VSS satisfying* (4.1.8), (4.1.9) *does not exist.*

Indeed, according to Proposition 4.3.1, for $p > p_0$, the trivial profile $V^0 \equiv 0$ is locally stable. This means that a connection $\{0\} \to \{V_0\}$ in X described by (4.3.2) does not exist. The same nonexistence result remains true in the critical case $p = p_0$. However, we will present below results on a centre manifold analysis showing that 0 is still stable at the critical exponent. In view of the rather complicated bifurcation structure for equation (4.1.8) which includes an arbitrarily large number of branches for $p \approx 1^+$ (Section 4.4), the proof of actual nonexistence of VSSs for $p \geq p_0$ and arbitrary m and N is a hard problem. On the other hand, the following nonexistence result is straightforward but we do not believe it to be sharp.

Proposition 4.3.3. *A non-trivial VSS does not exist for any $p \geq p_* = 1 + 4m/N$.*

Proof. Multiplying (4.1.8) by V and integrating by parts over $\mathbf{R}^N$ yields

$$-\|\bar{D}^m V\|_2^2 + \mu_* \|V\|_2^2 - \|V\|_{p+1}^{p+1} = 0,$$

where $\mu_* = 1/(p-1) - N/4m \le 0$ for $p \ge p_*$. □

4.3.3 A first estimate on the number of VSSs for $p < p_0$

It follows from (4.3.3) that in the subcritical case $p \in (1, p_0)$, there exists a finite number of unstable modes corresponding to the trivial equilibrium $V^0 \equiv 0$ of (4.3.2). The Morse index of $\mathcal{L}_1^*$ is given by the cardinal number

$$M(m,p,N) = \sharp\,\{\beta :\ |\beta| < 2mc_1 = N(p_0 - p)/(p-1)\}. \tag{4.3.5}$$

The operator $\mathcal{L}_1^* v - v^p$ is only known to be potential for $m = 1$, see Galaktionov et al. (1986), Escobedo and Kavian (1987) and Bricmont and Kupiainen (1996). Furthermore, equation (4.3.2) is not a gradient system for $m > 1$ (Section 4.5). The general properties of orbital connections for semilinear higher-order parabolic equations are unknown. For $m = 1$ such a classification (Henry 1985, Angenent 1986) is based on Sturm's Theorem on zeros associated with the Maximum Principle. Therefore, we cannot guarantee that each unstable mode generates stabilization to a non-trivial stationary profile (unlike the case $m = 1$ where this is actually true).

Nevertheless, completing this discussion, we expect that the number (4.3.5) characterizes the total finite number of nontrivial stationary solutions of the problem (4.1.8), (4.1.9), which are "nonlinear" asymptotic patterns for the PDE under consideration. This number of nonlinear patterns increases without bound as p decreases,

$$M(m,p,N) \to \infty \quad \text{as } p \to 1^+. \tag{4.3.6}$$

In the radial setting, (4.3.5) coincides with (4.1.11). The critical (bifurcation) exponents, at which $M(m,p,N)$ is discontinuous, are given by

$$c_1 - l/2m = 0 \implies p_l = 1 + 2m/(l+N), \quad l = 0,1,2,\dots. \tag{4.3.7}$$

Therefore, (4.1.3) is the first, maximal exponent corresponding to $l = 0$.

4.3.4 The stable manifold behaviour: a countable subset of linearized patterns

Unlike the nonlinear VSS patterns, the stable infinite-dimensional subspace $E^s = \mathrm{Span}\{\psi_\beta,\ \nu_{|\beta|} < 0\}$ of $\mathcal{L}_1^*$ generates linearized patterns decaying exponentially fast as $\tau \to \infty$. In view of the completeness and orthonormality of eigenfunctions of $\mathcal{L}_1^*$,

for initial data $v_0 \in X$ we use the uniformly converging eigenfunction expansion of solutions which are sufficiently smooth by parabolic regularity theory (Eidelman 1969, Friedman 1983)

$$v(\tau) = \sum a_\beta(\tau)\psi_\beta. \tag{4.3.8}$$

The expansion coefficients satisfy the dynamical system

$$a'_\beta = \nu_{|\beta|}a_\beta - \langle v^p, \psi_\beta\rangle \quad \text{for any } \beta. \tag{4.3.9}$$

The diagonally dominant structure of the system (4.3.9) shows that if the nonlinear term v^p forms an exponentially decaying perturbation as $\tau \to \infty$ (say, if v is small), then there exist patterns with exponential decay as $\tau \to \infty$

$$v(y,\tau) = Ce^{\nu_{|\beta|}\tau}(\psi^*_\beta(y) + o(1)), \quad C = C(u_0) \neq 0, \tag{4.3.10}$$

where ψ^*_β is a suitable eigenfunction with $\nu_{|\beta|} < 0$. In the asymptotic sense, these are exponentially decaying solutions of the linear equation $v_\tau = \mathcal{L}^*v$, and such results are well known in the linear perturbation theory, (Friedman 1983).

4.3.5 The centre manifold behaviour at $p = p_l$: logarithmic scaling factors

It follows from (4.3.7) that at any $p = p_l$, $\mathcal{L}^*_1$ has a nontrivial centre subspace. We describe the corresponding behaviour of radially symmetric asymptotic patterns, cf. (Galaktionov 2002) and (Egorov et al. 2002). For arbitrary even $l = 2, 4, ...$, the operator $\mathcal{L}^*_1$ has the simple eigenvalue 0 with a one-dimensional centre subspace $E^c = \mathrm{Span}\{\psi^*_l(|y|)\}$ and a finite number of isolated positive eigenvalues. Assuming the existence of a local centre manifold, we look for a solution of (4.3.2) in the form

$$v(\tau) = a_l(\tau)\psi^*_l(y) + w(\tau) \quad \text{for } \tau \gg 1, \quad w(\tau) = o(a_l(\tau)) \quad w \in (E^c)^\perp, \tag{4.3.11}$$

and arrive at the asymptotic ODE

$$a'_l = -\kappa_l|a_l|^{p-1}a_l(1 + o(1)) \quad \text{with} \quad \kappa_l = \langle(\psi^*_l)^p, \psi_l\rangle.$$

The positivity of the coefficient κ_l is of crucial importance (otherwise the behaviour is unstable) and is guaranteed at least for large l (see Section 4.4). This gives

$$a_l(\tau) = \pm C_l\tau^{-1/(p-1)}(1 + o(1)) \quad \text{as } \tau \to \infty,$$

where

$$C_l = [2m\,\kappa_l/(k+N)]^{-(l+N)/2m}.$$

Transforming back to the original variables $\{x, t, u\}$ gives the following asymptotic patterns at $p = p_l$ (cf. (4.1.5) for $l = 0$):

$$u(x,t) = \pm C_l (t \ln t)^{-(l+N)/2m} \left(\psi_l^*(|x|/t^{1/2m}) + o(1) \right) \quad \text{for } t \gg 1. \tag{4.3.12}$$

At the first critical exponent $p = p_0$, solutions (4.3.11) take the form

$$v(y,\tau) = \pm C_0 \tau^{-N/2m} (f(y) + o(1)) \to 0 \quad \text{as } \tau \to \infty.$$

Since this behaviour is on the centre manifold, (and $W^u(0) = \emptyset$), the trivial solution $v \equiv 0$ of (4.3.2) is stable, implying nonexistence of a non-trivial generically stable VSS and extending Corollary 4.3.2 to $p = p_0$.

The two types of asymptotic solutions described above combined with another detailed in (Galaktionov and Williams 2003b) are expected to form an "evolutionarily complete" countable subset of patterns in the diffusion-absorption problem under consideration in the sense that any nontrivial X-valued solution takes, as $t \to \infty$, the form of one of these patterns. Evolutionary completeness remains a hard open problem for many second and all of the higher-order semilinear parabolic equations considered in this thesis.

4.4 Very singular similarity profiles in the subcritical range $p \in (1, p_0)$

We return to the VSS profiles V satisfying the ODE problem (4.1.8), (4.1.9) in the subcritical range $p \in (1, p_0)$. Based on the linear analysis of Sections 3.3 and 4.3, we consider bifurcation problems in which we can construct solutions by parameter continuation and study their stability near to the critical values p_l.

4.4.1 Bifurcations at $p = p_l$: local existence and stability of the VSS

Taking p near the critical values as defined in (4.3.7), we look for small solutions to (4.1.8). At $p = p_l$ the linear operator $\mathcal{L}_1^*$ has a nontrivial kernel, hence, the following result.

Proposition 4.4.1. *Let, for an integer $l \geq 0$, the eigenvalue $\lambda_l = -l/2m$ of the operator* (3.3.4) *be of odd multiplicity. Then the critical exponent $p_l = 1 + 2m/(l+N)$ in* (4.3.7) *is a bifurcation point for the problem* (4.1.8), (4.1.9).

Proof. For a moment, given an $n \gg 1$, we denote by $(V^p)_n$ a suitable uniformly Lipschitz continuous truncation of the nonlinearity V^p such that $(V^p)_n \equiv V^p$ for $|V| \leq$

n and

$$(V^p)_n \to V^p \quad \text{as } n \to \infty \text{ uniformly on compact subsets.}$$

Consider in L^2_ρ the truncated equation

$$\hat{\mathcal{L}}^* V = -(1+c_1)V + (V^p)_n, \quad \hat{\mathcal{L}}^* = \mathcal{L}_1^* - (1+c_1)I \equiv \mathcal{L}^* - I. \tag{4.4.1}$$

The spectrum of $\hat{\mathcal{L}}^*$ is a translation of that of $\mathcal{L}^*$, (4.3.3), $\sigma(\hat{\mathcal{L}}^*) = \{-1 - l/2m\}$, and consists of strictly negative eigenvalues. The inverse operator $\hat{\mathcal{L}}^{*-1}$ is known to be compact (Egorov et al. 2002, Proposition 2.4). Therefore, in the corresponding integral equation

$$V = \mathbf{A}(V) \equiv -(1+c_1)\hat{\mathcal{L}}^{*-1}V + \hat{\mathcal{L}}^{*-1}(V^p)_n, \tag{4.4.2}$$

the right-hand side is a compact Hammerstein operator, (Krasnosel'skii 1964, Chap. 5). Bifurcations in the truncated problem (4.4.2) occur if the derivative $\mathbf{A}'(0) = -(1+c_1)\hat{\mathcal{L}}^{*-1}$ has the eigenvalue 1 of odd multiplicity, see Krasnosel'skii and Zabreiko (1984) and Krasnosel'skii (1964). Since $\sigma(\mathbf{A}'(0)) = \{(1+c_1)/(1+l/2m)\}$, we arrive at the critical values (4.3.7). By construction, the solutions of (4.4.2) for $p \approx p_l$ are small in L^2_ρ and, as can be seen from the properties of the inverse operator, in $H^{2m}_{\rho^*}$. Since the weight (3.3.8) is a monotone growing function as $|y| \to \infty$, using the known asymptotic properties of solutions of the ODE (4.1.8) (Section 4.2), $V \in H^{2m}_{\rho^*}$ is a uniformly bounded, continuous function. [It is worth mentioning that for even m solutions of (4.1.8) may blow-up at finite y (in striking contrast with second-order ODEs) forming singularities $\notin L^2_\rho$ locally.] Therefore, for $p \approx p_l$ we only have bounded, small solutions. Hence the same bifurcations occur in the original non-truncated equation (4.4.2) corresponding to $n = \infty$. □

Thus, $l = 0$ is always a bifurcation point since $\lambda_0 = 0$ is simple. In general, for $l = 1, 2, \ldots$ odd multiplicity occurs depending on the dimension N. In particular, for $l = 1$, the multiplicity is N, and for $l = 2$, it is $N(N+1)/2$. In the case of even multiplicity of λ_l, an extra analysis is necessary to guarantee that a bifurcation occurs, (Krasnosel'skii and Zabreiko 1984). It is important that for key applications, namely, for $N = 1$ and for the radial setting in $\mathbf{R}^N$, the eigenvalues (3.3.9) are simple and (4.3.7) are bifurcation points defining the critical exponents.

Since the nonlinear perturbation term in the integral equation (4.4.2) is an odd sufficiently smooth operator, we arrive at the following result describing the local behaviour of bifurcation branches, see Krasnosel'skii (1964) and Krasnosel'skii and Zabreiko (1984, Chap. 8).

Proposition 4.4.2. *Let λ_l be a simple eigenvalue of $\mathcal{L}^*$ with eigenfunction ψ_l. Denoting*

$$\kappa_l = \langle (\psi_l^*)^p, \psi_l \rangle, \tag{4.4.3}$$

we have that problem (4.1.8), (4.1.9) *has (i) precisely two small solutions for $p \approx p_l^-$*

and no solutions for $p \approx p_l^+$ if $\kappa_l > 0$, and (ii) precisely two small solutions for $p \approx p_l^+$ and no solutions for $p \approx p_l^-$ if $\kappa_l < 0$.

The two possibilities arise from the need of the product $\kappa_l(p_1 - p)$ to be positive.

In order to describe the asymptotics of solutions as $p \to p_l$, we apply the Lyapunov-Schmidt method (Krasnosel'skii and Zabreiko 1984, Chap. 8) to equation (4.4.2) with the operator $\mathbf{A}$ being differentiable at 0. Since under the assumptions of Proposition 4.4.2 the kernel $E_0 = \ker \mathbf{A}'(0) = \mathrm{Span}\{\psi_l^*\}$ is one-dimensional, denoting by E_1 the complementary (orthogonal to ψ_l^*) invariant subspace, we set $V = V_0 + V_1$, where $V_0 = \varepsilon_l \psi_l^* \in E_0$ and $V_1 = \sum_{k \neq l} \varepsilon_k \psi_k \in E_1$. Let P_0 and P_1, $P_0 + P_1 = I$, be projections onto E_0 and E_1 respectively. Projecting (4.4.2) with $n = \infty$ onto E_0 yields

$$\gamma_l \varepsilon_l = \langle \hat{\mathcal{L}}^{*-1}(V^p), \psi_l \rangle, \quad \gamma_l = 1 - (1 + c_1)/(1 + l/2m) = -(N + l)s/(p - 1)(2m + l), \tag{4.4.4}$$

where $s = p_l - p$. By the general bifurcation theory (see e.g. Krasnosel'skii and Zabreiko (1984, p. 355), noting that the operator $\mathbf{A}'(0)$ is a Fredholm operator with index zero), $V_1 = o(\varepsilon_l)$ as $\varepsilon_l \to 0$, so that ε_l is calculated from (4.4.4) as follows

$$\gamma_l \varepsilon_l = \varepsilon_l^p \langle \hat{\mathcal{L}}^{*-1}(\psi_l^*)^p, \psi_l \rangle + o(\varepsilon_l^p) \implies |\varepsilon_l|^{p-1} = \hat{c}_l \left((p_l - p) + o(1) \right), \ \hat{c}_l = (l+N)^2/4m^2\kappa_l,$$

where we have performed the calculations as follows

$$\langle \hat{\mathcal{L}}^{*-1}(\psi_l^*)^p, \psi_l \rangle = \langle (\psi_l^*)^p, (\hat{\mathcal{L}})^{-1} \psi_l \rangle = -\kappa_l/(1 + l/2m).$$

(here we have used the identity $(\hat{\mathcal{L}}^{*-1})^* = (\hat{\mathcal{L}})^{-1}$). In view of the orthonormality property (3.3.14), for $p = 1$ we have $\kappa_l = 1$, so that by continuity we can guarantee that

$$\kappa_l > 0 \quad \text{at least for all } p \approx 1^+. \tag{4.4.5}$$

Thus, we obtain a countable sequence of bifurcation points (4.3.7) satisfying $p_l \to 1^+$ as $l \to \infty$, with typical pitch-fork bifurcation branches appearing in a left-hand neighbourhood, for $p < p_l$. The behaviour of solutions in H^{2m}_ρ and uniformly takes the form

$$V_l(y) = \pm \left[\hat{c}_l (p_l - p) \right]^{1/(p-1)} \left(\psi_l^*(y) + o(1) \right) \quad \text{as } p \to p_l^-. \tag{4.4.6}$$

We now prove the main result concerning "local" existence and stability of the VSS solution with the similarity profile $V_0(y)$ corresponding to the first bifurcation point, $p = p_0$. If $\kappa_0 > 0$, as expected (this has been verified numerically), then two bifurcation branches exist for $p < p_0$.

Theorem 4.4.3. *For $p \approx p_0^-$, problem* (4.1.8), (4.1.9) *admits a solution $V_0(y)$ provided that $2m/N$ is small enough. Furthermore this is an asymptotically stable stationary solution of the rescaled equation* (4.3.2).

Proof. As we have shown, a continuous branch bifurcating at $p = p_0^-$ exists if

$$\kappa_0 = \langle ((\psi^*)_0^{p_0}, \psi_0 \rangle \equiv \int |F|^{2m/N} F > 0 \quad (\psi_0 \equiv 1). \tag{4.4.7}$$

In view of the positivity dominance of the rescaled fundamental solution F, $\int F = 1$, (3.3.5), we have that (4.4.7) holds by continuity provided that $2m/N \ll 1$. Therefore, in this case there exists a solution (4.4.6) with $l = 0$ satisfying for small $s = p_0 - p > 0$ uniformly

$$V_0(y) = (\hat{c}_0 s)^{1/(p-1)}[f(y) + o(1)], \quad \hat{c}_0 = N^2/4m^2\kappa_0. \tag{4.4.8}$$

We now estimate the spectrum of the linearized operator of equation (4.3.2)

$$\mathbf{D}_0 = \mathcal{L}_1^* - p|V_0|^{p-1}I. \tag{4.4.9}$$

Some of the eigenvalues of (4.4.9) follow from the original PDE (4.1.1). For instance, the stable eigenspace with $\hat{\lambda} = -1$, $\hat{\psi} = \frac{1}{p-1}V_0 + \frac{1}{2m}\nabla V_0 \cdot y \in L^2_\rho$, follows from the time-translational invariance of the PDE. For $N = 1$, translations in x yield another pair $\hat{\lambda} = -1/2m$, $\hat{\psi} = V_{0y} \in L^2_{\rho^*}$. For $N > 1$, in the non-radial setting, this $\hat{\lambda}$ has multiplicity N with eigenfunctions V_{0y_i}. These are not the first pair with the maximal real part.

Bearing in mind that the spectrum of the unperturbed operator $\mathcal{L}^*$ is real, (3.3.9), and has the unique, non-hyperbolic eigenvalue $\lambda_0 = 0$, we use (4.4.8) to obtain

$$\mathbf{D}_0 = \mathcal{L}^* + s(1 + o(1))\mathbf{C}, \tag{4.4.10}$$

where, as it follows from (4.4.7) and (4.4.8) at $p = p_0$, the perturbation has the form

$$\mathbf{C} = \frac{N^2}{4m^2}\left(1 - \frac{p_0}{\kappa_0}|F|^{2m/N}\right) I. \tag{4.4.11}$$

Therefore, we consider the spectrum of the perturbed operator

$$\tilde{\mathbf{D}}_0 = \mathcal{L}^* + s\mathbf{C}. \tag{4.4.12}$$

Since the operator $(\mathcal{L}^* - I)^{-1}\mathbf{C}$ is bounded,

$$(\tilde{\mathbf{D}}_0 - I)^{-1} = (I + s(\mathcal{L}^* - I)^{-1}\mathbf{C})^{-1}(\mathcal{L}^* - I)^{-1}$$

is compact for small $|s|$ as the product of compact and bounded operators. Hence, $\tilde{\mathbf{D}}_0$ also has only a discrete spectrum. By the classical perturbation theory of linear operators (see e.g. (Gohkberg and Krein 1969)), the eigenvalues and eigenvectors of $\tilde{\mathbf{D}}_0$ can be constructed as a perturbation of the discrete spectrum $\sigma(\mathcal{L}^*)$ consisting of eigenvalues of finite multiplicity. We are interested in the perturbation of the first

simple eigenvalue $\lambda_0 = 0$. Setting

$$\tilde{\lambda}_0 = s\mu_0 + o(s), \quad \tilde{\psi}_0 = \psi_0^* + s\varphi_0 + o(s) \quad \text{as} \quad s \to 0$$

and substituting these expansions in the eigenvalue equation $\tilde{\mathbf{D}}_0\tilde{\psi}_0 = \tilde{\lambda}_0\tilde{\psi}_0^*$ yields

$$\mathcal{L}^*\varphi_0 = (-\mathbf{C} + \mu_0 I)\psi_0. \tag{4.4.13}$$

We then obtain the solvability (orthogonality) condition

$$\langle(-\mathbf{C} + \mu_0 I)\psi_0^*, \psi_0\rangle = 0 \implies \mu_0 = \langle \mathbf{C}f, 1\rangle.$$

Using (4.4.11) yields $\mu_0 = -N/2m < 0$. Therefore, $\operatorname{Re}\tilde{\lambda}_0 < -sN/4m < 0$ for all $p \approx p_0^-$. Since, with these properties of the spectrum, the perturbation (4.4.9) of $\mathcal{L}^*$ remains a sectorial operator with $\sigma(\tilde{\mathbf{D}}_0) \subset \{\operatorname{Re}\lambda \le -sN/4m\}$ and $\|e^{\tilde{\mathcal{L}}^* 1^\tau}\|_{\mathcal{L}} \le Ce^{-N(p_0-p)\tau/4m}$ in the norm of $\mathcal{L}(H^{2m}_{\rho^*}, H^{2m}_{\rho^*})$ (Friedman 1983), $V_0(y)$ is exponentially stable in $H^{2m}_{\rho^*}$. □

We expect that condition (4.4.7) remains valid for any m and N so that $V_0(y)$ is stable without the restriction $2m \ll N$. There is strong numerical support for this (see Section 4.4.3), but, as yet, no rigorous proof. Possibly, to check conditions such as (4.4.7) we must currently rely on numerical evidence and then, as often happens in spectral theory and applications, Theorem 4.4.3 can be established with a hybrid analytic-computational proof. We also expect that the whole branch bifurcating from $p = p_0$ remains stable for all $p \in (1, p_0)$, though the proof would require one to establish that the discrete spectrum $\sigma(\mathbf{D}_0)$ never touches the imaginary axis. In particular, this difficult open problem means that a new (nonlinear) saddle-node bifurcation never occurs on this p_0-branch, i.e., it does not have any turning points.

Further, one can see that the other bifurcation branches are *unstable*. Taking any $l \ge 1$, instead of (4.4.10) we now have

$$\mathbf{D}_l = \mathcal{L}_1^* - p|V_l|^{p-1}I \equiv \mathcal{L}^* + \left[c_1 - sp_l\hat{c}_l(|\psi_l^*|^{p-1} + o(1))\right] I, \quad s = p_l - p. \tag{4.4.14}$$

From the definition of $\mathcal{L}_1^*$, (4.1.10), $c_1 > 0$ for all $p \approx p_l$, thus V_l for $l \ge 1$ is unstable.

The transition to a subset of linear patterns at $p = 1$. By (4.3.7), the sequence of critical exponents converges from above to $p = 1$ corresponding to the linear equation

$$\bar{u}_t = -(-\Delta)^m\bar{u} - \bar{u}. \tag{4.4.15}$$

Therefore, the expansion (4.4.6) gives an exceptional opportunity to see the *transition* from the non-linear patterns for $p > 1$ to the linear ones for $p = 1$. For $p \approx 1^+$ there

exists an arbitrarily large number of nonlinear patterns which become unbounded linear patterns in the case $p = 1$ (this trend is seen in Figure 4.1 to be discussed below). Some simple computations reveal the scaling factors of such a transition.

It is easy to determine all the linear (radial) patterns. Setting $\bar{u} = e^{-t}\tilde{u}$ in (4.4.15) yields the linear parabolic equation (3.3.2) with the known countable subset of asymptotic patterns, cf. (4.3.10). Hence, up to a constant multiplier, the subset of linear patterns is

$$\bar{u}_l(x,t) = e^{-t}t^{-(N+l)/2m}\psi_l^*(y), \quad y = x/t^{1/2m}; \quad l = 0, 1, 2, \dots . \tag{4.4.16}$$

It is important to note that due to the completeness of the eigenfunctions, Lemma 3.3.1, the pattern subset (4.4.16) is evolutionarily complete (these notions coincide in the linear case). On the other hand, using expansion (4.4.6), we obtain the following nonlinear asymptotic patterns corresponding to the original PDE (4.1.1) for $p \approx 1^+$:

$$u_l(x,t) \approx t^{-1/(p-1)}\,(\hat{c}_l(p_l - p))^{1/(p-1)}\,\psi_l^*(y). \tag{4.4.17}$$

Then the scaling factors in the pattern transition as $p \to 1^+$ are given by

$$\big(t^{-1}\tilde{c}_l(p_l - p)\big)^{-1/(p-1)}\,u_l(x,t) \to \psi_l^*(y) \equiv e^t t^{(N+l)/2m}\bar{u}_l(x,t).$$

For the ODE (4.1.8), the nonlinear VSS profiles are generated at $p = 1^+$ by the eigenfunctions of a linear Sturm-Liouville problem for the non-self adjoint operator $\mathcal{L}^*$, cf. (4.4.6).

4.4.2 Numerical calculations of the global bifurcation p-diagram

Our counting argument on the number of available solutions for a particular value of p is based on the number of bifurcation points (the Morse index of $\mathcal{L}_1^*$) which are available for $p < p_0$. Because of the existence of infinitely many solutions in the linear problem for $p = 1$, we conjecture that each branch bifurcating from $1 < p_l \le p_0$ is defined on $(1, p_l)$ and contributes exactly one additional exponentially decaying solution. Numerical results presented in Figure 4.1 support this as the branches are monotone in p with no branch ever contributing more than one solution. This is simpler than the blow-up problem in Chapter 3.6, where some non-monotone branches were seen to contribute multiple solutions, see Conjecture 3.6.1. To compute numerical approximations we begin with numerical approximations to (4.4.6) near the critical exponents p_l. These are then continued in p using the pseudo-arclength package AUTO (Doedel et al. 1997). All the numerically constructed similarity profiles $V(y)$ have asymptotics from the exponential bundle described in Section 4.2. This was not enforced numerically but is simply a property of the initial profiles used for continuation. Such solutions correspond to sharp agreement in the number of available solutions described in the estimate (4.1.11).

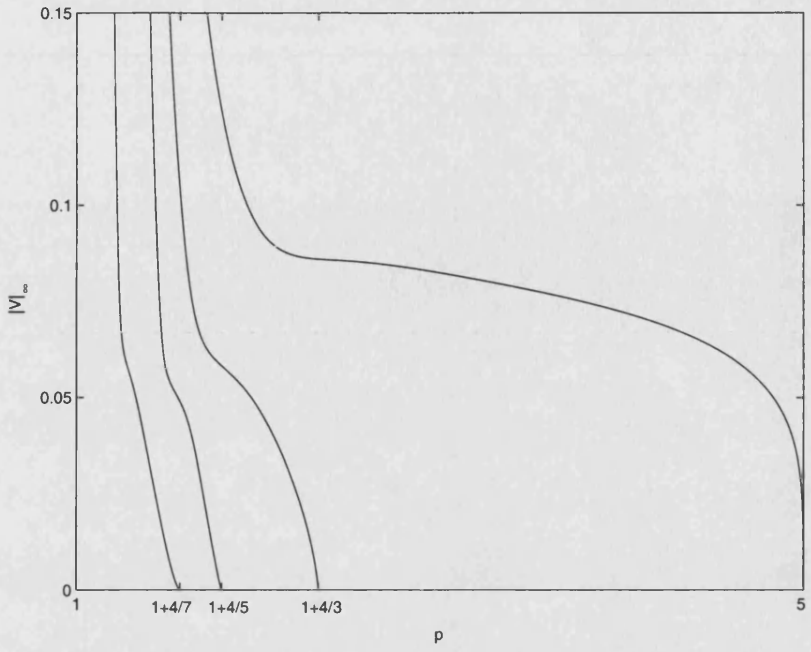

Figure 4.1: Bifurcation diagram with respect to p, $m = 2$, $N = 1$

4.4.3 VSS similarity profiles for various p, N and m

The two profiles with $m = 2$, $p = 2$ and $N = 1$ are presented in Figure 4.2a. Qualitatively, the picture remains unchanged in higher dimensions. In Figure 4.2b we present radially symmetric profiles $V(|y|)$ for $N = 2$ and 3. Topologically, there is no great distinction between the computed solutions for different values of N with all branches emanating from the bifurcation points of the associated linear operator. Further, the solutions and bifurcation diagrams are qualitatively similar for $m = 3$.

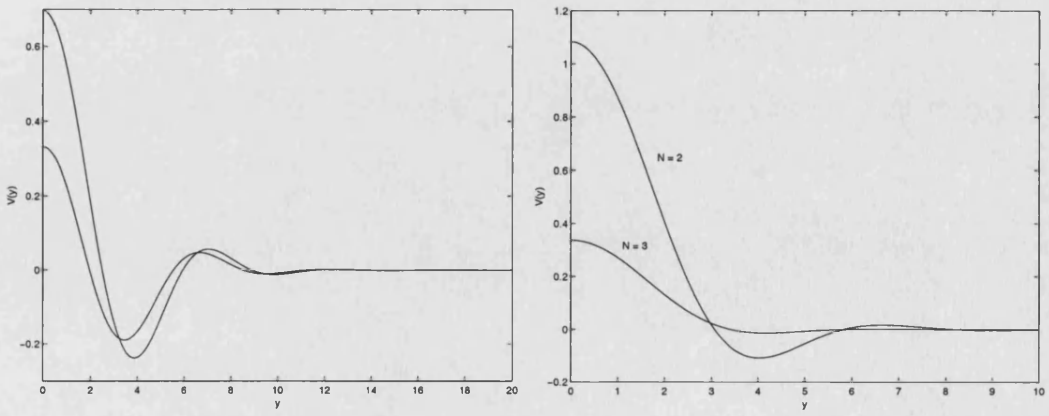

Figure 4.2: (a) Two similarity profiles V_0 and V_1 for $m = 2$, $p = 2$, $N = 1$. (b) The primary similarity profile V_0 for $m = 2$, $p = 3/2$, $N = 2$ and 3.

4.4.4 The local μ–bifurcation diagram

Following the branching approach of Chapter 3, in which we continued the solution branches in the parameter μ, we introduce the linear operator

$$\mathcal{L}^*_\mu = -(-\Delta)^m + \mu y \cdot \nabla + I/(p-1) \quad \text{with a parameter } \mu \geq 0, \tag{4.4.18}$$

and consider the corresponding equation

$$\mathcal{L}^*_\mu V - V^p = 0 \quad \text{in } \mathbf{R}^N \quad \text{with condition (4.1.9).} \tag{4.4.19}$$

For $\mu = 1/2m$, we get the original VSS-problem (4.1.8), (4.1.9). This μ-parameterization provides an additional approach to study the multiplicity of the VSS profiles. It is important for describing a transition to the elliptic problem occurring at $\mu = 0$,

$$-(-\Delta)^m V + V/(p-1) - V^p = 0 \quad \text{in } \mathbf{R}^N, \tag{4.4.20}$$

which admits a variational formulation in terms of critical points of the functional $\Phi(V) = -\frac{1}{2}\|\bar{D}^m V\|_2^2 + \frac{1}{2(p-1)}\|V\|_2^2 - \frac{1}{p+1}\|V\|_{p+1}^{p+1}$. For $N = 1$, (4.4.20) is a Hamiltonian dynamical system with known solution properties for $m = 2$, see Peletier and Troy (2001) and the references therein. In Chapter 3, μ-bifurcation diagrams were shown to be quite effective in studying blow-up similarity profiles for the semilinear $2m$-th order ODE occurring in the PDE (4.1.1) with the source term $+u^p$.

We now briefly describe bifurcation in the problem (4.4.19) from the trivial solution $V^0 \equiv 0$. We find the spectrum of $\mathcal{L}^*_\mu$ in $L^2_{\rho^*}$ by introducing the new independent variable $y = z/(2m\mu)^{1/2m}$. Then Lemma 3.3.1 yields

$$\mathcal{L}_\mu = 2m\mu\mathcal{L}^* + (-\mu N + 1/(p-1))\, I \implies \sigma(\mathcal{L}_\mu) = \{-\mu(N+l) + 1/(p-1)\},$$

whence the following result, analogous to Proposition 4.4.2.

Proposition 4.4.4. *Let the eigenvalue $\lambda_l = -l/2m$ in (3.3.9) be of odd multiplicity. Then*

$$\mu_l = 1/(N+l)(p-1) \tag{4.4.21}$$

is a bifurcation point in the problem (4.4.19).

Indeed, denoting $c = 1/(p-1) - \mu N$ and $\hat{\mathcal{L}^*}_\mu = \mathcal{L}^*_\mu - (1+c)I$, we have from (4.4.19)

$$\hat{\mathcal{L}^*}_\mu V = -(1+c)V + V^p.$$

The spectrum $\sigma(\hat{\mathcal{L}}_\mu) = \{-1 - \mu l\}$ consists of strictly negative eigenvalues. The proof is now analogous to that of Proposition 4.4.1 with the integral equation (4.4.1) replaced

by

$$V = \mathbf{A}_\mu(V) \equiv -(1+c)\hat{\mathcal{L}}_\mu^{-1}V + \hat{\mathcal{L}}_\mu^{-1}(V^p). \tag{4.4.22}$$

Again, bifurcations occur if the derivative $\mathbf{A}'_\mu(0) = -(1+c)\hat{\mathcal{L}}_\mu^{-1}$ has the eigenvalue 1 of odd multiplicity. Since $\sigma(\mathbf{A}_\mu{}'(0)) = \{(1+c)/(1+\mu l)\}$, this yields (4.4.21). Also, by construction, the solutions of (4.4.22) for $\mu \approx \mu_l$ are small in $L^2_{\rho^*}$, $H^{2m}_{\rho^*}$ and uniformly.

The local bifurcation structure in μ is similar to that for p (cf. Proposition 4.4.2). Namely, if λ_l is a simple eigenvalue of $\mathcal{L}^*$, then (4.4.2) has (i) precisely two small solutions for $\mu \approx \mu^-$ and no solutions for $\mu \approx \mu^+$ if $\kappa_l > 0$ and (ii) precisely two small solutions for $\mu \approx \mu^+$ and no solutions for $\mu \approx \mu^-$ if $\kappa_l < 0$. Under assumption $\kappa_l > 0$, pitch-fork bifurcations occur with branches appearing in a left-hand neighbourhood, for $\mu < \mu_l$, with the behaviour

$$V(y) = \pm\,[c_l(\mu_l - \mu)]^{1/(p-1)}\,[\psi_l^*(y) + o(1)], \quad \mu \to \mu_l^-; \quad c_l = (N+l)/\kappa_l. \tag{4.4.23}$$

We apply numerical methods to extend the local behaviour of the bifurcation diagram from the previous section. We will fix $N = 1$ and $m = 2$, and using initial data near the bifurcation points, continue solutions in μ using the numerical continuation code AUTO (Doedel et al. 1997). Taking $p = 2$, from (4.1.11) we expect at least two solutions. We conjecture that these solutions arise from the two unstable modes of the operator $\mathcal{L}_1^*$ in this case. Notice in Figure 4.3 that the two solutions available at $\mu = 1/4$ extend from branches connecting bifurcation points on either side of the value $\mu = 1/4$, $1 \to 1/5$ and $1/3 \to 1/7$. There are no other bifurcation points available greater than $1/4$.

All branches presented in Figure 4.3 leave the bifurcation points (4.4.21) as predicted by the asymptotics (4.4.23). However, for $\mu = 0$, the Hamiltonian system (4.4.20) does not admit any nontrivial solution (Peletier and Troy 2001). This gives rise to the closed orbits observed numerically in Figure 4.3.

4.5 For any $m > 1$ the rescaled operator is not potential

Let us return to the general problem of the stability of the similarity profiles constructed above locally close to bifurcation points. Assuming that $1 < p < p_0$, we consider the rescaled PDE (4.3.2) having VSS profiles $\{V_l\}$ as the stationary solutions. We have conjectured that, the first VSS similarity profile $V_0(y)$, corresponding to the branch bifurcating from $p = p_0^-$, is the only generically stable one describing the asymptotic behaviour for a dense subset of initial data $v_0 \in H^{2m}_\rho \cap L^\infty$. In other words, the stable branch which was proved in Theorem 4.4.3 to have originated from $p = p_0^-$ remains stable for all $1 < p < p_0$. We have strong numerical evidence supporting this conclusion. For $m = 1$, this is proved by various methods, see first results by the Lyapunov method (parabolic monotonicity) in (Galaktionov et al. 1986) and the references to Chap. 2

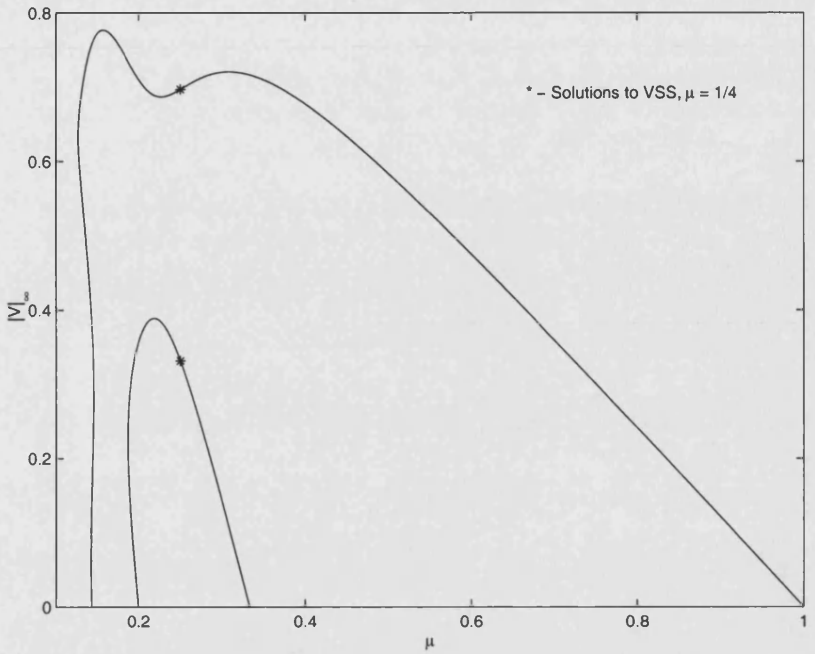

Figure 4.3: Bifurcation diagram with respect to μ

in (Samarskii et al. 1995). Even for $N = 1$ we do not know if equation (4.3.2) admits a Lyapunov function and is a gradient system. Moreover, we will present evidence to suggest that this is not the case for any $m > 1$.

Gradient systems for $m = 1$.

For rescaled equations such as (4.3.2) with $m = 1$ written in symmetric form

$$v_\tau = \frac{1}{\rho}\nabla \cdot (\rho \nabla v) + \frac{1}{p-1}\, v - v^p, \quad \rho = e^{|y|^2/4}, \tag{4.5.1}$$

the potential (variational) structure of the operator in L^2_ρ was used in (Escobedo and Kavian 1987) and in a number of subsequent papers; see additional references in Samarskii et al. (1995, Chap. 2). Indeed, since the linear operator in (4.5.1) is self-adjoint in L^2_ρ, a Lyapunov function is obtained by multiplying by ρv_τ and integrating over $\mathbf{R}^N$. Moreover, for the second-order parabolic equations with one spatial variable (or in $\mathbf{R}^N$ with radial symmetry), potential operators are dominant. Recall (Zelenyak 1968) that any quasilinear second-order uniformly parabolic equation with smooth coefficients

$$v_\tau = \mathbf{P}_2(v) \equiv a(y, v, v_y)v_{yy} + b(y, v, v_y) \tag{4.5.2}$$

on a bounded interval with typical (nonlinear) boundary conditions is a gradient system. Namely, there exists a smooth multiplier $\rho(y, v, w) > 0$, $w = v_y$, such that $\rho \mathbf{P}_2(v) = F'(v)$ is a potential operator. Hence, multiplying (4.5.2) by ρv_τ and integrating in y

yields a Lyapunov function, and for some function $\Phi(y, v, v_y)$ ($F(v) = \int \Phi(v)$ is the potential of $\rho \mathbf{P}_2(v)$), there holds

$$\frac{d}{d\tau} \int \Phi = \int \rho v_\tau^2 \ge 0 \tag{4.5.3}$$

on bounded evolution orbits. Indeed, using formal integration by parts, we get

$$\int \rho(a v_{yy} + b) v_\tau = \frac{d}{d\tau} \int \Phi(y, v, v_y) = \int (\Phi_v v_\tau + \Phi_w v_{y\tau}) \tag{4.5.4}$$
$$= \int (\Phi_v - D_y \Phi_w) v_\tau \equiv \int (\Phi_v - \Phi_{wy} - \Phi_{wv} v_y - \Phi_{ww} v_{yy}) v_\tau,$$

where $D_y = d/dy$ is the full derivative. Then ρ and Φ satisfy the system of PDEs

$$\rho a = -\Phi_{ww}, \quad \rho b = \Phi_v - \Phi_{wy} - \Phi_{wv} w.$$

Differentiating the second equation in w yields a linear first-order PDE for ρ

$$(\rho a)_y + (\rho a)_v w - (\rho b)_w = 0. \tag{4.5.5}$$

Introducing the new dependent variable $\rho = e^P > 0$ leads to an inhomogeneous first-order PDE for P and the existence of ρ is proved by the standard method of characteristics.

Higher-order rescaled equations do not possess a gradient structure. It is in striking contrast with the second-order equations, where Lyapunov functions often play a key role in the asymptotic analysis of blow-up and global solutions of quasilinear heat equations that the gradient structure is lost for $m > 1$. Without loss of generality, we prove this negative result for equation (4.3.2) with $m = 2$ and $N = 1$ denoting $\gamma_1 = 1/2m$, $\gamma_2 = \gamma_1 + c_1$.

Proposition 4.5.1. *The fourth-order parabolic equation*

$$v_\tau = \mathbf{P}_4(v) = -v_{yyyy} + \gamma_1 y v_y + \gamma_2 v - v^p \equiv -v_{yyyy} + b(y, v, v_y, v_{yy}, v_{yyy}) \tag{4.5.6}$$

is not a gradient system in the sense that (4.5.3) *does not hold for any* $\Phi(y, v, v_y, v_{yy}) \equiv \Phi(y, v, w, z)$ *and* $\rho(y, v, v_y, v_{yy}, v_{yyy})$.

Proof. Performing differentiation and formal integration by parts in (4.5.3), we obtain

$$\int \rho(-v_{yyyy} + b) v_\tau = \int (\Phi_v - D_y \Phi_w + (D_y)^2 \Phi_z) v_\tau \equiv \int (\mathcal{L}_3 \Phi + \Phi_{zz} v_{yyyy}) v_\tau,$$

where $\mathcal{L}_3 \Phi$ contains derivatives of v up to the third order, v_{yyy}. Comparing the terms

with higher-order derivatives gives a system of PDEs

$$\rho = -\Phi_{zz}, \quad \rho b = \mathcal{L}_3 \Phi. \tag{4.5.7}$$

The first equation shows that $\rho = \rho(y, v, w, z)$ and then taking from the second equation the coefficient of the third-order derivative $v_{yyy} = r$ yields the following linear first-order PDE:

$$\rho_y + \rho_v w + \rho_w z + \rho_z r/2 = 0.$$

Hence $\rho_z \equiv 0$, i.e., $\rho = \rho(y, v, w)$. Next, we get $\rho_w \equiv 0$, etc., and finally we have $\rho_y = 0$, i.e., $\rho \equiv 1$, which does not satisfy equation (4.5.3) unless $\gamma_1 = 0$. This implies that the system (4.5.7) has no solution. □

Thus, it seems that the only way to establish stability of the first VSS is to use the linearized operator which requires an estimate of the spectrum of the corresponding $2m$-th order non self-adjoint operators with non-constant coefficients. We have proven this in Theorem 4.4.3 for all $p \approx p_0$, provided that $2m/N \ll 1$. For arbitrary $p \in (1, p_0)$ this is an open problem, where sharp numerical methods can play a leading role, see further comments in Chapter 6.

4.6 On continuous subsets of similarity solutions

By the asymptotic analysis in Section 4.2, the similarity ODE (4.1.8) admits solutions with algebraic decay (3.2.14) accompanying the multi-parametric exponential bundle of dimension $m + 1$. Denoting such similarity solutions V_a, one can see they form a continuous subset of asymptotic patterns. Note that $V_a \in L^1$ if $p < p_0$ and $V_a \notin L^1$ for $p \geq p_0$. Obviously with algenraic decay, $V_a \notin L^2_\rho$ so that such similarity solutions have different domains of stability than the VSSs. In particular, the following simple but, in our opinion, typical characterization of their domain of stability holds.

Proposition 4.6.1. *Let $p > p_* = 1 + 4m/N$ and let V_a be a similarity profile in* (4.1.7) *satisfying* (4.1.8), (3.2.14) *for some constant $C \neq 0$. Let $u(x,t)$ be a solution of equation* (4.1.1) *such that $u(\cdot,t) - u_*(\cdot, 1+t) \in H^{2m}$ for all $t \geq 0$. Then*

$$\theta(y,t) \equiv (1+t)^{1/(p-1)} u(y(1+t)^{1/2m}, t) \to V_a(y) \quad \text{in } L^2 \text{ as } t \to \infty. \tag{4.6.1}$$

Proof. Multiplying the equation for the difference $w = u - u_*$, $w_t = -(-\Delta)^m w - (u^p - u_*^p)$, by w and integrating over $\mathbf{R}^N$, we obtain

$$\frac{1}{2}\frac{d}{dt}\|w\|_2^2 = -\int |\bar{D}^m w|^2 - \langle u^p - u_*^p, u - u_* \rangle \leq 0,$$

so that $\|w(t)\|_2^2 \leq C$ for $t > 0$. By scaling $\|u - u_*\|_2^2 \equiv (1+t)^\nu \|\theta - V_a\|_2^2$, with exponent

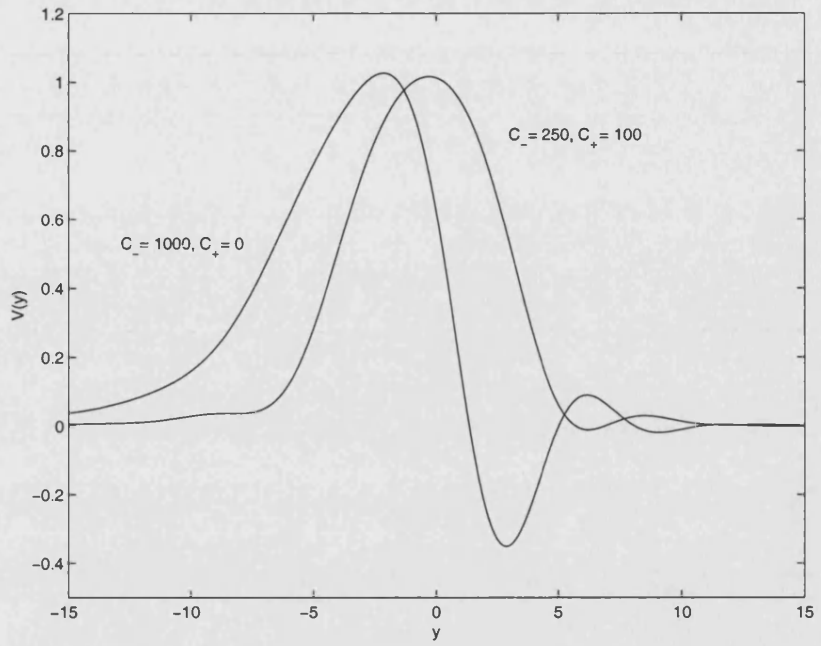

Figure 4.4: Solutions with algebraic decay, $m = 2$, $p = 2$ and $N = 1$

$\nu = -2/(p-1) + N/2m > 0$, (4.6.1) follows. □

In Figure 4.4 we present examples of profiles from this continuous family, which is extremely wide. Namely, for $N = 1$, we expect that there are asymmetric profiles $V_a(y)$ satisfying

$$|y|^{2m/(p-1)} V_a(y) \to C_\pm \quad \text{as } y \to \pm\infty, \quad \text{with arbitrary } C_\pm \in \mathbf{R}. \tag{4.6.2}$$

4.7 Conclusions

In this Chapter we have begun the extension of the large body of work for the classical semilinear heat equation with absorption $u_t = \Delta u - u^p$ to the important case of higher-order parabolic equations with monotone operators $u_t = -(-\Delta)^m u - u^p$. While some of our results are incomplete, not being valid over all parameter values, we have established the key existence and stability results asymptotically and numerically. As we have demonstrated, the same dynamics governs equations of the form (4.1.1) for all $m \geq 1$ but new ideas will be required to establish this rigorously throughout the whole parameter range in the absence of the self-adjoint, potential and order-preserving structures which are lost in the higher-order case.

Chapter 5

Blow-up and global asymptotics of the unstable Cahn-Hilliard equation with a homogeneous nonlinearity

5.1 Introduction

5.1.1 The model and discussion

In this Chapter we consider a fourth-order model combining features of the previous two Chapters which represents, in some ways, an intermediate model between those already studied and the classical second-order problems. In particular, we study the long-time and blow-up asymptotic behaviour of the fourth-order semilinear parabolic equation

$$u_t = -\Delta(\Delta u + u^p) \quad \text{in } \mathbf{R}^N \times \mathbf{R}_+, \quad p > 1, \quad u^p := |u|^{p-1}u. \tag{5.1.1}$$

We consider the Cauchy problem for (5.1.1) with initial data

$$u(x,0) = u_0(x) \quad \text{in } \mathbf{R}^N, \quad u_0 \in L^1(\mathbf{R}^N) \cap L^\infty(\mathbf{R}^N), \tag{5.1.2}$$

assuming in most cases that $u_0(x)$ has exponential decay as $x \to \infty$.

Equation (5.1.1) is a model connected with various applications. For instance, it arises as the limit case of the phenomenological, "unstable" Cahn-Hilliard equation for $N = 1$ and 2 and $p = 3$, see the references in Novick-Cohen and Segel (1984) and Elliott and Songmu (1986),

$$u_t = -(\gamma u_{xx} - u^3 + \gamma_1 u)_{xx} - \gamma_2 u.$$

It is also a reduced model from solidification theory with $N = 1$ or 2 and $p = 2$, (Novick-Cohen 1992, Bernoff and Bertozzi 1995). Equations of this form also arise in the theory of thermo-capillary flows in thin layers of viscous fluids with free boundaries, (Funada 1984).

Writing (5.1.1) in the form

$$Pu_t = \Delta u + u^p \tag{5.1.3}$$

with the positive operator $P = (-\Delta)^{-1}$ on the right-hand side ($\tilde{u} = (-\Delta)^{-1}u$ means $\Delta\tilde{u} = -u$ in $\mathbf{R}^N$) defines a pseudo-parabolic second-order equation. Many aspects of such equations are well understood with both the existence and uniqueness of local and global classical solutions and the blow-up of solutions known from the 1970's; see the first results in (Levine 1973) and the references in the surveys (Galaktionov and Vazquez 2002, Levine 1990).

We are mainly interested in the study of blow-up behaviour of the solutions to (5.1.1), (5.1.2). In this sense (5.1.1) is an exceptional model and (5.1.3) clearly indicates that, at least formally, we can expect some similarities of blow-up singularity formation phenomena with the classical semilinear heat equation from Combustion Theory (1.3.1). On the other hand, the unstable nonlinear operator in (5.1.1) is the classical *porous medium equation* but backwards in time

$$u_t = -\Delta u^p. \tag{5.1.4}$$

It is not well-posed and leads to blow-up of solutions and all derivatives in arbitrarily small times; see the concavity techniques applied in (Levine and Payne 1974).

In standard form (5.1.1) (rather than (5.1.3)) is a fourth-order semilinear parabolic equation. In this sense, (5.1.1) can be treated as an "intermediate" canonical model between second and fourth-order parabolic equations. Another related class of fourth-order models admitting both blow-up and deacay comes from the theory of thin films and general long-wave unstable equations (Bertozzi and Pugh 1998), where a typical *quasilinear* equation takes the form

$$u_t = -(uu_{xxx} + u^3u_x)_x. \tag{5.1.5}$$

Equations of this form are known to admit non-negative solutions see (Witelski, Bernoff and Bertozzi 2003) and the references therein. Because there is no mechanism to preserve finite support in (5.1.1) (unlike in (5.1.5)) there are no compactly supported or steady-state solutions for $p < p_S = (N+4)/(N-4)_+$. Thus we will concentrate on solutions defined in $\mathbf{R}^N \times (0,T)$.

The primary goal of this Chapter is to present some general principles of formation of stable generic blow-up and global asymptotics for this Cahn-Hilliard equation. To this end, we construct various subsets of self-similar solutions of (5.1.1) in different ranges

of the parameters p and N. We establish that, in general,

(i) (5.1.1) admits a countable discrete subset of blow-up similarity solutions, and

(ii) there exists an unbounded continuous family of global similarity solutions decaying as $t \to \infty$.

Lastly, we study the stability of some crucial branches of similarity solutions. Construction of approximate self-similar patterns which can play an important part in the description of asymptotic properties of the PDE (5.1.1) may be found in Galaktionov and Williams (2003a).

In the remainder of this section we discuss some basic properties of (5.1.1). In Section 5.2 we introduce the blow-up and global similarity solutions, perform a local asymptotic analysis of the corresponding ODEs and pose the spectral properties of the linearized operators in the framework of Section 3.3. In Section 5.3 we present an existence proof of blow-up similarity solutions and show numerically that the minimal profile is an attractor for a wide set of initial data. A countable subset of solutions is then constructed via a singular perturbation expansion. In Section 5.4 we study classes of global solutions of (5.1.1) and show that, unlike the blow-up case, the family of similarity solutions is continuous and we rigorously determine the stable branch.

5.1.2 A potential operator and gradient system

Equation (5.1.1) is uniformly parabolic with all spatial differential operators appearing in divergence form. It admits a unique, classical, local in time solution and the standard parabolic theory applies, (Friedman 1983). The operator on the right-hand side of (5.1.1), $-\Delta(\Delta u + u^p)$, is potential, with Lyapunov function

$$E[u](t) = \frac{1}{2}\|\nabla u\|_2^2 - \frac{1}{p+1}\|u\|_{p+1}^{p+1}, \quad u \in H^2(\mathbf{R}^N) \cap L^{p+1}(\mathbf{R}^N), \tag{5.1.6}$$

which is monotone on bounded orbits,

$$\frac{d}{dt}E[u](t) = -\|u_t\|_{H^{-1}}^2 \le 0.$$

For such gradient systems, the ω-limit set of any uniformly bounded orbit,

$$\omega(u_0) = \{f \in C(\mathbf{R}^N) : \exists\ \{t_k\} \to \infty \text{ such that } u(\cdot, t_k) \to f \quad \text{uniformly}\}$$

is known to consist of stationary solutions: $-\Delta(\Delta f + f^p) = 0$ in $\mathbf{R}^N$ for any $f \in \omega(u_0)$. If the subset of stationary solutions consists of isolated equilibria, the asymptotic behaviour does not essentially differ from the classical second-order theory where any bounded orbits are known to approach a stationary profile as $t \to \infty$ (Sell and You 2002). However, one can see from (5.1.3) that for this problem the only admissible

stationary solution is $u \equiv 0$, so that the large-time (and of course blow-up for which $E_0 < 0$) behaviour is essentially non-stationary.

5.1.3 Finite-time blow-up

Despite the gradient structure, from known results on pseudo-parabolic equations, (Levine 1973), it follows that classical solutions whose initial data satisfy an energy inequality,

$$E(u_0) = \frac{1}{2}\|\nabla u_0\|_2^2 - \frac{1}{p+1}\|u_0\|_{p+1}^{p+1} < 0 \tag{5.1.7}$$

cannot be extended beyond a finite blow-up time $T < \infty$. In the particular case of $p = 3$, $N = 1$ this can be interpreted as a condition on the initial mass of positive solutions, (Witelski et al. 2003),

$$M \equiv \int_{-\infty}^{\infty} u_0 > M_c = \frac{4\sqrt{2}\pi}{3}.$$

Finite-time blow-up is a well known phenomenon in long-wave unstable thin-film equations of the form (5.1.5), (Novick-Cohen and Segel 1984, Novick-Cohen 1992, Bertozzi and Pugh 1998, Bertozzi and Pugh 2000, Bernoff and Bertozzi 1995). Because not all initial data will satisfy this condition and because of the gradient structure, we will also look for decaying solutions. In the case of both decaying and blowing up solutions the role of similarity variables is key.

5.2 Preliminaries: similarity variables for global and blow-up asymptotics

Equation (5.1.1) is invariant under the group of scaling transformations

$$t \mapsto \lambda t, \quad x \mapsto \lambda^{1/4} x, \quad u \mapsto \lambda^{-1/2(p-1)} u, \quad \lambda > 0.$$

This symmetry suggests the introduction of the following rescaled variables

$$u(x,t) = [\sigma(T-t)]^{-1/2(p-1)}\theta(y,\tau), \quad y = x/[\sigma(T-t)]^{1/4}, \quad \tau = -\ln[\sigma(T-t)], \tag{5.2.1}$$

where $\sigma = 1$ corresponds to blow-up at the unknown blow-up time $t = T^-$, and $\sigma = -1$ to infinite time decay as $t \to \infty$ with a reference time T (generically, we will take $T = 0$ in this case). Without loss of generality, we assume that the solution $u(x,t)$ blows-up at the finite time $t = T$ in the sense of (1.2.1) and the corresponding blow-up set contains the origin. Despite the inclusion of the Laplacian of a nonlinear term it is easily established from parabolic regularity theory that blow-up, if it occurs in any Sobolev norm also occurs in L^∞ (Friedman 1983) . Thus, we do not have

the possibility, as in nonlinear diffusion (5.1.4), of blow-up only in a derivative of the solution (Henry 1985, Novick-Cohen 1998).

The rescaled solution $\theta(y,\tau)$ satisfies the semilinear equation

$$\theta_\tau = \mathbf{A}(\theta) \equiv -\Delta(\Delta\theta + \theta^p) - \frac{\sigma}{4} y \cdot \nabla\theta - \frac{\sigma}{2(p-1)}\theta, \tag{5.2.2}$$

and we are interested in the possible asymptotic dynamics of solutions for $\tau \gg 1$.

An exact similarity solution to (5.2.2) is independent of τ giving an elliptic boundary value problem for the similarity profile f,

$$\mathbf{A}(f) = 0 \quad \text{in } \mathbf{R}^N. \tag{5.2.3}$$

Because $\mathbf{A}$ is not potential (see the example in Section 4.5), classical variational approaches do not apply.

We restrict our attention to the one-dimensional or radial geometry, where (5.2.3) is a fourth-order ODE and in most cases we impose symmetry conditions at the origin $y = 0$ and a suitable decay condition (possibly exponential) at infinity:

$$f'(0) = 0, \quad f'''(0) = 0; \quad \text{and } f(y) \to 0 \quad \text{as } y \to \infty. \tag{5.2.4}$$

5.2.1 Conservative similarity solutions and the first critical exponent

Under appropriate decay conditions at infinity (say, exponential), equation (5.1.1) is *conservative* as

$$\frac{d}{dt}\int_{\mathbf{R}^N} u dx = -\int_{\mathbf{R}^N} \Delta(\Delta u + u^p) dx = 0. \tag{5.2.5}$$

Given an exact similarity solution

$$u_S(x,t) = [\sigma(T-t)]^{-1/2(p-1)} f(y) \tag{5.2.6}$$

and assuming that $f \in L^1(\mathbf{R}^N)$, we have that

$$\int_{\mathbf{R}^N} u_s(x,t) dx = [\sigma(T-t)]^{-1/2(p-1)+N/4} \int_{\mathbf{R}^N} f(y) dy, \tag{5.2.7}$$

which satisfies (5.2.5) only if $p = p_0$, where

$$p_0 = 1 + 2/N \tag{5.2.8}$$

is the critical exponent in the problem (it is interesting that p_0 coincides with the Fujita exponent for the semilinear heat equation (1.3.1)). In fact, it is the *first* critical exponent and in Section 5.4 we show that there exists a countable sequence of further

critical exponents

$$p_k = 1 + 2/(N+k), \quad k = 0, 1, 2, \dots . \tag{5.2.9}$$

It follows from (5.2.8) that in the crucial one-dimensional case, $N = 1$, we will concentrate on $p = p_0 = 3$. However, we expect that similarity solutions will govern the dynamics for all p, regardless of the conservation property, see Section 5.3.6. Moreover, from (5.2.7) we have that, for $N = 1$ any similarity solution for $p < 3$ must have $\int_{\mathbf{R}} f dy = 0$ for all initial data with bounded mass if it is to play a part in the long-time behaviour of (5.1.1) in the case of blow-up.

5.2.2 Local asymptotic properties of self-similar solutions

First, we need to describe the possible asymptotics of small solutions to (5.2.3) satisfying $f(y) \to 0$ as $y \to \infty$, see (5.2.4). Consider the linearization of (5.2.3) about $f = 0$,

$$f'''' + \frac{2(N-1)}{y} f''' + \frac{\mu}{y^2} f'' - \frac{\mu}{y^3} f + \frac{\sigma}{4} y f' + \frac{\sigma}{2(p-1)} f = 0, \quad \mu = (N-1)(N-3). \tag{5.2.10}$$

Proceeding as in Section 3.2.2, we set $z = y^\alpha$ with $\alpha = 4/3$ reducing the above to

$$-f'''' - a_1 f' - a_2 z^{-1} f + \mathbf{D}(z) f = 0, \tag{5.2.11}$$

where $a_1 = \sigma/4\alpha^3$, $a_2 = \sigma/2(p-1)\alpha^4$ and

$$\mathbf{D}(z) f = \sum_{j=1}^{3} \gamma_j z^{j-4} f^{(j)}$$

is a linear operator with bounded coefficients as $z \to \infty$. This equation has exactly the form of equations (3.2.10) and (4.2.3) for the particular case $m = 2$. From that previous analysis we immediately have that as $y \to \infty$, there exists

a two-dimensional exponential bundle for the global case $\sigma = -1$, and (5.2.12)

a one-dimensional exponential bundle for the blow-up case $\sigma = 1$. (5.2.13)

Equation (5.2.11) also admits solutions with algebraic decay (rather than exponential) as $z \to \infty$ described by the first-order operator

$$-a_1 f' - a_2 z^{-1} f = 0 \quad \Longrightarrow \quad f(z) = c\, z^{-3/(2(p-1))}, \ c \neq 0.$$

For the linearized equation (5.2.10) the leading order behaviour is algebraic,

$$f(y) = A|y|^{-2/(p-1)}(1 + o(1)) \quad \text{as } |y| \to \infty, \tag{5.2.14}$$

with a constant $A \neq 0$. For blow-up similarity solutions (5.2.6), the limit-time profile is then bounded for any $x \neq 0$ and has the form (cf. (3.2.16))

$$u_s(x, T^-) = A|x|^{-2/(p-1)}.$$

Clearly, this is not an admissible solution for the conservative case given finite initial mass and thus for $p = p_0$ we must have $C \equiv 0$ and exclusively exponential decay.

5.2.3 The spectral properties of the rescaled linear operators

The structure of the rescaled equation (5.2.2) is very strongly related to the linear operators $\mathcal{L}$ (3.2.4) and $\mathcal{L}^*$ (3.3.1) introduced in Chapter 3.2. In fact,

$$\mathbf{A}'(0) = -\Delta^2 + \frac{1}{4} y \cdot \nabla + \frac{1}{2(p-1)} I \equiv \mathcal{L} + c_* I, \quad c_* = \frac{N(p_0 - p)}{4(p-1)}. \tag{5.2.15}$$

Thus we can use all the properties of the operators $\mathcal{L}$ and $\mathcal{L}^*$ previously described but now we restrict $m = 2$. This means for instance that the first four eigenvalues and eignevectors of $\mathcal{L}$ are given by (3.3.15).

5.3 Blow-up similarity profiles for $p = 3$ in one dimension

While the linear part of the ODE (5.2.3) coincides with those previously studied in Chapters 3 and 4, the dynamics simplify for the conservative case $p = p_0 = 1 + 2/N$ as the ODE is *integrable*. Due to this integrability, we will not need to employ the $\mu-$bifurcation strategy of Chapter 3 to establish existence of solutions, instead we will prove it directly. The case, $p = 3$ and $N = 1$ is of key importance in our analysis and highlights the typical techniques required to describe a countable subset of similarity blow-up patterns.

5.3.1 Preliminaries

The ODE for the similarity profile (5.2.2) can be integrated once to give (with $\sigma = 1$)

$$f''' + \frac{1}{4} y f + (f^3)' = 0 \quad \text{for } y > 0, \quad f'(0) = 0, \tag{5.3.1}$$

where we have removed the algebraically decaying mode (5.2.14), $f(y) = Ay^{-1}(1 + o(1))$ $y \to \infty$, by looking for L^1-solutions satisfying the conservation of mass condition (5.2.5). It follows from (5.2.13) that we are left with a *one-parameter* family of decaying solutions satisfying

$$f(y) = Cy^{-1/3} e^{-\beta y^{4/3}} (1 + o(1)) \quad \text{as } y \to +\infty, \quad 0 \leq C < \infty; \quad \beta = 3/4^{4/3}, \tag{5.3.2}$$

(this asymptotic bundle is generated by the linear part (5.2.10) of the operator). In order to construct a solution to (5.3.1) we will use a shooting type argument from $y = +\infty$. All admissible profiles have the asymptotic behaviour (5.3.2) and also satisfy the symmetry condition at the origin.

We will now study the behaviour of solutions on the manifold (5.3.2) parameterized by C. Denoting $f(y;C)$ as the function which satisfies equation (5.3.1) with decay from the bundle (5.3.2), the goal is to find the set of C, such that

$$G(C) \equiv f'(0;C) = 0. \tag{5.3.3}$$

Because the function $G(C)$ in (5.3.3) is analytic in C (see below), equation (5.3.3) has at most a countable subset of roots which can accumulate at $C = \infty$ only, and this actually happens. We begin with the global existence of the family $\{f(y;C)\}$.

Lemma 5.3.1. *For any $C > 0$, the solution $f(y;C)$ to (5.3.1), (5.3.2) is well defined for all $y \in \mathbf{R}$.*

Proof. This follows from the local properties of the operator in (5.3.1) which are close to those for the second-order case $f'' + f^3 = 0$ which, obviously, does not admit blow-up of solutions at finite y. Integrating (5.3.1), $f'' = -f^3 + \frac{1}{4}\int f y dy$, multiplying by f' and integrating again over a sufficiently small interval yields

$$\frac{1}{2}f'^2 = -\frac{1}{4}f^4 + \frac{1}{4}\int f' \int fy + \text{const} \le \frac{1}{4}\int |f'| \int |fy| + \text{const}, \tag{5.3.4}$$

where the right-hand side is not more than quadratic in f'. Therefore, $f(y)$ cannot blow-up at a finite point y_* along a sequence since (5.3.4) guarantees that $f'(y_*)$ is finite. □

In fact, this holds for all $p > 1$.

5.3.2 Existence of the first monotone blow-up similarity pattern

The proof that there exists a C_1 such that (5.3.3) holds involves three steps. First, we show in the limit as $C \to 0^+$ solutions are strictly monotone decreasing on $[0, \infty)$ and, second, that in the limit $C \to +\infty$ all solutions cannot be monotone. Then, by a standard continuity argument we have that there must exist an intermediate $C = C_1 > 0$ corresponding to an admissible solution.

Proposition 5.3.2. *For all $0 < C \ll 1$, solutions $f(y;C)$ are strictly monotone decreasing in y.*

Proof. Rescaling $f = Cg$, we have

$$g''' + \frac{1}{4}yg + C^2(g^3)' = 0 \quad \text{in } \mathbf{R}_+. \tag{5.3.5}$$

In view of the behaviour at infinity (5.3.2), by standard results on continuous dependence for ODEs (Coddington and Levinson 1955), it follows that as $C \to 0^+$,

$$f(y;C) = C(\phi_0(y) + o(1)) \quad \text{uniformly in } \mathbf{R}_+, \tag{5.3.6}$$

where ϕ_0 solves the linear ODE $\phi''' + \frac{1}{4}\phi' y = 0$ satisfying (5.3.2) with $C = 1$. All the derivatives of f converge similarly. Let us now show that $\phi_0(y)$ is strictly monotone decreasing. Assume that y_i is the first (from $y = \infty$) local maximum point of ϕ_0, $\phi_0'(y_i) = 0$ and $\phi_0'(y) < 0$ on (y_i, ∞). Integrating over (y_i, ∞), we obtain the contradiction, $\phi_0''(y_i) = \int_{y_i}^{\infty} s\phi_0(s)ds > 0$. □

Proposition 5.3.3. *There exists a $C_* > 0$ such that $f(y;C_*)$ has a local maximum point at some $y_* \geq 0$ and $f(y;C_*) > 0$ on $[y_*, \infty)$.*

Proof. Assume for contradiction that $f(y;C)$ is strictly monotone decreasing in $\mathbf{R}_+$ for all $C > 0$, then $f(0;C) > 0$. One can see from the rescaled ODE (5.3.5) that the solutions $f(y;C)$ cannot be bounded for $y \in \mathbf{R}_+$ uniformly in $C > 0$. Therefore, there exists a sequence $\{C_k\} \to \infty$ such that $a_k = f(0;C_k) \to \infty$. Performing the scaling

$$g = f/a_k, \quad z = ya_k, \tag{5.3.7}$$

we arrive at a perturbed ODE for the sequence $\{g = g_k(z)\}$

$$g_k''' + (g_k^3)' = -\frac{1}{4a_k^4} z g_k \quad \text{for } z > 0, \quad g_k(0) = 1, \tag{5.3.8}$$

where $0 < g_k(z) \leq 1$ and $g_k(z)$ is monotone decreasing in z. Since $\{g_k\}$ is a uniformly bounded sequence of solutions of the asymptotically perturbed ODE (5.3.8) with regular coefficients, by the Ascoli-Arzelá theorem (Hirsch and Lacombe 1999) and standard ODE estimates (Coddington and Levinson 1955), we have that along a subsequence, $g_k \to \bar{g}$ uniformly on compact subsets in z, where $\bar{g}$, $0 \leq \bar{g} \leq 1$, must be a monotone decreasing solution of the unperturbed ODE

$$(\bar{g}'' + \bar{g}^3)' = 0, \quad \bar{g}(0) = 1. \tag{5.3.9}$$

Since all the solutions of (5.3.9) are oscillatory, which is easily checked by integrating twice, this leads to a contradiction. Therefore, there exists a sufficiently large $C_* > 0$ such that $f(y;C_*)$ is not strictly monotone in $\mathbf{R}_+$ and has a local maximum point. □

Theorem 5.3.4. *There exists a constant $C_1 \in (0, C_*)$ such that* (5.3.3) *holds for*

$C = C_1$ and $f_1(y) = f(y; C_1)$ is a strictly monotone decreasing symmetric positive similarity profile.

Proof. Introducing the subset

$$W_1 = \{\mu > 0 : \ f(y; C) \text{ is strictly monotone decreasing in } \mathbf{R}_+ \text{ for all } C \in (0, \mu)\},$$

we have that $W_1 \neq \emptyset$ by Proposition 5.3.2 and W_1 is bounded above by Proposition 5.3.3. Hence, there exists

$$C_1 = \sup W_1 \leq C_*, \tag{5.3.10}$$

where by construction $f_1(y) = f(y; C_1)$ is monotone decreasing for $y \geq 0$, and it follows by inspection of the ODE that $f_1'(y)$ must vanish at the origin, i.e., (5.3.3) holds. □

We now describe a countable subset of the similarity profiles satisfying (5.3.1) and (5.3.2) with some $C > C_1$. Similarly, we show that as C increases, the function $f(y; C)$ becomes more and more oscillatory for $y > 0$. Indeed, performing the scaling (5.3.7) and passing to the limit $C = C_k \to \infty$, we obtain a bounded solution $\bar{g}$ satisfying (5.3.9) admitting oscillatory solutions only. Hence, $f(y; C)$ can have an arbitrarily large number of oscillations for $y > 0$ with $C \gg 1$. As in the proof of Theorem 5.3.4, for any $k = 2, 3, ...$, we define the subsets

$$W_k = \{\mu > C_{k-1} : \ f(y; C) \text{ has at most } k \text{ local extrema for } y \geq 0 \text{ for all } C \in [C_{k-1}, \mu)\}.$$

Then, once C_{k-1} is known starting with $k = 2$, we have that $W_k \neq \emptyset$ and by the oscillatory behaviour for $C \gg 1$, W_k is bounded from above. Hence, we define

$$C_k = \sup W_k > C_{k-1}, \quad k = 2, 3, \dots, \tag{5.3.11}$$

and by construction, $f_k(y) = f(y; C_k)$ satisfies the symmetry condition at the origin (otherwise, it is not the supremum in (5.3.11)).

Such a construction, while giving an infinite sequence of similarity profiles, does not describe the important properties of the functions $f_k(y)$, such as positivity (or at least "positivity dominance") nor the actual distribution of local extrema and inflection points of the profiles. This will be done by a more delicate asymptotic matching procedure. These results are formal but some of them can be rigorously justified asymptotically, as $k \to \infty$.

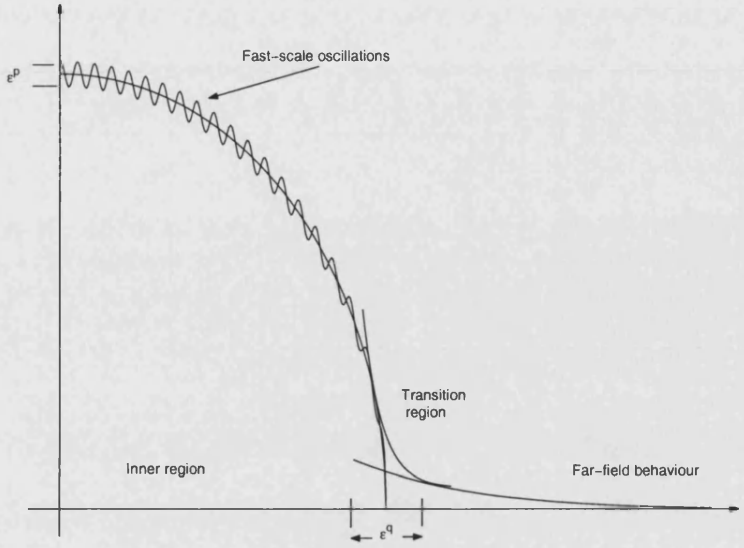

Figure 5.1: Sketch of the regions for construction of asymptotic profiles.

5.3.3 Asymptotic construction of a countable subset of similarity profiles

As is common in matched asymptotics expansions, we will consider three regions (as described in Figure 5.1). The two primary regions are the inner region localized near the origin, where the solution is concentrated, and a far-field outer region as described by the asymptotic bundle (5.3.2). Joining the two is a narrow transition region. Because the characteristics of the family are determined by the far-field behaviour, we will begin by considering the refined aymptotics as $y \to \infty$.

Outer region: the far field behaviour. To determine the asymptotic behaviour as $y \to \infty$ in greater detail, we produce a refined asymptotic description of solutions from the exponential bundle (5.3.2). Because we are interested in the analyticity of $G(C)$ we will write f as a power series of the form

$$f(y;C) = \textstyle\sum_{n=0}^{\infty} C^{2n+1}\phi_n(y), \tag{5.3.12}$$

where ϕ_0 is given in (5.3.6) and the rest of the terms are obtained from the relation

$$\mathcal{L}\phi_n \equiv \phi_n''' + \frac{1}{4}y\phi_n = -\sum_{\substack{1\le i,j,k\le n \\ i+j+k=n+1}} (\phi_i\phi_j\phi_k)', \quad n = 2, 3, \dots, \tag{5.3.13}$$

with the condition $\phi_n(y) = o(\phi_0(y))$ as $y \to \infty$. Using the expansion (5.3.2), it can be

shown that for $y \gg 1$,

$$\phi_n(y) = \left[\gamma_n + o((1+y)^{-1})\right] y^{-(4n+1)/3} e^{-(2n+1)\beta y^{4/3}}, \tag{5.3.14}$$

with suitable constants $|\gamma_n| \le 1$. By direct substitution

$$\gamma_{n+1}\left[\frac{1}{4} - \left((2n+1)\frac{4\beta}{3}\right)^3\right] = -(2n+1)\frac{4\beta}{3} \sum_{\substack{1\le i,j,k\le n \\ i+j+k=n+1}} \gamma_i\gamma_j\gamma_k,$$

hence,

$$\begin{aligned} |\gamma_{n+1}| \le & \left|\frac{(2n+1)\frac{4\beta}{3}}{\frac{1}{4} - \left((2n+1)\frac{4\beta}{3}\right)^3}\right| \left|\sum_{\substack{1\le i,j,k\le n \\ i+j+k=n+1}} \gamma_i\gamma_j\gamma_k\right| \\ \le & \frac{3^3 2^{2/3}}{13}\frac{1}{(2n+1)^2}\left|\sum_{\substack{1\le i,j,k\le n \\ i+j+k=n+1}} \gamma_i\gamma_j\gamma_k\right| \qquad \text{for } n \ge 1. \end{aligned}$$

However, there are $\binom{n}{2} = n(n+1)/2$ terms in the sum, thus,

$$|g_{n+1}| \le \frac{3^3}{13\,2^{1/3}}\frac{n(n+1)}{(2n+1)^2}\tilde{\gamma}^3 \le \frac{3^3}{13\,2^{7/3}}\tilde{\gamma}^3,$$

where $\tilde{\gamma} = \max_{i\le n}|\gamma_i|$ Since $3^3/(13\,2^{7/3}) < 1$, taking $\gamma_0 = 1$ and recognizing that this formula is valid for all $n \ge 1$ we may take $\tilde{\gamma} = \gamma_0 = 1$ implying $|\gamma_n| \le 1$ for all n.

Moreover, the right-hand side of (5.3.14) gives uniform estimates of ϕ_n in $\mathbf{R}_+$, which establish convergence of (5.3.12) for $y \ge y_0 \gg 1$. By the Weierstrass theorem (Hirsch and Lacombe 1999), the solution $f(y;C)$ in (5.3.12) obtained as a uniformly converging series of analytic functions is analytic in C at least for $y_0 \gg 1$. Therefore, on extension to $y \in [0, y_0)$, as a solution of an ODE with analytic coefficients and analytic dependence on C in the Dirichlet boundary condition at $y = y_0$, it is analytic in C for any $y \in \mathbf{R}_+$ (Coddington and Levinson 1955). Hence, (5.3.3) is an analytic function having isolated zeros only and we arrive at the following conclusion.

Proposition 5.3.5. *The problem* (5.3.1), (5.3.2) *has at most a countable subset of solutions.*

From this Proposition we expect that the discrete nature of the function $G(C)$ will be made evident by close examination of the inner and transition regions.

A singular perturbation problem. We begin by looking for possible solutions

localized in a neighbourhood of the origin $y = 0$. We rescale as

$$f(y) = ag(z), \quad y = az, \quad \text{where } a = f(0; C), \tag{5.3.15}$$

with a an as yet unspecified function of C (to be determined for the similarity profiles $f_k(y)$). Under the assumption that $a(C) \to \infty$ as $C \to \infty$ (possibly along a subsequence), we define

$$\varepsilon = a^{-4} \ll 1,$$

and under the rescaling (5.3.15), equation (5.3.1) leads to a singularly perturbed ODE

$$\varepsilon g''' + \frac{1}{4} z g + (g^3)' = 0. \tag{5.3.16}$$

We supplement this with the conditions

$$g(0) = 1, \qquad g'(0) = 0, \qquad g''(0) = b\varepsilon^{-m}, \tag{5.3.17}$$

where b and $m > 0$ are as yet unspecified. In order to match to the known asymptotic behaviour, we will also require that g has the correct asymptotic behaviour as $z \to \infty$. At first glance this problem may appear to be over specified as we have a third-order problem and four conditions. However, as there can be only a countable set of solutions, we also need a way to distinguish the admissible values of ε and hence the set C_k such that $G(C_k) = 0$.

The specific requirement $g''(0) = b\varepsilon^{-m}$ is arbitrary and made for convenience only. It indicates that a faster scale will be necessary to resolve the additional oscillatory structure as described by the perturbed problem (5.3.8). A standard single scale expansion can be carried out but gives the asymptotic expression $G(C) \equiv 0$ which is clearly unsatisfactory.

The inner region. In the inner region we pose an expansion of the form

$$g(z) = g_0(z) + \theta g_1(z, t) + o(\theta), \qquad |\theta| \ll 1 \tag{5.3.18}$$

with the scale θ and the variable $t(z)$ as yet unspecified. The leading solution, $g_0(z)$ is determined by

$$\frac{1}{4} z g_0 + (g_0^3)' = 0, \qquad g_0(0) = 1,$$

and hence

$$g_0(z) = \left(1 - \frac{z^2}{12}\right)^{1/2}. \tag{5.3.19}$$

To leading order, this also satisfies $g'(0) = g_0'(0) = 0$ but not the condition on the second derivative. Most importantly, this solution is only defined on $z \in (0, \sqrt{12})$. In

order to meet the condition $g''(0) = b\varepsilon^{-m}$, we introduce the fast scale $z = \varepsilon^{1/2}Z$ whence

$$\frac{d^3g}{dZ^3} + \frac{1}{4}\varepsilon^{1/2}zg + 3g^2\frac{dg}{dZ} = 0$$

and define

$$t = t_0 + \varepsilon t_1 \tag{5.3.20}$$

with the function $t_0 = h(Z)$ as yet unspecfied.

Under this change of variables for $g = g(z,t)$ we have

$$\left(\frac{d^3g}{dt^3} + 3\frac{h''}{(h')^2}\frac{d^2g}{dt^2} + \frac{h'''}{(h')^3}\frac{dg}{dt}\right) + \frac{\varepsilon^{1/2}}{4}\frac{zg}{(h')^3} + \frac{1}{(h')^2}\frac{d}{dt}(g^3) = 0, \tag{5.3.21}$$

where

$$\frac{dg}{dt} = \frac{\partial g}{\partial t} + \frac{\varepsilon^{1/2}}{h'(Z)}\frac{\partial g}{\partial z}.$$

Using (5.3.18) in (5.3.21) defines a sequence of problems at the various asymptotic orders:

$$O(1): \quad \frac{\partial^3 g_0}{\partial t^3} + \frac{1}{(h')^2}\frac{\partial g_0^3}{\partial t} = 0, \tag{5.3.22}$$

$$O(\varepsilon^{1/2}): \quad \frac{3}{h'}\frac{\partial^3 g_0}{\partial t^2 \partial z} - \frac{z}{4g_0(z)^2 h'}\frac{\partial^2 g_0}{\partial t \partial z} + \frac{1}{4}z\frac{g_0}{(h')^3} + 3\frac{g_0^2}{(h')^2}\frac{\partial g_0}{\partial z} = 0, \tag{5.3.23}$$

$$O(\theta): \quad \frac{\partial^3 g_1}{\partial t^3} + \frac{3g_0^2}{(h')^2}\frac{\partial (g_0^2 g_1)}{\partial t} = 0, \tag{5.3.24}$$

$$O(\varepsilon^{1/2}\theta): \quad \frac{3}{h'}\frac{\partial^3 g_1}{\partial t^2 \partial z} + \frac{z}{4g_0^3}\left(g_1 - \frac{\partial^2 g_1}{\partial t^2}\right) + \frac{3}{(h')^3}\left(2g_0 g_1\frac{\partial g_0}{\partial z} + g_0^2\frac{\partial g_1}{\partial z}\right) = 0. \tag{5.3.25}$$

By definition the leading order equation (5.3.22) is satisfied by $g_0(z)$. From the $O(\theta)$ equation we have separation of the fast and slow scales only if

$$(h')^2 = g_0^2.$$

Thus, to leading order,

$$t = \int_0^Z \left(1 - \varepsilon\frac{u^2}{12}\right)^{1/2} du = \frac{1}{\varepsilon^{1/2}}\left[\frac{z}{2}\left(1 - \frac{z^2}{12}\right)^{1/2} + \sqrt{3}\sin^{-1}\left(\frac{z}{2\sqrt{3}}\right)\right]. \tag{5.3.26}$$

With this definition of t the $O(\varepsilon)$ equation, (5.3.23), is also satisfied by $g_0(z)$. Further, the definition of $t = h(Z)$ and the boundary conditions applied at $t = z = 0$ imply that the solution to (5.3.24) equation is given by

$$g_1(z,t) = B(z)(1 - \cos\sqrt{3}t).$$

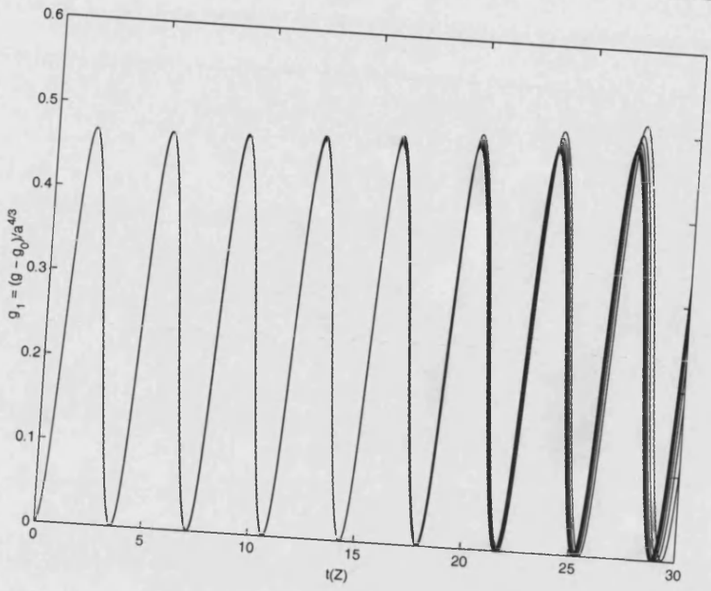

Figure 5.2: Convergence of numerical solutions to $g_1(z,t)$.

The slowly-varying envelope $B(z)$ is determined by solving the final equation (5.3.25),

$$\frac{B'}{B} = -\frac{g_0'}{g_0} \quad \text{hence} \quad B(z) = \frac{b}{3g_0(z)}.$$

Combining all this together we have

$$g = g_0(z) + \theta \frac{b}{g_0(z)}(1 - \cos\sqrt{3}t) + o(\theta), \tag{5.3.27}$$

where $\theta = \varepsilon^{1-m}$. This requires $m < 1$ and we have assumed that $\theta \neq \varepsilon^{1/2}$.

The transition region The inner solution is only defined on $z \in (0, \sqrt{12})$ and does not satisfy the far-field behaviour (5.3.2), thus we introduce the transition co-ordinate $\bar{z}$ and solution in the transition region $\bar{g}(\bar{z})$ by

$$z = \sqrt{12} + \varepsilon^{1/3}\bar{z}, \qquad g = \varepsilon^{1/6}\bar{g}. \tag{5.3.28}$$

In the transition region, $\bar{g}$ solves

$$\frac{d^3\bar{g}}{d\bar{z}^3} + \frac{1}{4}\left(\sqrt{12} + \varepsilon^{1/3}\bar{z}\right)\bar{g} + \frac{d}{d\bar{z}}\left(\bar{g}^3\right) = 0. \tag{5.3.29}$$

Posing the asymptotic form $\bar{g} = \bar{g}_0 + \bar{\theta}\bar{g}_1 + o(\bar{\theta}), |\bar{\theta}| \ll 1$ the leading order equation is

$$\frac{d^3\bar{g}_0}{d\bar{z}^3} + \frac{\sqrt{3}}{2}\bar{g}_0 + \frac{d}{d\bar{z}}\left(\bar{g}_0^3\right) = 0, \tag{5.3.30}$$

which has a one-parameter family of exponentially decaying solutions

$$\bar{g}_0 \simeq A_0 e^{-\frac{3^{1/6}\bar{z}}{2^{1/3}}} \qquad \text{as } \bar{z} \to \infty, \tag{5.3.31}$$

and a three-parameter family of slowly growing solutions,

$$\bar{g}_0 \simeq \left(\frac{-\bar{z}}{3^{1/2}}\right)^{1/2} + \frac{\bar{a}_1}{(-\bar{z})^{1/2}} + \bar{a}_2 \frac{\cos\frac{2}{3^{3/4}}(-\bar{z})^{3/2}}{(-\bar{z})^{1/2}} + \bar{a}_3 \frac{\sin\frac{2}{3^{3/4}}(-\bar{z})^{3/2}}{(-\bar{z})^{1/2}} \quad \text{as } \bar{z} \to -\infty. \tag{5.3.32}$$

This behaviour may be determined in the standard way by setting $\bar{g}_0 = \tilde{g}_0 + \tilde{g}_1$, where $|\tilde{g}_1| \ll |\tilde{g}_0|$. The leading equation for $\tilde{g}_1$ is

$$\frac{d^3\bar{g}_1}{d\bar{z}^3} + \frac{\sqrt{3}}{2}\bar{g}_1 - \frac{(\bar{z}\bar{g}_1)'}{\sqrt{3}} = 0, \tag{5.3.33}$$

which has an exact solution in terms of the Airy functions Ai and Bi,

$$\bar{g}_1 = c_1 Ai^2(\bar{z}) + c_2 Ai(\bar{z})Bi(\bar{z}) + c_3 Bi^2(\bar{z}), \qquad c_i \in \mathbf{R}. \tag{5.3.34}$$

This fact is important for the reliable numerical integration of (5.3.30).

Matching. To determine the sequence $\{C_k,\ k \gg 1\}$ and the corresponding values $f(0; C_k) = a(C_k)$, we match the inner and outer solutions to the asymptotic behaviour of the transition region. Expanding the components of the inner solution (5.3.27) near the transition point, we have

$$g_0 = \varepsilon^{1/6}\left(-\frac{\bar{z}}{3^{1/2}}\right)\left(1 + \varepsilon^{1/3}\frac{\bar{z}}{83^{1/2}} + \ldots\right), \tag{5.3.35}$$

$$g_1 = \varepsilon^{-1/6} b \left(-\frac{3^{1/2}}{\bar{z}}\right)^{1/2} \left[1 - \cos\frac{\sqrt{3}t_0}{\varepsilon^{1/2}}\cos\frac{2}{3^{3/4}}(-\bar{z})^{3/2} - \sin\frac{\sqrt{3}t_0}{\varepsilon^{1/2}}\sin\frac{2}{3^{3/4}}(-\bar{z})^{3/2}\right]. \tag{5.3.36}$$

Thus, in this region, $g \simeq g_0 + \theta g_1 = O(\varepsilon^{1/6}) + O(\theta\varepsilon^{-1/6})$ and $\bar{g} = O(1) + O(\theta\varepsilon^{-1/3})$ which only matches completely for $\theta = \varepsilon^{1/3}$, or $m = 2/3$. Re-defining the coefficients in (5.3.32) by

$$\bar{g}_0 \simeq \left(\frac{-\bar{z}}{3^{1/2}}\right)^{1/2} + \frac{\bar{a}_1}{(-\bar{z})^{1/2}}\left[1 - \bar{a}_2\cos\frac{2}{3^{3/4}}(-\bar{z})^{3/2} - \bar{a}_3\sin\frac{2}{3^{3/4}}(-\bar{z})^{3/2}\right], \tag{5.3.37}$$

we have agreement when

$$\bar{a}_1 = b\,3^{-3/4}, \quad \bar{a}_2 = \cos\frac{3^{1/2}t_f}{\varepsilon^{1/2}}, \quad \bar{a}_3 = \sin\frac{3^{1/2}t_f}{\varepsilon^{1/2}}, \tag{5.3.38}$$

where $t_f = \int_0^{\sqrt{12}} \sqrt{1 - \frac{v^2}{12}} dv = \frac{3^{1/2}\pi}{2}$. Notice in particular that this demands

$$\bar{a}_2^2 + \bar{a}_3^2 = 1. \tag{5.3.39}$$

To determine the values of the parameters A_i and a_i we notice that equation (5.3.30) is translation invariant, as is the asymptotic behaviour for $\bar{z} \to \infty$, but not (to leading order) as $\bar{z} \to -\infty$. To see this we consider the solution to (5.3.30) as a shooting problem in the single parameter A_0. However,

$$\bar{g}(\bar{z}; A_0) = \bar{g}(\bar{z} - \bar{z}_0; 1), \qquad \text{where } \bar{z}_0 = \frac{2^{1/3}}{3^{1/6}} \ln A_0.$$

Clearly this translation does not change the ODE. To leading order, this same translation only affects the coefficient $\bar{a}_1$ in (5.3.32),

$$\bar{a}_1 \mapsto \bar{a}_1 + \frac{\bar{z}_0}{2 \cdot 3^{1/4}}, \quad \bar{a}_2 \mapsto \bar{a}_2, \quad \bar{a}_3 \mapsto \bar{a}_3. \tag{5.3.40}$$

However, such a translation generically destroys the rescaling from (5.3.32) to (5.3.37). Thus, we must look for A_0 such that we have the exact form (5.3.37). From the translation argument we have that $\bar{a}_1$ is monotone increasing in A_0 and the constraint (5.3.39) implies, by simple algebra, that there are precisely two sets of solutions which are simply the negatives of each other. Hence there are two possible solutions satisfying

$$\bar{a}_1 = -\tilde{a}_1, \qquad \bar{a}_2 = -\tilde{a}_2, \qquad \bar{a}_3 = -\tilde{a}_3,$$

where $\bar{a}_1 = \bar{a}_1(A_0)$ and $\tilde{a}_1 = \tilde{a}_1(A_1)$ related by

$$A_1 = A_0 e^{-2^{5/3}3^{1/6}\bar{a}_1}.$$

Numerical computation gives these two values to be ...

$$A_0 \simeq .045..., \qquad A_1 \simeq .448..., \qquad \bar{a}_1 \simeq .341... .$$

Using this value for $\bar{a}_1$ in the asymptotic expression (5.3.27) gives excellent agreement for z near zero to full numerical solutions, as seen in Figure 5.3.

In the far field, the behaviour has the form

$$g \simeq C\varepsilon^{1/12} z^{-1/3} e^{-\beta 12^{4/3} z^{4/3}/\varepsilon^{1/3}}$$

and matching to the transition region gives

$$A_0 = \frac{C}{12^{1/3}} \varepsilon^{1/12} e^{-\beta 12^{4/3}/\varepsilon^{1/3}}, \tag{5.3.41}$$

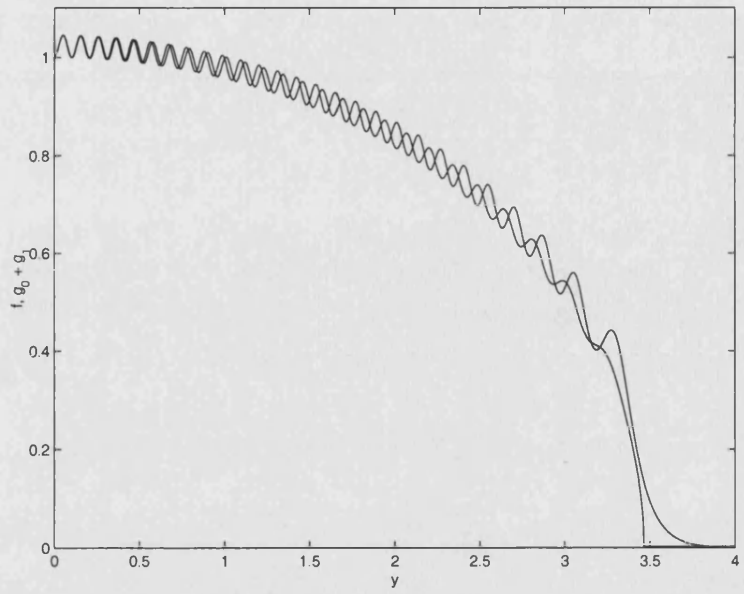

Figure 5.3: Comparison of numerical and asymptotic solutions

which, recognizing that $A_i = O(1)$ fixes [2]

$$\varepsilon = 2^2 3^5 \frac{1}{(\ln C)^3} + 2^2 3^6 \frac{\ln \ln C}{(\ln C)^4} + \ldots \qquad \text{as } C \to \infty.$$

Most importantly, given that $\bar{a}_2$ and $\bar{a}_3$ are unique (up to a change in sign in both coefficients), we have from (5.3.38)

$$\frac{3\pi}{2\varepsilon^{1/2}} = k\pi + (\phi + o(1))\pi, \tag{5.3.42}$$

for an unknown phase shift ϕ/π. Using this in the definition of ε gives

$$a_k = \sqrt{\frac{2k}{3}} \qquad \text{as } k \to \infty.$$

Also, the discrete spectrum is fixed

$$C_k \sim k^{1/6} e^{4^{4/3} k^{2/3} / 3^{1/3}} \qquad \text{as } k \to \infty.$$

Using the computed values of the coefficients and expansions we present a comparision of the numerical and asymptotic solutions in Figure 5.3. Notice the phase lag in the t_0-variable. This can be corrected by further terms in the expansion but, even to this order captures the correct number of fast scale oscillations. The Z variable over-predicts this by about one half for this value of ε.

[2] Further expansion of (5.3.41) also determines A_1 but not $\bar{a}_1$. (J.D. Evans, personal communication, 2003)

Numerical solution in the transition region. Because of the fast oscillation in (5.3.32) and the slow convergence to this profile (the next terms are $O(1/\bar{z})$), the accurate numerical computation of the coefficients (5.3.41) is not straightforward, in many ways it is the most difficult ODE problem in this thesis. In fact, it is known that for second-order equations of the type

$$y''(t) + g(t)y(t) = 0, \qquad g(t) \to \infty \text{ as } t \to \infty$$

(of which the Airy functions are particular solutions) standard Runge-Kutta or Linear Multi-step Methods are not only poorly suited, but are incapable of producing reliable solutions in double precision arithmetic for large t (Iserles 2002b). As such, the values were computed using a Modified Magnus Method employing Filon quadratures (Iserles 2002a, Iserles 2003).

5.3.4 Numerical solution of the ODE

In (5.3.3) we introduced the shooting function G whose zeroes correspond to admissible blow-up profiles. By numerically integrating the ODE (5.3.1) with the far-field behaviour (5.3.2), we have been able to approximate this function, as seen in Figure 5.4. Labelling, as above, the solutions to (5.3.1) corresponding to the $n-$th zero of G as f_n, we find that $f_n(y)$ has precisely n maxima on $\mathbf{R}$. In Figure 5.5 we present the first profile f_1 given in Theorem 5.3.4, which has the simplest bell-shaped form. It is evolutionarily stable for a broad range of initial data (see the next Section). For visual clarity we separately present the profiles $\{f_{1+4n}\}$ and $\{f_{2+4n}\}$ for $n = 0, ..., 15$.

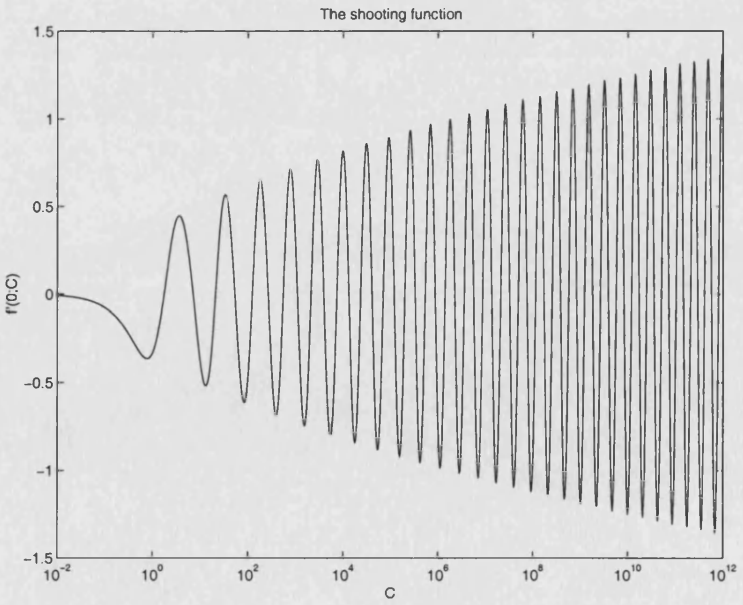

Figure 5.4: Numerical approximation to $G(C)$.

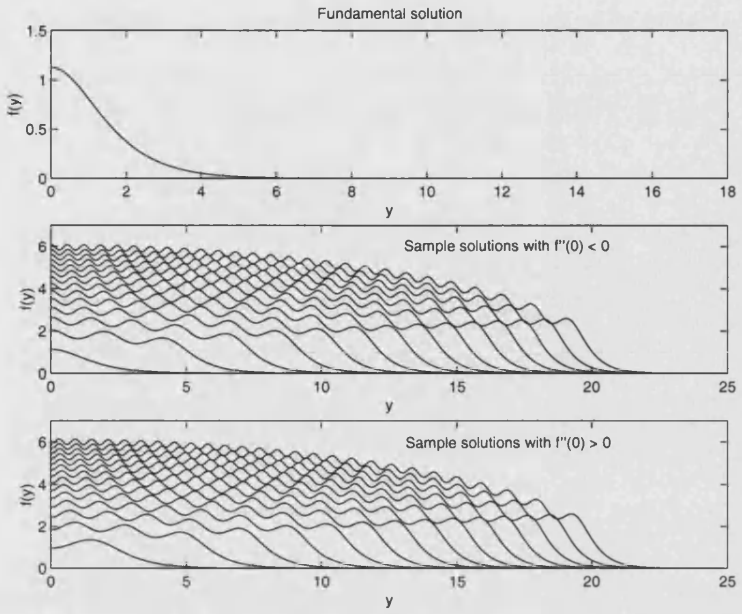

Figure 5.5: Various numerical solutions to (5.3.1)

5.3.5 Exponential asymptotic stability of the first blow-up pattern with profile f_1: numerical evidence

Proposition 5.3.5 together with the above matching analysis for $k \gg 1$ imply that there is a discrete family of solutions to the similarity ODE, and hence a discrete subset of admissible masses for the final time profiles

$$M_k = \int f_k(y)dy, \quad k = 1, 2, ..., . \tag{5.3.43}$$

We now justify that the first blow-up pattern with profile f_1 is the only stable one.

Returning to the rescaled evolutionary PDE (5.2.2) which for $N = 1$ and $p = 3$ takes the form

$$\theta_\tau = \mathbf{A}(\theta) \equiv -\theta_{yyyy} - \frac{1}{4}(\theta y)_y - (\theta^3)_y, \tag{5.3.44}$$

with initial data θ_0 we study the asymptotic behaviour of the global orbit $\{\theta(\tau)\}$. First we prove the following property of its ω-limit set $\omega(\theta_0)$.

Proposition 5.3.6. *With the definition* (5.2.1) *of the rescaled solution,*

$$0 \notin \omega(\theta_0). \tag{5.3.45}$$

Proof. We have from (5.3.44) that $\mathbf{A}'(0) = \mathcal{L} - \frac{1}{4}I$ with known spectral and sectorial properties (see section 3.3) and by Lemma 3.3.1 $\sigma(\mathbf{A}'(0)) = \{-(k+1)/4, k \geq 0\}$. The principle of the linearized stability (Lunardi 1995, Chap. 9) implies that any sufficiently small solution $\theta(\tau)$ decays as $\tau \to \infty$ exponentially fast and that for some

constant $C_0 > 0$,

$$|\theta(y,\tau)| \le C_0 e^{-\tau/4} \quad \text{uniformly in } \mathbf{R}.$$

Then one can see that from scaling (5.2.1) with $p = 3$ we have $|u(x,t)| \le C_0$ for all $t \approx T^-$, i.e., u does not blow-up at $t = T$ contradicting the choice of the scaling parameters. □

The linear part of the operator $\mathbf{A}$, $\mathcal{L} - \frac{1}{4}I$, is not self-adjoint and we do not expect that $\mathbf{A}$ is a potential operator nor that (5.3.44) is a gradient system. Therefore, the stability properties of the first similarity profile f_1 depend on the spectrum of the linearized operator

$$\begin{aligned}\mathbf{A}'(f_1) &= \mathcal{L} - \frac{1}{4}I - 3\frac{d^2}{d^2y}(f_1^2 I) \\ &= \mathcal{L} - \frac{1}{4}I - 3\frac{d^2(f_1^2)}{dy^2}I - 6\frac{d(f_1^2)}{dy}\frac{d}{dy} - 3f_1^2\frac{d^2}{dy^2},\end{aligned} \tag{5.3.46}$$

where we use the functional setting similar to that for $\mathcal{L}$ in Section 5.2.3.

Proposition 5.3.7. *$\mathbf{A}'(f_1) : H^4_\rho \to L^2_\rho$ is a bounded linear operator with the discrete spectrum $\sigma(\mathbf{A}'(f_1)) = \{\mu_l\}$.*

Proof. We recall that by Theorem 5.3.4, $f_1(y)$ has exponential decay as $y \to \infty$, so that (5.3.46) is a lower-order perturbation with smooth, bounded and exponentially decaying coefficients of the operator (3.2.4) and hence $\mathbf{A}'(f_1)$ is a bounded operator; see (Gohkberg and Krein 1969). In view ofthe known spectrum of $\mathcal{L}$ having a compact resolvent $(\mathcal{L} - \lambda I)^{-1}$ in L^2_ρ (Egorov et al. 2002) and taking $(\mathbf{A}'(f_1) - cI)^{-1}$ with a constant $c \gg 1$, we have that the additional terms in (5.3.46) form a compact perturbation of the integral operator. Hence, the spectrum of $\mathbf{A}'(f_1)$ is discrete. □

Note that the two first real positive eigenvalues of $\mathbf{A}'(f_1)$ are easily calculated explicitly:

$$\mu_0 = 1, \;\; \phi_0 = (yf_1(y))' \quad \text{and} \quad \mu_1 = 1/4, \;\; \phi_1 = f_1'(y), \tag{5.3.47}$$

corresponding to the invariance of the original PDE (5.1.1) under the group of translations in t and x respectively. As is usual in blow-up problems, since the blow-up scaling (5.2.1) does not admit such translations (the time T and the blow-up point $x = 0$ are fixed), these unstable modes are not available for the rescaled PDE (5.3.44).

An actual estimate of the real part of the remainder of the eigenvalues $\{\mu_l, l \ge 2\} \subset \mathbb{C}$ of $\mathbf{A}'(f_1)$ is non-trivial. Instead we present a numerical calculation, from directly simulating the PDE, in Figure 5.1.1a. We have chosen symmetric monotone decreasing initial data having a smaller mass

$$\int u_0 < M_1 = \int f_1$$

than the similarity solution. Figure 5.1.1b shows the time-evolution of the mass of this solution for $\tau \gg 1$ establishing convergence to M_1 (recall from Chapter 2 that our numerical scheme was designed to preserve mass). From a variety of numerical experiments, we conjecture that the next eigenvalue satisfies

$$\text{Re } \mu_2 \simeq -.51....$$

This calculation is based on measuring the L^∞ convergence in the rescaled co-ordinates over a compact set in the similarity variable y. Measurement over all of x shows

$$\text{Re } \mu_2 \simeq -1/4$$

instead. This is understood analagously to Propostion 5.3.6. Solutions with mass different from the final time profile cannot, because of conservation, lose that mass, but, similarly, it cannot contribute to the final-time profile in the rescaled co-ordinates. This extra mass (positive or negative) is damped to zero in the rescaled co-ordinates as described in Propostion 5.3.6 and hence with exponential rate $-1/4$. However, this is not a property of the linearized operator about the first similarity profile. This discrepancy is indicated in Figure 5.6. Numerical simulation of the full PDE with

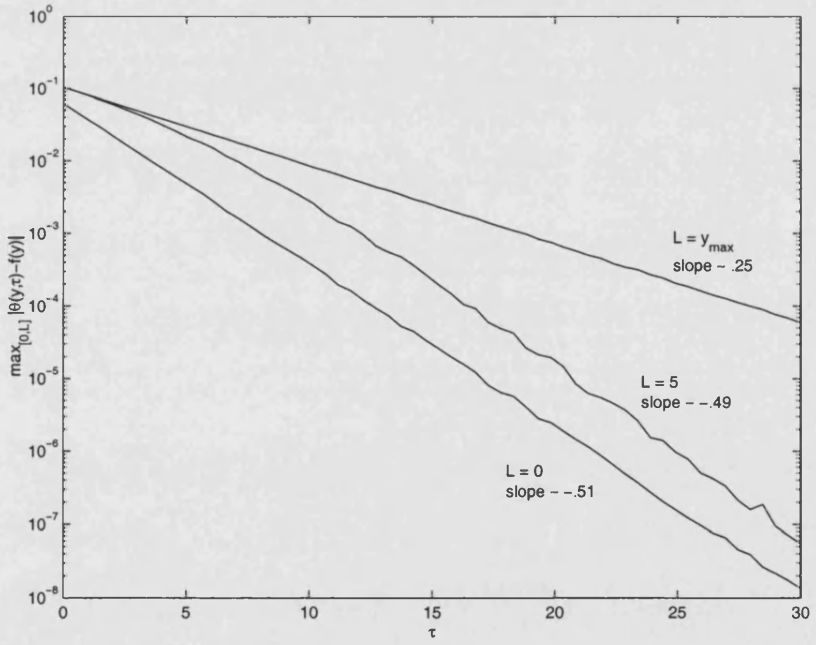

Figure 5.6: Rate of convergence to the similarity profile.

stationary profiles other than f_1 shows them to be exponentially unstable and the linearized operator

$$\mathbf{A}'(f_k) = \mathcal{L} - \frac{1}{4}I - 3\frac{d^2}{dy^2}(f_k^2 I) \tag{5.3.48}$$

has eigenvalues with positive real parts. Ordering the sequence of eigenvalues $\{\mu_l\}$ such that their real parts are non-increasing, means that

$$\operatorname{Re}\mu_2 > 0 \qquad \text{for all } \; k \geq 2. \tag{5.3.49}$$

This has been checked numerically in a number of PDE experiments. For instance, Figures 5.1.1c and 5.1.1d display the unstable evolution given by the initial function $\theta_0 = f_5$ with the larger mass $\int \theta_0 = \int f_5 > \int f_1$.

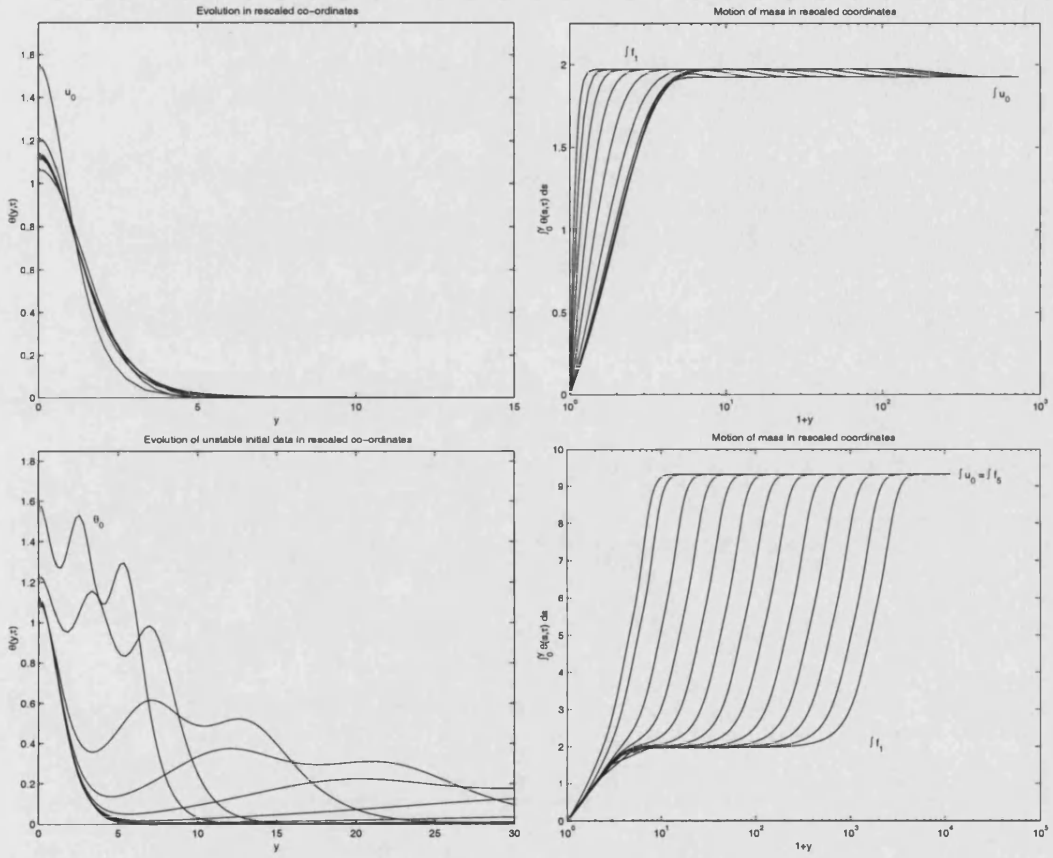

Figure 5.7: Evolution of solutions to (5.1.1). (a) Convergence to f_1 in rescaled co-ordinates. (b) Motion of the mass for initial mass $\int u_0 < \int f_1$. (c) Instability of f_5. (d) Motion of the mass for initial mass $\int u_0 = \int f_5 > \int f_1$.

5.3.6 General p

The case of general p is more complicated than for the conservative case as without conservation the ODE remains truly fourth-order. One seeming exception to this is the second critical exponent $p_1 = 2$ (recall (5.2.8)) for which one can also derive a third-order ODE. These are the solutions which conserve momentum. For simplicity

we consider only $N = 1$. Multiplying by x in the PDE (5.1.1) we have

$$0 = -\int_{\mathbf{R}} x(u_{xx} + u^p)_{xx} dx = \frac{d}{dt}\int_{\mathbf{R}} ux\, dx = \frac{d}{dt}\left[(T-t)^{1/2(p-1)+1/2}\int_{\mathbf{R}}^{N} f(y) y\, dy\right].$$

Thus, $p_1 = 2$ defines the exponent for which momentum is conserved (generically, $p_1 = 1 + 2/(N+1)$). Multiplying the ODE (in $\mathbf{R}$) with y and integrating we have

$$f'''y - f'' + \frac{1}{4}y^2 f + (f^2)'y - f^2 = -f''(0) - f^2(0) = C \in \mathbf{R}, \tag{5.3.50}$$

where the constant C determines the size of algebraic decay at infinity. Recall that from (5.2.14) with $p = 2$ the asymptotic algebraic behaviour is $f(y) \sim 4C/y^2$ for $y \gg 1$. For the case $C = 0$, the far-field behaviour is purely exponential. However, for this case

$$f''(0) = -f^2(0) < 0,$$

thus there are only such solutions with a local maximum at the origin (recall Figure 5.5). This family, $\{f = f_\mu(y)\}$, may be investigated by integrating (5.3.50) from $y = 0$ subject to

$$f(0) = \mu, \quad f'(0) = 0, \quad f''(0) = -\mu^2, \quad \mu \in \mathbf{R},$$

looking for μ such that $f(y) \to 0$ exponentially fast as $y \to \infty$. Numerical experiment indicates there is only one such solution and that it has non-zero mass, $\int f_{\mu^*} > 0$ and hence can play no part in the asymptotics of the full PDE.

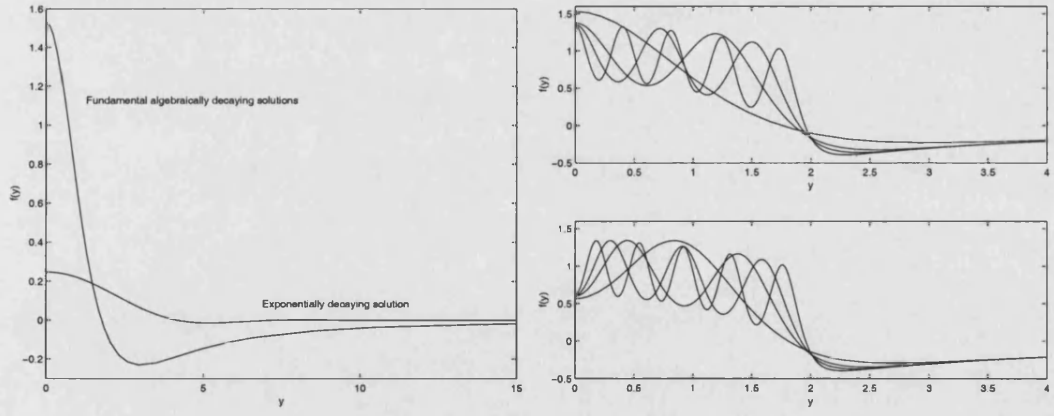

Figure 5.8: Solutions to (5.3.50). (a) The solution with exponential decay and the fundamental algebraically decaying one. (b) Examples from the family of algebraically decaying solutions.

For C not identically zero solutions can again be constructed by continuation in C but now the condition of zero mass must be enforced creating, once again, a fourth-order

system. For all $C \in \mathbf{R}$ we solve

$$f'''y - f'' + \frac{1}{4}y^2 f + (f^2)'y - f^2 = C$$
$$F' = f$$
$$F(0) = 0, \quad \lim_{y\to\infty} F = 0, \quad f \to C/y^2 \ \text{ as } \ y \to \infty$$

for C such that $f'(0;C) = 0$. In Figure 5.8 we present example solutions with algebraic decay as well as the exponentially decaying profile. For the algebraic solutions, a similar rescaling and singular perturbation approach may be employed to construct the countable spectrum of solutions as for the case $p = 3$. Notice however that now the inner solution is defined on a region which is independent of C and that the inner solutions have oscillations whose amplitude is also independent of C, cf. Figure 5.5. By direct simulation of the full PDE with various values of $p \neq 3$ we conjecture that solutions to (5.2.3) govern the blow-up dynamics for all p, not just in the conservative case. For instance, for $p = 2$ solutions converge, on compact sets in y, to the fundamental algrebraically decaying solution in Figure 5.8a.

5.4 Global similarity and approximate similarity patterns

Taking $\sigma = -1$ (and $T = 0$) in (5.2.1) yields the rescaling of global in time solutions. We now study the asymptotic behaviour as $\tau \to \infty$ of solutions satisfying the parabolic PDE

$$\theta_\tau = \mathbf{A}(\theta) \equiv -\Delta(\Delta\theta + \theta^p) + \frac{1}{4}y \cdot \nabla\theta + \frac{1}{2(p-1)}\theta. \tag{5.4.1}$$

5.4.1 Similarity patterns for the one-dimensional equation with $p = 3$

As in the case of blow-up in Section 5.3, we begin with the analysis of global self-similar solutions

$$u_s(x,t) = t^{-1/4} f(y), \quad y = x/t^{1/4},$$

where f satisfies the ODE obtained from (5.2.3), (5.2.2) by integration

$$f''' - \frac{1}{4}yf + (f^3)' = 0, \quad f'(0) = 0. \tag{5.4.2}$$

We are looking for profiles f with exponential decay at infinity, so that these are L^1-solutions satisfying the conservation law (5.2.5). Recall that unlike the blow-up case (5.3.1), the ODE (5.4.2) admits a two-dimensional exponential bundle as $y \to \infty$ (cf. (5.2.12)). This essentially simplifies the existence analysis and implies a continuous subset of similarity profiles.

Theorem 5.4.1. *The ODE* (5.4.2) *has an unbounded continuous family of exponentially decaying solutions.*

Proof. Step 1: asymptotics as $y \to \infty$. By a standard local analysis, one can check that, in addition to the two-dimensional exponential bundle of solutions (5.2.12) and those with the algebraic decay (5.2.14), (5.4.2) has a three-dimensional bundle of growing solutions as $y \to \infty$

$$f(y) = \frac{y}{\sqrt{12}} + \frac{1}{y}\left[C_1 \cos\left(\frac{y^{3/2}}{3}\right) + C_2 \sin\left(\frac{y^{3/2}}{3}\right) + C_3\right] + ..., \tag{5.4.3}$$

where C_1, C_2, C_3 are arbitrary parameters.

Step 2: shooting argument. Fix a constant $a \geq 0$ and by $f(y; C)$ denote the solution of (5.4.2) with conditions

$$f(0) = a, \quad f''(0) = C.$$

As in Section 5.3, one can show that $f(y; C)$ is globally defined. Using the stability of the three-dimensional bundle (5.4.3) concentrated around the stable explicit solution

$$f_*(y) = y/\sqrt{12} \to \infty, \quad y \to \infty, \tag{5.4.4}$$

we have that there exists a sufficiently large $C_1 > 0$ such that $f(y; C)$ belongs to the bundle (5.4.3) for all $C \geq C_1$. Such profiles may be constructed in the limit $C \to \infty$ using the rescaling $g(z) = f(y)/a$, $z = y\sqrt{C/a}$. On the other hand, via symmetry by reflection, for all $-C \gg 1$, $f(y)$ approaches as $y \to \infty$ the bundle around the explicit profile $-f_*(y)$. Introducing the subset

$$W = \{\mu < C_1 : \ f(y; C) \text{ belongs to (5.4.3) for all } C \in (\mu, C_1)\},$$

we have that there exists a finite $C = \inf W$, and by construction, $C = C(a)$ provides us with a profile $f(y; C(a))$ which belongs to the exponential bundle (5.2.12) as $y \to \infty$.

□

Note that this implies that there exists a solution with all $f(0) = a \in \mathbf{R}$. On Figure 5.9 we present the bifurcation mass-diagram of this continuous family of similarity profiles. As we already know, there exists another case $p = 2$, $N = 1$, where the fourth-order ODE (5.2.3) reduces to a simpler third-order one. The existence results here are quite similar and the family of solutions is continuous. The shooting approach may be extended to one-dimensional or radial ODEs for arbitrary p and dimension N, where some critical cases occur to be studied next.

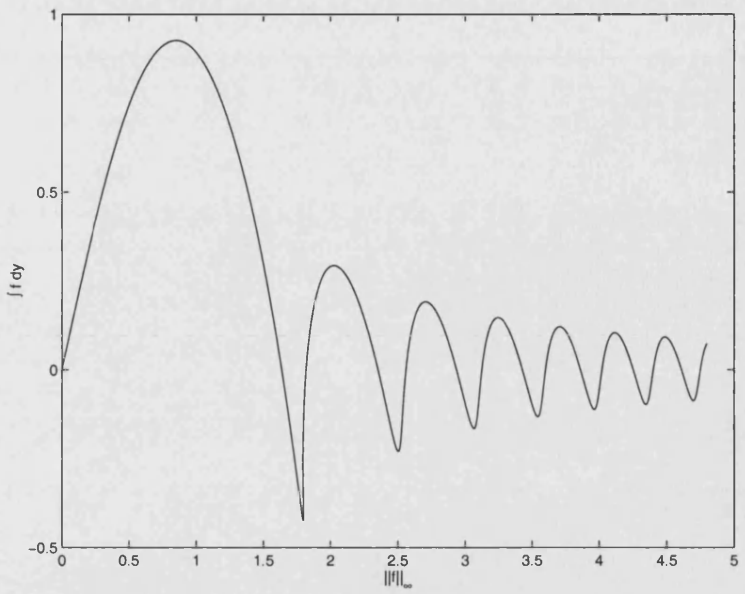

Figure 5.9: Mass bifurcation diagram.

5.4.2 The minimal mass-branch is evolutionarily stable

It follows from Figure 5.9 that for any fixed initial mass $m_0 = \int u_0 \neq 0$ there exists a finite (or empty if $|\int u_0| > m^*$) subset of similarity solution with the given mass. Moreover, for $m_0 = 0$ besides $f(y) \equiv 0$, there exists a countable family of such solutions. The crucial problem for such a case is the stability of those solutions in the PDE sense. Let us show that the *minimal branch* in Figure 5.9 corresponding to the limit

$$f \to 0 \quad \text{as } m_0 \to 0 \tag{5.4.5}$$

is evolutionarily stable at least for all small masses $m_0 > 0$ (or $m_0 < 0$ setting $f \mapsto -f$). As a typical example, we perform such computations for the N-dimensional case bearing in mind that the first critical exponent is now $p = p_0 = 1 + 2/N$. Consider the corresponding elliptic equation

$$\mathbf{A}(f) \equiv -\Delta^2 f + \frac{1}{4} y \cdot \nabla f + \frac{N}{4} f - \Delta f^p = 0, \quad \int f = m_0. \tag{5.4.6}$$

First, as an example, we establish a local result on the existence of such similarity patterns.

Proposition 5.4.2. *Let $p = p_0$. For any sufficiently small m_0, (5.4.6) admits a solution satisfying*

$$f = m_0 F + O(m_0^p) \qquad (\textit{with } F \textit{ is as in } (3.3.4)). \tag{5.4.7}$$

Proof. Setting $f = m_0 v$ yields the perturbed equation

$$\mathcal{L}^* v = |m_0|^{p-1} \Delta v^p, \quad \int v = 1. \tag{5.4.8}$$

Using the spectral properties of $\mathcal{L}^*$, as described in Lemma 3.3.1, we look for a solution $v = F + w$, where $w \in \mathcal{L}^{\perp}\{F\}$ (note that $\lambda_0 = 0$ is simple), and obtain solvability for sufficiently small masses as in the proof of Theorem 4.4.3. □

To study the stability of this branch, we consider the linearized operator

$$\mathbf{A}'(f)Y = \mathcal{L}^* Y - \Delta(p|f|^{p-1}Y) \equiv \mathcal{L}^* Y + |m_0|^{2/N} \Delta(p|f|^{p-1}Y) + \dots. \tag{5.4.9}$$

For small m_0, $\mathbf{A}'(f)$ is a perturbation of $\mathcal{L}^*$ with the known spectrum (3.3.9). Similarly to Theorem 4.4.3 we have that $\mathbf{A}'(f)$ has a discrete spectrum which is a perturbation of that of $\mathcal{L}^*$. Recall from the orthogonality condition (3.3.14) that $\psi_0^* = F$ is the only eigenfunction of $\mathcal{L}^*$ with non-zero mass (in fact it equals unity, see (3.3.4)). Thus, requiring that the mass of profiles be preserved means that the eigenfunctions Y of $\mathbf{A}'(f)$ must come from $\mathcal{L}^{*\perp}(F)$ and that the eigenvalues are perturbations of the eigenvalues of $\mathcal{L}^*$ for $l \geq 1$ i.e. no perturbation of the first eigenvalue $\lambda_0 = 0$ may occur as a change in this eigenvalue would lead to a change in time of the mass of the solution. Proceeding as Section 4.4 we have, by direct calculation, that, to leading order, the perturbed spectrum is given by

$$\sigma(\mathbf{A}'(f)) = \left\{ -\frac{l}{4} + |m_0|^{2/N} \left\langle \Delta(p|\psi_0^*|^{p-1}\psi_l^*, \psi_l \right\rangle, l = 1, 2, \cdots \right\}$$

This guarantees that, in the limit of small m_0 the real parts of the eigenvalues are bounded away from zero from below and that this branch is stable. Note that this expansion is not valid near the subsequent zeros of mass seen in Figure 5.9 as the L^∞ norm is not zero and hence the form (5.4.7) does not hold.

5.4.3 The p-bifurcation diagram for similarity profiles

In order to understand the global bifurcation diagram of similarity profiles, we need to determine the spectrum of critical exponents. Writing the elliptic equation (5.2.3) in the form

$$\mathcal{L}^* f + c_* f = \Delta f \quad \text{in } \mathbf{R}^N, \quad f(y) \to 0 \text{ exponentially fast as } y \to \infty, \tag{5.4.10}$$

we proceed as in Section 4.4.

Proposition 5.4.3. *Let, for an integer $l \geq 0$, the eigenvalue $\lambda_l = -l/4$ of the operator*

(3.2.4) *be of odd multiplicity. Then the critical exponents*

$$p_l = 1 + 2/(N + l), \qquad l = 0, 1, 2, ... \tag{5.4.11}$$

are bifurcation points for the problem (5.4.10).

After performing a smooth truncation of the nonlinearity Δf^p the proof follows analgously to that of Proposition 4.4.1.

By using the explicit representation of the resolvent of $\mathcal{L}^*$ (Egorov et al. 2002), this differential equation reduces to an integral one with compact Hammerstein's operators to which the classical nonlinear bifurcation techniques (Krasnosel'skii and Zabreiko 1984) applies. Using this approach, asin Section 4.4, we briefly describe the results calculated directly from the differential equation.

By Lemma 3.3.1, the linear operator in (5.4.10) has the spectrum $\sigma(\mathcal{L}^* - c_* I) = \{c_* - l/4,\, l \geq 0\}$. Therefore, any p for which $c_* - l/4 = 0$, i.e., the critical exponents (5.4.11) are bifurcation points for problem (5.4.10) provided that $\lambda_l = -l/4$ is of odd multiplicity (e.g., this is always true for $N = 1$ or in the radial geometry where the eigenvalues are always simple). In order to describe the local behaviour of the bifurcation branches at $p \approx p_l$, we fix an l and set

$$p = p_l + \varepsilon \quad \text{with } p_l = 1 + 2/(N + l).$$

It follows that $c_* = l/4 - \mu_l \varepsilon + O(\varepsilon^2)$, with $\mu_l = (N + l)^2/8$, so that equation (5.4.10) takes the form

$$\left(\mathcal{L}^* + \frac{l}{4} I\right) f - \mu_l \varepsilon f + O(\varepsilon^2) = \Delta f^p. \tag{5.4.12}$$

Using the Lyapunov-Schmidt method ((Krasnosel'skii and Zabreiko 1984), Chap. 8), we find that near the bifurcation point the solution takes the form

$$f = [\nu_l (p_l - p)]^{-1/(p-1)} \psi_l^* + ... \quad \text{as } p \to p_l^-, \text{ where } \nu_l = (N + l)^2/8\kappa_l \tag{5.4.13}$$

and

$$\kappa_l = \langle \Delta(\psi_l^*)^{p_l}, \psi_l \rangle = \langle (\psi_l^*)^{p_l}, \Delta\psi_l \rangle . \tag{5.4.14}$$

The expansion (5.4.13) is written down under the assumption that (5.4.14) holds, which is to be checked numerically. Notice however, that

$$\kappa_0 = \kappa_1 = 0, \qquad \text{for all } N \geq 1,$$

as $\psi_0 = 1$ and ψ_1 is linear. Thus the branches leave these bifurcation points vertically, suggesting a continuous family of solutions for these critical exponents. Of course, this is consistent with Theorem 5.4.1. Also, $\lim l \to \infty \kappa_l = 0$.

On stability of the p_2-branch. Let us now show that the first non-vertical branch, from $p = p_2$, is stable for $p \approx p_2$. This is done by estimating the real parts of the eigenvalues of the linearized operator given in (5.4.10), which for $l = 2$ has the form

$$\mathbf{A}'(f) = \mathcal{L}^* + \frac{1}{2}I + \varepsilon \mathbf{C} + o(\varepsilon), \quad \mathbf{C} = \mu_l I + p_2 \nu_2 \Delta(\psi_2^*)^{p_2}, \tag{5.4.15}$$

where we substitute the expansion of f given by (5.4.13). By $\{\bar{\lambda}_l = \bar{\lambda}_l(\varepsilon)\}$, $\varepsilon = p_2 - p$, we denote the discrete spectrum of $\mathbf{A}'(f)$.

For $N = 1$, due to conservation of mass (for any $p \le p_0 = 3$) and of momentum (for any $p \le p_1 = 2$), the first modes with positive unperturbed eigenvalues of $\mathcal{L}^* + \frac{1}{2}I$ ($\varepsilon = 0$), $\bar{\lambda}_0(0) = 1/2$ and $\bar{\lambda}_1(0) = 1/4$ are not taken into account and we need to check the perturbed third eigenvalue $\bar{\lambda}_2(\varepsilon)$. The same holds for $N > 1$ in the radial setting deleting all eigenvalues corresponding to asymmetric eigenfunctions and hence $\bar{\lambda}_1$. Since this unperturbed eigenvalue vanishes, $\lambda_2(0) = 0$, by the perturbation methods (Gohkberg and Krein 1969), the eigenvalue expansion takes the form $\lambda_2(\varepsilon) = \varepsilon\mu + o(\varepsilon)$ with the eigenfunction $\bar{\psi}(\varepsilon) = \psi_2 + \varepsilon\varphi + o(\varepsilon)$. Substituting these approximations into the eigenvalue equation

$$\mathbf{A}'(f)\bar{\psi}_2(\varepsilon) = \bar{\lambda}_2(\varepsilon)\bar{\psi}_2(\varepsilon),$$

similar to computations in the proof of Theorem 4.4.3 we obtain from the orthogonality condition that $\mu = -(N+2)/4$. Hence, for small $\varepsilon = p_2 - p > 0$,

$$\bar{\lambda}_2(\varepsilon) = -(p_2 - p)(N+2)/4 + o(p_2 - p), \quad \text{i.e., } \operatorname{Re} \lambda_2(\varepsilon) < 0. \tag{5.4.16}$$

This means the exponential asymptotic stability of the similarity patterns on the p_2-bifurcation branch for all $p_2 - p > 0$ sufficiently small. We expect that the whole branch remains stable but this needs to be justified numerically (or otherwise).

Chapter 6

Conclusions and further work

This thesis is devoted to the study of the general principles of singularity formation phenomena for higher-order nonlinear parabolic equations. This work has its roots in the long and important study of second-order quasilinear heat equations, with many important questions answered by the mid 1990s. While the main analytical tool for this original work, the Maximum Principle, is no longer available for higher-order problems, many of the known phenomena persist. We have undertaken this study with a mixture of analysis, asymptotics and numerical computation of both PDEs and ODEs. While this work is broad it is by no means complete. In fact, there are many directions that it can be continued. First and foremost, while we have achieved a certain understanding of these phenomena, many results remain unproven. For this, fundamentally new mathematics will be required as the current tools are insufficient. I do not see this occuring in the near future. There are however many areas of immediate concern.

6.1 Extension to quasilinear models

All the problems discussed have been semilinear. One natural continuation is to quasilinear and eventually fully nonlinear problems. The results of Chapter 3 generalize immediately to the problem

$$u_t = u(-(-\Delta)^m u + u^p), \quad x \in \mathbf{R}^N, u \geq 0, p > 1,$$

which is a generalization of a model from plasma physics for $m = 1$ (Friedman and McLeod 1986) and of curve shortening flows (Angenent and Velázquez 1995). Looking for finite-time blow-up solutions, we introduce the rescaled co-ordinates

$$\theta(y,\tau) = u(x,t)/(T-t)^{1/p}, \qquad y = x/(T-t)^{(p-1)/2mp}, \qquad \tau = -\ln(T-t),$$

whence θ solves

$$\theta_\tau = \theta(-(-\Delta)^m\theta + \theta^p) + \frac{p-1}{2mp} y \cdot \nabla\theta + \frac{\theta}{p}.$$

Linearizing, as in Chapter 3, about the constant solution $1/p^{1/p}$ shows that the spectrum of the new linearized operator is precisely a shift of that of $\mathcal{L}$. Moreover, this shift gives a very simple estimate for the number of similarity solutions available, there should be at least k solutions for $p > p_k = k/(k-2m)$. In the limit case $k \to \infty$,i.e. $p \to 1^+$ we can construct the countable spectrum of solutions exactly. These are regional blow-up profiles of the form (for $m = 2$)

$$u(x,t) = (T-t)^{-1} f(x)$$

where $f(x)$ solves

$$\begin{aligned} &-f'''' + f = 0, \qquad x \in (-x_k, x_k), \\ &f \equiv 0 \qquad\qquad \text{else}, \\ &f(-x_k) = f'(-x_k) = f''(-x_k) = f(x_k) = f'(x_k) = f''(x_k) = 0, \end{aligned}$$

and x_k is the $k-$th root of $\tan(x) = \tanh(x)$. These structures need to be investigated in further detail.

Another obvious extension would be to generalize the results and methods of Chapter 5 to consider models of the form

$$u_t = -(-\Delta)^{m_1}(|u|^{p_1-1}u) \pm (-\Delta)^{m_2}(|u|^{p_2-1}u) \quad x \in \mathbf{R}^N, m_1 > m_2 \geq 1, p_2 > p_1 \geq 1.$$

Many similar features to those already described persist for such models with stable or unstable higher-order porous medium operators. The very optimistic goal of such work would be the eventual complete classification of operators of thin-film type

$$h_t = -\nabla \cdot (h^{p_1}\Delta\nabla h \pm \Delta h^{p_2}).$$

6.2 Hyperbolic models

The problems of finite-time blow-up and localization are not unique to parabolic models. One hyperbolic example of great physical interest is the complex Ginzburg-Landau equation

$$i\Phi_t + (1+i\delta)\Delta\Phi + (1-i\varepsilon)|\Phi|^2\Phi = 0, \quad x \in \mathbf{R}^N, \quad t > 0. \tag{6.2.1}$$

A reduction of this equation with $\varepsilon = \delta = 0$ is the famous nonlinear Schrödinger equation which is known to exhibit many of the same blow-up phenomena as described in Chapter 3 (Sulem and Sulem 1999). The geometry of self-similar solutions for CGL is

more complicated than for the models thus far examined as can be seen in the similarity transformation

$$\xi \equiv \frac{|x|}{L(t)}, \quad \tau \equiv \int_0^t \frac{1}{L^2(s)} ds, \quad u(\xi,\tau) = L(t)\Phi(x,t). \tag{6.2.2}$$

The rescaled solution u satisfies

$$iu_\tau + (1-i\varepsilon)\left(u_{\xi\xi} + \frac{N-1}{\xi}u_\xi\right) + (1+i\delta)|u|^2 u + ia(\tau)(\xi u)_\xi = 0, \tag{6.2.3}$$

where

$$a = -L\frac{dL}{dt} = -\frac{1}{L}\frac{dL}{d\tau}.$$

The simplest form of blow-up behaviour arises when $a(\tau)$ is constant. These are the self-similar solutions and we have

$$L(t) = \sqrt{2a(T-t)} \quad \text{and} \quad \tau = \ln(T-t)/2a. \tag{6.2.4}$$

The constant a above is a non-linear eigenvalue for the reduced equation, and its value needs to be determined as part of the solution process. Thus the transformation has an unknown essential parameter in it, unlike any of the previous parabolic problems. As for the NLS (Sulem and Sulem 1999), we look for self-similar solutions of (6.2.3) of the form $u(\tau,\xi) = e^{i\tau}Q(\xi)$ which leads to the following ODE for Q:

$$(1-i\varepsilon)\left(Q_{\xi\xi} + \frac{(N-1)}{\xi}Q_\xi\right) - Q + ia(\xi Q)_\xi + (1+i\delta)|Q|^2 Q = 0. \tag{6.2.5}$$

Through a combination of matched asymptotics and WKB approximations applied to (6.2.5) we have begun to understand the stability of similarity solutions to this problem, the structure of multi-bump profiles and the parameter ranges over which such solutions exist. Critically, we have an ODE non-existence argument of solutions at the critical dimension $N = 2$ which agrees for a previous modulation argument and can extend our results (continuously in $N \geq 1$) to the physically important region of $N = 3$. An example of these results is summarized in Figure 6.1. Interestingly, it appears that there is a region of the parameter ε where a multi-bump solution occurs, but not a ground-state solution. This is intriguing because in all the numerical experiments we have performed on various problems, only the profiles with the simplest shape have been found to be stable. However, no spectral theory for the associated linear operators exists and techniques from bifurcation theory have not been employed to consider the number of admissable solutions. In fact, whether this spectrum is finite, countably infinite or uncountable is an important open problem. Perhaps it can be tackled with a combination of bifurcation and spectral arguments as we did in Chapter 3 for the semilinear parabolic blow-up problem.

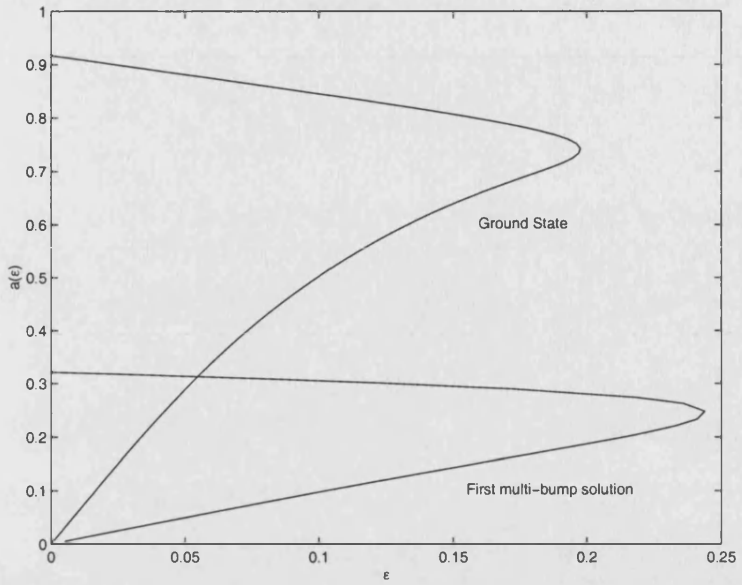

Figure 6.1: Bifurcation curves for $N = 3$.

6.3 Adaptivity in higher-dimension

All of the simulations presented thus far have concentrated on calculations in one dimension or radially symmetric solutions in higher dimensions. This is not a severe limitation for the problems at hand as we have, in the first instance, concentrated on one-dimensional or radially symmetric patterns. To fully understand stability and more complicated patterns, in higher-dimensions we need to be able to extend the ideas of Chapter 2 to arbitrary dimension. Many strategies are currently competing in this area, see the survey (Huang and Russell 2001) and the references therein. We are working on another approach which we believe has certain key advantages and is based directly on the idea that equidistribution is a mapping with specified Jacobian (Budd and Williams 2003). In its simplest form this idea highlights the enormous leap in moving beyond one dimension. Unfortunately, the condition

$$J = \frac{1}{M(x)}, \qquad x \in \mathbf{R}^N, \tag{6.3.1}$$

only specifies one equation in N-dimensions, which appears to be satisfactory only in dimension $N-1$. One way to close this system is to look amongst all the solutions to (6.3.1) for (the) one which minimizes

$$L[x] = \int |x(\xi) - \xi|^2 d\xi. \tag{6.3.2}$$

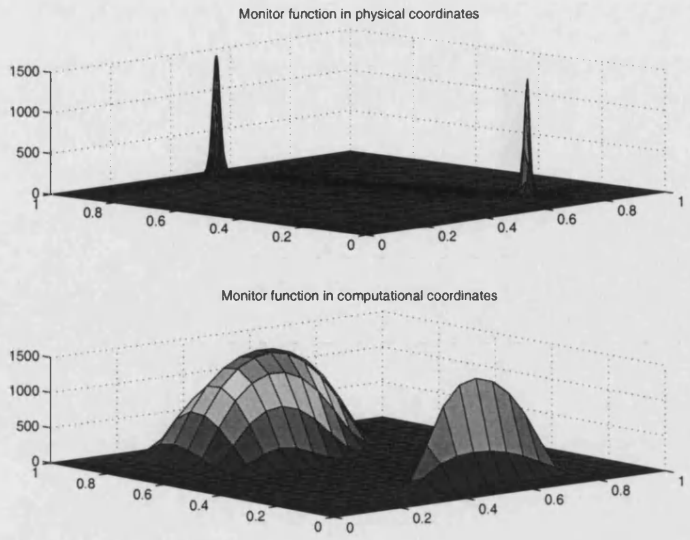

Figure 6.2: Monitor function in computational and physical co-ordinates.

Heuristically, this is a very natural requirement from a numerical analysis point of view as this is, by definition, the map closest to the identity in the L^2 sense. Further, this augmented problem has been well studied in the context of Optimal Transport (Villani 2003) dating back to Monge and Kantorovich. It is known that there exists a unique solution satisfying a Monge-Ampere problem

$$x = \nabla P(\xi), \qquad |D^2 P| = \frac{m(\xi)}{M(\nabla P)}, \qquad \xi \in \mathbf{R}^N, \tag{6.3.3}$$

supplemented with the condition that the boundary maps to the boundary. This is a pure Neumann condition which takes the form

$$\nabla P \cdot \xi = \xi \cdot \hat{n} \qquad \text{on } \partial\Omega \quad \text{where } \Omega = [0,1]^N.$$

In the context of meteorological fluid dynamics this transformation has been used to great effect by Cullen and Purser (1984) and co-workers to study the semi-geostrophic equations, see the references in (Piggott 2002). This formulation is also a natural geometric requirement as it requires the mesh to be *irrotational*, a property seen to be desirable in practice (Cao, Huang and Russell 2002). We have begun an extension of the MMPDE approach described in Chapter 2 by solving the parabolic Monge-Ampere equation

$$P_t = \ln\left(M(\nabla P)|D^2 P|\right). \tag{6.3.4}$$

This has the nice properties that it preserves the convexity of P (and hence the well-posedness of the mapping $x = \nabla P$), and for $M = M(\xi)$ possesses a Lyapunov function

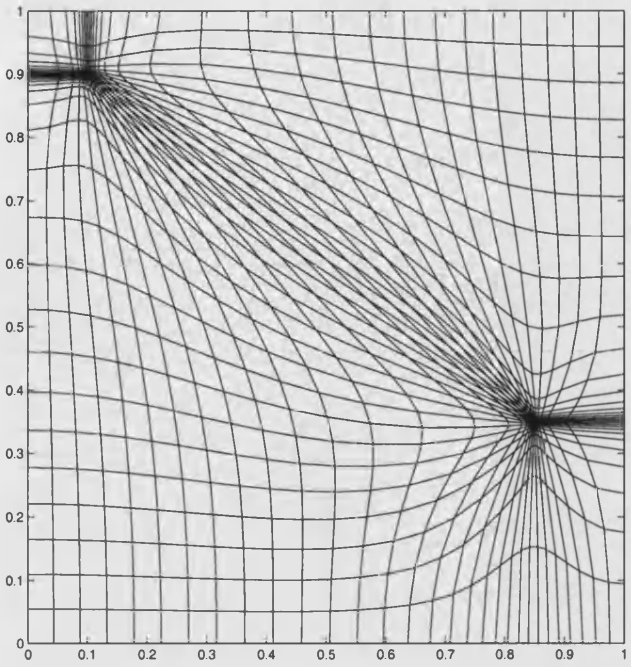

Figure 6.3: Associated mesh.

whose minimizer is unique and is amenable to fast solution techniques. The key to the efficient implementation of adaptive methods in $N > 1$ is the splitting of the physical and mesh PDEs in the solution process. This means that given a solution, a monitor function is defined in computational space and fixed. Once the new grid has been solved, the solution is updated on the new grid. This means that we can concentrate on the problem

$$P_t = \ln\left(M(\xi)|D^2 P|\right). \tag{6.3.5}$$

instead of the more difficult problem (6.3.4). An example of this in practice is presented in Figures 6.2 and 6.3. Here we have taken a monitor function representing singularity formation at two points in the region $[0,1]^2$ and solved (6.3.5) until steady-state. In Figure 6.2 we present the monitor function in both physical and computational coordinates. Here we can see the effects of adaptivity–solutions are 'smoother' in the new variable. Lastly, in Figure 6.3 we show the associated mesh in which we can see the localization near the 'singularities'.

6.4 Numerical computation of spectra for higher-order non-autonomous non self-adjoint operators

Throughout this thesis the numerical solution of initial-boundary value problems for PDEs, initial value problems for ODEs and continuation of boundary value problems

for ODEs has gone hand in hand with analysis, be it rigorous or formal. The one exception has been in the computation of spectra. Instead of an approximation of the full spectra of our linear operators we have only used PDE computations to estimate the magnitude of the real part of dominant eigenvalues. This is not due to lack of effort! Much progress has been made in this direction (in the context of the numerical evaluation of the Evans function) for operators for which all coefficients are bounded in the limit $y \to \infty$. This is fine for travelling wave problems but, for all similarity transformations one must contend with operators of the form $y \cdot \nabla$ for which all the existing theory and methods breakdown.

Generically we are interested in approximating the following problem:

$$(\mathcal{L} + C)\phi = \mu\phi$$

where C is a compact perturbation of the operator $\mathcal{L}^{-1}$ whose spectral properties are known. Unfortunately, we know that the eigenfunctions of $\mathcal{L}$ oscillate at infinity, this, coupled with the growing first derivative term makes the computations very difficult. Because of the importance of equations of this form careful study needs to be undertaken.

References

Ad'jutov, M. M. and Lepin, L. A. (1984). Absence of blowing up similarity structures in a medium with a source for constant thermal conductivity, *Differ. Equat.* **20**(7): 1279–1281.

Amick, C. J. and Toland, J. F. (1992). Homoclinic orbits in the dynamic phase space analogy of an elastic strut, *Euro. J. Appl. Math.* **3**: 97–114.

Angenent, S. B. (1986). The Morse-Smale property for a semi-linear parabolic equation, *J. Differ. Equat.* **62**: 427–442.

Angenent, S. and Velázquez, J. (1995). Asymptotic shape of cusp singularities in curve shortening, *Duke Math. J.* **77**(1): 71–110.

Ascher, U. M., Mattheij, R. M. M. and Russell, R. D. (1988). *Numerical Solution of Boundary Value Problems for Ordinary Differential Equations*, Prentice Hall, New Jersey.

Barenblatt, G. I. (1996). *Scaling, Self-similarity, and Intermediate Asymptotics*, Cambridge University Press, Cambridge.

Bebernes, J. and Eberly, D. (1989). *Mathematical Problems from Combustion Theory*, Springer-Verlag, New York.

Bebernes, J. and Troy, W. (1987). Nonexistence for the Kassoy problem, *SIAM J. Math. Anal.* **18**(4): 1157–1162.

Beckett, G., Mackenzie, J. A., Ramage, A. and Sloan, D. (2001). On the numerical solution of one-dimensional PDEs using adaptive methods based on equidistribution., *J. Comp. Phys.* **167**(2): 372–392.

Ben-Artzi, M., Koch, H. and Saut, J.-C. (2000). Dispersion estimates for fourth order Schrödinger equations, *C. R. Acad. Sci. Paris Série I Math.* **330**: 87–92.

Berger, M. and Kohn, R. (1988). A rescaling algorithm for the numerical calculation of blowing-up solutions, *Comm. Pure Appl. Math.* **41**(6): 841–863.

Bernoff, A. J. and Bertozzi, A. L. (1995). Singularities in a modified Kuramoto-Sivashinsky equation describing interface motion for phase transition, *Physica D* **85**: 375–404.

Bertozzi, A. and Pugh, M. (1998). Long-wave instabilities and saturation in thin film equations, *Comm. Pur. Appl. Math.* **LI**: 625–651.

Bertozzi, A. and Pugh, M. (2000). Pugh, finite-time blow-up of solutions of some long-wave unstable thin film equations, *Indiana Univ. Mathematics J.* **49**(4): 1323–1366.

de Boor, C. (1973). Good approximation by splines with variable knots. II, Vol. 363 of *Springer Lecture Note Series*, Springer-Verlag, Berlin.

Brenan, K., Campbell, S. and Petzold, L. (1996). *Numerical Solution of Initial Value Problems in Differential-Algebraic Equations*, second edn, SIAM, Philadelphia.

Brezis, H. and Friedman, A. (1983). Nonlinear parabolic equations involving measures as initial conditions, *J. Math. Pures Appl.* **62**: 73–97.

Brezis, H., Peletier, L. A. and Terman, D. (1986). A very singular solution of the heat equation with absorption, *Arch. Rat. Mech. Anal.* **95**: 185–209.

Bricmont, J. and Kupiainen, A. (1996). Stable nongaussian profiles, *Nonlinear Anal., TMA* **26**: 583–593.

Bricmont, J., Kupiainen, A. and Lin, G. (1994). Renormalization-group and asymptotics of solutions of nonlinear parabolic equations, *Comm. Pure Appl. Math* **47**.

Budd, C. J., Chen, S. and Russell, R. D. (1999). New self-similar solutions of the nonlinear Schrödinger equation with moving mesh computations, *J. Comp. Phys.* **152**(2): 756–789.

Budd, C. J. and Galaktionov, V. A. (1998). Stability and spectra of blow-up in problems with quasi-linear gradient diffusivity, *Proc. Roy. Soc. London A* **454**: 2371–2407.

Budd, C. J., Galaktionov, V. A. and Williams, J. F. (2002). Self-similar blow-up in higher-order semilinear parabolic equations. submitted to SIAM Applied Math (`http://www.maths.bath.ac.uk/MATHEMATICS/ preprints.html`).

Budd, C. J., Huang, W. and Russell, R. D. (1996). Moving mesh methods for problems with blow-up, *SIAM J. Sci. Comput.* **17**(2): 305–327.

Budd, C. J. and Piggott, M. D. (2001). The geometric integration of scale-invariant ordinary and partial differential equations, *J. Comput. Appl. Math.* **1-2**(128): 399–422.

Budd, C. J., Piggott, M. D. and Williams, J. F. (2003). The geometric integration of the porous medium equation. Pre-print.

Budd, C. J. and Williams, J. F. (2003). Equidistribution, optimal transport and adaptivity in arbitrary dimension. Pre-print.

Budd, C., Rottschäffer, V. and Williams, J. (2003). Blow-up multi-bump self-similar solutions to the complex Ginzburg-Landau equation. Submitted to Euro. J. Appl. Math. (`http://www.maths.bath.ac.uk/MATHEMATICS/ preprints.html`).

Bulirsch, R. and Stoer, J. (1980). *Introduction to Numerical Analysis*, Springer-Verlag, New York.

Cao, W., Huang, W. and Russell, R. D. (2002). A moving mesh method based on the geometric conservation law., *SIAM J. Sci. Comput.* **24**(1): 118–142.

Carey, G. F. and Dinh, H. T. (1985). Grading functions and mesh redistribution, *SIAM J. Numer. Anal.* **5**(22): 1028–1040.

Chapman, C. J. and Proctor, M. R. E. (1980). Nonlinear Rayleigh-Benard convection between poorly conducting boundaries, *J. Fluid Mech.* **101**: 759–782.

Chaves, M. and Galaktionov, V. A. (2001). Regional blow-up for a higher-order semilinear parabolic equation, *Euro. J. Appl. Math.* **12**: 601–623.

Coddington, E. A. and Levinson, N. (1955). *Theory of Ordinary Differential Equations*, McGraw-Hill Book Company, Inc., New York/London.

Cullen, M. J. P. and Purser, R. J. (1984). Properties of the Lagrangian theory of semi-geostrophic frontogenesis, *J. Atmos. Sci.* **41**: 1477–1497.

Doedel, E. J., Champneys, A. R., Fairgrieve, T. F., Kuznetsov, Y. A., Sandstede, B. and Wang, X.-J. (1997). AUTO97: Continuation and bifurcation software for ordinary differential equations, *Technical report*, Department of Computer Science, Concordia University, Montreal, Canada. Available at `ftp://ftp.cs.concordia.ca/pub/doedel/auto`.

Eberly, D. (1988). Nonexistence for the Kassoy problem in dimensions 1 and 2, *J. Math. Anal. Appl.* **129**(2): 401–408.

Egorov, Y. V., Galaktionov, V. A., Kondratiev, V. A. and Pohozaev, S. I. (2002). Asymptotic behaviour of global solutions to higher-order semilinear parabolic equations in the supercritical range, *Comptes Rendus Acad. Sci. Paris, Série I* **335**: 805–810. (Full text in `http://mip.ups-tlse.fr`).

Eidelman, S. D. (1969). *Parabolic Systems*, North-Holland Publ. Comp., Amsterdam/London.

Elliott, C. and Songmu, Z. (1986). On the cahn-hilliard equation, *rch. Rat. Mech. Anal.* **96**: 339–357.

Escobedo, M. and Kavian, O. (1987). Variational problems related to self-similar solutions of the heat equation, *Nonlinear Anal., TMA* **11**: 1103–1133.

Fibich, G., Ilan, B. and Papanicolau, G. (2002). Self-focusing with fourth-order dispersion, *SIAM J. Appl. Math.* **62**(4): 1437–1462.

Filippas, S. and Kohn, R. V. (1992). Refined asymptotics for the blow-up of $u_t - \Delta u = u^p$, *Comm. Pure Appl. Math.* **45**: 821–869.

Frank-Kamenetskii, D. A. (1969). *Diffusion and Heat Transfer in Chemical Kinetics*, Plenum Press, New York.

Friedman, A. (1983). *Partial Differential Equations*, Robert E.Krieger Publ. Comp., Malabar.

Friedman, A. and McLeod, B. (1986). Blow-up of solutions of nonlinear degenerate parabolic equations, *Arch. Rat. Mech. Anal.* **96**(1): 55–80.

Funada, J. (1984). Nonlinear diffusion equation for interfacial waves generating by the marangoni effect, *Note of Res. Inst. Math. Sci., Kyoto Univ.* **510**.

Galaktionov, V. A. (2001). On a spectrum of blow-up patterns for a higher-order semilinear parabolic equations, *Proc. Royal Soc. London A* **457**: 1–21.

Galaktionov, V. A. (2002). Critical global asymptotics in higher-order semilinear parabolic equations. To appear.

Galaktionov, V. A., Kurdyumov, S. P. and Samarskii, A. A. (1986). On asymptotic "eigenfunctions" of the cauchy problem for a nonlinear parabolic equation, *Math. USSR Sbornik* **54**: 421–455.

Galaktionov, V. A. and Pohozaev, S. I. (2003). Existence and blow-up for higher-order semilinear parabolic equations: majorizing order-preserving operators, *Indiana Univ. Math. J.* **51**: 1321–1338.

Galaktionov, V. A. and Poshashkov, S. A. (1986). Application of new comparison theorems to the investigation of unbounded solutions of nonlinear parabolic equations., *Diff. Equat.* **22**(7): 809–815.

Galaktionov, V. A. and Vazquez, J. L. (1991). Asymptotic behaviour of nonlinear parabolic equations with critical exponents. A dynamical systems approach, *J. Funct. Anal.* **100**: 435–462.

Galaktionov, V. A. and Vazquez, J. L. (1994). Extinction for a quasilinear heat equation with absorption II. A dynamical systems approach, *Comm. Part. Differ. Equat.* **19**: 1107–1137.

Galaktionov, V. A. and Vazquez, J. L. (2002). The problem of blow-up in nonlinear parabolic equations, *Discr. Cont. Dyn. Syst.* **8**: 399–433.

Galaktionov, V. A. and Williams, J. F. (2002). Blow-up in a fourth-order semilinear parabolc equation from convection explosion theory. In Press Euro. J. Appl. Math.

Galaktionov, V. A. and Williams, J. F. (2003a). Blow-up and global asymptotics of the unstable Cahn-Hilliard equation with a homogeneous nonlinearity. Submitted to Nolnlinearity (`http://www.maths.bath.ac.uk/MATHEMATICS/preprints.html`).

Galaktionov, V. A. and Williams, J. F. (2003b). On very singular similarity solutions of a higher-order semilinear parabolic equation. Submitted (`http://www.maths.bath.ac.uk/MATHEMATICS/preprints.html`).

Gel'fand, I. M. (1963). Some problems in the theory of quasilinear equations, *Amer. Math. Soc. Transl. (Ser. 2)* **29**: 295–381. See Section 15 by G.I. Barenblatt.

Gertsberg, V. L. and Sivashinsky, G. I. (1981). Large cells in nonlinear Rayleigh-Benard convection, *Prog. Theor. Phys.* **66**: 1219–1229.

Giga, Y. and Kohn, R. (1987). Characterizing blowup using similarity variables, *Indiana Univ. Math. J.* **36**(1): 1–40.

Giga, Y. and Kohn, R. V. (1985). Asymptotically self–similar blow-up of semilinear heat equations, *Comm. Pure Appl. Math.* **38**: 297–319.

Gohkberg, I. C. and Krein, M. G. (1969). *Introduction to the Theory of Linear Nonselfadjoint Operator*, Vol. 18 of *Transl. Math. Monogr.*, AMS.

Guerra, I., Peletier, M. A. and Williams, J. F. (2003). Stabilization and blow-up in a non-local problem from statistical mechanics. Preprint.

Hairer, E., Lubich, C. and Wanner, G. (2002). *Geometric Numerical Integration*, Vol. 31 of *Springer series in Compuational Mathematics*, Springer-Verlag, Berlin.

Henry, D. B. (1985). Some infinite-dimensional Morse-Smale systems defined by parabolic partial differential equations, *J. Differ. Equat.* **59**: 165–205.

Hirsch, F. and Lacombe, G. (1999). *Elements of Functional Analysis*, number 193 in *Graduate texts in mathematics*, Springer-Verlag, Berlin/New York.

Hocking, L. M., Stewartson, K. and Stuart, J. T. (1972). A nonlinear instability burst in plane parallel flow, *J. Fluid Mech.* **51**: 702–735.

Huang, W., Ren, Y. and Russell, R. D. (1994a). Moving mesh methods based on moving mesh partial differential equations, *J. of Comp. Phys.* **113**(2): 279–290.

Huang, W., Ren, Y. and Russell, R. D. (1994b). Moving mesh partial differential equations (MMPDEs) based on the equidistribtion principle, *SIAM J. Numer. Anal.* **31**(3): 709–730.

Huang, W. and Russell, R. D. (1996). A moving collocation method for solving time dependent partial differential equations, *Appl. Num. Math.* **20**(1-2): 101–116.

Huang, W. and Russell, R. D. (1997). Analysis of moving mesh partial differential equations with spatial smoothing, *SIAM J. Numer. Anal.* **34**(3): 1106–1126.

Huang, W. and Russell, R. D. (2001). Adaptive mesh movement—the mmpde approach and its applications. numerical analysis, *J. Comput. Appl. Math.* **1-2**: 383–398.

Iserles, A. (2002a). On the global error of discretization methods for highly-oscillatory ordinary differential equations, *BIT* **42**: 561–599.

Iserles, A. (2002b). Think globally, act locally: solving highly-oscillatory ordinary differential equations, *Appl. Num. Anal.* **43**: 145–160.

Iserles, A. (2003). On the numerical quadrature of highly-oscillating integrals I: Fourier transforms. DAMTP Tech. Rep. 2003/NA05.

Joulin, G., Mikishev, A. B. and Sivashinsky, G. I. (n.d.). A Semenov-Rayleigh-Benard problem. Preprint.

Kamin, S. and Peletier, L. A. (1985). Singular solutions of the heat equation with absorption, *Proc. Amer. Math. Soc.* **95**: 205–210.

Kamin, S. and Peletier, L. A. (1986). Large time behaviour of solutions of the porous media equation with absorption, *Israel J. Math.* **55**: 129–146.

Kamin, S. and Véron, L. (1988). Existence and uniqueness of the very singular solution of the porous media equation with absorption, *J. Analyse Math.* **51**: 245–258.

Krasnosel'skii, M. A. (1964). *Topological Methods in the Theory of Nonlinear Integral Equations*, Pergamon Press, Oxford/Paris.

Krasnosel'skii, M. A. and Zabreiko, P. P. (1984). *Geometrical Methods of Nonlinear Analysis*, Springer-Verlag, Berlin/Tokyo.

Levine, H. A. (1973). Some nonexistence and instability theorems for solutions of formally parabolic equations of the form $Pu_t = -Au + F(u)$, *Arch. Rat. Mech. Anal.* **51**: 371–386.

Levine, H. A. (1990). The role of critical exponents in blow-up problems, *SIAM Review* **32**: 262–288.

Levine, H. A. and Payne, L. (1974). Nonexistence theorems for the heat equation with nonlinear boundary conditions and for the porous meduim equation backward in time, *J. Differ. Equat.* **16**: 319–334.

Lions, J. L. (1969). *Quelques méthodes de résolution des problèmes aux limites non linéaires*, Gauthier–Villars, Paris.

Lunardi, A. (1995). *Analytic Semigroups and Optimal Regularity in Parabolic Problems*, Birkhäuser, Basel/Berlin.

Mackenzie, J. A. and Robertson, M. L. (2002). A moving mesh method for the solution of the one-dimensional phase-field equations., *J. Comput. Phys.* **181**(2): 526–544.

Novick-Cohen, A. (1992). Blow-up and growth in the directional solidification of dilute binary alloys, *Appl. Anal.* **47**: 241–257.

Novick-Cohen, A. (1998). The Cahn-Hilliard equation: mathematical and modeling perspectives., *Adv. Math. Sci. Appl.* **8**(2): 965–985.

Novick-Cohen, A. and Segel, L. (1984). Nonlinear aspects of the Cahn-Hilliard equation, *Phys. D* **10**: 277–298.

Peletier, L. and Troy, W. (2001). *Spatial Patterns: Higher-order Models in Physics and Mechanics*, Birkhäuser, New York.

Piggott, M. D. (2002). *Geometric Integration of Differential Equations*, PhD thesis, University of Bath.

Samarskii, A. A., Galaktionov, V. A., Kurdyumov, S. P. and Mikhailov, A. P. (1995). *Blow-up in Quasilinear Parabolic Equations*, Walter de Gruyter, Belrin/New York.

Saucez, P., Wouwer, A. V., Schiesser, W. E. and Zegeling, P. (2001). Method of lines study of nonlinear dispersive waves. Submitted.

Sell, G. R. and You, Y. (2002). *Dynamics of Evolutionary Equations*, Vol. 143 of *Appl. Math. Sci.*, Springer-Verlag.

Semenov, N. (1935). *Chemical Kinetics and Chain Reaction*, Clarendon Press, Oxford.

Shampine, L. F. and Kierzenka, J. (2001). A BVP solver based on residual control and the Matlab PSE, *ACM Transactions on Mathematical Software* **27**(3): 299–316.

Stockie, J., MacKenzie, J. A. and Russell, R. D. (2000). A moving mesh method for one-dimensional hyperbolic conservation laws., *SIAM J. Sci. Comput.* **22**(5): 1791–1813.

Sulem, C. and Sulem, P.-L. (1999). *The Nonlinear Schrödinger Equation*, Vol. 139 of *Appl. Math. Sci.*, Springer-Verlag, Berlin.

Vainberg, M. A. and Trenogin, V. A. (1974). *Theory of Branching of Solutions of Non-Linear Equations*, Noordhoff Int. Publ., Leiden.

Villani, C. (2003). *Topics in Optimal Transport*, Vol. 58 of *Graduate Studies in Mathematics*, AMS, Providence.

Williams, J. F., Xu, X. and Russell, R. D. (2003). Movcol4: A high resolution moving collocation scheme for evolutionary equations. Pre-print.

Witelski, T. P., Bernoff, A. J. and Bertozzi, A. L. (2003). Blow-up and dissipation in a critical-case unstable thin film equation. Submitted to Euro. J. Appl. Math.

Zel'dovich, Y. B., Barenblatt, G. I., Librovich, V. B. and Makhviladze, G. M. (1985). *The Mathematical Theory of Combustion and Explosions*, Consultants Bureau (Plenum), New York/London.

Zel'dovich, Y. B. and Raizer, Y. P. (1966). *Physics of Shock Waves and High-Temperature Hydrodynamic Phenomena* Vols I and II, Academic Press, New York.

Zelenyak, T. (1968). Stabilization of solutions of boundary value problems for a second order parabolic equation with one space variable, *Differ. Equat.* **4**: 17–22.